COLLECTED PAPERS on Off-shell Science

Vol. 39

January 2024 – December 2024

Motoichi OHTSU[1,2]

1 Chief Director
(General Incorporated Association)
Research Origin for Dressed Photon
2 Prof. Emeritus, The University of Tokyo
and Tokyo Institute of Technology

MEMBERS

[I] RESEARCH ORIGIN FOR DRESSED PHOTON (RODreP) *

Chief Director

Motoichi OHTSU** (Dr. Eng.)

Directors

Masayuki NAYA (Dr. Eng.)
Hirofumi SAKUMA (Ph. D.)

Auditor

Satoshi SUGIURA

Advisors

Izumi OJIMA (Dr. Sci.)
Junji MIYAHARA (Dr. Eng.)
Masuo FUKUI (Dr. Eng.)
Naoya TATE (Dr. Eng.)

Visiting Scientists

Hayato SAIGO (Dr. Sci.) (Nagahama Inst. Bio-Sci. and Tech.)
Itsuki BANNO (Univ. Yamanashi)
Suguru SANGU (Dr. Eng.) (Ricoh Co. Ltd.)
Etsuo SEGAWA (Dr. Eng.) (Yokohama National Univ.)
Seiken SAITO (Dr. Sci.) (Kogakuin Univ.)
Kazuya OKAMURA (Dr. Sci.) (Chubu Univ.)
(also, Senior Researcher, RODreP)

Secretary

Mari KAZAMA

(*)（General Incorporated Association）Research Origin for Dressed Photon
(RODreP)
Phone: 090-1603-0562
E-mail: ohtsu@rodrep.or.jp
URL: https://rodrep.or.jp/
(Labs.)
c/o Bdg.1, Yokohama Research Center, NICHIA Corp.
3-13-19 Moriya-cho, Kanagawa-ku, Yokohama-shi, Kanagawa 221-0022, Japan
(Executive office)
Adthree Publishing Co., Ltd.
4-27-37 Higashi-Nakano, Nakano-ku, Tokyo164-0003, Japan
The 3rd Floor, Sunrise Bldg. II, 5-20 Shin-Ogawa-cho, Shinjuku-ku, Tokyo 162-0814, Japan

（一般社団法人）ドレスト光子研究起点
Phone: 090-1603-0562
E-mail: ohtsu@rodrep.or.jp
URL: https://rodrep.or.jp/
（研究所）
〒221-0022　神奈川県横浜市神奈川区守屋町 3－13－19
日亜化学工業（株）　横浜研究所　1 号館 1 階
（事務局）
〒162-0814　東京都新宿区新小川町 5-20　サンライズビルⅡ ３F
株式会社アドスリー

(**) Professor Emeritus, The University of Tokyo and Tokyo Institute of Technology
東京大学名誉教授、東京工業大学名誉教授

THE 2nd OFF-SHELL SCIENCE GRAND PRIZE

[1] Call for application, an award winner, and award ceremony
【第二回オフシェル科学大賞：　募集案内、受賞者発表、授賞式】

VIDEO LECTURES

[1] 大津元一、「ドレスト光子フォノンの最適散逸と自律的移動経路」(2024 年 9 月)

その１　https://www.youtube.com/watch?v=bTSnf4_6q58
その２　https://www.youtube.com/watch?v=I8Ly0HZAAHU

[2] 大津元一、「3 次元量子ウォークモデルによる偏光に関する光子ブリーディングの記述」(2024 年 3 月)

その１　https://www.youtube.com/watch?v=ZyB7sVHuYgM
その２　https://www.youtube.com/watch?v=SibIxg99LYw

[3] 大津元一、「ドレスト光子量子ウォークモデルへのエネルギー散逸の導入」(2024 年 1 月)

その１　https://www.youtube.com/watch?v=ixulubpp9hY
その２　https://www.youtube.com/watch?v=k1boE-R45VE

LIST OF PAPERS

[(pp. XX-XX); pages in this issue of the COLLECTED PAPERS**]**

[I] ORIGINAL PAPERS

N.A.

[II] PRESENTATIONS IN INTERNATIONAL CONFERENCES

[1] N. Tate, "SiC-based photon-breeding device for characteristic polarization modulation," Abstract of the 14th Japan-Korea Joint Workshop on Digital Holography and Information Photonics (DHIP 2024), 15-18 December 2024, Seoul, Korea, paper number M1-2, p.23.
[Invited paper]

[2] H. Du, T. Kadowaki, N, Tate, T. Kawazoe, Y. Oki, M. Ohtsu, K. Hayashi, "Spectral-Polarization-Selective Magneto-Optical Effect by Al-doped 4H-SiC Device with DPP-Assisted Annealing," Abstract of the Conference on Lasers and Electro-Optics (CLEO24), 05-10 May 2024, Charlotte Convention Center, Charlotte, North Carolina, USA, paper number SM1O.5.

[III] REVIEW PAPERS

[1] H. Sakuma, I. Ojima, and M. Ohtsu, "Perspective on an Emerging Frontier of Nanoscience Opened up by Dressed Photon Studies," *Nanoarchitectonics*, Vol. 5, Issue 1 (2024) pp.1-23.

[IV] PREPRINT DEPOSITORIES

[IV-1] OFF-SHELL ARCHIVE

[Original papers]

[1] M. Ohtsu, E. Segawa, K. Yuki, and S. Saito, "Quantum walk analyses of the off-shell scientific features of dressed-photon–phonon transfers among a small number of nanometer-sized particles," *Off-shell Archive* (July, 2024)
Offshell: 2407O.001.v1.

DOI 10.14939/2407O.001.v1,
https://rodrep.or.jp/en/off-shell/original_2407O.001.v1.html

[2] M. Ohtsu, E. Segawa, K. Yuki, and S. Saito, "Optimum dissipation for governing the autonomous transfer of dressed photons," *Off-shell Archive* (May, 2024) Offshell: 2405O.001.v1.
DOI 10.14939/2405O.001.v1,
https://rodrep.or.jp/en/off-shell/original_2405O.001.v1.html

[Review papers]

[1] M. Ohtsu, "Off-shell scientific nature of dressed photon energy transfer and dissipation," *Off-shell Archive* (April, 2024) Offshell: 2404R.001.v110.
DOI 10.14939/2404R.001.v1
https://rodrep.or.jp/en/off-shell/review_2404R.001.v1.html

[IV-2] arXiv

[1] H. Sakuma, I. Ojima, and K. Okamura, "Reexamination of the hierarchy problem from a novel geometric perspective," arXiv: 2406.01626v1 [physics.gen-ph] 1 June 2024.

[V] PUBLISHED BOOKS

N.A.

[VI] PRESENTATIONS IN DOMESTIC CONFERENCES

[1] I. Banno, "Current-induced Non-equlibrium Structure IV," Abstracts of the 85th Jpn. Soc. Appl. Phys. Autumn Meeting, September 16-20, 2024 (Toki Messe and Online) meeting), paper number 18p-A33-13.
【坂野斎、「流れが誘導する平衡から遠い量子構造IV」、第85回応用物理学会秋季学術講演会予稿集（2024年9月16-20日：朱鷺メッセ＆オンライン）講演番号18p-A33-13】

[2] H.Saigo, "Off-shell Science and Causality," Abstracts of the 85th Jpn. Soc. Appl. Phys. Autumn Meeting, September 16-20, 2024 (Toki Messe and Online meeting), paper number 18p-A33-14.
【西郷甲矢人、「オフシェル科学と因果性」、第85回応用物理学会秋季学術講演会予稿集（2024年9月16-20日：朱鷺メッセ＆オンライン）講演番号18p-A33-14】

[3] K. Okamura, “Dressed photons from network quantum fields,” Abstracts of the 85th Jpn. Soc. Appl. Phys. Autumn Meeting, September 16-20, 2024 (Toki Messe and Online meeting), paper number 18p-A33-15.
【岡村和弥、「ネットワーク量子場からのドレスト光子」、第85回応用物理学会秋季学術講演会予稿集（2024年9月16-20日：朱鷺メッセ＆オンライン）講演番号18p-A33-15】

[4] K. Saito, “The wave functions of quantum walks on regular graphs,” Abstracts of the 85th Jpn. Soc. Appl. Phys. Autumn Meeting, September 16-20, 2024 (Toki Messe and Online meeting), paper number 18p-A33-16.
【齋藤正顕, 「正則グラフ上の量子ウォークの波動関数について」、第85回応用物理学会秋季学術講演会予稿集（2024年9月16-20日：朱鷺メッセ＆オンライン）講演番号18p-A33-16】

[5] M. Ohtsu, E. Segawa, K. Yuki, S. Saito, “Optimum dissipation for governing the autonomous transfer of dressed photons,” Abstracts of the 85th Jpn. Soc. Appl. Phys. Autumn Meeting, September 16-20, 2024 (Toki Messe and Online meeting), paper number 18p-A33-17.
【大津元一、瀬川悦生、結城謙太、「ドレスト光子の自律的移動経路を決める最適散逸」、第85回応用物理学会秋季学術講演会予稿集（2024年9月16-20日：朱鷺メッセ＆オンライン）講演番号18p-A33-17】

[6] E. Segawa, S. Saito, K. Yuki, M. Ohtsu, “Paths on the graph chosen autonomously by dressed photons from the quantum walk model,” Abstracts of the 85th Jpn. Soc. Appl. Phys. Autumn Meeting, September 16-20, 2024 (Toki Messe and Online meeting), paper number 18p-A33-18.
【瀬川悦生、齋藤正顕、結城謙太、大津元一、「量子ウォークモデルから見たドレスト光子が自律的に選択するグラフ上のパス」、第85回応用物理学会秋季学術講演会予稿集（2024年9月16-20日：朱鷺メッセ＆オンライン）講演番号18p-A33-18】

[7] S. Sangu, “Generation of Highly Excited States of Dressed Photon via Matter Structure,” Abstracts of the 85th Jpn. Soc. Appl. Phys. Autumn Meeting, September 16-20, 2024 (Toki Messe and Online meeting), paper number 18p-A33-19.
【三宮俊、「物質構造を介したドレスト光子高励起状態の生成」、第85回応用物理学会秋季学術講演会予稿集（2024年9月16-20日：朱鷺メッセ＆オンライン）講演番号18p-A33-19】

[8] M. Ohtsu, E. Segawa, K. Yuki, and S. Saito, “Principles of autonomous transfer of dressed photons,” Abstracts of laser seminar, organized by the Laser Society of Japan, August 12, 2024 (Fukui Univ., Fukui)
【大津元一、瀬川悦生、結城謙太、齋藤正顕、「ドレスト光子の自律的移動と

その原理」、2024年レーザー学会　レーザー普及セミナー予稿集（2024年8月12日：福井大学遠赤外領域開発研究センター、福井）】
[Invited presentation]

[9] I. Banno, “Current-induced Non-equlibrium Structure III,” Abstracts of the 71st Jpn. Soc. Appl. Phys. Spring Meeting, March 22-25, 2024 (Tokyo City Univ. and Online meeting), paper number 24a-11F-1.
【坂野斎、「流れが誘導する平衡から遠い量子構造Ⅲ」、第71回応用物理学会春季学術講演会予稿集（2024年3月22-25日：東京都市大学＆オンライン）講演番号24a-11F-1】

[10] H. Sakuma, “On the emergence of spacetime and existence of dressed photon,” Abstracts of the 71st Jpn. Soc. Appl. Phys. Spring Meeting, March 22-25, 2024 (Tokyo City Univ. and Online meeting), paper number 24a-11F-2.
【佐久間弘文、「時空領域の創発とドレスト光子の存在について」、第71回応用物理学会春季学術講演会予稿集（2024年3月22-25日：東京都市大学＆オンライン）講演番号24a-11F-2】

[11] H.Saigo, “Off-shell Science and the Concept of Spacetime,” Abstracts of the 71st Jpn. Soc. Appl. Phys. Spring Meeting, March 22-25, 2024 (Tokyo City Univ. and Online meeting), paper number 24a-11F-3.
【西郷甲矢人、「ドレスト光子の物理量代数について」、第71回応用物理学会春季学術講演会予稿集（2024年3月22-25日：東京都市大学＆オンライン）講演番号24a-11F-3】

[12] K. Okamura, “Measurement theory for algebraic quantum fields,” Abstracts of the 71st Jpn. Soc. Appl. Phys. Spring Meeting, March 22-25, 2024 (Tokyo City Univ. and Online meeting), paper number 24a-11F-4.
【岡村和弥、「代数的量子場の測定理論」、第71回応用物理学会春季学術講演会予稿集（2024年3月22-25日：東京都市大学＆オンライン）講演番号24a-11F-4】

[13] E. Segawa, H, Ohno, and L. Matsuoka, “Can quantum walk find the shortest path ?,”Abstracts of the 71st Jpn. Soc. Appl. Phys. Spring Meeting, March 22-25, 2024
(Tokyo City Univ. and Online meeting), paper number 24a-11F-5.
【瀬川悦生、大野博道、松岡雷士，「量子ウォークは近道を探せるか？」、第71回応用物理学会春季学術講演会予稿集（2024年3月22-25日：東京都市大学＆オンライン）講演番号24a-11F-5】

[14] M. Ohtsu, E. Segawa, K. Yuki, S. Saito, “Three-dimensional quantum walk analysesof photon breeding with respect to photon spin,” Abstracts of the 71st Jpn. Soc. Appl. Phys. Spring Meeting, March 22-25, 2024 (Tokyo City Univ. and Online meeting), paper number 24a-11F-6.

【大津元一、瀬川悦生、結城謙太、齋藤正顕、「偏光に関する光子ブリーディングの3次元量子ウォーク解析」、第71回応用物理学会春季学術講演会予稿集（2024年3月22-25日：東京都市大学＆オンライン）講演番号24a-11F-6】

[15] S. Sangu, H. Saigo, and M. Ohtsu, "Influence of Matter-System Geometry on Dressed-Photon Localization and Dissipation ," Abstracts of the 71st Jpn. Soc. Appl. Phys. Spring Meeting, March 22-25, 2024 (Tokyo City Univ. and Online meeting), paper number 24a-11F-7.
【三宮俊、西郷甲矢人、大津元一、「ドレスト光子の局在および散逸における物質系の幾何学的構造の影響」、第71回応用物理学会春季学術講演会予稿集（2024年3月22-25日：東京都市大学＆ オンライン）講演番号24a-11F-7】

[16] M. Naya, M. Sato, S. Hakuta, M. Mitomo, K. Ijiro, T. Saiki, "Laser light controlled microdroplet robot," Abstracts of the 44th annual meeting of the Laser Society of Japan, January 16-19, 2024 (The National Museum of Emerging Science and Innovation, Tokyo) paper number A08-18p-VI-01.
【納谷昌之、佐藤守、白田真也、三友秀之、居城邦治、斉木敏治、「レーザ光制御マイクロ液滴ロボット」、レーザー学会学術講演会第44回年次大会予稿集（2024年1月16日-19日）、（日本科学未来館、東京） 講演番号A08-18p-VI-01】
[Invited presentation]

[17] M. Ohtsu, "A quantum walk model for dressed photons with energy dissipation ," Abstracts of the 44th annual meeting of the Laser Society of Japan, January 16-19, 2024 (The National Museum of Emerging Science and Innovation, Tokyo) paper number S03-18p-VIII-05.
【大津元一、「エネルギー散逸のあるドレスト光子の量子ウォークモデル」、レーザー学会学術講演会第44回年次大会予稿集（2024年1月16日-19日）、（日本科学未来館、東京）講演番号S03-18p-VIII-05】
[Invited presentation]

[18] E. Segawa, "Mathematics of energy transfer problem of quantum walk," Abstracts of the 44th annual meeting of the Laser Society of Japan, January 16-19, 2024 (The National Museum of Emerging Science and Innovation, Tokyo) paper number S03-18p-VIII-06.
【瀬川悦生、「量子ウォークのエネルギー遷移問題の数理」、レーザー学会学術講演会第44回年次大会予稿集（2024年1月16日-19日）、（日本科学未来館、東京）講演番号S03-18p-VIII-06】
[Invited presentation]

[19] S. Sangu, "Superradiance process of dressed photons induced by spatial defect structures," Abstracts of the 44th annual meeting of the Laser Society of Japan,

January 16-19, 2024 (The National Museum of Emerging Science and Innovation, Tokyo) paper number S03-18p-VIII-07.
【三宮俊、「欠陥構造が引き起こすドレスト光子の超放射過程」、レーザー学会学術講演会第44回年次大会予稿集（2024年1月16日−19日）、（日本科学未来館、東京）講演番号S03-18p-VIII-07】
[Invited presentation]

[VII] AWARDS AND CONFERMENTS

[1] E. Segawa, The 2nd Off-shell science grand prize, October 28, 2024.
【瀬川悦生、第二回オフシェル科学大賞、2024 年 10 月 28 日】

[2] M. Ohtsu, The Order of the Sacred Treasure, Gold Rays with Neck Ribbon, May 13, 2024.
【大津元一、瑞宝中綬章、2024 年 5 月 13 日】

CUMULATIVE LIST: Off-shell Archive

2024

38 Quantum walk analyses of the off-shell scientific features of dressed-photon–phonon transfers among a small number of nanometer-sized particles

Authors M.Ohtsu, E.Segawa, K.Yuki, and S.Saito
DOI 10.14939/2407O.001.v1
URL https://rodrep.or.jp/en/off-shell/original_2407O.001.v1.html
Date 2024.07.26

37 Optimum dissipation for governing the autonomous transfer of dressed photons

Authors M.Ohtsu, E.Segawa, K.Yuki, and S.Saito
DOI 10.14939/2405O.001.v1
URL https://rodrep.or.jp/en/off-shell/original_2405O.001.v1.html
Date 2024.05.27

36 Off-shell scientific nature of dressed photon energy transfer and dissipation

Authors M.Ohtsu
DOI 10.14939/2404R.001.v1
URL https://rodrep.or.jp/en/off-shell/review_2404R.001.v1.html
Date 2024.04.10

2023

35 Analyses of photon breeding with respect to photon spin by using a three-dimensional quantum walk model

Authors M.Ohtsu, E.Segawa, K.Yuki, and S.Saito
DOI 10.14939/2311O.001.v1
URL https://rodrep.or.jp/en/off-shell/original_2311O.001.v1.html
Date 2023.11.13

34 A quantum walk model with energy dissipation for a dressed-photon–phonon confined by an impurity atom-pair in a crystal

Authors M.Ohtsu, E.Segawa, K.Yuki, and S.Saito
DOI 10.14939/2304O.001.v1
URL https://rodrep.or.jp/en/off-shell/original_2304O.001.v1.html
Date 2023.04.10

33 Spatial distribution of dressed-photon–phonon confined by an impurity atom-pair in a crystal

Authors M.Ohtsu, E.Segawa, K.Yuki, and S.Saito
DOI 10.14939/2301O.001.v1
URL https://rodrep.or.jp/en/off-shell/original_2301O.001.v1.html
Date 2023.01.18

2022

32 Dressed-photon–phonon creation probability on the tip of a fiber probe calculated by a quantum walk model

Authors M.Ohtsu, E.Segawa, K.Yuki, and S.Saito
DOI 10.14939/2212O.001.v1
URL https://rodrep.or.jp/en/off-shell/original_2212O.001.v1.html
Date 2022.12.02

31 Numerical calculation of a dressed photon energy transfer based on a quantum walk model

Authors M.Ohtsu, E.Segawa, and K.Yuki
DOI 10.14939/2206O.001.v1
URL https://rodrep.or.jp/en/off-shell/original_2206O.001.v1.html
Date 2022.06.22

30 Off-shell science theories on interaction for dressed photons

Authors M.Ohtsu
DOI 10.14939/2201R.001.v1

URL https://rodrep.or.jp/en/off-shell/review_2201R.001.v1.html
Date 2022.01.31

2021

29 Progresses in theoretical studies of off-shell science for dressed photons
Authors M.Ohtsu
DOI 10.14939/2110R.002.v1
URL https://rodrep.or.jp/en/off-shell/review_2110R.002.v1.html
Date 2021.10.22

28 Generation Mechanism of Dressed Photon and Unique Features of Converted Propagating Light
Authors M.Ohtsu
DOI 10.14939/2110R.001.v1
URL https://rodrep.or.jp/en/off-shell/review_2110R.001.v1.html
Date 2021.10.01

27 A Quantum Walk Model for Describing the Energy Transfer of a Dressed Photon
Authors M.Ohtsu
DOI 10.14939/2109R.001.v1
URL https://rodrep.or.jp/en/off-shell/review_2109R.001.v1.html
Date 2021.09.03

26 The dressed photon as a member of the off-shell photon family
Authors M.Ohtsu
DOI 10.14939/2103R.001.v1
URL https://rodrep.or.jp/en/off-shell/review_2103R.001.v1.html
Date 2021.03.02

2020

25 Past, present, and future studies on the longitudinal electric field components of light

Authors M.Ohtsu
DOI 10.14939/2008R.001.v1
URL https://rodrep.or.jp/en/off-shell/review_2008R.001.v1.html
Date 2020.08.21

24 Errata: Route to Off-Shell Science
Authors M.Ohtsu
DOI 10.14939/2006R.001.v2
URL https://rodrep.or.jp/en/off-shell/review_2006R.001.v2.html
Date 2020.08.17

23 Route to Off-Shell Science
Authors M.Ohtsu
DOI 10.14939/2006R.001.v1
URL https://rodrep.or.jp/en/off-shell/review_2006R.001.v1.html
Date 2020.06.25

22 Nutation in energy transfer of dressed photons between nano-particles
Authors M.Ohtsu and T.Kawazoe
DOI 10.14939/2005O.001.v1
URL https://rodrep.or.jp/en/off-shell/original_2005O.001.v1.html
Date 2020.05.15

21 Progress in off-shell science in analyzing light–matter interactions for creating dressed photons
Authors M.Ohtsu
DOI 10.14939/2004R.001.v1
URL https://rodrep.or.jp/en/off-shell/review_2004R.001.v1.html
Date 2020.04.25

20 The present and future of numerical simulation techniques for off-shell science
Authors M.Ohtsu
DOI 10.14939/2003R.001.v1
URL https://rodrep.or.jp/en/off-shell/review_2003R.001.v1.html

Date 2020.02.27

2019

19 Note on the physical meaning of the cosmological term

Authors H.Sakuma and H.Ochiai

DOI 10.14939/1909O.001.v2

URL https://rodrep.or.jp/en/off-shell/original_1909O.001.v2.html

Date 2019.12.20

18 History, current developments, and future directions of near-field optical science

Authors M.Ohtsu

DOI 10.14939/1912R.001.v1

URL https://rodrep.or.jp/en/off-shell/review_1912R.001.v1.html

Date 2019.12.20

17 Dressed photon phenomena that demand off-shell scientific theories

Authors M.Ohtsu

DOI 10.14939/1911R.001.v1

URL https://rodrep.or.jp/en/off-shell/review_1911R.001.v1.html

Date 2019.11.12

16 Note on the physical meaning of the cosmological term

Authors H.Sakuma and H.Ochiai

DOI 10.14939/1909O.001.v1

URL https://rodrep.or.jp/en/off-shell/original_1909O.001.v1.html

Date 2019.09.10

15 Infrared lasers using silicon crystals

Authors M.Ohtsu and T.Kawazoe

DOI 10.14939/1908R.001.v1

URL https://rodrep.or.jp/en/off-shell/review_1908R.001.v1.html

Date 2019.08.01

14 Indications from dressed photons to macroscopic systems based on hierarchy and autonomy

Authors M.Ohtsu
DOI 10.14939/1906R.001.v1
URL https://rodrep.or.jp/en/off-shell/review_1906R.001.v1.html
Date 2019.07.06

13 Novel functions and prominent performance of nanometric optical devices made possible by dressed photons

Authors M.Ohtsu
DOI 10.14939/1904R.001.v1
URL https://rodrep.or.jp/en/off-shell/review_1904R.001.v1.html
Date 2019.04.02

2018

12 Embarking on theoretical studies for off-shell science guided by dressed photons

Authors M.Ohtsu
DOI 10.14939/1811R.001.v1
URL https://rodrep.or.jp/en/off-shell/review_1811R.001.v1.html
Date 2018.12.26

11 Theory of Single Susceptibility for Near-_eld Optics Equally Associated with Scalar and Vector Potentials

Authors I.Banno
DOI 10.14939/1809O.002.v1
URL https://rodrep.or.jp/en/off-shell/original_1809O.002.v1.html
Date 2018.12.26

10 Gigantic Ferromagnetic Magneto-Optical Effect in a SiC Light-emitting Diode Fabricated by Dressed-Photon–Phonon-Assisted Annealing

Authors M.Ohtsu and T.Kawazoe
DOI 10.14939/1809R.001.v1
URL https://rodrep.or.jp/en/off-shell/review_1809R.001.v1.html

Date 2018.12.26

9 Micro-Macro Duality for Inductions/Reductions

Authors I.Ojima

DOI 10.14939/1809O.001.v1

URL https://rodrep.or.jp/en/off-shell/original_1809O.001.v1.html

Date 2018.12.26

8 Logical Fallacy of using the Electric Field in Non-resonant Near-field Optics

Authors I.Banno and M.Ohtsu

DOI 10.14939/1808O.001.v1

URL https://rodrep.or.jp/en/off-shell/original_1808O.001.v1.html

Date 2018.12.26

7 Principles and Practices of Si Light Emitting Diodes using Dressed Photons

Authors M.Ohtsu and T.Kawazoe

DOI 10.14939/1805R.001.v1

URL https://rodrep.or.jp/en/off-shell/review_1805R.001.v1.html

Date 2018.12.26

6 Photon localization revisited

Authors I.Ojima, M.Ohtsu and H.Saigo

DOI 10.14939/1804O.002.v1

URL https://rodrep.or.jp/en/off-shell/original_1804O.002.v1.html

Date 2018.12.26

5 Experimental estimation of the maximum size of a dressed photon

Authors M.Ohtsu and T.Kawazoe

DOI 10.14939/1802R.001.v1

URL https://rodrep.or.jp/en/off-shell/review_1802R.001.v1.html

Date 2018.12.26

2017

4 Creation and Measurement of Dressed Photons: A Link to Novel Theories

Authors M.Ohtsu and H.Sakuma
DOI 10.14939/1712R.001.v1
URL https://rodrep.or.jp/en/off-shell/review_1712R.001.v1.html
Date 2018.12.26

3 Spatial and Temporal Evolutions of Dressed Photon Energy Transfer

Authors M.Ohtsu, T.Kawazoe, H.Saigo
DOI 10.14939/1710R.001.v1
URL https://rodrep.or.jp/en/off-shell/review_1710R.001.v1.html
Date 2018.12.26

2 High-Power Infrared Silicon Light-emitting Diodes Fabricated and Opereted using Dressed Photones

Authors M.Ohtsu and T.Kawazoe
DOI 10.14939/1804O.001.v1
URL https://rodrep.or.jp/en/off-shell/original_1804O.001.v1.html
Date 2018.12.24

1 New Routes to Studying the Dressed Photon

Authors M.Ohtsu
DOI 10.14939/OffShell.1709R.001.v1
URL https://rodrep.or.jp/en/off-shell/review_1709R.001.v1.html
Date 2018.12.23

THE 2nd OFF-SHELL SCIENCE GRAND PRIZE

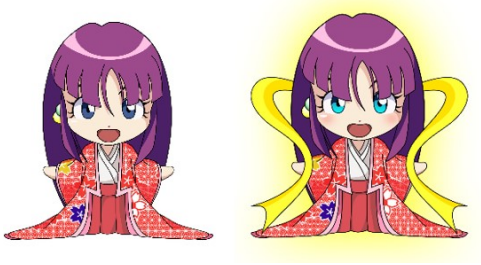

未来を拓く
オフシェル科学大賞

募集

量子場は現代物理学における根本概念ですが、粒子描像に還元できる「オンシェル」的な側面の研究に比べ、相互作用の本質に関わる「オフシェル」的な側面への数理的な研究は未開発の状態でした。しかし最近のナノ寸法の複合系の量子場であるドレスト光子の理論的研究により、相互作用する量子場を正面から扱う「オフシェル科学」の先導的研究が著しく進みました。その結果ドレスト光子が関わる新奇な実験結果が説明され、理論と実験との結びつきが強まると同時に、物理学や数学の幅広い研究分野との予期せぬ新たな連携が生まれつつあります。

未来の科学技術の発展に貢献するため、第２回（2024年度）は
オフシェル科学研究の促進に資する優れた「問題」を募集します。

応募の中から優れた「問題」(3件程度）を選び表彰します。
副賞として**30万円**（1件あたり）を差し上げます（※注1）。

応募資格
若手中堅の研究者

応募方法
次の二書類を提出
①問題提案書（※注2.3）
　1.問題の題名（20字以内）
　2.問題の内容説明（3,000字以内）
②応募者の経歴、研究業績など（※注3）

審査方法
有識者で構成する審査委員会による書類審査

募集日程等
◆募集締め切り：令和6年　8月16日（金）
◆受賞者発表　：令和6年 10月18日（金）
（審査結果は下記の法人のHPなどで公表します。）

応募書類提出先
上記の二書類を下記に郵送（応募締め切り日の消印有効）

〒221-0022
神奈川県横浜市神奈川区守屋町3-13-19　１号館１階
一般社団法人　ドレスト光子研究起点
第２回オフシェル科学大賞事務局　宛

（※注1）次回以降の募集ではこれらの受賞問題を提示し その解決に重要な貢献をする論文を募集し表彰します。
（※注2）Symmetry誌のSpecial Issue “Quantum Fields and Off-shell Sciences”所収の論文などを参考の上、問題をご考案、ご執筆下さい。これらの論文リストは下記ウェブサイトをご覧下さい。
（※注3）問題提案書用紙、及び経歴書等などの記載用紙は下記ウェブサイト、又は右のQRコードからダウンロードして下さい。

お問い合わせ▶ rodrep-general@rodrep.or.jp
https://rodrep.or.jp/

第２回オフシェル科学大賞　受賞者発表

６名の有識者からなる審査委員会における厳正な審査の結果、第２回オフシェル科学大賞（注１）の受賞者を下記のように決定しました。近日中に受賞者に賞状、副賞、賞金が授与されます。

令和６年 10 月 18 日

（一般社団法人）ドレスト光子研究起点（注２）　　代表理事　大津 元一

【受賞者】　瀬川 悦生様　（横浜国立大学 教授）

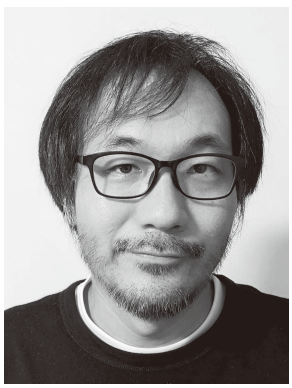

【受賞理由】オフシェル科学の発展の促進に資する優れた問題を提案した。

◉提案の名称　ドレスト光子の出力最大にする最適な閉曲面上の埋め込みを探せ

◉提案の概要説明　従来のネットワークの隣接関係のみが反映される標準的モデル（グローバーウォークモデル）ではドレスト光子のエネルギー移動の独特の不思議な振る舞いを再現するには不十分である。そこで、このモデルから脱却し、「ネットワークの背後にある閉曲面埋め込み」という幾何的な新たな考察を加え、ドレスト光子の挙動が端的に再現されるモデルを構築し、新しい世界を拓く。これが実現すればドレスト光子、オフシェル科学、そして生体微生物によるエネルギー輸送などへ波及し、広範な分野の相乗効果が期待される。上記の実現のために与えられたネットワークに対し、「初期にはいろいろな場所に訪問し、その経験をいかして時間の経過とともに『自律的に』適切な経路を選ぶ」ようすが記述される閉曲面上の埋め込みを探すことをここに問題として提示する。

（注１）光と物質との相互作用などに関わる量子場とその関連現象を扱うのがオフシェル科学です。発展の著しいこの科学は古くからある伝統的なオンシェル科学とは補完的であることから、未踏の問題が立ちはだかっています。「オフシェル科学大賞」は（一般社団法人）ドレスト光子研究起点によって設立され、第１回に続き今回もこれらの未踏の問題を提起した研究者を表彰しました。また将来これらの問題をが解決された場合、解決した研究者を表彰する予定です。

（注２）（一般社団法人）ドレスト光子研究起点はオフシェル科学の基礎研究を行う研究機関です。研究振興のため上記のオフシェル科学大賞の募集、研究助成などの事業も行っています。詳細は法人のホームページ **https://rodrep.or.jp/** をご参照下さい。右の QR コードもご利用できます。

第2回オフシェル科学大賞

授賞式

令和6年10月28日（月）

（一般社団法人）ドレスト光子研究起点

（ https://rodrep.or.jp/ ）　代表理事：大津　元一

1978年
5月9日

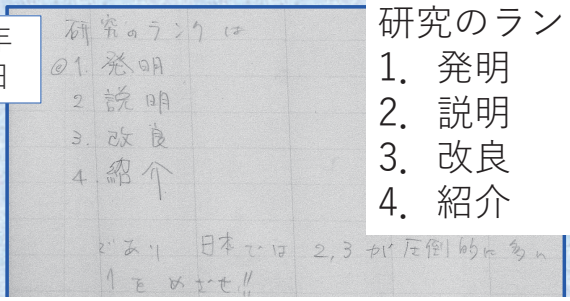

研究のランクは
1. 発明
2. 説明
3. 改良
4. 紹介

3U's

Universal?
Unique?
Ultimate?

忘れえぬ言葉1のハイライト　1．大学院の講義にて
https://youtu.be/eiESFHMIX2U?feature=shared

・ナノ寸法の微小な量子場であるドレスト光子、その原理を扱うオフシェル科学の基礎研究を行う研究機関です。
・研究振興のためオフシェル科学大賞の募集、研究助成等の事業も行います。

オフシェル科学大賞

近年その発展が著しいオフシェル科学は古くからある伝統的なオンシェル科学とは補完的であることから、未踏の問題が立ちはだかっています。

本賞はこれらの未踏の問題を提起した研究者を表彰するものです。今後もさらに問題提起を募集していきます。また将来これらの問題が解決された場合、その研究者も表彰する予定です。

本賞の趣旨に近いもの

第2回は問題の提起に対して

1. 米国のクレイ数学研究所によって2000年に発表された下記の7つの問題
   （懸賞金は100万ドル）→ミレニアム懸賞問題
   ヤン-ミルズ方程式と質量ギャップ問題、リーマン予想、P≠NP予想、
   ナビエ・ストークス方程式の解の存在と滑らかさ、ホッジ予想、ポアンカレ予想、
   バーチ・スウィンナートン＝ダイアー予想
2. ベルリン科学アカデミーの懸賞　受賞者はH. R. Hertz (1857-1894)
3. フランス科学アカデミーの懸賞　受賞者はA.-L. de Lavoisier (1743-1794)
4. ブザンソン学術・文芸・技能アカデミーの懸賞論文
   1）雄弁賞　350リーブル、2）文芸賞（250リーブル）、3）技能賞（200リーブル）
5. ディジョン・アカデミーの懸賞　受賞者はJ. J. Rousseau (1712-1778)

国内では

6.「物性研究」5周年記念懸賞論文 テーマ「物性物理学をどのように発展させるか」
   募集期間1969. 3.1～1969. 8.20. 賞金5万円

問題の解決に対して

将来：問題の解決に対して

第2回の受賞者

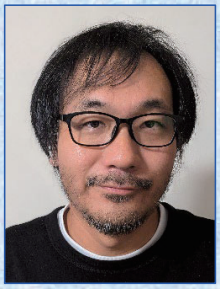

瀬川悦生　様
（横浜国立大学　教授）

【受賞理由】 オフシェル科学の発展の促進に資する優れた問題を提案した。

◎提案の名称 ドレスト光子の出力最大にする最適な閉曲面上の埋め込みを探せ

[I] ORIGINAL PAPERS

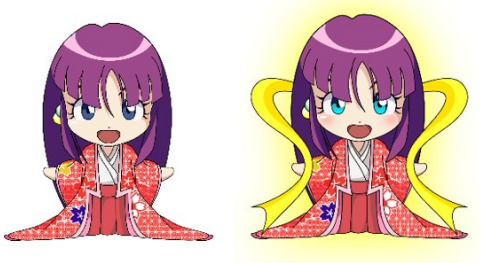

[II] PRESENTATIONS

IN INTERNATIONAL CONFERENCES

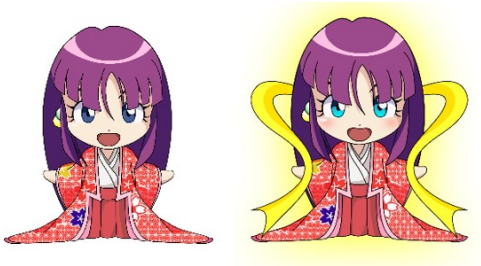

SiC-based photon-breeding device for characteristic polarization modulation

Naoya Tate
Kyushu University
744 Motooka, Nishi-ku, Fukuoka, 819-0395, Japan
Tel.:+81-92-802-3694, E-mail:tate@ed.kyshu-u.ac.jp
OCIS codes: (230.0230) Optical devices; (350.4238) Nanophotonics and photonic crystals.

Photon-breeding devices have been investigated as novel electrical-to-optical energy-conversion devices. The nanoscale structure of a material with dopants is appropriately modified by dressed-photon-phonon (DPP) annealing [1]. Accordingly, the production and radiation of cloned photons are physically stimulated by energy conversion. To date, Si lasers, SiC-LED, ZnO-LED, and others have been developed. Recently, polarization modulation using 4H-SiC materials has been experimentally demonstrated [2]. Electro-optical and magneto-optical devices are widely utilized as polarization rotators. However, they require external setups to induce electric or magnetic fields of sufficient strength. By contrast, SiC devices can be operated without external fields. Therefore, smaller, lighter, and thinner devices can be fabricated. In this study, we experimentally verified several performance characteristics and clarified nano-optical mechanisms during polarization rotation.

In general, the DPP phenomena are utilized twice in an experimental demonstration; for device fabrication and device operation. For fabrication, the SiC substrate is annealed through Joule heating produced by current injection to diffuse the Al dopants. During annealing, the substrate is irradiated with laser light to create DPPs that surround the dopant clusters. Driven by the created DPPs, electron-hole recombination occurs, emitting light. Because the energy of the emitted light dissipates from the substrate, the efficiency of the Joule heating decreases. Consequently, a unique spatial distribution of dopants is automatically formed. Then, for operation, the light to be modulated is input to the device, as shown in Fig. 1(a), and only the surface current is injected into the device. Via this surface current, the magnetic fields are injected into the device substrate. The fields interact with the created DPPs by the input light, and then the corresponding photons, with some modulation by the fields, are emitted. Polarization-modulated light is then obtained as a macroscale optical output. Notably, the polarization modulation is controllable by several experimental conditions of DPP annealing. As a characteristic demonstration, we focused on the wavelength dependency of the polarization modulation. As Fig. 1(b) shows, the Verdet constants of the device before annealing, which indicate the strength of the magneto-optical effect, are 3.47×10^4 and 1.68×10^4 rad/T·m at wavelengths of 457 and 532 nm, respectively. Following annealing using $\lambda = 532$ nm of light, the Verdet constant with only $\lambda = 532$ nm was increased to 4.75×10^4 rad/T·m.

These findings can clarify the nanoscale mechanism behind the novel polarization modulation, which is expected to result from nanoquantum interactions between the magnetic fields and DPPs. This a topic that has not been discussed in detail. In future research, we will implement a SiC device designed for a compact application system that relies solely on this device for development.

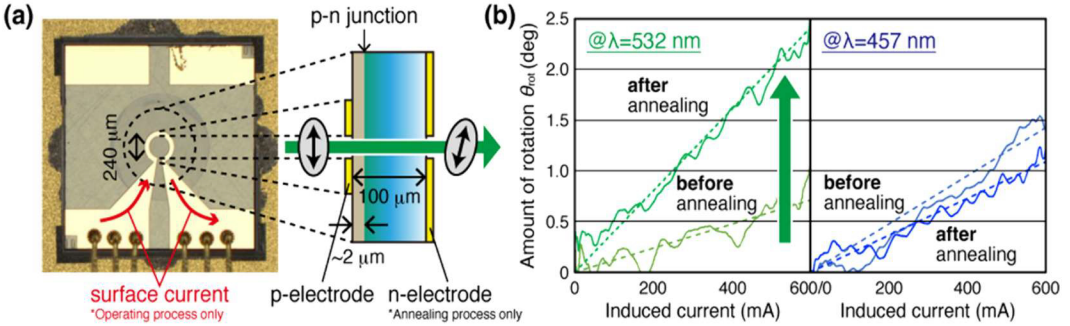

Fig. 1 (a) Appearance (left) and cross section (right) of the SiC device. (b) Comparison of polarization rotation angle θ_{rot} relative to the injected current between $\lambda = 532$ nm and $\lambda = 457$ nm optical inputs.

We thank Prof. Motoichi Ohtsu of the Research Origin for Dressed Photons and Dr. Tadashi Kawazoe at NICHIA for several important discussions, as well as Mr. Takuya Kadowaki at NICHIA for providing the SiC devices. This study was supported by JSPS KAKENHI (Grant No. JP22H04952).

References

[1] M. Ohtsu, *Nanophotonics* **1**, 83–97 (2012).
[2] T. Kadowaki, T. Kawazoe, M. Ohtsu, *Sci. Rep.* **10**, 12967 (2020).

Spectral-Polarization-Selective Magneto-Optical Effect by Al-doped 4H-SiC Device with DPP-Assisted Annealing

Haoze Du[1]*, Takuya Kadowaki[2], Naoya Tate[1], Tadashi Kawazoe[2], Yuji Oki[1], Motoichi Ohtsu[3], Kenshi Hayashi[1]

1. Graduate School and Faculty of Information Science and Electrical Engineering, Kyushu University, 744 Motooka, Nishi-ku, Fukuoka 819-0395, Japan

2. Nichia Corporation, 3-13-19 Moriya-cho, Kanagawa-ku, Yokohama, Kanagawa, 221-0022, Japan

3. Research Origin for Dressed Photon, 3-13-19 Moriya-cho, Kanagawa-ku, Yokohama, Kanagawa, 221-0022, Japan

**duhaoze@laserlab.ed.kyushu-u.ac.jp*

Abstract: An Al-doped 4H-SiC device exhibits a large Verdet constant at a specific wavelength and polarization state via DPP-assisted annealing under the corresponding conditions. Thus, it can function as a novel MO-SLM for high-performance spectroscopic systems. © 2022 The Author(s)

1. Introduction

The magneto-optical (MO) effect has been applied in many fields of modern optics, including optical information and optical communications, owing to the modulation of the phase of the light by inducing an external magnetic field on a specific material [1]. Recently, we reported a novel polarization rotator by doping Al atoms into 4H-SiC crystal and performing dressed-photon-phonon- (DPP)-assisted annealing, which produces a larger MO effect with a Verdet constant of 9.51×10^4 rad/T·m at a wavelength of 450 nm, while maintaining a high transmittance of 99.3% [2]. In particular, the device does not require external magnetic fields, only local magnetic fields caused by surface currents induce the MO effect.

The MO effect is induced by parallel spins in clusters of doped Al atoms that are formed by dressed-photon-phonon (DPP)-assisted annealing [3]. During annealing, a bias voltage was applied to the crystal to provide Joule heating for the thermal diffusion of the Al dopants, while the crystal was simultaneously irradiated with nonabsorbable laser light. Consequently, an optimal spatial distribution of Al clusters was established [2]. The distribution, photons, electrons, and phonons in the crystal create a novel quantum field, which is defined as the DPP [4]. The distribution of Al clusters varied according to the experimental conditions of annealing, such as the wavelength and polarization of the laser light. Therefore, the polarization rotation is expected to depend on the wavelength and polarization of the input light. To verify this hypothesis, we prepared multiple devices under various annealing conditions and examined the wavelength and polarization state dependence of the Verdet constants. Furthermore, based on the results, a characteristic physical model of the phase modulation in the device was clearly identified.

2. Experiment

In this study, SiC devices, whose width and length were 2 mm and thickness was 100 μm were prepared, as shown in Fig. 1 (b). Al atoms were doped with injection concentration of 1×10^{19} cm^{-3} and depth of 600 nm. During DPP-assisted annealing, a forward bias voltage of 22 V (current density: 0.6 A/cm^2) was applied to the devices that were irradiated by a 532 nm laser (optical power: 14 mW). A crossed Nichols setup was prepared, as shown in Fig. 1 (a), to verify the MO properties of the devices. The device was placed in the crossed Nichols setup to be irradiated by linearly polarized light and obtain a component of polarization-rotated light through the device. The optical intensity V_{pmt} of the light was measured using a photomultiplier tube. The amount of polarization rotation θ_{rot} was deduced by calculating the change of the intensity V_{pmt}, as $V_{pmt}=I(1-\cos2\theta_{rot})/2$. The Verdet constant v of the device was calculated by $\theta_{rot}=Bvd$, where B and d denote the magnetic induction and length of the interaction distance, respectively.

The results are shown in Fig. 2. The Verdet constants of the device before annealing are 3.14×10^4 rad/T·m and 1.80×10^4 rad/T·m at wavelengths of 457 nm and 532 nm, respectively. After annealing using a wavelength of 532 nm, the Verdet constants at 457 nm and 532 nm increased to 3.29×10^4 rad/T·m and 5.57×10^4 rad/T·m, respectively. Thus, the Verdet constant clearly increases at the same wavelength of light as that used for annealing.

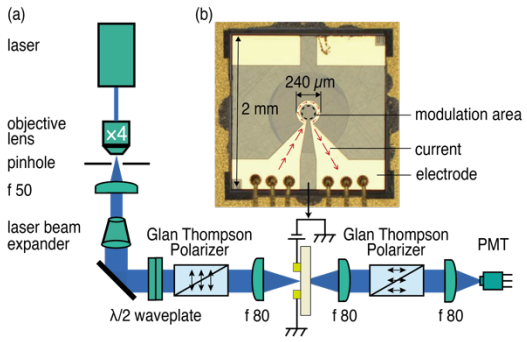

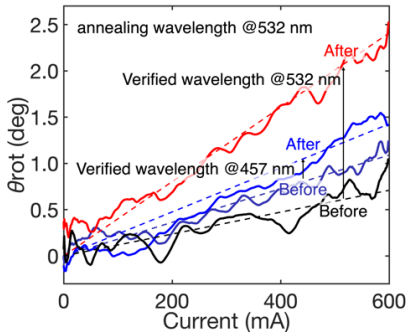

Fig. 1. (a) Experimental setup evaluating the MO property of the SiC device, (b) appearance of the device. Fig. 2. Polarization rotation angle θ_{rot} relative to the amount of surface current.

3. Discussion

The significant increase in the Verdet constant at specific wavelengths is related to the autonomous spatial distribution of the Al clusters, which exhibits consistent separation. During the DPP-assisted annealing, the phonons localized in the Al clusters exchange momentum with the electrons due to the creation of DPP, and then emit photons. Specifically, the photons can be emitted when the momentum (h/a) between the electrons in conduction band and the positive holes in valence band is equal to the total momentum of the phonons (h/na) localized in the Al clusters with a separation of d=na [5]. Since the photons emitted so that the Joule energy is consumed to form the Al clusters of the same separation. Moreover, the photons emitted with the same energy as the irradiated light during the DPP-assisted annealing, such uniformly spaced Al clusters can efficiently create DPP when irradiated light at the same wavelength and induce an increase in the Verdet constant.

4. Conclusion

In this study, we demonstrated for the first time the relationship between wavelength and the Verdet constant before and after annealing at various wavelengths to determine the range and resolution of the spectral selectivity in the Verdet constants. Future research endeavors will focus on elucidating the relationship between DPP-assisted annealing conditions and the spectral selectivity of Verdet constants. This understanding will be used to design a SiC device that can be applied in spectroscopic systems. Such SiC devices can be used to construct thin, small, pixelized current-controlled MO-SLMs suitable for higher-performance spectroscopic systems.

This study was supported by JSPS KAKENHI (Grant No.: JP22H04952).

5. References

[1] K.J. Carothers, R.A. Norwood, J. Pyun, “High Verdet constant materials for magneto-optical Faraday rotation: A review,” Chem. Mate. 34.6, 2531-2544 (2022).
[2] T. Kadowaki, T. Kawazoe, M. Ohtsu, “SiC transmission-type polarization rotator using a large magneto-optical effect boosted and stabilized by dressed photons,” Sci. Rep. 10, 12967 (2020).
[3] B. Song, *et. al.*, “Observation of glassy ferromagnetism in Al-doped 4H-SiC,” J. Am. Chem. Soc. 131, 1376–1377 (2009).
[4] M. Ohtsu, “Dressed photon technology,” Nanophotonics 1, 83–97 (2012).
[5] M. Ohtsu, T. Kawazoe, Advanced Materials Letters 10.12 (2019): 860-867

[III] REVIEW PAPERS

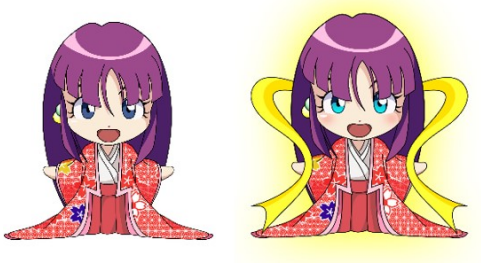

Nanoarchitectonics
http://ojs.wiserpub.com/index.php/NAT/

UNIVERSAL WISER PUBLISHER

Research Article

Perspective on an Emerging Frontier of Nanoscience Opened up by Dressed Photon Studies

Hirofumi Sakuma*, **Izumi Ojima**, **Motoichi Ohtsu**

Research Origin for Dressed Photon (RODreP) Yokohama, Kanagawa 221-0022, Japan
E-mail: sakuma@rodrep.or.jp

Received: 30 November 2022; **Revised:** 12 January 2023; **Accepted:** 28 February 2023

Abstract: The core parts of developing dressed photon (DP) research that require advanced knowledge of highly mathematical quantum field theory and their potentially important impacts on the wide spectrum of long-term scientific activities in general, not necessarily restricted to those in the natural science sector, are succinctly explained in this article. Although a considerable number of remarkable technological achievements in the field of nanophotonics have been attained by utilizing DP phenomena, from the theoretical viewpoint, they remain enigmatic, as in the case of dark matter and energy in cosmology. Under such circumstances, an intriguing working hypothesis (WH) for DPs is proposed by the authors of this article through a combination of Ojima's micro-macro duality theory and the Greenberg-Robinson theorem, claiming that the space-like momentum contribution is an inevitable element for quantum field interactions to occur. Note that, as the Schrödinger's cat thought experiment clearly shows, the widespread common quantum mechanics knowledge is incapable of explaining how the invisible quantum world is connected to our familiar visible classical world. In the above-mentioned WH, the main reason why we cannot explain either DPs or dark entities in cosmology is shown to have roots in the fact that the prevailing theories have not revealed an important role of spacelike momentum in connecting the quantum and classical worlds. Our new WH further shows that the entire universe is connected by an instantaneous spacelike entropic spin network, as in the case of quantum spin entanglement explained in mainstream physics. Since such a network may have a close relation with the nonlocal consciousness field, which seems to be the final frontier of physics, our perspective on such a possibility is briefly given in the final section of this paper.

Keywords: dressed photon, silicon light-emitting devices, micro-macro duality, off-shell quantum field, dark energy, dark matter, twin universes

Nomenclature

AI	Artificial intelligence
B	Boron
CC	Cross-correlation coefficient
CCC	Conformal cyclic cosmology
CP	Clebsch parameterization

DOI: https://doi.org/10.37256/nat.5120243508

CW	Continuous wave
DHR	Doplicher-Haag-Roberts
DP	Dressed photon
EPR	Einstein-Podolsky-Rosen
FWHM	Full-width at half-maximum
GNS	Gel'fand-Naimark-Segal
GR	Greenberg-Robinson
KG	Klein-Gordon
LED	Light-emitting diode
LSZ	Lehmann-Symanzik-Zimmermann
MMD	Micro-macro duality
NDE	Near-death experience
NL	Nakanishi-Lautrup
nm	Nanometer
NPi	ith-nanoparticle when i is attached to NP
PB	Photon breeding
PCVD	Photochemical vapor deposition
PMMA	Polymethyl methacrylate
PP	Psi phenomenon
QED	Quantum electrodynamics
QFT	Quantum field theory
QM	Quantum mechanics
SCSB	Simultaneous conformal symmetry breaking

1. Introduction

The aim of this article is to disseminate an important implication of dressed photon (DP) research [1], initiated by an inspired vision of the third author (M. O.) around the beginning of the 1990s, in the context of the progress to be made in many fields of natural and social sciences. A DP is an experimentally identifiable subtle electromagnetic field manifesting in a spherical form whose diameter varies in the range of less than several tens of nanometers (nm). Without exception, a DP is generated around a point-like singularity, such as the tip of an optical fiber or an impurity atom embedded in a given uniform medium. Figure 1 shows typical situations in which DPs can be generated.

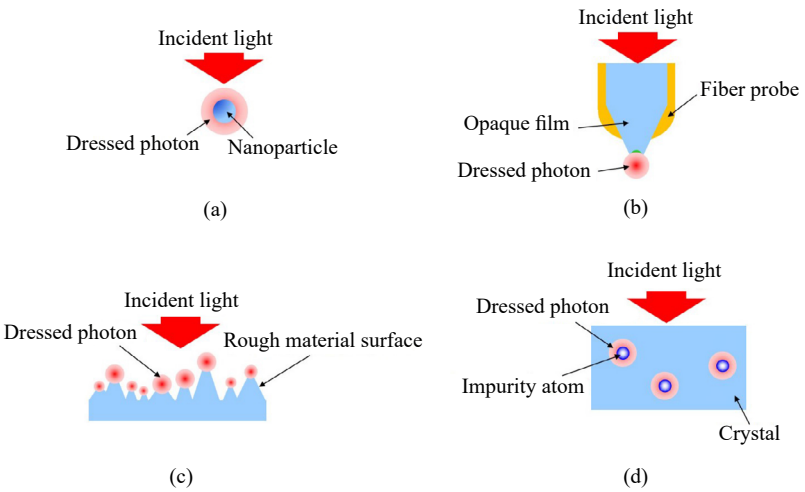

Figure 1. Experimental methods for generating DPs: (a) on a nanometer-sized particle; (b) on the tip of a fiber probe; (c) on bumps of a rough material surface; (d) on impurity atoms in a crystal

Responding to the demands of the times, during the first decade of this century, DP studies [2] created a new history in the field of optics. However, this rise of the DP research movement did not attract as much attention as one would think since DP phenomena are quite elusive in the sense that no existing theory can explain the generation mechanism. In some references, DP phenomena are described as well-known evanescent light fields, but we strongly support the view that these are quite different entities, namely, the former are generated by nonlinear light-matter field interactions, while the latter are boundary-trapped electromagnetic fields satisfying the linear Maxwell equation.

To understand why we cannot have a satisfactory theory of DP phenomena, first, we have to know the present status of quantum physics. Since many of the potential readers of this journal would not be experts in the field of advanced quantum field theory (QFT), giving the positioning of our targeted problem (the difficulty of formulating DP theory) in the Big Picture of QFT would be quite helpful. Actually, the difficulty arises from the disciplinary fragmentation existing between classical and quantum physics. The great and spectacular progress in quantum physics achieved in the 20th century made us regard classical physics as a somewhat obsolete discipline compared to quantum physics, which naturally led us to believe that the laws of quantum physics are the "genuine" physical laws, while those of classical physics are not exactly correct but approximate laws.

In fact, in standard physics textbooks, finding a simple explanatory phrase stating that electromagnetic waves are not longitudinal seems to be not rare, despite the fact that the existence of such longitudinal waves was reported, although not frequently, in eminent literature, for instance, Physical Review [3]. Recall that in "advanced" quantum electrodynamics (QED), through the process [4] of quantizing the electromagnetic field, the longitudinal mode is eliminated as an intangible and unobservable mode. We think that we often find the abovementioned phrase in physics textbooks because of a strong influence from the "advanced" QED without paying any attention to the "obsolete" classical physics. This being the case, borrowing a geological terminology, we can say that there exists a sharp made-up "theoretical fault" to be cleared at the dynamic boundary of the two realms of quantum and classical electromagnetism.

We believe that the ill effect of this "theoretical fault" is not restricted to electromagnetism but seems to widely penetrate into a considerable number of disciplines in physical sciences studying phenomena occurring at the boundary of the quantum and classical worlds. The widespread problem of the Schrödinger's cat thought experiment referred to in the abstract must be a well-known example. The endeavor to remove the "theoretical fault" is regarded as consistent integration of the quantum and classical worlds, and the micro-macro duality (MMD) [5, 6] theory to be explained here is a unique proposal aiming at such consistent integration of the quantum and classical worlds. The term consistent integration of different fields represents our central theme of the perspective we are going to explain in this article.

For those who do not have any prior knowledge of DPs, in section 2, we start our main discussion by briefly explaining DP phenomena and associated prominent technologies. To give a concise and lucid "bird's eye view"-type picture of the present status of QFT, namely, the aforementioned "Big Picture" of QFT, we will explain the essence of MMD theory in section 3, which plays a key role in our theoretical discussions. Then, in section 4, we will extend our discussion first to a spacelike Maxwell electromagnetic field and will discuss a novel heuristic model of DPs. In the final section 5, after briefly touching on a novel cosmology that is least expected from DP studies, an ambitious perspective on a possible connection between the "instantaneous" spacelike off-shell quantum field and yet-to-be-defined nonlocal consciousness field is tentatively given. Since consciousness is much more elusive than DPs and it has not gained "citizenship" in the world of physical sciences, our discussion on consciousness is not given from the viewpoint of pro and con arguments but from an advocate position.

2. A brief overview of DP phenomena and technologies

Numerous research papers and monographs describing the details of various DP experiments have been published thus far by the third author M. O. In this section, among others, we will give brief commentaries on ten highlighted phenomena that cannot be explained within the conventional framework of optics. The existence of these phenomena serves as an underlying motive of our novel research that we call "off-shell science", the present status of the theoretical construction of which is given in the subsequent sections 3 and 4, together with the reason why we call it "off-shell science", while the term "on-shell science" is reserved for the conventional framework. The list of ten phenomena is as follows:

1. The DP energy transfers back and forth between the two nanoparticles (NPs). (cf. Ch. 1 of [1] and [7])

2. The DP field is conspicuously disturbed and demolished by the insertion of NP_2 for detection. (cf. Ch. 1 of [7])
3. The efficiency of the DP energy transfer between the two NPs is the highest when the sizes of the NPs are equal. (cf. [8])
4. An electric-dipole-forbidden transition is allowed. (cf. Ch. 3 of [1])
5. The DP energy autonomously transfers among NPs. (cf. [9])
6. The irradiation photon energy $h\nu$ can be lower than the excitation energy of the electron E_{excite}. (cf. [10])
7. The maximum size $a_{(DP, Max)}$ of the DP is 40-70 nm. (cf. [11])
8. The spatial distribution of Boron (B) atoms varies and autonomously reaches a stationary state due to DP-assisted annealing, resulting in strong light emission from the Si crystal. (cf. Ch. 2 of [12])
9. The length and orientation of the B atom pair in the Si crystal are autonomously controlled by DP-assisted annealing. (cf. Ch. 3 of [12])
10. A light-emitting device fabricated by DP-assisted annealing exhibits photon breeding (PB) with respect to the photon energy, i.e., the emitted photon energy $h\nu_{em}$ is equal to the photon energy $h\nu_{anneal}$ used for the annealing. (cf. Ch. 1 and Ch. 3 of [12])

2.1 *Creation and detection of dressed photons*

A DP field is created in a complex system composed of photons and electrons (or excitons) in an NP (Figure 1(a)). This means that the photon "dresses" the exciton energy, and thus, this field was named a DP [13]. As an example of further dressing of the material energy, coupling between a DP and a phonon has been found.

To detect the DP that is created and localized on NP_1, the DP must be converted to propagating scattered light. This can be performed by inserting NP_2 into the DP field. Propagating scattered light is created by this insertion, and it reaches a photodetector in the far field, where it is detected. Although NP_1 and NP_2 may be considered a light source and a detector in this process, one should note the following two phenomena:

Phenomenon 1: The DP energy transfers back and forth between the two NPs.

Phenomenon 2: The DP field is conspicuously disturbed and demolished by the insertion of NP_2 for detection.

Furthermore, the following phenomenon was also found [8].

Phenomenon 3: The efficiency of the DP energy transfer between the two NPs is the highest when the sizes of the NPs are equal.

This phenomenon was named size-dependent resonance. Although the long-wavelength approximation has been popularly used in conventional optical scientific studies on light-matter interactions, it is invalid in the case of a DP because the spatial extent of a DP is much smaller than the wavelength of light. Due to this invalidity, the following phenomenon was found.

Phenomenon 4: An electric-dipole-forbidden transition is allowed.

The results of the above basic studies have ingeniously contributed to the realization of innovative generic technologies. For example, nanometer-sized optical functional devices were developed by using semiconductor NPs. They have enabled transmission and readout of optical signals via DP energy transfer and subsequent dissipation. Practical NOT logic gate and AND logic gate devices operated at room temperature have been fabricated by using InAs NPs [14]. The advantages include their superior performance levels and unique functionality, such as single-photon operation [15], extremely low energy consumption [16], and autonomous energy transfer [9]. These advantages originate from the unique operating principles of DP devices achieved by exploiting Phenomena 3 and 4. Furthermore, an inherent phenomenon was used for device operation.

Phenomenon 5: The DP energy autonomously transfers among NPs.

A non-von Neumann-type computing system has been proposed by using DP devices [17]. The ability to solve a decision-making problem [18] and an intractable computational problem [19] has been demonstrated.

The following two sections review two more examples of these technologies and present novel phenomena that originate from the intrinsic nature of DPs.

2.2 *Nanofabrication technology*

This part starts by reviewing an example of nanofabrication technology that uses a fiber probe (Figure 1(b)) or an

aperture for creating a DP. Next, a more practical technology is reviewed, in which neither a fiber probe nor an aperture is required.

2.2.1 *Technology using a fiber probe or an aperture*

This part reviews photochemical vapor deposition (PCVD) that involves molecular dissociation by a DP and subsequent deposition of the dissociated atoms on a substrate. $Zn(C_2H_5)_2$ was adopted as a specimen molecule. A DP was created on the tip of a fiber probe by irradiating the end of the fiber probe with light. Gaseous $Zn(C_2H_5)_2$ molecules, filled in a vacuum chamber, dissociated when these molecules moved into the DP field. The dissociated Zn atoms subsequently landed on a substrate and were adsorbed on the substrate. By repeating these processes, the number of adsorbed Zn atoms increased, resulting in the deposition of Zn atoms and the formation of a nanometer-sized metallic Zn-NP on the substrate.

For comparison, the wavelength in the case of dissociating $Zn(C_2H_5)_2$ molecules by using conventional propagating light had to be shorter than 270 nm (photon energy = 4.59 eV) to excite an electron in the $Zn(C_2H_5)_2$ molecule. By noting this requirement, the following ingenious contrivances (i) and (ii) were employed to confirm that the $Zn(C_2H_5)_2$ molecules were dissociated by the above DP.

(i) The wavelength of the propagating light for creating the DP was set longer than 270 nm. However, the $Zn(C_2H_5)_2$ molecules were expected to be dissociated by the DP on the tip due to the following phenomenon.

Phenomenon 6: The irradiation photon energy $h\nu$ can be lower than the excitation energy of the electron E_{excite}.

That is, since the created DP is the quantum field accompanying the energies of the excitons (E_{excite}) and phonons (E_{phonon}) at the tip of the fiber probe, its energy is expressed as $h\nu_{DP} = h\nu + E_{excite} + E_{phonon}$. Thus, even though $h\nu < E_{excite}$, the DP energy $h\nu_{DP}$ can be greater than E_{excite} [10].

(ii) The $Zn(C_2H_5)_2$ molecules were replaced by $Zn(acac)_2$ molecules [20]. $Zn(acac)_2$ is a well-known optically inactive molecule that has never been shown to be dissociated by propagating light. However, from **Phenomenon 4**, the possibility of it being dissociated by the DP was expected.

Figures 2(a) and 2(b) show images of Zn-NPs formed on sapphire substrates by dissociating $Zn(C_2H_5)_2$ molecules [10]. The wavelengths of the propagating light for creating the DP were as long as 684 nm and 488 nm. Figure 2(c) shows an image of a Zn-NP for which $Zn(acac)_2$ molecules were used [20]. The wavelength of the propagating light for creating the DP was 457 nm.

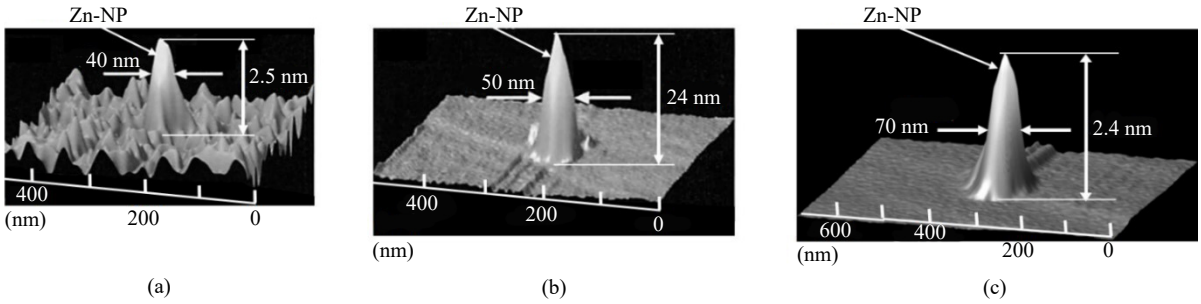

Figure 2. Shear-force microscopic images of Zn-NPs formed on sapphire substrates. The dissociated molecules are $Zn(C_2H_5)_2$ ((a) and (b)) and $Zn(acac)_2$ (c). The wavelengths of the propagating light for creating the DP are 684 nm (a), 488 nm (b), and 457 nm (c).

The maximum size $a_{(DP, Max)}$ of the DP was estimated from the above experimental results [11]. For this estimation, the increasing rate R of the full-width at half-maximum (FWHM) of the formed Zn-NP was measured [21].

The measured results showed that R was the maximum when the FWHM was equal to the tip diameter $2a_P$ of the fiber probe (a_P = 4.4 nm: tip radius). This was due to the size-dependent resonance of the DP energy transfer between the tip of the fiber probe and the formed Zn-NP (**Phenomenon 3**). Although a further increase in the deposition time increased the FWHM, R decreased to zero. Finally, the FWHM saturated. Figure 2 shows the profiles acquired after this saturation.

The FWHMs in Figure 2 were 40-70 nm. They were independent of the tip diameter, the wavelength and power of

the light used for irradiating the end of the fiber probe, and the species of molecules used. Since the spatial profile and size of the DP transferred from the tip of the fiber probe corresponded to those of the NP deposited on the substrate, the FWHMs in Figure 2 indicate the following phenomenon.

Phenomenon 7: The maximum size $a_{(DP, Max)}$ of the DP is 40-70 nm.

By using the above PCVD technology, a variety of two-dimensional patterns were formed by scanning a fiber probe [22]. To increase the working efficiency for pattern formation, a novel lithography technology was developed in which the fiber probe was replaced by a two-dimensional photomask [23]. A fully automatic practical photolithography machine was developed and used to form a diffraction grating pattern with a half pitch as narrow as 22 nm [24]. It also produced a two-dimensional array of the nanometer-sized optical devices reviewed in subsection 2.1 [25] and practical devices for soft X-rays (a Fresnel zone plate [26] and a diffraction grating [27]).

2.2.2 *Technology that uses neither fiber nor aperture*

This part reviews a technology for autonomous smoothing of a material surface that requires neither fiber probes nor apertures. The material to be smoothed is installed in a vacuum chamber, and the chamber is filled with gaseous molecules. By irradiating the material surface with light, DPs are created at the tips of the bumps on the rough material surface (Figure 1(c)). That is, the bumps play the role of fiber probes for creating DPs. If the molecules move into the DP field, they are dissociated. The chemically active atoms created as a result of this dissociation selectively etch the tips of the bumps away, while the flat part of the surface remains unchanged. The etching autonomously starts upon light irradiation, and the surface roughness gradually decreases as etching progresses. The etching autonomously stops when the bumps are annihilated and the DPs are no longer created.

The disc surface of a synthetic silica substrate (30 mm diameter) was etched by using gaseous Cl_2 molecules. Although light with a wavelength shorter than 400 nm was required for conventional photodissociation, the present method used visible light with a wavelength of 532 nm based on **Phenomenon 6**. Etching by active Cl atoms decreased the surface roughness to as low as 0.13 nm. A laser mirror was produced by coating a high-reflection film on the smoothed substrate surface. Its damage threshold for high-power ultraviolet laser light pulses was evaluated to be as high as twice that of the commercially available strongest mirror whose substrate surface was polished by a conventional chemical-mechanical polishing technology [28].

Gaseous O_2 molecules can also be used for autonomous etching because the O atoms created by dissociation are chemically active. The advantage is that etching can be carried out in atmospheric conditions by using O_2 molecules in air, and thus, a vacuum chamber is not required. Figure 3(a) shows the experimental results of etching a plastic polymethyl methacrylate (PMMA) surface [29]. Although ultraviolet light with a wavelength shorter than 242 nm was required for the conventional photodissociation of O_2 molecules, light with a longer wavelength λ_{DP} = 325 nm was used here due to **Phenomenon 6**. For comparison, Figure 3(b) shows the result of etching using conventional photodissociation, for which the wavelength $\lambda_{\text{Conventional}}$ of the light used was as short as 213 nm.

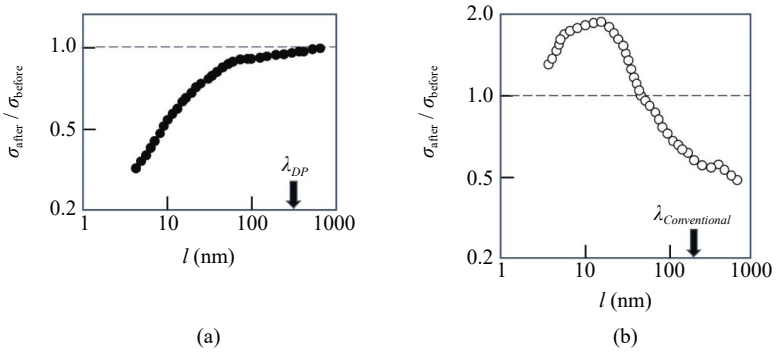

Figure 3. Ratio of the standard deviation of the roughness of the PMMA surface before and after etching. (a) and (b) are the results acquired by illuminating the surface with light with a wavelength of λ_{DP} = 325 nm and $\lambda_{\text{Conventional}}$ = 213 nm, respectively. The downward arrows represent the values of l that are equal to the above wavelengths.

In Figures 3(a) and 3(b), the surface roughness was evaluated from its standard deviation $\sigma(l)$. The horizontal axis l represents the period of the roughness of the surface. The vertical axis represents the ratio $\sigma_{after}/\sigma_{before}$ between the $\sigma(l)$ values before (σ_{before}) and after (σ_{after}) etching [29]. Figure 3(a) shows that $\sigma_{after}/\sigma_{before} < 1$ in the range $l < \lambda_{DP}$, through which the contribution of the subwavelength-sized DP is confirmed. A drastic decrease in $\sigma_{after}/\sigma_{before}$ can be observed in the range $l <$ 40-70 nm, which again confirms **Phenomenon 7** regarding the maximum size of the DP. In contrast to Figure 3(a), Figure 3(b) shows that $\sigma_{after}/\sigma_{before} < 1$ in the range $l > \lambda_{Conventional}$. This means that the etching was effective only in the superwavelength range.

Since DPs are always created at the tips of the bump on the material surface under light irradiation, the present autonomous etching has been applied to smoothing of a variety of surfaces and materials: the side surface of a diffraction grating [30], the surface of a photomask used for conventional ultraviolet lithography [31], and the surfaces of GaN crystals [32], transparent ceramics [33], and diamonds [34].

2.3 *Silicon light-emitting devices*

Crystalline Si has long been a key material supporting the development of modern technology. However, because Si is an indirect-transition-type semiconductor, it has been considered to be unsuitable for light-emitting devices. The momentum conservation law requires an interaction between an electron-hole pair and phonons for radiative recombination. However, the probability of this interaction is very low. Nevertheless, Si has been the subject of extensive study for the fabrication of light-emitting devices [35, 36]. The above problems have been solved by using DPs because the phonons in a DP can provide momenta to the electron to satisfy the momentum conservation law [37, 12]. For device fabrication, DPs were created by irradiating a Si crystal with light. For device operation, DPs were created by electronic excitation.

For fabrication, an As atom- or Sb atom-doped n-type Si substrate was used. As the first step, the substrate surface was transformed to a p-type material by implanting B atoms, forming a p-n homojunction. Metallic films were coated on the substrate surface to serve as electrodes. As the next step, this substrate was processed by a fabrication method named DP-assisted annealing. Joule heat was generated by current injection, which caused the B atoms to diffuse. During this Joule annealing, the substrate surface was irradiated with light (wavelength λ_{anneal} = 1.342 μm). Because its photon energy $h\nu_{anneal}$ (= 0.925 eV) was sufficiently lower than the bandgap energy E_g (= 1.12 eV) of Si, the light could penetrate into the Si substrate without suffering absorption. Then, the light reached the p-n homojunction to create a DP on an impurity B atom (Figure 1(d)). The phonons in the created DP could provide momenta to a nearby electron to satisfy the momentum conservation law, resulting in stimulated emission of light. The emitted light propagated from the crystal to the outside, which indicated that part of the Joule energy used for diffusing B atoms was dissipated in the form of optical energy, resulting in local cooling that locally decreased the diffusion rate. As a result, through the balance between heating via the Joule energy and cooling via the stimulated emission, the spatial distribution of B atoms varied and autonomously reached a stationary state. This stationary state was expected to be the optimum for efficient creation of DPs and for efficient light emission because the probability of spontaneous emission was proportional to that of the stimulated emission described above. After DP-assisted annealing, the Huang-Rhys factor, a parameter representing the magnitude of the coupling between electron-hole pairs and phonons, was experimentally evaluated to be 4.08 [38]. This was 10^2-10^3 times higher than that before DP-assisted annealing.

The above fabricated device was operated as a light-emitting diode (LED) by simple current injection. By injecting a current of 3.0 A into the device with an areal size of 0.35 mm by 0.35 mm, a continuous wave (CW) output optical power as high as 2.0 W was obtained at a substrate temperature of 77 K. A power as high as 200 mW was obtained at room temperature (283 K) [39]. These results confirmed that the following phenomenon occurs.

Phenomenon 8: The spatial distribution of B atoms varies and autonomously reaches a stationary state due to DP-assisted annealing, resulting in strong light emission from the Si crystal.

Note that the photon energy emitted from conventional LEDs is governed by E_g. However, for the present Si-LED, the light emission spectra acquired at a temperature of 283 K and an injection current of 2.45 A [39] clearly showed a high spectral peak $h\nu_{em}$ at $E_g - 3E_{phonon}$, where E_{phonon} is the phonon energy. The origin of this spectral peak was attributed to the spatial distribution of B atoms that was autonomously controlled during DP-assisted annealing [40]. The measured three-dimensional spatial distribution of B atoms at the p-n homojunction indicated that the B atoms were apt to form pairs with a length $d = 3a$ (a is the lattice constant of the Si crystal (= 0.54 nm)) and that the formed pairs

were apt to orient along a plane parallel to the top surface of the Si crystal [41]. That is, the following phenomenon was found.

Phenomenon 9: The length and orientation of the B atom pair in the Si crystal are autonomously controlled by DP-assisted annealing.

Note that the required phonon momentum must be h/a for radiative recombination of the electron (at the bottom of the conduction band at the X-point in reciprocal space) and the positive hole (at the top of the valence band at the Γ-point) to occur. Since the phonon momentum is $h/3a$ when $d = 3a$, the DP created and localized at this B atom pair provides the momenta of three phonons to the electron. As a result, hv_{em} is expressed as $E_g - 3E_{phonon}$, and its value is 0.93 eV (E_{phonon} = 65 meV), which is nearly equal to the photon energy hv_{anneal} (= 0.95 eV) irradiated during DP-assisted annealing. This indicates that the irradiated light served as a breeder that created a photon with energy $hv_{em} = hv_{anneal}$ and manifested the following phenomenon.

Phenomenon 10: A light-emitting device fabricated by DP-assisted annealing exhibits photon breeding (PB) with respect to the photon energy; i.e., the emitted photon energy hv_{em} is equal to the photon energy hv_{anneal} used for the annealing.

PB was also observed with respect to the photon spin. That is, the polarization direction of the emitted light was identical to that of the light irradiated during DP-assisted annealing [41].

The fabricated Si-LED was demonstrated to work as a relaxation oscillator upon injection of a direct current, yielding an emission pulse train [42]. As an advanced version of this experiment, the 2nd-order cross-correlation coefficient (CC) was measured to evaluate the photon statistical features of the emission from small light spots on the device surface, which took the form of a pulse train (duration and repetition frequency of 50 ps and 1 GHz, respectively) [43]. Figure 4 shows the value of the CC evaluated by a Hanbury Brown-Twiss experimental setup [44]. It presents two features. One is that the CC is smaller than unity in the range of time difference of the measurements by two independent detectors $|\tau| < 20$ ns. This indicates the photon antibunching phenomenon that is an inherent feature of a single photon. The other feature is that the CC takes a nonzero value at $\tau = 0$, although it is less than 1×10^{-2}. This small nonzero value is attributed to the photons generated from multiple light spots located in close proximity to each other on the Si-LED surface.

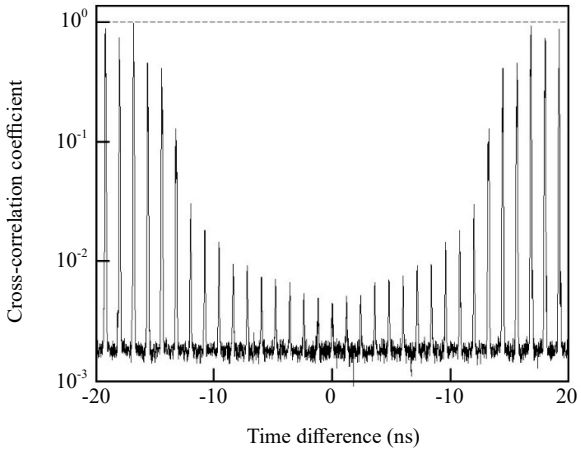

Figure 4. Second-order CC measured as a function of the time difference of the measurements by two independent detectors

These two features suggest the possibility that an emitted cluster of photons behaves as if it is a single photon. This possibility can be conjectured to be related to the localizable property of the spin-zero particle we noted [43] in relation to the Wightman theorem [45]. Namely, if the observable positions of given spin-zero quantum particles are sufficiently close, then the cluster of these particles would behave as if it is a single quantum particle with the accumulated amount of energy.

At the end of this section, the fact that Si lasers have also been fabricated by DP-assisted annealing should be briefly reviewed. One example is a CW single-mode laser with a ridge waveguide structure of 500 μm length operated

under room temperature (Figures 5(a) and 5(b)) [46]. Another example is a similarly operated quasi-CW multi-mode high-power laser (maximum output power = 100 W) with a long cavity (30 mm length) (Figure 5(c)) [7, 47]. PB was also observed for these devices.

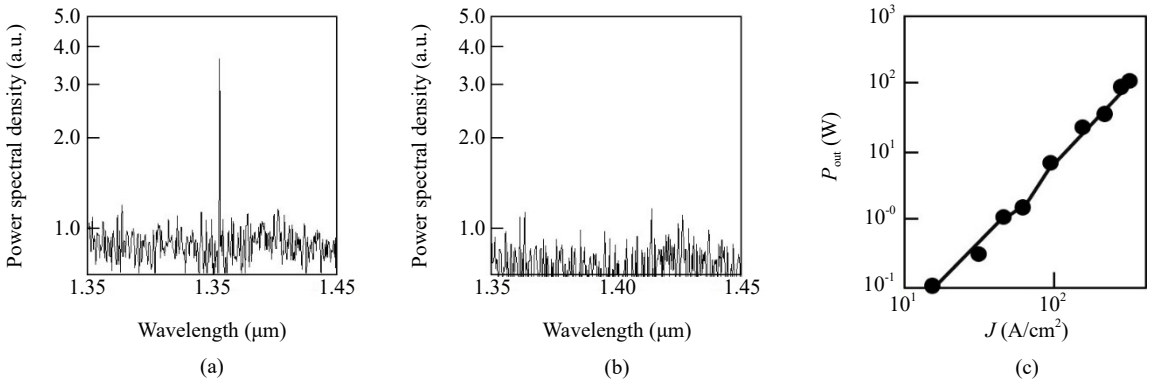

Figure 5. Light emission spectra and output optical power of Si lasers. (a) and (b) Single-mode laser: spectral profiles above (injected current density J = 42 A/cm^2) and below (J = 38 A/cm^2) the threshold, respectively. The threshold current density Jth is 40 A/cm^2. (c) High-power laser: Relation between J and the output optical power.

3. On the essence of micro-macro duality theory

3.1 *From macro to micro as an inductive approach*

We can safely say that for the majority of researchers in the fields of physics and engineering, except for experts in theoretical or mathematical physics, knowledge of QFT must be foreign to them, even though they are familiar with the standard framework of quantum mechanics (QM), where the state and associated physical quantities of a given quantum system are represented by a unit vector and self-adjoint operators defined on the Hilbert space $\mathfrak{H}$, respectively. The aim of this and the following subsections is therefore twofold: to clarify the important difference between QM and QFT and to plainly explain MMD theory, which adopts a methodology of algebraic formulation of the relativistic quantum field. Since these two subjects are highly mathematical in nature, we will explain the basic outline of their conceptual structures without touching on the sophisticated mathematics involved.

The fundamental framework of QFT consists of a couple of elemental concepts, namely, the quantum observable, which characterizes a given micro quantum system, and the quantum state, which determines the way in which the former manifests itself macroscopically. The aim of QFT as a physical theory is to explain how the structural interdependent relation changes in four-dimensional spacetime, which is called the dynamics of the system. In considering the characteristics of the quantum observable and quantum state, noting that these concepts are not directly recognizable concepts through visible phenomena in the macro classical world is particularly important. To appreciate their realistic meanings, we will inevitably employ analogies with classical physics (called the quantum-classical correspondence) together with the correct understanding of measurement processes.

The related important aspect of the quantum field is the fact that, unlike the classical field, not all of it is observable. In the algebraic QFT with which MMD theory is described, the quantum field is investigated through the associated noncommutative algebra $\mathfrak{F}$, and an observable is shown to be an element of a certain partial ring $\mathfrak{A}$ of $\mathfrak{F}$ ($\mathfrak{A} \in \mathfrak{F}$). A well-known example of an unobservable is a quantity that satisfies Fermi statistics. Although a "Fermi state" (a state in which fermionic fields exist) does not create any problems, we cannot directly observe such a quantity because it obeys the anticommutation relation that breaks the Einstein causality. Since electrons and protons are well-known and important fermions in particle physics, we see that the quantum field inevitably includes such an invisible field as to break the Einstein causality. We think that the outcome of the Bell's inequality test [48] for the Einstein-Podolsky-Rosen (EPR) dispute [49] seems to be consistent with this fact.

The starting point of MMD theory is the abstract sector theory of Doplicher-Haag-Roberts (DHR) [50-52], where sector means a collection of states for which the principle of superposition in quantum physics holds well. Recall that

in the classical special theory of relativity, the Poincaré group as the transformation group acting on the outer physical fields plays an important role in identifying the invariants of the fields. A similar situation holds for the inner quantum field $\mathfrak{F}$ and its transformation group G. In the case where $\mathfrak{F}$ possesses the internal symmetry associated with the action of G, the observable $\mathfrak{A}$, is usually given by the fixed partial ring of $\mathfrak{F}$ denoted by the symbol.

$$\mathfrak{A} = \mathfrak{F}^G, (\mathfrak{A} \in \mathfrak{F}, G = Gal(\mathfrak{F} / \mathfrak{A})) \tag{1}$$

where *Gal* denotes the Galois group fixing $\mathfrak{A}$ in $\mathfrak{F}$.

Since experimental validation is the most important element of physical theories, we can regard DHR's sector theory as an ambitious attempt to construct a quantum field theory based solely on the information on observable $\mathfrak{A}$. The key ingredient of their attempt is called the DHR selection criterion, which sorts the appropriate representations to be considered for satisfactory implementation of their scheme. The detailed explanation of it is beyond the scope of this article. The bottom line of DHR's sector theory is that by applying the selection criterion, based solely on the appropriate data on $\mathfrak{A}$, we can construct not only G but also $\mathfrak{F}$ to satisfy Equation (1).

3.2 *From micro to macro as a deductive approach*

In this subsection, we clarify the emergence process of the macro classical world; namely, we show, by improving the basic concept of sector in DHR's theory, how the macro classical world emerges from the micro quantum world. There are two important aspects of this emergence process. One is related to the degrees of freedom of the physical variables under consideration, and the other is directly tied to the specific problem of generalization of sector notion from the viewpoint of physics.

At the beginning of the previous subsection, we started our discussion by referring to the readers' unfamiliarity of QFT compared to QM. One of the decisive differences between QM and QFT comes from the difference in the degrees of freedom of the physical variables belonging to the dynamical system under consideration. If the number of degrees is finite, then the dynamics of a given system can be described by QM, whereas in the case of infinite degrees of freedom, QFT takes over. The Stone-von Neumann uniqueness theorem states that there exists only one sector for a QM system, which clearly shows that for a QM system, there is no room for the classical world to emerge since a sector is the states for which the principle of superposition in quantum physics holds well. In other words, a sector is defined as the irreducible representation of $\mathfrak{A}$. In what follows, we use the terms state and representation synonymously. In algebraic QFT, the state ω of $\mathfrak{A}$ is alternatively referred to as the Gel'fand-Naimark-Segal (GNS) representation $(\mathfrak{H}_\omega, \pi_\omega)$ where $\mathfrak{H}$ and π denote the Hilbert space and a linear operator on it, respectively.

DHR's sector theory constructed in the manner described above, however, suffers from serious flaws from the viewpoint of a physical theory. In theoretical physics, a seminal work of Nambu [53] on the notion of (spontaneous) symmetry breaking of physical fields made this idea of paramount importance since a considerable number of intriguing phenomena can be explained by such a process. Unfortunately, G in DHR's sector theory automatically has a unitary representation, and all the states reduce to the state with a G-invariant vacuum without symmetry breaking. In addition, from the definition of a sector as an irreducible representation of $\mathfrak{A}$ DHR's sector theory clearly cannot deal with thermodynamic states as mixed states.

Therefore, conceptual extension of the sector notion is definitely needed to overcome this difficulty. An effective remedy for this difficulty was proposed by Ojima [5]. Usually, by the equivalence of representations $\pi_1(A)$ and $\pi_2(A)$ of physical quantity A, we mean the unitary equivalence of $\pi_2(A) = U\pi_1(A)U^{-1}$, where U denotes a unitary operator. If we employ this, then π_1 and π_2 become nonequivalent even in the case that their difference is only multiplicity, for instance, of the form $\pi_1 = \pi$ and $\pi_2 = \pi \oplus \pi$. Ojima reached the solution that, as the classification of representations, if we employ the notion of quasi-equivalence $\pi_1 \approx \pi_2$ in which multiplicity is set aside, namely, unitary equivalence up to multiplicity, then the difficulty of DHR's sector theory can be overcome. The minimum unit of this new classification is called a generalized sector having factor representation with a trivial center.

We can show that for two arbitrary factor representations π_1 and π_2 if they are not quasi-equivalent, then they are disjoint. For the representation that is not a factor, there exist nontrivial centers as a commutative ring that enable break down of the representation uniquely into the form of the direct sum of disjoint factor representations through the process of simultaneous diagonalization. Thus, we see that these nontrivial centers play the role of the order parameters

describing the classical world, which is the emergence provcess of the macro classical world based on MMD theory.

3.3 *On nonlinear field interactions*

A typical example of the research on quantum field interactions is collision experiments in elementary particle physics. Theoretically speaking, the important elements in such experiments are as follows:

(1) the interacting nonlinear Heisenberg field φ, which must have a complicated spatiotemporal structure whose amplitude becomes predominant in the narrow spatiotemporal domain around the collision event, and

(2) the initial and final (noninteracting free) states of the field $\phi^{in/out}$ long before and after the collision event, which can be mathematically described as asymptotic fields $\phi^{as} \to \phi^{in/out}$ realized at $x^0 \to \mp\infty$, where x^0 denotes time in the spacetime Lorentzian coordinates $x = (x^0, x^1, x^2, x^3)$.

For simplicity, we assume that the field φ is a scalar field parameterized by a given mass m. The equations of motion for φ and ϕ^{as} become

$$(\Box + m^2)\varphi(x) = (\text{polynomial in } \varphi) := J_H \tag{2}$$

$$(\Box + m^2)\phi^{as}(x) = 0 \tag{3}$$

where the nonlinear term J_H is called the Heisenberg source current. Note that compared to the φ field, a nonlinear term is missing for the ϕ^{as} field. Without caring about the detailed explanation of mathematical expressions employed in the following system of equations (Equations (4) to (7)), if we formally write down φ, then we have

$$\varphi(x) \to \phi^{in/out}(x) \quad (\text{as } x^0 \to \mp\infty) \tag{4}$$

$$\varphi(x) = S^{-1}\{(\omega_0 \otimes id)(T[\varphi(x) \otimes 1]\exp(iJ_H \otimes \phi^{in}))\} \tag{5}$$

$$= \{(\omega_0 \otimes id)(T[\varphi(x) \otimes 1]\exp(iJ_H \otimes \phi^{out}))\}S^{-1} \tag{6}$$

The two symbols $\{S\}$ defined as

$$S = \{(\omega_0 \otimes id)(T\exp(iJ_H \otimes \phi^{in}))\} = \{(\omega_0 \otimes id)(T\exp(iJ_H \otimes \phi^{out}))\} \tag{7}$$

and $\{\exp(iJ_H \otimes \phi^{in/out})\}$ are the S(cattering)-matrix operator and an extended version of the Kac-Takesaki operator for an infinite dimensional system, and Equations (5) and (6) are called the Haag-GLZ expansion of φ.

Fortunately, there exists a helpful translation to decipher the above "hieroglyphic" description of quantum field interactions, which is called asymptotic completeness. It states that in the extremely long time limit of a scattering process controlled by the S matrix operator, the Heisenberg field φ generated from J_H can be transformed into asymptotic field(s) ϕ^{as} specified by Equation (3), and this field

(i) satisfies, with sufficient accuracy, the on-shell condition for the associated 4-momentum p^μ having the form $p^\nu p_\nu = m^2 \geq 0$, where the sign convention of the Lorentzian metric signature $(+---)$ is employed and "shell" in the present context means the mass-shell parameterized by m, and

(ii) can also be described with the same accuracy by a pair of creation and annihilation operators.

The combined behaviors (i) and (ii) of the asymptotic field(s) ϕ^{as} are what Equations (5) and (6) mean, and the important relation between φ and ϕ^{as} is given by the Lehmann-Symanzik-Zimmermann (LSZ) formula [54].

Presumably, those familiar with optics would note why the key element S given in Equation (7) is called the scattering matrix. When a propagating electromagnetic field hits a small particle, it is reflected in a certain fashion depending on the given physical situation, which is called scattering of the electromagnetic wave. The quantum field interaction focusing on $\phi^{in/out}$ mentioned above resembles this scattering phenomenon in form, where $\phi^{in/out}$ correspond to the incident and reflected outgoing light fields far from the particle. The substantial difference is that the Heisenberg field φ arises from the nonlinear interactions of quantum fields, while the scattering process in optics can be described solely in terms of the linear Maxwell equation. In relation to this substantial difference, readers should pay attention

to Haag's no-go theorem [55] stating that there exist no unitary transformations connecting ϕ^{in} and ϕ^{out}. This no-go theorem clearly shows that the existing QFT cannot satisfactorily describe the nonlinear field interactions.

Nevertheless, we think that the impact of the LSZ formula on the particle physicist community is quite significant in the sense that it provides a quite useful formula for particle collision experiments by circumventing the awkward problem of nonlinearity. We further think that the advent of the LSZ formula would create the atmosphere in their community that the study of invisible off-shell quantum fields (fields free from the on-shell condition) directly related to nonlinear interactions is either an unattractive (in the sense that it is behind the scenes) or a too difficult theme such that many of them would not think much about it.

In introductory section 1, we referred to the "theoretical fault" existing between the quantum and classical worlds. The prevailing tendency of focusing mainly on the on-shell aspects of physical fields also seems to be related to the "theoretical fault" since nonlinear field interactions play essential roles in connecting the two worlds. To conclude this subsection and in preparation for developing our discussion further in the following subsection, here, we refer to the Greenberg-Robinson (GR) theorem [56, 57] claiming that the involvement of off-shell spacelike momentum field $p^{\nu}p_{\nu} = m^2 < 0$ (cf. $p^{\nu}p_{\nu} = m^2 \geq 0$ explained in item (i) of field(s) ϕ^{as}) is necessary for nonlinear quantum field interactions to occur.

4. Spacelike Maxwell's field and a novel DP model

The contents of electromagnetism in this section and of novel cosmology in the subsequent section are the epitome of our series of recent studies reported in several papers. The latest research outcomes in the respective fields were reported by Sakuma et al. [43, 58].

4.1 *Spacelike electromagnetic field*

In particle physics, a spacelike momentum field $p^{\nu}p_{\nu} = m^2 < 0$ is often considered the field of a tachyon (or tachyonic particle) moving with superluminal velocity. However, a wave packet moving with superluminal velocity is shown to be quite unstable [59], while a simple sinusoidal-type wave does not create any problems. Therefore, assuming that any spacelike momentum field p^{μ} does not give an expression of a particle but represents a nonlocal wavelike field is natural.

Having noted this important characteristic of spacelike fields, we now explain how the Maxwell equation can be extended into the spacelike momentum domain, which is required by the GR theorem for us to consider nonlinear quantum field interactions. Since the Coulomb mode relating to longitudinal waves missing in the conventional theory of QED must be the key element, we start by reinvestigating the dynamical process in which the longitudinal mode plays an important role in the Maxwell equation.

$$j^{\mu} = \partial_{\nu}F^{\mu\nu} = \partial_{\nu}(\partial^{\mu}A^{\nu} - \partial_{\nu}A^{\mu}) = [-\partial^{\nu}\partial_{\nu}A^{\mu} + \partial^{\mu}(\partial_{\nu}A^{\nu})] \tag{8}$$

where j^{μ} and $F^{\mu\nu}$ denote an electric current and the electromagnetic field strength with vector potential A^{μ}. The mixed form of the energy-momentum tensor for Equation (8) is given by

$$T^{\nu}_{\mu} = -F_{\mu\sigma}F^{\nu\sigma} + \frac{1}{4}\eta^{\nu}_{\mu}F_{\sigma\tau}F^{\sigma\tau} \tag{9}$$

where η^{ν}_{μ} denotes the Lorentzian metric tensor with signature (+ − − −).

The quantization of the electromagnetic field cannot be done without using a gauge-fixing condition of some kind, which means that we have to specify $\partial_{\nu}A^{\nu}$ in a physically meaningful fashion. Here, we employ the Nakanishi-Lautrup (NL) B-field formalism [4] already referred to in section 1, which realizes manifestly covariant quantization. In the NL formalism, the Lorentz gauge condition $\partial_{\nu}A^{\nu} = 0$ can be generalized through the introduction of covariant linear gauges of the form.

$$\mathscr{L}_{\mathrm{B}} = B\partial_\nu A^\nu + \frac{\alpha}{2}B^2; \quad \partial_\nu A^\nu + \alpha\beta = 0, \partial^\nu\partial_\nu B = 0 \tag{10}$$

where $\mathscr{L}_{\mathrm{B}}$, B and α are a gauge-fixing Lagrangian density, the B-field and a real parameter, respectively. The second and third equations in Equation (10) give the gauge-fixing condition and the equation the B-field satisfies, respectively.

From the viewpoint of our present analysis focusing on the substantial (physical) property of nonvanishing longitudinal mode $\partial_\nu A^\nu$, the Feynman gauge corresponding to $\alpha = 1$ in Equation (10) is particularly important. The total Lagrangian density $\mathscr{L}_{\mathrm{total}}$ and its first variation with this gauge become

$$\mathscr{L}_{\mathrm{total}} = -\frac{1}{4}F_{\mu\nu}F^{\mu\nu} - \frac{1}{2}(\partial_\nu A^\nu)^2, \rightarrow [-\partial_\nu F^{\mu\nu} + \partial^\mu(\partial_\nu A^\nu)]\delta A_\mu = 0. \tag{11}$$

By comparing the second equation in Equation (11) with Equation (8), we obtain

$$\partial^\nu\partial_\nu A^\mu = 0, \partial_\nu A^\nu = -B, \partial^\nu\partial_\nu B = 0. \tag{12}$$

In the conventional analysis of the energy-momentum conservation of Equation (9), we usually interpret $\partial^\nu T_\mu{}^\nu = F_{\mu\nu}j^\nu = 0$ as the consequence of $j^\nu = 0$, namely, no electric current exists. Note, however, that since Equation (8) reduces to $\{j^\mu = \partial_\nu F^{\mu\nu} = \partial^\mu(\partial_\nu A^\nu)\}$ by the first equation in Equation (12), this also holds well for the case in which we have $\partial^\nu T_\mu{}^\nu = F_{\mu\nu}\partial^\mu(\partial_\nu A^\nu) = 0$ under the condition that nonzero current $\partial^\mu(\partial_\nu A^\nu)$ (physically different from the electric current) is parallel to a Poynting vector field associated with $F_{\mu\nu}(F_{\mu\nu} \perp \partial^\mu(\partial_\nu A^\nu))$. Thus, we have shown that a longitudinal wave "current" having the form of

$$(j^\mu =)\partial_\nu F^{\mu\nu} = \partial^\mu(\partial_\nu A^\nu)) \tag{13}$$

is a physical current that satisfies the energy-momentum conservation, and we further see that for this particular choice of Feynman's gauge-fixing condition, the B-field equation $\partial^\nu\partial_\nu B = 0$ in Equation (12) formally corresponds to the gauge-invariant condition relating to conservation of "the current" $\{(j^\mu) = \partial^\mu(\partial_\nu A^\nu)\}$.

Next, we consider the extension of the Maxwell equation to the spacelike momentum domain $p^\nu p_\nu = m^2 < 0$. For the brevity of notation, in what follows, we redefine $\partial_\nu A^\nu$ as ϕ, namely,

$$\phi := \partial_\nu A^\nu, \quad \partial^\nu\partial_\nu\phi = 0 \tag{14}$$

The "gauge-invariant" orthogonality condition $F_{\mu\nu}(\partial^\nu\phi) = 0$ derived above is mathematically equivalent to a relativistic hydrodynamic equation of a barotropic (isentropic) fluid [58]. This observation suggests that we employ the method of the (two-parameter λ, ϕ) Clebsch parameterization (CP) to represent vector potential U^μ of spacelike electromagnetic field $S^{\mu\nu}$ since these two parameters play the role of canonically conjugate variables in the Hamiltonian dynamics of the barotropic fluid [60]. The detailed derivation of U^μ and $S^{\mu\nu}$ was already given in a few references [61-63], so here, we only show the main results, which can be classified into two, categories I and II. For the reason mentioned above, we call the spacelike electromagnetic field defined below the Clebsch dual (electromagnetic) field.

Category I

U^μ belonging to this category satisfies the lightlike condition of $(U^\nu)^* U_\nu = 0$, where $(\cdot)*$ denotes the complex conjugate of $(\cdot)$. In this case, U_μ is defined in terms of two parameters λ and ϕ satisfying the following equations.

$$U_\mu = \lambda\partial_\mu\phi, \quad \partial^\nu\partial_\nu\lambda - \left(\kappa_0\right)^2\lambda = 0, \quad \partial^\nu\partial_\nu\phi = 0 \tag{15}$$

where κ_0 (or its inverse $l_{dp} := (\kappa_0)^{-1}$) denotes an important constant called the DP constant referred to in section 2. For concise representations of $S^{\mu\nu}$ and the associated energy-momentum tensor $\hat{T}_\mu{}^\nu$, we introduce two gradient vector fields that are perpendicular to each other:

$$L_\mu := \partial_\mu \lambda, \quad C_\mu := \partial_\mu \phi, \quad C^\nu L_\nu = 0. \tag{16}$$

With these new notations, the covariant representation of $S^{\mu\nu}$ is given by a simple bivector of the form

$$S_{\mu\nu} = L_\mu C_\nu - L_\nu C_\mu, \tag{17}$$

and we can show that U_μ is a tangential vector field along a null geodesic satisfying the wave equation on the right side:

$$U^\nu \partial_\nu U_\mu = -S_{\mu\nu} U^\nu = 0, \Longleftrightarrow \partial^\nu \partial_\nu U^\mu - (\kappa_0)^2 U^\mu = 0. \tag{18}$$

The energy-momentum tensor $\hat{T}_\mu{}^\nu$ corresponding to Equation (9) is defined as

$$\hat{T}_\mu{}^\nu = S_{\mu\sigma} S^{\nu\sigma} = \rho C_\mu C^\nu, \quad \rho := L^\nu L_\nu < 0, \tag{19}$$

$$\partial_\nu \hat{T}_\mu{}^\nu = S_{\mu\sigma} \partial_\nu S^{\nu\sigma} = S_{\mu\sigma} (\kappa_0)^2 U^\sigma = 0. \tag{20}$$

We see that $\hat{T}_\mu{}^\nu$ has dual representations of wave field $S_{\mu\sigma} S^{\nu\sigma}$ and particle field $\rho C_\mu C^\nu$, and the condition of negative density $\rho < 0$ corresponds to the removal of the particle mode in QED.

Category II

For spacelike U_μ that satisfies $(U^\nu)^* U_\nu < 0$ and is advected along a geodesic, it is redefined as

$$U_\mu := \frac{1}{2}(\lambda C_\mu - \phi L_\mu), \quad U^\nu \partial_\nu U_\mu = 0, \tag{21}$$

$$\partial^\nu \partial_\nu \lambda - (\kappa_0)^2 \lambda = 0, \quad \partial^\nu \partial_\nu \phi - (\kappa_0)^2 \phi = 0, \quad C^\nu L_\nu = 0. \tag{22}$$

The form of $S_{\mu\nu}$ remains the same as Equation (17), while $\hat{T}_\mu{}^\nu$ in this case assumes the form of

$$\hat{T}_\mu{}^\nu = \hat{S}_{\mu\sigma}{}^{\nu\sigma} - \frac{1}{2} \hat{S}_{\alpha\beta}{}^{\alpha\beta} \eta_\mu{}^\nu, \ \hat{S}_{\alpha\beta\gamma\delta} := S_{\alpha\beta} S_{\gamma\delta}. \tag{23}$$

Since $\hat{S}_{\alpha\beta\gamma\delta}$ has the same antisymmetric properties as the Riemann tensor $R_{\alpha\beta\gamma\delta}$, including the first Bianchi identity $\hat{S}_{\alpha[\beta\gamma\delta]} = 0$, $\hat{T}_\mu{}^\nu$ becomes isomorphic to the Einstein tensor $G_\mu{}^\nu := R_\mu{}^\nu - R g_\mu{}^\nu / 2$.

4.2 *Novel heuristic model of a DP*

In the preceding subsection, we have shown that the spacelike electromagnetic field $S_{\mu\nu}$ can be decomposed into a spacelike bivector of the form $\partial^\nu \partial_\nu \lambda - (\kappa_0)^2 \lambda = 0$. In our efforts to develop a heuristic model of a DP, we think that the analogy called the quantum-classical correspondence referred to in subsection 3.1 is quite helpful. As such a helpful analogy, we consider first the comparison between the above spacelike Klein-Gordon (KG) equation regarding λ and the Dirac equation

$$(i\gamma^\nu \partial_\nu + m)\Psi = 0, \tag{24}$$

which can be regarded as the "square root" of the timelike KG (type) equation: $(\partial^\nu \partial_\nu + m^2)\Psi = 0$. The Dirac equation for $(\partial^\nu \partial_\nu - (\kappa_0)^2)\Psi = 0$ therefore becomes

$$i(\gamma^\nu \partial_\nu + \kappa_0)\Psi = 0. \tag{25}$$

Additionally, for the Dirac equation (24), there exists an electrically neutral Majorana representation in which

all the values of the γ matrix become purely imaginary, so it reduces to $(\gamma^{\nu}{}_{(M)}\partial_{\nu}+m)\Psi=0$, which is isomorphic to Equation (25). Therefore, in our quantum-classical correspondence for this particular case, we can say that the Majorana field is the quantum counterpart of the classical solution of $\partial^{\nu}\partial_{\nu}\lambda-(\kappa_0)^2\lambda=0$.

Due to Pauli's exclusion principle, for the Majorana field as the fermionic field, the same state cannot be occupied by two fields. Therefore, the key question regarding the formulation of the (bosonic) Clebsch dual electromagnetic field is how the fermionic Majorana field fits into the former field. To answer this question, let us consider two different states of Majorana fields whose angular and linear momenta are given by ($M_{\mu\nu}$, p^{μ}) and ($N_{\mu\nu}$, q^{μ}), respectively. Note that two such fields can share the same Pauli-Lubanski vector W_{μ} describing the spin state of moving particles. Namely,

$$M_{\mu\nu}\,p^{\nu}=N_{\mu\nu}q^{\nu}=W_{\mu}, \tag{26}$$

where linear momenta p^{μ} and q^{ν} are orthogonal, i.e., $p^{\nu}q_{\nu}=0$. As we have shown in the preceding subsection, the spacelike electromagnetic field $S_{\mu\nu}$ is represented by a couple of simple bivector fields L_{μ} and C_{μ} that are perpendicular to each other (Equations (16) and (22)). Therefore, such a dynamic configuration in the classical Clebsch dual representation is consistent with the condition $p^{\nu}q_{\nu}=0$, and the bosonic property of spin 1 is realized by sharing the same W_{μ}, the sum total of which becomes 1.

To obtain a heuristic model of a DP, we utilize the theoretical analysis performed by Aharonov et al. [64], who studied the resulting behavior of the spacelike KG equation perturbed by a point source of the form $\delta(x^0)\delta(r)$, where r denotes the spatial coordinate(s). In our present analysis, we employ a spherical coordinate system in which r denotes the radial coordinate. Their analyses showed that the resulting time-dependent behavior of the solution is expressed as the superposition of a superluminal (spacelike) stable oscillatory mode and a timelike linearly unstable mode whose combined amplitude with a local peak initially tends to flatten with a speed slower than the light velocity. A timelike unstable solution arising from the perturbed spacelike KG equation has the form of $\hat{\lambda}(x^0,r)=\exp(\pm k_0x^0)R(r)$, where $R(r)$ satisfies

$$R''+\frac{2}{r}R'-(\hat{\kappa}_r)^2=0,\quad (\hat{\kappa}_r)^2\coloneqq(k_0)^2-(\kappa_0)^2>0, \tag{27}$$

the solution of which is known as the Yukawa potential

$$R(r)=\exp(-\hat{\kappa}_r r)/r, \tag{28}$$

which rapidly falls off as r increases.

In the classical scenario, we can usually interpret a pair of these unstable solutions as follows. While $\hat{\lambda}_{(-)}\coloneqq\exp(-k_0x^0)R(r)$ decays, $\hat{\lambda}_{(+)}=\exp(+k_0x^0)R(r)$ exponentially grows to nonlinearly interact with the environmental field missing in our present model. As a tentative quantum mechanical scenario, we conjecture the following possibility. First, we regard this pair of solutions as a particle-antiparticle pair of the Majorana field: one is going forward in time, and the other is going backward. The reason why we can have such a pair is that the Clebsch dual electromagnetic field $S_{\mu\nu}$ has a simple bivector structure of the form Equation (17). If their spin axes are antiparallel, then the particle-antiparticle pair would combine as a boson to form an (spin 0) electric field, and if they are parallel, then we would have a (spin 1) magnetic field. Here, we regard this state change from two independent timelike Majorana fields produced by a point-like perturbation to a combined bosonic field as an internal field interaction. In addition, we further assume that the solution $R(r)$ given by Equation (27) is quantized such that $(\hat{\kappa}_r)^2=(n\kappa_0)^2$, where n denotes a positive integer. This quantization defines the discrete energy levels of the DP and the upper limit of the size of the DP explained in section 2.

5. Toward the integration of visible and invisible fields

As we have mentioned at the end of introductory section 1, a novel vision of cosmology, particularly regarding dark energy, arising from DP studies is what we least expected. A source-free Maxwell equation of electromagnetism

(in four-dimensional spacetime) and the de Sitter solution (closely related to the spacelike KG equation explained in subsection 4.1) in cosmology share the same characteristic of self-similarity, namely, they are scale independent. We think that self-similarity must be a key factor that connects a DP as a nanoscale entity with dark energy in cosmology. In concluding this article on a novel nanoscience perspective, we think that touching on such an unexpected finding demonstrating the vast potential of nanoscience to be explored is quite appropriate. In what follows, we first briefly refer to our recent studies [58] on dark energy and matter as a concrete example of the integration of visible and invisible fields and then extend our discussion to include the problem of consciousness, which would be the final frontier of the physical sciences.

In retrospect, our new proposal on the dark energy model is quite simple once we accept the notion of a Clebsch dual electromagnetic field giving the spacelike momentum field for quantum field interactions. In the preceding subsection 4.2, we have referred to Equation (26) showing how a bosonic Clebsch dual field can be constructed from the fermionic Majorana field. Recall that the reason why we introduce the Clebsch dual field is that the GR theorem explained in subsection 3.3 requires such a field for quantum field interactions. In this respect, we can say that, conceptually, the Clebsch dual field plays the role of virtual photons in the conventional QED. Since the spatial dimension of our universe is three, the maximum number of momentum vectors satisfying Equation (26) is also three. Namely, we have

$$M_{\mu\nu}\, p^{\nu} = N_{\mu\nu} q^{\nu} = L_{\mu\nu} r^{\nu} = W_{\mu}. \tag{29}$$

A Clebsch dual field arises from any pair of $[(p^{\mu}, q^{\mu}), (q^{\mu}, r^{\mu}), (r^{\mu}, q^{\mu})]$, each of which can be regarded as a "virtual photon field" moving along one direction of (x^1, x^2, x^3). Quantum mechanically, since the Clebsch dual field is composed of a Majorana field, the state represented by Equation (29) is the compound Rarita-Schwinger state of the Majorana field with spin 3/2.

The important role played by this compound state is as follows. We can regard this state $\left|M3\right\rangle_g$ as the "ground" state of the "virtual photon field". Since electromagnetic field interactions are ubiquitous phenomena in the universe, incessant occurrences of excitation-deexcitation processes between the ground $\left|M3\right\rangle_g$ and nonground states occur, which would make $\left|M3\right\rangle_g$ a "stable unseen off-shell state" from the viewpoint of a macroscopic time scale although the states of virtual photons are extremely ephemeral. At the end of subsection 4.1, we noted that the energy-momentum tensor $\hat{T}_{\mu}^{\ \nu}$ of the Clebsch dual field is isomorphic to the Einstein tensor $G_{\mu\nu}$ which facilitates obtaining $\left|M3\right\rangle_g$ in the theory of general relativity. Recall that $\hat{T}_{\mu}^{\ \nu}$ is itself a spacelike unobservable quantity. However, by referring to the fundamental knowledge of QFT regarding observable quantities explained in relation to Equation (1), we conjecture that the trace of $\hat{T}_{\mu}^{\ \nu}$ is an observable quantity since, by the abovementioned isomorphism, it is proportional to the scalar curvature R of the spacetime as the invariant of general coordinate transformation. The most well-known model of dark energy is what we call the cosmological term $\lambda g_{\mu\nu}$, and the value of λ derived by Planck satellite observations [65] is $\lambda_{\text{obs}} \approx 3.2 \times 10^{-53}\ \text{m}^{-2}$. Although our model $\hat{T}_{\mu}^{\ \nu}$ is quite different from $\lambda g_{\mu\nu}$,we can define a reduced cosmological constant λ_{DP} as the trace of $\hat{T}_{\mu}^{\ \nu}$ and the λ_{DP} estimated by the DP experiments explained in subsection 2.2 turns out to be $\lambda_{DP} \approx 2.47 \times 10^{-53}\ \text{m}^{-2}$, which is very close to λ_{obs}.

Regarding the physical meaning of the cosmological term $\lambda g_{\mu\nu}$, the long-standing controversy since the time of Einstein has not yet been settled. We think that the major problem is the fact that metric tensor $g_{\mu\nu}$ by itself is not an appropriate set of quantities to represent the gravitational field since for the flat spacetime, we can introduce a multitude of metric tensors depending on the coordinate system we choose. Our proposal for resolving this problem is to use the following identity [63] on Weyl curvature tensor $W_{\alpha\beta\gamma\delta}$:

$$W_{\mu\alpha\beta\gamma} W_{\nu}^{\ \alpha\beta\gamma} - \frac{1}{4} g_{\mu\nu} W^2 = 0, \quad W^2 := W_{\alpha\beta\gamma\delta} W^{\alpha\beta\gamma\delta}. \tag{30}$$

Based on this identity, we can redefine metric tensor $g_{\mu\nu}$ as

$$g_{\mu\nu} := \frac{4W_{\mu\alpha\beta\gamma} W_{\nu}^{\alpha\beta\gamma}}{W^2}, \tag{31}$$

under the condition that $W^2 \neq 0$. Then, the cosmological term $\lambda g_{\mu\nu}$ with a certain meaningful constant λ becomes the energy-momentum tensor of the conformal gravitational field, of which justification in relation to the novel definition of entropy introduced by Aoki et al. [66] is given in the latest paper by Sakuma et al. [58].

The crucial assumption of $W^2 \neq 0$ is closely related to our novel cosmology, which is similar to conformal cyclic cosmology (CCC) proposed by Penrose [67]. The essential characteristic of CCC is that the universe repeats an infinite cycle of life and death through the interaction of the nodal "null universe" with a conformal light field. The decisive difference between our cosmology and CCC lies in the fact that while the twins (as a matter and antimatter pair) in the augmented universe play key roles in the former scenario, a single universe undergoes a cyclic process through its internal dynamics in the latter scenario. In our model, the creation and annihilation of twin universes can be compared to the pair creation and annihilation of elementary particles, and the configuration of twin universes in a 5-dimensional Minkowski space is uniquely determined by the dark energy field in our model [68]. In Figure 6, we give a schematic diagram showing how twin universes undergo everlasting cyclic changes.

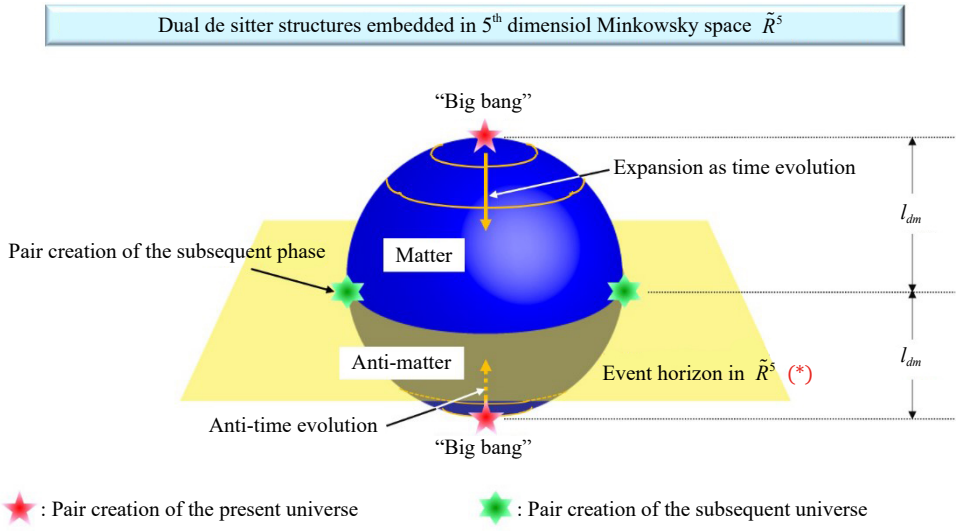

Figure 6. Schematic diagram on the infinite cyclic motions of twin universes. Twin material universes are born from the nodal "null universe" with conformal light field and will return to its original light field eons later by the process of a pair annihilation at the event horizon $\tilde{R}^5$.

In our new model, the abovementioned nodal null universe is represented by light fields that consist of the light field we are familiar with and the Clebsch dual light field of category I. In our cosmological scenario, the transition from the nodal null universe to the metric twin universes occurs as the result of simultaneous conformal symmetry breaking (SCSB) of electro-magnetic and gravitational fields. By SCSB of the electromagnetic field, we mean the appearance of the Clebsch dual light field of category II leading to the dark energy field λ_{DP}, and SCSB of the gravitational field corresponds to the emergence of a nonzero W^2 field in Equation (30). In their latest study on cosmology, Sakuma et al. [58] further showed that there exists a strong correlation between Weyl curvature tensor $W_{\alpha\beta\gamma\delta}$ and the gravitational entropy field having the form of a spin network, from which an intriguing dark matter model emerges.

Regarding the problem of fixing a constant for the cosmological term $\lambda g_{\mu\nu}$, they argue that the choice of

$$\lambda_{dm} := -\frac{1}{3}\lambda_{DP} > 0, \quad \lambda_{DP} \approx -2.47\times10^{-53}\,\mathrm{m}^{-2}, \tag{32}$$

would be an appropriate estimate consistent with the observational evidence that the abundance ratio between dark matter and dark energy is approximately 1:3. The reason why we have negative λ_{DP} here is because we employ the sign convention $(+---)$ for metric tensor $g_{\mu\nu}$. Since the abundance ratio of ordinary matter is approximately 5 percent, the overall spacetime structure must be determined by dark matter and energy. We conjecture that Equation (32) reflects a formal equipartition of spacetime energy of the form

Dark matter $\Longrightarrow (\lambda_{dm}, 0, 0, 0)$
Dark energy $\Longrightarrow (0, -\lambda_{dm}, -\lambda_{dm}, -\lambda_{dm})$

from which we can say that our universe has a nearly flat spacetime structure.

In addition, as we have shown in Figure 6, the parameter $l_{dm} := \sqrt{(\lambda_{dm})^{-1}}$ gives the characteristic length scale of our universe. Immediately after the SCSB event, the magnitude of the emergent W^2 would be quite small. However, the local maxima of W^2 work as the cores of universal gravitation, so such cores become the seeds of galactic formation. Note that the smallness of W^2 means that the spacetime structure of the early universe was isotropic, so contrary to the widely prevalent theory based on a cosmic inflation scenario, our new theory naturally explains the isotropy of the early universe.

As we have explained in the arguments developed thus far, the essential ingredient of invisible fields is the spacelike momentum field breaking the Einstein causality. Although the GR theorem referred to in subsection 3.3 does not seem to attract the attention of mainstream physicists, we think that a currently spotlighted research theme such as quantum entanglement must be closely related to it. In subsection 4.1, we showed that DP constant $l_{dp} = (\kappa_0)^{-1}$ is a key parameter for spacelike momentum of electromagnetic field (cf. Equation (15)). One of the quite intriguing findings from the viewpoint of nanoscience is that DP constant $l_{dp} \approx 50$ nm gives the geometric mean of the smallest Planck length l_p and the largest characteristic length scale of our universe $l_{dm} = \sqrt{(\lambda_{dm})^{-1}}$, where λ_{dm} is given by Equation (32). Namely, l_{dp} is considered as "the central scale of our universe" called Heisenberg cut dividing our micro and macro universes, and our newly proposed model on DP genesis shows that DPs come into existence through the interactions between the visible materialistic field and the invisible spacelike momentum of electromagnetic field.

The final remarks we would like to make on the invisible spacelike momentum field that would connect every component in our universe instantaneously are its relationship with elusive consciousness. Presumably, an emerging view on this problem currently in the spotlight would be a notion called "singularity" of artificial intelligence (AI) [69]. According to this view, the singularity is loosely defined as the critical point in AI evolution beyond which AI will outperform human even in the realm of creativity. However, we should not miss the fact that a world-renowned mathematical physicist Penrose strongly disagrees with the existence of AI singularity. In one of his books entitled Shadows of the Mind [70], Penrose eloquently argues that, on the basis of Gödel's incompleteness theorems published for the second Hilbert problems [71], the activities of human consciousness including those of mathematics cannot be reduced to algorithmic processes on which AI essentially depends.

We can say that views on human consciousness conflicting with AI singularity are shared by not a few scientists and philosophers even in the western community. Hungarian philosopher of science László [72], the founder of the Club of Budapest, holds a unique view that the western science and the eastern esoteric philosophy can be united harmoniously. The following arguments on human consciousness we are going to develop are in line with such a basic philosophy of László. Since the electromagnetic field is an inevitable mediator for the normal operation of cranial nerve systems, we think assuming that conscious activities are related to such an invisible spacelike electromagnetic field is quite natural, especially when we consider the possible existence of what we call paranormal (or Psi) phenomena (PP), such as clairvoyance, telepathy and near-death experience (NDE). In modern societies where our sense of values has been heavily influenced by materialism, we tend to regard such PP as fantasies or hallucinations. However, there exist numerous scientific reports supporting their credibility [73], including a special report in which Alexander, a highly trained neurosurgeon at Harvard, described his own NDE [74] in detail as a bona fide challenge to the prevailing Western materialistic world view. We think that such an emerging societal situation in which we have conflicting world

views is, in a sense, similar to the situation we touched on in section 1, where we have two conflicting explanations of the existence of a longitudinal mode of an electromagnetic wave: the one based on fragmented knowledge, although it belongs to scientifically "advanced" QED, where a longitudinal mode is excluded as a ghost mode, and the other based on the quite sound but undistinguished scientific approach.

In coping with the problem of consciousness, the most difficult aspect of it would be how to deal with qualitative attribute such as motivation in life, selfish and unselfish acts, in addition to the interpretation of what we call mysterious experiences including inspiration, which is surely beyond the scope of the present physical sciences. Of course, now we do not have a clear vision on the way we should go, but we should bear in mind that, if we look back at the history of science, we find numerous stories in which inspirational experiences beyond description played a central role in making breakthrough achievements. In his autobiography [75], Nikola Tesla, a legendary genius in electrical engineering, tells us such an inspirational experience on the revolutionary idea of induction motor, which came suddenly to him as a "revelation" when he was reciting a verse of the "Sunset Speech" from Goethe's Faust. It seems that he could directly access to the blueprint for future technology by resonating with the currently unknown field beyond spacetime.

We think that, as the well-known Fourier analysis shows, if everything is composed of a certain energetic wave field, then the resonance may be interpreted as frequency matching. As Tesla's experience implies, such a frequency matching may be the ultimate way to learn the innermost secret of reality. In this respect, a medical practice such as wave adjustment therapy taken as a kind of pseudoscience may turn out to be a natural and sensible therapy. If we turn our eyes toward economic activities that are of vital importance to our societies, as in the case of medical care, we find that economics has reached an impasse over the question of how to deal with human factors such as motivation in life, selfish and unselfish acts already mentioned just before the anecdote of Tesla. In economics, the action of (self-interested) individual is simply modeled to maximize utility (function) as a measure of consumption. This oversimplification seems to be a modeling effort in pursuit of the formality of mathematical science and, by virtue of this, economics became the queen of social sciences. However, we can say that this very aspect of economics led to the unwanted degradation of economics in the sense that the model prediction does not reflect the real economic activities.

To overcome this drawback, Okabe [76] has launched an ambitious initiative called Humanomics as an investigation of the new form of economics in which the well-being (as a qualitative human factor) of constituent members in our communities and economic development (as a gross quantitative factor of macro-economics) are to be achieved in a consistent fashion. We think that the challenging endeavor of Humanomics is closely related to our main theme of consistent integration of different fields mentioned in section 1. In Okabe's proposal, an individual human is no longer a self-interested person, but a practitioner carving a new life of the self-improvement with the awareness that we are souls contributing to the harmonious development of our world. One of the fundamental premises of Humanomics is based on an unprecedented system of wisdom learning on the human existence established through a decades-long pilot study project. The whole project was led by Takahashi [77, 78], an eminent leader who is conversant with the wide spectrum of PP Alexander experienced and was supported by the active participation of numerous collaborators in the fields of medical practice, management, education, etc.

Our research on DPs initiated by the third author M. O. has been a continuous challenge of breaking the firmly established framework (or paradigm) of the existing theory of electromagnetism. Especially in the early stages, Ohtsu's DP research was considered quite abnormal such that almost all senior researchers in the field of optics ignored it. Concerning the dauntless challenging spirit of M. O., the first author H. S. thinks that Hancock [79], a British investigative journalist and bestselling writer who has been providing many thought-provoking ideas on the lost civilization of Atlantis, seems to share a similar challenging spirit. According to Hancock, his attempt to find evidence of the lost civilization was ridiculed by scientific communities in the 20th century. However, the situation has gradually changed with the accumulation of new archaeological evidence, especially recent quite convincing geophysical evidence of the catastrophic Younger Dryas event [80] reported in the Proceedings of the National Academy of Sciences, which confirms the period of the sudden fall of Atlantis told by Plato. Hancock speculates that Atlanteans did not have much interest in materialistic worlds compared to nonmaterialistic spiritual worlds because they knew that the former occupy extremely small portions of the entire world, just as our lifetime span on the earth is negligibly small compared to the eternal life of the spirit. Interestingly, such a world view of Atlanteans speculated by Hancock is exactly the same as what Alexander experienced in his NDE.

Suppose that souls are actually eternal entities experiencing infinite cycles of birth and death between the visible

and invisible worlds, as in the case of twin universes in our cosmology; then, we can say that the existence of DPs and the associated cosmology symbolize not only human existence but also Hancock's favorite Hermetic verse of "As above, so below". We believe that nanoscience will play the central role of a springboard in inducing a large paradigm shift in science.

Acknowledgments

We gratefully acknowledge valuable and helpful comments from the anonymous reviewers, by which the quality and readability of this article is improved. The first author thanks M. Inutake, Emeritus Professor of Tohoku University, for his keen interest in our studies on novel type of diffraction-free laser beams and the first author's thank extends to M. Okabe, Emeritus Professor of Keio University, who kindly provided the cutting-edge information on his ambitious initiative for economics together with useful suggestion to improve the quality of the first draft of this article.

Conflict of interest

The authors declare no conflict of interest.

References

[1] Ohtsu M. *Dressed photons*. Berlin: Springer; 2014. p.89-214. Available from: https://doi.org/10.1007/978-3-642-39569-7.
[2] Ohtsu M. From classical to modern near-field optics and the future. *Optical Review*. 2014; 21: 905-910. Available from: https://doi.org/10.1007/s10043-014-0143-5.
[3] Cicchitelli L, Hora H, Postle R. Longitudinal field components for laser beams in vacuum. *Physical Review A*. 1990; 41(7): 3727-3732. Available from: https://doi.org/10.1103/physreva.41.3727.
[4] Nakanishi N, Ojima I. (eds.) *Covariant operator formalism of gauge theories and quantum gravity*. Singapore: World Scientific; 1990. Available from: https://doi.org/10.1142/0362.
[5] Ojima I. A unified scheme for generalized sectors based on selection criteria: Order parameters of symmetries and of thermality and physical meanings of adjunctions. *Open Systems and Information Dynamics*. 2003; 10(3): 235-279. Available from: https://doi.org/10.1023/A:1025175907589.
[6] Ojima I. Micro-macro duality in quantum physics. In: Hida T. (ed.) *Stochastic Analysis: Classical and Quantum - Perspectives of White Noise Theory*. Singapore: World Scientific; 2005. p.143-161. Available from: https://doi.org/10.1142/9789812701541_0012.
[7] Ohtsu M. Off-shell application in nanophotonics. Amsterdam: Elsevier; 2021. p.1-17. https://doi.org/10.1016/C2020-0-02956-7.
[8] Sangu S, Kobayashi K, Ohtsu M. Optical near fields as photon-matter interacting systems. *Journal of Microscopy.* 2001; 202(2): 279-285. Available from: https://doi.org/10.1111/j.1365-2818.2001.00805.x.
[9] Naruse M, Leibnitz K, Peper F, Tate N, Nomura W, Kawazoe T, et al. Autonomy in excitation transfer via optical near-field interactions and its implications for information networking. *Nano Communication Networks*. 2011; 2(4): 189-195. Available from: https://doi.org/10.1016/j.nancom.2011.07.002.
[10] Kawazoe T, Kobayashi K, Takubo S, Ohtsu M. Nonadiabatic photodissociation process using an optical near field. *The Journal of Chemical Physics*. 2005; 122(2): 024715. Available from: https://doi.org/10.1063/1.1828034.
[11] Ohtsu M. History, current developments, and future directions of near-field optical science. *Opto-Electronic Advances*. 2020; 3(3): 190046. Available from: https://doi.org/10.29026/oea.2020.190046.
[12] Ohtsu M. *Silicon light-emitting diodes and lasers*. Cham: Springer; 2016. Available from: https://doi.org/10.1007/978-3-319-42014-1.
[13] Ohtsu M. Progress in dressed photon technology and the future. In: Ohtsu M, Yatsui T. (eds.) *Progress in Nanophotonics 4*. Cham: Springer; 2017. p.1-18. Available from: https://doi.org/10.1007/978-3-319-49013-7_1.
[14] Kawazoe T, Ohtsu M, Aso S, Sawado Y, Hosoda Y, Yoshizawa K, et al. Two-dimensional array of room-temperature nanophotonic logic gates using InAs quantum dots in mesa structures. *Applied Physics B.* 2011; 103:

537-546. Available from: https://doi.org/10.1007/s00340-011-4375-9.
[15] Kawazoe T, Tanaka S, Ohtsu M. Single-photon emitter using excitation energy transfer between quantum dots. *Journal of Nanophotonics*. 2008; 2(1): 029502. Available from: https://doi.org/10.1117/1.3026554.
[16] Naruse M, Holmström P, Kawazoe T, Akahane K, Yamamoto N, Thylén L, et al. Energy dissipation in energy transfer mediated by optical near-field interactions and their interfaces with optical far-fields. *Applied Physics Letters*. 2012; 100(24): 241102. Available from: https://doi.org/10.1063/1.4729003.
[17] Naruse M, Tate N, Aono M, Ohtsu M. Information physics fundamentals of nanophotonics. *Reports on Progress in Physics*. 2013; 76(5): 056401. Available from: https://doi.org/10.1088/0034-4885/76/5/056401.
[18] Kim SJ, Naruse M, Aono M, Ohtsu M, Hara M. Decision maker based on nanoscale photo-excitation transfer. *Scientific Reports*. 2013; 3: 2370. Available from: https://doi.org/10.1038/srep02370.
[19] Aono M, Naruse M, Kim SJ, Wakabayashi M, Hori H, Ohtsu M, et al. Amoeba-inspired nanoarchitectonic computing: Solving intractable computational problems using nanoscale photoexcitation transfer dynamics. *Langmuir*. 2013; 29(24): 7557-7564. Available from: https://doi.org/10.1021/la400301p.
[20] Kawazoe T, Kobayashi K, Ohtsu M. Near-field optical chemical vapor deposition using $Zn(acac)_2$ with a non-adiabatic photochemical process. *Applied Physics B*. 2006; 84: 247-251. Available from: https://doi.org/10.1007/s00340-006-2224-z.
[21] Lim J, Yatsui T, Ohtsu M. Observation of size-dependent resonance of near-field coupling between a deposited Zn dot and the probe apex during near-field optical chemical vapor deposition. *IEICE Transactions on Electronics*. 2005; E88-C(9): 1832-1835. Available from: https://doi.org/10.1093/ietele/e88-c.9.1832.
[22] Polonski VV, Yamamoto Y, Kourogi M, Fukuda H, Ohtsu M. Nanometric patterning of zinc by optical near-field photochemical vapour deposition. *Journal of Microscopy*. 1999; 194(2-3): 545-551. Available from: https://doi.org/10.1046/j.1365-2818.1999.00497.x.
[23] Yonemitsu H, Kawazoe T, Kobayashi K, Ohtsu M. Nonadiabatic photochemical reaction and application to photolithography. *Journal of Luminescence*. 2007; 122-123: 230-233. Available from: https://doi.org/10.1016/j.jlumin.2006.01.115.
[24] Inao Y, Nakasato S, Kuroda R, Ohtsu M. Near-field lithography as prototype nano-fabrication tool. *Microelectronic Engineering*. 2007; 84(5-8): 705-710. Available from: https://doi.org/10.1016/j.mee.2007.01.043.
[25] Kawazoe T, Kobayashi K, Akahane K, Naruse M, Yamamoto N, Ohtsu M. Demonstration of nanophotonic NOT gate using near-field optically coupled quantum dots. *Applied Physics B*. 2006; 84: 243-246. Available from: https://doi.org/10.1007/s00340-006-2234-x.
[26] Kawazoe T, Takahashi T, Ohtsu M. Evaluation of the dynamic range and spatial resolution of nonadiabatic optical near-field lithography through fabrication of Fresnel zone plates. *Applied Physics B*. 2010; 98: 5-11. Available from: https://doi.org/10.1007/s00340-009-3680-z.
[27] Koike M, Miyauchi S, Sano K, Imazono T. X-ray devices and the possibility of applying nanophotonics. In: Ohtsu M. (ed.) *Nanophotonics and Nanofabrication*. Germany: Wiley-VCH; 2009. p.179-191.
[28] Hirata K. Realization of high-performance optical element by optical near-field etching. In: *Laser-based Micro- and Nanopackaging and Assembly V*. California, United States: SPIE; 2011. p.79210M. Available from: https://doi.org/10.1117/12.875808.
[29] Yatsui T, Nomura W, Ohtsu M. Realization of ultraflat plastic film using dressed-photon-phonon-assisted selective etching of nanoscale structures. *Advances in Optical Technologies.* 2015; 2015: 701802. Available from: https://doi.org/10.1155/2015/701802.
[30] Yatsui T, Hirata K, Tabata Y, Miyake Y, Akita Y, Yoshimoto M, et al. Self-organized near-field etching of the sidewalls of glass corrugations. *Applied Physics B*. 2011; 103: 527-530. Available from: https://doi.org/10.1007/s00340-011-4569-1.
[31] Teki R, Kadaksham AJ, House M, Harris-Jones J, Ma A, Babu SV, et al. Alternative smoothing techniques to mitigate EUV substrate defectivity. In: *Extreme Ultraviolet (EUV) Lithography III.* California, United States: SPIE; 2012. p.83220B. Available from: https://doi.org/10.1117/12.916497.
[32] Yatsui T, Nomura W, Stehlin F, Soppera O, Naruse M, Ohtsu M. Challenges in realizing ultraflat materials surfaces. *Beilstein Journal of Nanotechnology*. 2013; 4: 875-885. Available from: https://doi.org/10.3762/bjnano.4.99.
[33] Nomura W, Yatsui T, Yanase Y, Suzuki K, Fujita M, Kamata A, et al. Repairing nanoscale scratched grooves on polycrystalline ceramics using optical near-field assisted sputtering. *Applied Physics B*. 2010; 99: 75-78. https://doi.org/10.1007/s00340-009-3797-0.
[34] Yatsui T, Nomura W, Naruse M, Ohtsu M. Realization of an atomically flat surface of diamond using dressed photon–phonon etching. *Journal of Physics D: Applied Physics*. 2012; 45(47): 475302. Available from: https://doi.org/10.1088/0022-3727/45/47/475302.

[35] Hirschman KD, Tsybeskov L, Duttagupta SP, Fauchet P. Silicon-based visible light-emitting devices integrated into microelectronic circuits. *Nature*. 1996; 384: 338-341. Available from: https://doi.org/10.1038/384338a0.
[36] Lu ZH, Lockwood DJ, Baribeau JM. Quantum confinement and light emission in SiO_2/Si superlattices. *Nature.* 1995; 378: 258-260. Available from: https://doi.org/10.1038/378258a0.
[37] Kawazoe T, Mueed MA, Ohtsu M. Highly efficient and broadband Si homojunction structured near-infrared light emitting diodes based on the phonon-assisted optical near-field process. *Applied Physics B.* 2011; 104: 747-754. Available from: https://doi.org/10.1007/s00340-011-4596-y.
[38] Yamaguchi M, Kawazoe T, Ohtsu M. Evaluating the coupling strength of electron–hole pairs and phonons in a 0.9 μm-wavelength silicon light emitting diode using dressed-photon–phonons. *Applied Physics A*. 2014; 115: 119-125. Available from: https://doi.org/10.1007/s00339-013-7904-z.
[39] Ohtsu M, Kawazoe T. Principles and practices of Si light emitting diodes using dressed photons. *Advanced Materials Letters*. 2019; 10(12): 860-867. Available from: https://doi.org/10.5185/amlett.2019.2264.
[40] Tanaka Y, Kobayashi K. Optical near field dressed by localized and coherent phonons. *Journal of Microscopy.* 2008; 229(2): 228-232. Available from: https://doi.org/10.1111/j.1365-2818.2008.01891.x.
[41] Kawazoe T, Nishioka K, Ohtsu M. Polarization control of an infrared silicon light-emitting diode by dressed photons and analyses of the spatial distribution of doped boron atoms. *Applied Physics A*. 2015; 121: 1409-1415. Available from: https://doi.org/10.1007/s00339-015-9288-8.
[42] Wada N, Kawazoe T, Ohtsu M. An optical and electrical relaxation oscillator using a Si homojunction structured light emitting diode. *Applied Physics B*. 2012; 108: 25-29. Available from: https://doi.org/10.1007/s00340-012-5100-z.
[43] Sakuma H, Ojima I, Ohtsu M, Kawazoe T. Drastic advancement in nanophotonics achieved by a new dressed photon study. *Journal of the European Optical Society-Rapid Publications.* 2021; 17: 28. Available from: https://doi.org/10.1186/s41476-021-00171-w.
[44] Hanbury Brown R, Twiss RQ. A test of a new type of stellar interferometer on Sirius. *Nature*. 1956; 178, 1046-1048. Available from: https://doi.org/10.1038/1781046a0.
[45] Wightman AS. On the localizability of quantum mechanical systems. *Reviews of Modern Physics*. 1962; 34(4): 845-872. Available from: https://doi.org/10.1103/RevModPhys.34.845.
[46] Tanaka H, Kawazoe T, Ohtsu M, Akahane K. Decreasing the threshold current density in Si lasers fabricated by using dressed-photons. *Fluorescent Materials*. 2015; 1(1): 1-7. Available from: https://doi.org/10.1515/fma-2015-0001.
[47] Kawazoe T, Hashimoto K, Sugiura S. High-power current-injection type silicon laser using nanophotonics. In: *EMN Meeting on Nanocrystals, 17-21 October 2016, Xi'an, China*. China: EMN; 2016. p.9-11.
[48] Aspect A, Grangier P, Roger G. Experimental tests of realistic local theories via Bell's theorem. *Physical Review Letters*. 1981; 47(7): 460. Available from: https://doi.org/10.1103/PhysRevLett.47.460.
[49] Einstein A, Podolsky B, Rosen N. Can quantum-mechanical description of physical reality be considered complete? *Physical Review*. 1935; 47(10): 777-780. Available from: https://doi.org/10.1103/PhysRev.47.777.
[50] Doplicher S, Haag R, Roberts JE. Fields, observables and gauge transformations I. *Communications in Mathematical Physics*. 1969; 13: 1-23. Available from: https://doi.org/10.1007/BF01645267.
[51] Doplicher S, Haag R, Roberts JE. Fields, observables and gauge transformations II. *Communications in Mathematical Physics*. 1969; 15: 173-200. Available from: https://doi.org/10.1007/BF01645674.
[52] Doplicher S, Roberts JE. Why there is a field algebra with a compact gauge group describing the superselection structure in particle physics. *Communications in Mathematical Physics*. 1990; 131(1): 51-107. Available from: https://doi.org/10.1007/BF02097680.
[53] Nambu Y, Jona-Lasinio G. Dynamical model of elementary particles based on an analogy with superconductivity. I. *Physical Review*. 1961; 122(1): 345-358. Available from: https://doi.org/10.1103/physrev.122.345.
[54] Lehmann H, Symanzik K, Zimmermann W. Zur formulierung quantisierter feldtheorien. *Il Nuovo Cimento*. 1955; 1: 205-225. Available from: https://doi.org/10.1007/bf02731765.
[55] Streater RF, Wightman AS. *PCT, spin and statistics, and all that*. Princeton: Princeton University Press; 1964.
[56] Dell'Antonio GF. Support of a field in *p* space. *Journal of Mathematical Physics*. 1961; 2(6): 759-766. Available from: https://doi.org/10.1063/1.1724219.
[57] Jost R. *The general theory of quantized fields*. Providence, RI, USA: American Mathematical Society; 1965.
[58] Sakuma H, Ojima I, Saigo H, Okamura K. Conserved relativistic Ertel's current generating the vortical and thermodynamic aspects of space–time. *International Journal of Modern Physics A*. 2022; 37(22): 2250155. Available from: https://doi.org/10.1142/s0217751x2250155x.
[59] Bers A, Fox R, Kuper CG, Lipson SG. The impossibility of free tachyons. In: Kuper CG, Peres A. (eds.) *Relativity*

and Gravitation. New York, USA: Gordon and Breach Science Publishers; 1971.
[60] Lamb H. *Hydrodynamics*. 6th ed. Cambridge: Cambridge University Press; 1930. p.248-249.
[61] Sakuma H, Ojima I, Ohtsu M. Dressed photons in a new paradigm of off-shell quantum fields. *Progress in Quantum Electronics.* 2017; 55: 74-87. Available from: https://doi.org/10.1016/j.pquantelec.2017.07.006.
[62] Sakuma H. Virtual photon model by spatio-temporal vortex dynamics. In: Yatsui T. (ed.) *Progress in Nanophotonics 5*. 2018. Cham: Springer; 2018. p.53-77. Available from: https://doi.org/10.1007/978-3-319-98267-0_2.
[63] Sakuma H, Ojima I, Ohtsu M, Ochiai H. Off-shell quantum fields to connect dressed photons with cosmology. *Symmetry*. 2020; 12(8): 1244. Available from: https://doi.org/10.3390/sym12081244.
[64] Aharonov Y, Komar A, Susskind L. Superluminal behavior, causality, and instability. *Physical Review*. 1969; 182(5): 1400-1403. Available from: https://doi.org/10.1103/physrev.182.1400.
[65] @Hongwan Liu. The cosmological constant is measured as the dimensionless quantity. [cited 2013 December 24.] https://www.quora.com/What-is-the-best-estimate-of-the-cosmological-constant/answer/Hongwan-Liu [Accessed 24th February 2019]
[66] Aoki S, Onogi T, Yokoyama S. Charge conservation, entropy current and gravitation. *International Journal of Modern Physics A*. 2021; 36(29): 2150201. Available from: https://doi.org/10.1142/s0217751x21502018.
[67] Penrose R. Before the big bang: an outrageous new perspective and its implications for particle physics. In: *Proceedings of EPAC 2006*. Edinburgh, Scotland: EPAC; 2006. p.2759-2762. Available from: https://accelconf.web.cern.ch/e06/PAPERS/THESPA01.PDF.
[68] Sakuma H, Ojima I. On the dressed photon constant and its implication for a novel perspective on cosmology. *Symmetry.* 2021; 13(4): 593. Available from: https://doi.org/10.3390/sym13040593.
[69] Kurzweil R. *The singularity is near: When humans transcend biology*. New York: Viking Penguin; 2005.
[70] Penrose R. *Shadows of the mind*. Oxford: Oxford University Press; 1994.
[71] Simons Foundation. *Hilbert's problems: 23 and math*. https://www.simonsfoundation.org/2020/05/06/hilberts-problems-23-and-math/ [Accessed 16th December 2022].
[72] László E. *Ervin Laszlo*. https://ervinlaszlobooks.com/ [Accessed 21st December 2022].
[73] Kelly EF, Kelly EW, Crabtree A, Gauld A, Grosso M, Greyson B. *Irreducible mind: Toward a psychology for the 21st century*. Lanham: Rowman & Littlefield; 2007.
[74] Alexander E. *Proof of heaven: A neurosurgeon's journey into the afterlife*. New York: Simon & Schuster; 2012.
[75] Tesla N. *My inventions: The autobiography of Nikola Tesla*. New York: Experimenter Publishing Company, Inc.; 1919.
[76] Okabe M. *Humanomics: Exploring economics based on human nature (in Japanese)*. Tokyo, Japan: Nippon Hyoronsha, 2022.
[77] Takahashi K. *The path of prayer: For a supreme dialogue*. Trans Ridley C. Tokyo, Japan: Sampoh Publishing Co., Ltd.; 2014.
[78] Takahashi K. *The soul doctrine as a way of life: 5 inner revolutions to change life and work*. Trans Brooks W. Tokyo, Japan: Sampoh Publishing Co., Ltd; 2017.
[79] Hancock G. *About the speaker, Graham Hancock*. https://www.alternatives.org.uk/event/ancient-apocalypse [Accessed 5th October 2022].
[80] Firestone RB, West A, Kennett JP, Becker L, Bunch TE, Revay ZS, et al. Evidence for an extraterrestrial impact 12,900 years ago that contributed to the megafaunal extinctions and the Younger Dryas cooling. *Proceedings of the National Academy of Sciences*. 2007; 104(41): 16016-16021. Available from: https://doi.org/10.1073/pnas.0706977104.

[IV] PREPRINT DEPOSITORIES

[IV-1] OFF-SHELL ARCHIVE

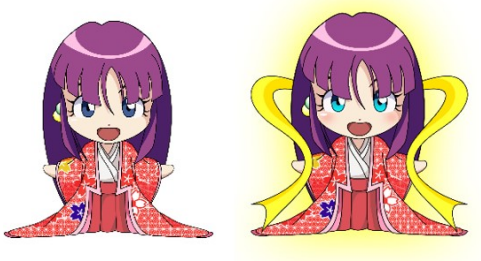

Quantum walk analyses of the off-shell scientific features of dressed-photon–phonon transfers among a small number of nanometer-sized particles

M. Ohtsu[1], E. Segawa[2], K. Yuki[3], and S. Saito[4]

[1]Research Origin for Dressed Photon,3-13-19 Moriya-cho, Kanagawa-ku, Yokohama, Kanagawa 221-0022, Japan

[2]Yokohama National University, 79-8 Tokiwadai, Hodogaya-ku, Yokohama, Kanagawa 240-8501, Japan

[3]Middenii, 3-3-13 Nishi-shinjuku, Sinjuku-ku, Tokyo 160-0023, Japan

[4]Kogakuin University, 2665-1, Nakano-machi, Hachioji, Tokyo 192-0015, Japan

Abstract

This paper reports the results of numerical calculation of the output signal intensity emitted from a nanometer-sized particle (NP) located at the center of the surrounding NPs. A blown-up quantum walk model is used for these calculations. When the number of these NPs is as small as 4–6, the output signal intensity shows a drastic increase. This increasing feature agrees with the experimental results and implies that the dressed-photon–phonon autonomously transfers in a microscopic system composed of a small number of NPs, which is a typical off-shell scientific phenomenon.

1. Introduction

A dressed photon (DP) is a quantum field created by the interaction between photons and electrons (or excitons) in a nanometer-sized particle (NP) under light irradiation. The created DP localizes at the NP. It is an off-shell quantum field because its momentum has large uncertainty due to its subwavelength size [1, 2].

Since the DP creation originates from the light–matter interaction in a microscopic space, a spacelike momentum field must be introduced into the electromagnetic field theory. This has recently been successful in off-shell science, allowing physical pictures of the creation process to be drawn. These successful pictures have revealed the following [3,4]:

(1) A microscopic material field (a timelike momentum field) interacts with a vector boson field.

(2) In addition to a stable pair of Majorana fermions (a spacelike momentum field), an unstable pair consisting of a Majorana particle and anti-particle (timelike momentum fields) is created.

(3) Although this unstable pair annihilates within a short time duration, a novel light field (a timelike momentum field) remains at the microscopic material. This is the DP.

Furthermore, the DP couples with a phonon to create a new quantum field, named a dressed-photon–phonon (DPP). The spatial behavior of the transfer of this created DPP was analyzed by using

a quantum walk (QW) model [5], and the results of this analysis agreed well with experimental results [6-12]. This paper reports the results of numerical calculations that were carried out for studying the experimentally found unique features of DPP transfer among a small number of NPs.

2. Review of experimental results

This section reviews experiments conducted to improve the optical/electrical energy conversion efficiency of a silicon photodiode (Si-PD: Hamamatsu Photonics K.K., Si photodiode S2388: Active surface area 5.8 mm × 5.8 mm) [13,14]. As schematically explained by Fig. 1(a), small and large NPs (NP_S and NP_L) were used, which were made of CdSe spherical particles. Their average diameters were 2.0 nm and 2.8 nm, respectively. These NPs were dispersed in a mixed solution of toluene and an ultraviolet (UV)-curable resin. The volume density of the dispersed NPs was controlled so that the average distance between NPs was around 40 nm. Half of the Si-PD surface was spin-coated with a resin containing a mixture of NP_S and was cured by UV radiation, whereas the other half of the surface was coated with the same resin without the NP mixture. F_{DPP} and F_0 in Fig. 1(a) represent the cured resin films on the Si-PD surface with and without the NPs, respectively. After the DPP transfers from NP_S to NP_L in F_{DPP} and creates an exciton in the higher energy level of NP_L, the exciton relaxes to the lowest energy level to emit a photon. It should be noted that the energy of this photon is red-shifted* due to the relaxation of the exciton.

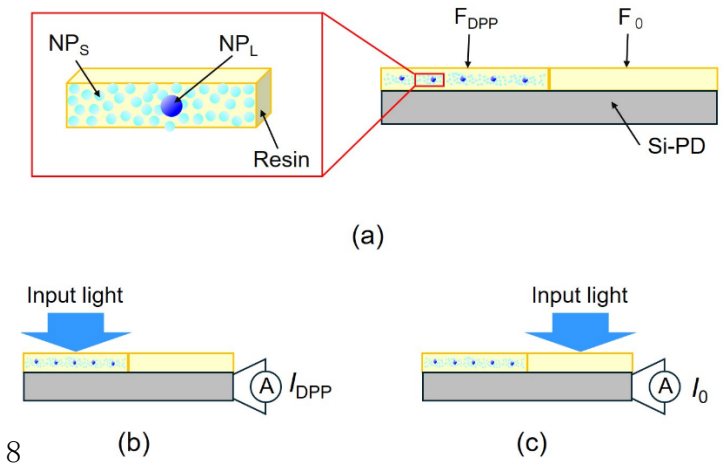

Fig. 1 A silicon photodiode on which a cured resin film is coated.

(a) Cross-sectional profile.

(b), (c) Generated photocurrents (I_{DPP} and I_0) by radiating input light onto the films F_{DPP} and F_0, respectively.

By using a deuterium lamp and a halogen lamp (wavelength: 300–400 nm) as input light sources, the photocurrents I_{DPP} and I_0, generated in the Si-PD under the films F_{DPP} and F_0, respectively, were measured. Since the Si-PD is sensitive to visible light, the photocurrent I_{DPP} (Fig. 1(b)) is larger than I_0 (Fig. 1(c)). The rate of increase of the photocurrent is defined by

$$\Delta\eta \equiv \left(I_{\mathrm{DPP}} - I_0\right)/I_0 \,. \tag{1}$$

Figure 2 shows the measured value of $\Delta\eta$ [13,14], which shows that $\Delta\eta$ is larger than 10 % when the ratio $n\left(=n_{\mathrm{S}}/n_L\right)$ between the numbers n_{S} and n_L of $\mathrm{NP_S}$ and $\mathrm{NP_L}$ is in the range of 2–6. This drastic increase and the unique dependence on n are typical off-shell scientific phenomena that have never been observed in the case of conventional on-shell scientific methods. The following sections analyze these phenomena by employing an off-shell scientific QW numerical calculation.

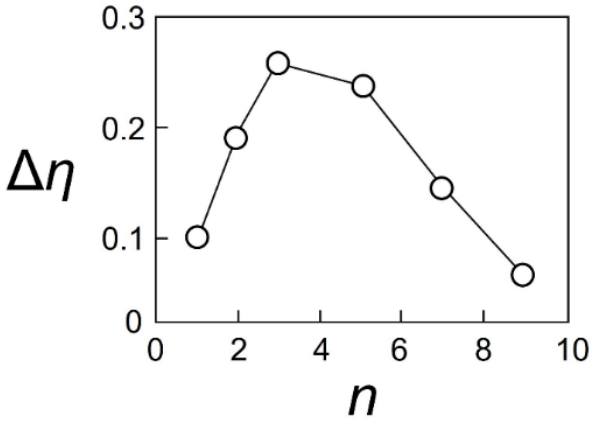

Fig. 2 Measured values of the rate of increase $\Delta\eta$ of the photocurrent.
The horizontal axis is the ratio n between the numbers of $\mathrm{NP_S}$ and $\mathrm{NP_L}$.

(*) This is conversion from UV to visible light energy. It has been advantageously used not only to improve optical/electrical energy conversion efficiency but also to protect the Si-PD surface from deterioration induced by UV exposure [13,14].

3. A blown-up quantum walk model

This section presents a QW model for analyzing the unique features of the DPP transfer from $\mathrm{NP_S}$ to $\mathrm{NP_L}$. Here, the optical/electrical energy conversion process in Fig. 1 does not have to be included in this model because this conversion occurs after the DPP transfer completes.

Figure 3 schematically explains how to apply the incident light (input signal) to $\mathrm{F_{DPP}}$ in Fig. 1 and generate the emitted light (output signal). The DPP transfer in the three-dimensional $\mathrm{F_{DPP}}$ is modelled by two-dimensional arrangements of $\mathrm{NP_S}$ and $\mathrm{NP_L}$ in Fig. 4, in which n $\mathrm{NP_S}$ (white circles ○) are arranged around one $\mathrm{NP_L}$ (gray circle ●). A DPP is created at these $\mathrm{NP_S}$s by light irradiation (an input signal) and transfers to the $\mathrm{NP_L}$. Since the different-sized $\mathrm{NP_S}$ and $\mathrm{NP_L}$ were used in the experiment only to allow the exciton to relax to the lowest energy level of $\mathrm{NP_L}$ and since the relaxation process is unrelated to the DPP transfer from $\mathrm{NP_S}$ to $\mathrm{NP_L}$, this size difference does not have to be considered in the present QW model.

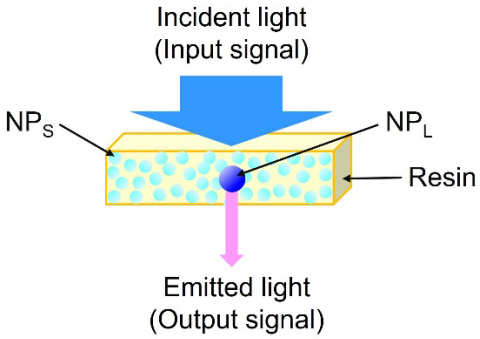

Fig. 3 How to apply the incident light (input signal) to F_{DPP} and generate the emitted light (output signal).

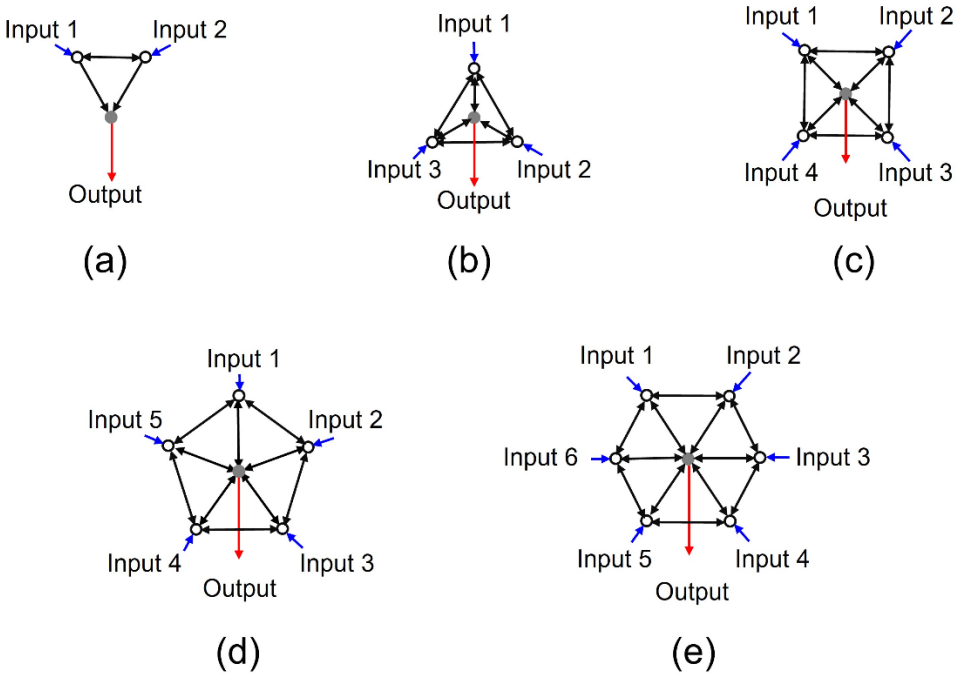

Fig. 4 Two-dimensional arrangements of NP_S and NP_L.
They are represented by white circles (○) and a gray circle (●), respectively.
(a)-(e) are for $n = 2 - 6$.

The two-dimensional QW model of the arrangements in Fig. 4 has been formulated for calculating the intensity of a generated output signal [15]. In this model, in the case of Fig. 4(c) ($n = 4$), as an example, the sites for four input signals (white circles ○) are blown up, and four internal sites are attached. They are represented by small black circles on the circumferences of the white circles in Fig. 5. These attachments are to establish routes of transfer in and out of the DPP (represented by a pair of curved arrows). These internal sites are also attached to the blown-up site for the output signal (gray circle ● in Fig. 5). Finally, a side cycle (a closed loop represented by an

∞-shaped thick gray curve in Fig. 5) is selected to identify the DPP transfer route that passes through both the internal sites for input and output signals. Such internal sites and side cycle are attached also to the arrangements in Figs. 4(a), (b), (d), and (e). Their details are described in Ref. [15].

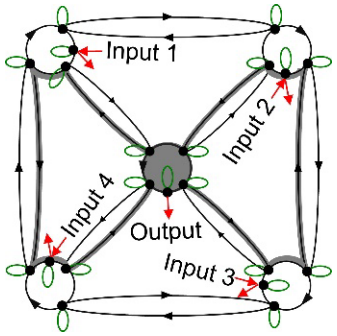

Fig. 5 Schematic explanation of a blown-up quantum walk model.

Internal sites are represented by small black circles on the circumferences of the four white circles and a gray circle. The closed loop is a side cycle that is represented by an ∞-shaped thick gray curve.

In order to represent the experimentally observed phenomenon of photon breeding with respect to photon momentum [10], it is assumed that the DP-phonon coupling constant χ [5] takes different values for the DP that hops along the directions parallel (χ_1) and anti-parallel (χ_2) to that of the incident light propagation. That is, the possibility of photon breeding occurring is assumed to be higher in the case of $\chi_1 > \chi_2$ than that of $\chi_1 < \chi_2$. The difference between these constants is represented by introducing a parameter ε into

$$\chi_1 / \chi_2 = \sqrt{(1+\varepsilon)/(1-\varepsilon)}\,. \tag{2}$$

For comparing with the case of $\chi_1 < \chi_2$, the value of ε is allowed to vary in the range of

$$-1 < \varepsilon < 1\,. \tag{3}$$

From the QW model constructed above, Ref. [15] derived the stationary value P_{OS} of the output signal intensity, which was the value realized a sufficiently long time after the input signal was applied (refer to Fig. 10(a) in Section 5). The results demonstrated the following unique off-shell scientific features of the DPP transfer:

(1) P_{OS} increases with increasing n and asymptotically approaches $(1+\varepsilon)^2$.

(2) P_{OS} is 1 at $n = 2$, which is independent of ε.

(3) P_{OS} for $n = 3$ is equal to that for $n = 6$.

(4) P_{OS} is 1 in the case of $\varepsilon = 0$, which is independent of n.

(5) P_{OS} is independent of χ/J, where J is the hopping energy of the DP [5].

4. Results of numerical calculations

Numerical calculations were carried out by referring to the theoretical results (1)–(5) in Section 3. Figure 6 shows the calculated relation between $n(=2\text{-}12)$ and P_{OS}. Here, the value χ/J was fixed at 1 by referring to (5) in Section 3. Figs. 6(a)-(c) and (e)-(g) are the relations for $\varepsilon>0$ ($\chi_1>\chi_2$) and for $\varepsilon<0$ ($\chi_1<\chi_2$), respectively. Figure 6(d) is for $\varepsilon=0$ ($\chi_1=\chi_2$).

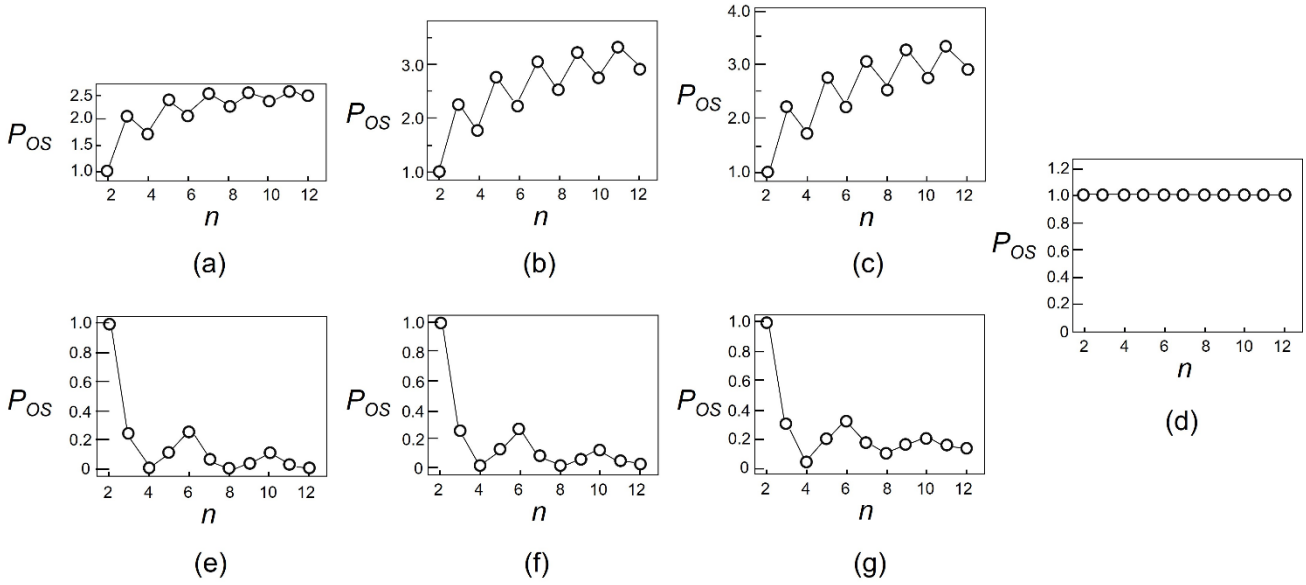

Fig. 6 Calculated relation between n and P_{OS}.
The value χ/J was fixed at 1.

(a)-(c) ε =0.600, 0.923, and 0.981 (χ_1/χ_2 =2, 5, and 10). (d) $\varepsilon=0$ (χ_1/χ_2 =1).

(e)-(g) ε =-0.981, -0.923, and -0.600 (χ_1/χ_2 =0.1, 0.2, and 0.5).

Figure 7 shows the relation between χ_1/χ_2 in Eq. (2) and S_n. Here, S_6 and S_{12} are the sums of P_{OS} in Fig. 6 over $n=2\text{-}6$ and $n=2\text{-}12$, respectively. This figure indicates that the value S_n is small when $\chi_1/\chi_2<1$. However, it increases rapidly with increasing χ_1/χ_2 when $\chi_1/\chi_2>1$. As a result, S_n takes a large value in the case of $\chi_1>\chi_2$. This result agrees with the experimental result for photon breeding with respect to photon momentum.

In Figs. 6(a)-(c), P_{OS} increases with increasing n while varying in a pulsatory manner, as schematically explained by the broken curve and white circles in Fig. 8(a), respectively. (For comparison, Figs. 6(e)-(g) show that P_{OS} decreases with pulsatory variations, as explained by Fig. 8(b).) Increases in Figs. 6(a)-(c) and Fig. 8(a) represent the typical on-shell scientific feature because

P_{OS} often increases with increasing number of NPs in a macroscopic-sized system composed of a large number of NPs. In contrast, the pulsatory variation, which is conspicuously seen in the case of a small number n, is the off-shell scientific feature of the microscopic-sized system. In order to analyze this pulsatory feature, the magnitude of deviation of the white circle from the broken curve in Fig. 8(a) is defined by

$$\Delta p_{\mathrm{OS}}(n) \equiv \frac{\left|P_{\mathrm{OS}}(n) - P_{\mathrm{OS}}(n-1)\right|}{P_{\mathrm{OS}}(n) + P_{\mathrm{OS}}(n-1)}. \tag{4}$$

Figure 9(a) is the calculated result for $\varepsilon > 0$. It shows that $\Delta p_{\mathrm{OS}}(n)$ takes a large value in the range of $n = 4\text{-}6$, which agrees with the experimental results in Fig. 2, and thus, the correlation with photon breeding with respect to photon momentum is confirmed*. For comparison, Fig. 9(b) shows the results for $\varepsilon < 0$, in which the value of $\Delta p_{\mathrm{OS}}(n)$ shows a complicated dependency on n. Especially for $\varepsilon = -0.981$, it takes large values at n=4, 5, 8, 9, and 12. It originates from very small values of P_{OS} (Figs. 6(a)-(c) and 7) due to the low probability of photon breeding occurring.

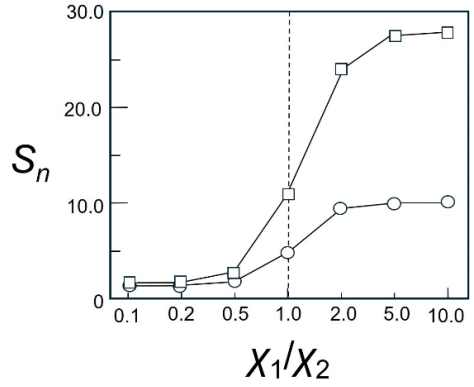

Fig. 7 Relation between χ_1/χ_2 and S_n.
S_6 and S_{12} are the sums of P_{OS} in Fig. 6 over $n = 2\text{-}6$ and $n = 2\text{-}12$, respectively.

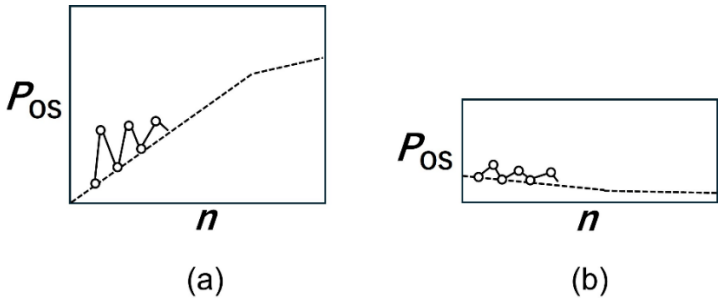

Fig. 8 Schematic explanation of the variations (broken curves) of P_{OS} and pulsatory deviation (white circles) from the broken curves.
(a) and (b) are for the case of $\varepsilon > 0$ and $\varepsilon < 0$, respectively.

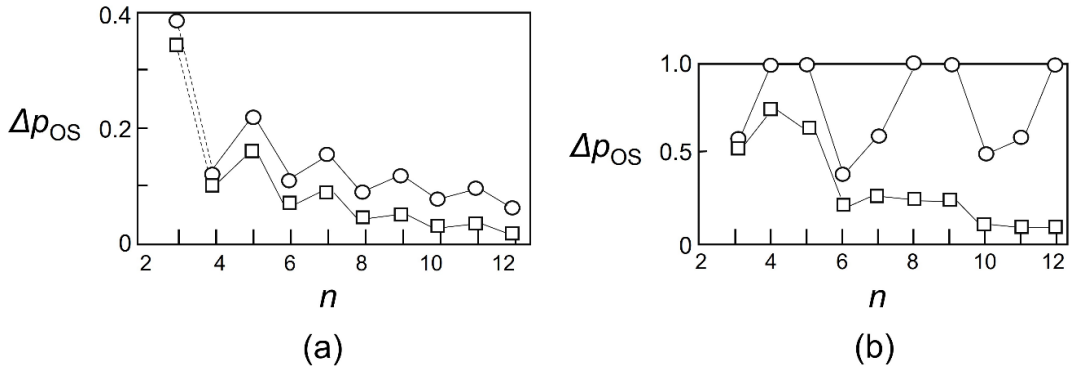

Fig. 9 Relation between n and $\Delta p_{\mathrm{OS}}(n)$.

(a) For the case of $\varepsilon > 0$. White circles and squares are for ε =+0.981 and +0.600, respectively.

(b) For the case of $\varepsilon < 0$. White circles and squares are for ε =-0.981 and -0.600, respectively.

(*) Figure 9(a) shows that $\Delta p_{\mathrm{OS}}(n)$ takes a distinctly large value at $n = 3$. Since it originates from feature (2) in Section 3, further studies on the QW model are required to explore this origin.

5. Discussion

In Fig. 9(a), large values of $\Delta p_{\mathrm{OS}}(n)$ in the range $n = 4\text{-}6$ imply that the phenomena occurring in a microscopic system composed of a small number n are very different from those in a macroscopic system. Although the macroscopic phenomena follow the popular on-shell scientific principle of least action, the large values in Fig. 9(a) mean that the DPP in the microscopic system is free from this principle and can transfer in an autonomous manner. Such autonomous transfer has been implied by a variety of experimental results on DPPs, including the experimental results in Fig. 2 [11].

In further studies on the autonomous transfer, it could be advantageous to analyze the temporal variation of the output signal intensity $P_{\mathrm{O}}(t)$ in the transient time period that starts immediately after the input signal is applied to the system. Figure 10(a) shows the profile of $P_{\mathrm{O}}(t)$. Figures 10(b) and (c) show the calculated time t_{s} required to converge to the stationary value P_{OS} for $\varepsilon > 0$ and for $\varepsilon < 0$, respectively. This time t_{s} depends on n for $\varepsilon > 0$ (Fig. 10(b)). In contrast, it is independent of n for $\varepsilon < 0$ (Fig. 10(c)). Calculations also found that the time t_{s} depended on the value of χ/J, which is different from feature (5) in Section 3.

Furthermore, within the transient time period ($t < t_{\mathrm{S}}$), $P_{\mathrm{O}}(t)$ pulsates in the case of $\varepsilon > 0$, and can take a larger value (white square in Fig. 10(a)) than P_{OS}. This pulsatory variation feature implies that the DPP tries to find the transfer routes in Fig. 5 in a unique manner to autonomously fix the optimum route to the $\mathrm{NP_L}$. To investigate this further, temporal variations of the DPP creation probabilities should be evaluated more quantitatively, not only for the output terminal $\mathrm{NP_L}$ but also

for each NP_S.

Since the positions and sizes of NP_S and NP_L can fluctuate when they are dispersed in the UV-curable resin in Fig. 1(a) [16], the QW model in Figs. 4 and 5 should be slightly modified by taking these fluctuations into account. Furthermore, it may be advantageous to replace the two-dimensional model in Fig. 4 by a three-dimensional one [10]. More accurate comparisons between calculated and experimental results are expected by doing so.

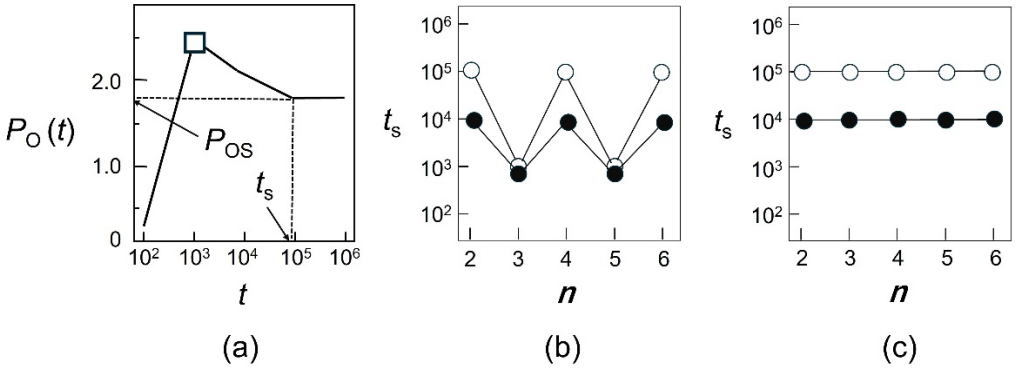

Fig. 10 Temporal variation of the output signal intensity $P_O(t)$.

(a) Profile of $P_O(t)$ for n=5 and ε=+0.981. t_s represents the time required to converge to the stationary value P_{OS}. The white square represents the value at the peak of the pulsatory variation, which is larger than P_{OS}.

(b) For the case of $\varepsilon > 0$. White and black circles are for ε=+0.981 and +0.923, respectively.

(c) For the case of $\varepsilon < 0$. White and black circles are for ε=-0.981 and -0.923, respectively.

6. Summary

This paper reported the results of numerical calculations of the output signal intensity emitted from a nanometer-sized particle (NP: output terminal), which was located at the center of surrounding NPs (input terminals). A blown-up quantum walk model was used for these calculations, and the results indicated that the output intensity increased with increasing number of surrounding NPs. However, when this number was as small as 4–6, the intensity deviated from this trend and showed a drastic increase. This agreed with the experimental results. This deviation implied that the DPP autonomously transferred in a microscopic system composed of a small number of NPs, which is a typical off-shell scientific phenomenon.

References

[1] M. Ohtsu, I. Ojima, and H. Sakuma, “Dressed Photon as an Off-Shell Quantum Field,” Progress in Optics Vol.64, (ed. T.D. Visser) pp.45-97 (Elsevier, 2019).

[2] M. Ohtsu, , *Off-Shell Applications In Nanophotonics*, Elsevier, Amsterdam (2021) p.5.

[3] H. Sakuma, I. Ojima, M. Ohtsu, and T. Kawazoe, Drastic advancement in nanophotonics achieved by a new dressed photon study, “JEOS-RP (2021) **17**: 28.

[4] H. Sakuma, I. Ojima, and M. Ohtsu, “Perspective on an Emerging Frontier of Nanoscience Opened up by Dressed Photon Studies,” *Nanoarchitectonics*, Vol. 5, Issue 1 (2024) pp.1-23.

[5] M. Ohtsu, “A Quantum Walk Model for Describing the Energy Transfer of a Dressed Photon,” *Off-shell Archive* (September, 2021) OffShell: 2109R.001.v1.

DOI 10.14939/2109R.001.v1, http://offshell.rodrep.org/?p=345

[6] M. Ohtsu, E. Segawa, and K. Yuki, “Numerical calculation of a dressed photon energy transfer based on a quantum walk model,” *Off-shell Archive* (June, 2022) OffShell: 2206O.001.v1.

DOI 10.14939/2206O.001.v1

https://rodrep.or.jp/en/off-shell/original_2206O.001.v1.html

[7] M. Ohtsu, E. Segawa, K. Yuki, and S. Saito, “Dressed-photon—phonon creation probability on the tip of a fiber probe calculated by a quantum walk model,” *Off-shell Archive* (December, 2022) OffShell: 2212O.001.v1.

DOI 10.14939/2212O.001.v1

https://rodrep.or.jp/en/off-shell/original_2212O.001.v1.html

[8] M. Ohtsu, E. Segawa, K. Yuki, and S. Saito,’ “Spatial distribution of dressed-photon–phonon confined by an impurity atom-pair in a crystal,” *Off-shell Archive* (January, 2023) Offshell: 2301O.001.v1.

DOI 10.14939/2301O.001.v1

https://rodrep.or.jp/en/off-shell/original_2301O.001.v1.html

[9] M. Ohtsu, E. Segawa, K. Yuki, and S. Saito,’ “A quantum walk model with energy dissipation for a dressed-photon–phonon confined by an impurity atom-pair in a crystal,” *Off-shell Archive* (April, 2023) Offshell: 2304O.001.v1.

DOI 10.14939/2304O.001.v1

https://rodrep.or.jp/en/off-shell/original_2304O.001.v1.html

[10] M. Ohtsu, E. Segawa, K. Yuki, and S. Saito,’ “Analyses of photon breeding with respect to photon spin by using a three-dimensional quantum walk model,” *Off-shell Archive* (November, 2023) Offshell: 2311O.001.v1.

DOI 10.14939/2311O.001.v1

https://rodrep.or.jp/en/off-shell/original_2311O.001.v1.html

[11] M.Ohtsu "Off-shell scientific nature of dressed photon energy transfer and dissipation," Offshell: 2404R.001.v1.

DOI 10.14939/2404R.001.v1

https://rodrep.or.jp/en/off-shell/review_2404R.001.v1.html

[12] M.Ohtsu, E.Segawa, K.Yuki, and S.Saito "Optimum dissipation for governing the autonomous transfer of dressed photons," Offshell: 2405O.oo1.v1.

DOI 10.14939/2405O.001.v1

https://rodrep.or.jp/en/off-shell/original_2405O.001.v1.html

[13] M. Naruse, T. Kawazoe, R. Ohta, W. Nomura, M. Ohtsu, "Optimal mixture of randomly dispersed quantum dots for optical excitation transfer via optical near-field interactions," Phys. Rev. B **80**, 125325 (2009)

[14] M. Naruse, K. Leibnitz, F. Peper, N. Tate, W. Nomura, T. Kawazoe, M. Murata, M. Ohtsu, “Autonomy in excitation transfer via optical near-field interactions and its implications for information networking,” Nano Commun. Networks **2**, (2011) pp. 189-195.

[15] E. Segawa, S. Saito, K. Yuki, M. Ohtsu, "Paths on the graph chosen autonomously by dressed photons from the

quantum walk model, " Abstracts of the 85th Jpn. Soc. Appl. Phys. Autumn Meeting, (September 16-20, 2024) (Toki Messe, Niigata) paper number 18p-A33-18. To be presented (in Japanese).
[16] W. Nomura, T. Yatsui, T. Kawazoe, M. Naruse, and M. Ohtsu, "Structural dependence of optical excitation transfer via optical near-field interactions between semiconductor quantum dots," Appl. Phys. - Lasers and Optics, Vol. 100, July 2010, pp.181-187.

Optimum dissipation for governing the autonomous transfer of dressed photons

M. Ohtsu[1], E. Segawa[2], K. Yuki[3], and S. Saito[4]

[1]Research Origin for Dressed Photon,3-13-19 Moriya-cho, Kanagawa-ku, Yokohama, Kanagawa 221-0022, Japan

[2]Yokohama National University, 79-8 Tokiwadai, Hodogaya-ku, Yokohama, Kanagawa 240-8501, Japan

[3]Middenii, 3-3-13 Nishi-shinjuku, Sinjuku-ku, Tokyo 160-0023, Japan

[4]Kogakuin University, 2665-1, Nakano-machi, Hachioji, Tokyo 192-0015, Japan

Abstract

This paper claims that the unique features of dressed photon (DP) transfer are governed by the DP energy dissipation. First, problems on theoretical descriptions of DP creation, transfer, and measurement are presented, and strategies for solving them are also indicated. Second, experimental results of DP measurement are reviewed. It is pointed out that these results follow a principle that differs from the on-shell scientific principle of least action. Third, in order to analyze these results, a theoretical non-unitary quantum walk model is presented by considering energy dissipation. Finally, calculated results are presented, suggesting that an optimum dissipation constant of the dressed-photon–phonon energy exists. It is also claimed that the transfer path with such optimum dissipation is autonomously determined to minimize the decreases in the emitted light power. In other words, this determination is governed by the off-shell scientific principle of largest output signal.

1. Introduction

A large number of novel phenomena that originate from the nature of the dressed photon (DP) have been experimentally found and applied to realize innovative technologies [1]. As an introduction to this paper, this section summarizes the principles of DP creation, transfer, and measurement [2], as follows:

[1] Creation (Fig. 1(a)): A DP is created on a nanometer-sized particle (NP) by the interaction between a light field and a microscopic material field.

[2] Transfer (Fig. 1(b) and (c)): If a second NP (NP_2) is placed in close proximity to the first NP (NP_1) (Fig.1(b)), the DP on NP_1 transfers to NP_2. This transfer between these NPs is bi-directional because it originates from the interaction between the NPs. Even when the number of NPs is increased to N (Fig. 1(c): NP_1 to NP_N), bi-directional transfer of the DP also occurs.

[3] Measurement (Fig. 1(d)): For measuring the DP, a larger-sized NP (NP_L) is placed at the end of

an array of smaller-sized NPs (NP_S) [3]. After the DP reaches NP_L by repetitive bi-directional transfers between the adjacent NP_Ss, an exciton is created in a higher energy level in NP_L. A part of its energy dissipates to the heat-bath, and the exciton relaxes to the lowest energy level. Subsequently, the exciton annihilates within a short time, resulting in propagating light emission, which is the DP energy dissipation to the external macroscopic space. This propagating light can be measured in the macroscopic space by using a conventional measurement instrument.

This paper claims that DP transfer is governed by the dissipation in the measurement process of **[3]**. Sections 2 reviews the problems that must be solved for giving theoretical descriptions of DP creation, transfer, and measurement, and also presents strategies for solving them. Section 3 reviews the experimental results of DP measurements and indicates that DPs have unique features that do not follow the conventional on-shell scientific principle. For analyzing these features, Section 4 proposes a method of introducing the concept of dissipation into the theorical quantum walk (QW) model. Section 5 describes the theoretical results and compares them with experimental ones. Section 6 presents a summary.

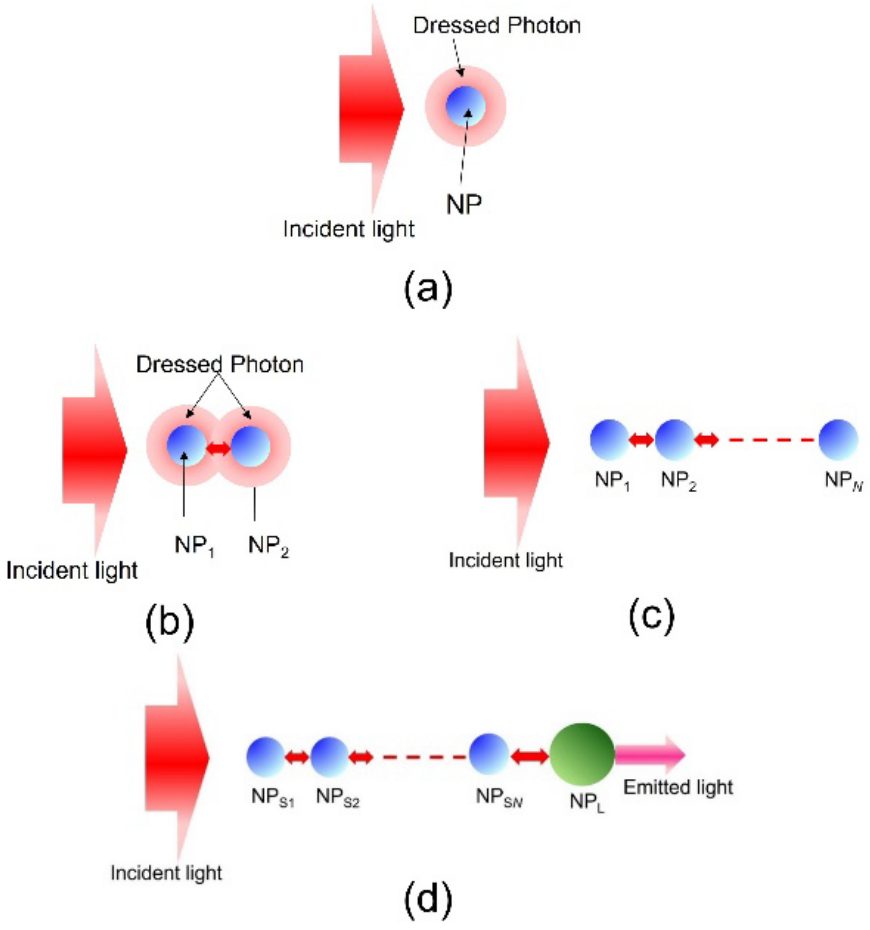

Fig. 1 Dressed photon (DP) creation, transfer, and measurement.

(a) DP creation. (b) Bi-directional transfer of DP between two nanometer-sized particles (NPs).

(c) Bi-directional transfer, where the number of NPs in (b) is increased from two to *N*.

(d) DP measurement.

2. Problems and strategies for solving them

Basic problems in the modern science have to be solved for theoretically describing DP creation, transfer, and measurement indicated in Fig. 1 in a unified manner. These problems, strategies for solving them, and the solutions derived so far by novel off-shell scientific methods are summarized as follows:

[1] Creation: Since the DP creation in Fig. 1(a) originates from the light–matter interaction in a microscopic space, a spacelike momentum field must be introduced into the electromagnetic field theory. Although conventional on-shell science has never succeeded in doing so, off-shell science has recently succeeded in drawing physical pictures of the creation process. These successful pictures are [4,5]:

(1) A microscopic material field (a timelike momentum field) interacts with a vector boson field.

(2) In addition to a stable pair of Majorana fermions (a spacelike momentum field), an unstable pair consisting of a Majorana particle and anti-particle (timelike momentum fields) is created (pair creation).

(3) Although this unstable pair annihilates within a short time duration (pair annihilation), a novel light field (a timelike momentum field) remains at the microscopic material. This is the DP.

[2] Transfer: Since DP transfer is a dynamic process in a microscopic complex system, the concept of interaction between NPs via exchange of a DP must be introduced into the theoretical model, and the position of the DP must be identified (Figs. 1(b) and (c)). Recent studies have found that a QW is a promising theoretical model for this introduction and identification [6-11]. This is because the principle of the QW and the nature of the DP have at least two common features:

(a) Nonreciprocity: A mathematical formulation of the QW uses nonreciprocal algebra that is composed of vectors and matrices. On the other hand, as has been described in **[1]** above, the DP is a field that originates from the interaction between NPs. Since the interaction is a typical nonreciprocal physical process, the QW and DP have a common feature, represented by nonreciprocity. This allows the QW to describe the interaction and the bi-directional DP transfer.

(b) Site: The QW deals with the phenomenon of the energy transfer from one site to its neighbor. On the other hand, since the DP is spatially localized$^{(*)}$, its quantum mechanical position operator can be defined. Thus, in the case where the site of the QW is the NP on which the DP is created, the position of the DP can be identified as the position of this site.

[3] Measurement: The DP transfer in Figs. 1(b) and (c) can neither be monitored nor measured in a macroscopic space because it occurs only in a microscopic space. For measurement, the DP energy must be delivered from the microscopic to the macroscopic space via energy dissipation (Fig. 1(d)). By introducing this dissipation into QW theory, it is transformed from unitary to non-unitary. The dissipation at the NP_Ss in a microscopic space plays a leading role in this delivery. The main purpose of this paper is to describe this role.

Table 1 summarizes the reviews **[1]** - **[3]** above. The concepts and strategies in this table are correlated among **[1]** - **[3]**.

Table 1 Concepts required for describing the DP creation/transfer/measurement and strategies for description

	[1] Creation	**[2] Transfer**	**[3] Measurement**
Phenomena and spaces	Light–matter interaction in a microscopic space	Dynamic behavior of a complex system in a microscopic space	Energy transfer from microscopic to macroscopic space
Concepts	Interaction	Nonreciprocity and sites	Dissipation
Strategies	Introducing the spacelike momentum field	Using a unitary QW model	Using a non-unitary QW model

(*) The theory of DP creation teaches that the spin of the electric DP is zero [4,5], which has also been experimentally confirmed. Such a zero-spin field is spatially localized, as indicated by Wightman's theorem [12].

3. Experimental results

This section reviews the experimental results in Fig. 1(d) [2]. As is schematically explained by Fig. 2(a), the experiments used a three-dimensional arrangement of a large number of small NPs (NP_Ss) dispersed in a box-shaped template. A large NP (NP_L) is placed on the top of this box and is used as an output port [13]. Since the semiconductor CdSe NP used for the experiments absorbs some amount of the light power, the DP energy dissipates and decreases by repeating the DP transfer between adjacent NPs. Thus, the propagating light power emitted from NP_L decreases by increasing the number of NP_Ss that are dispersed between the input and output ports (by increasing the direct distance L between these ports). The rate of the decrease due to the internal dissipation above is formulated as $\exp\left(-\alpha_{loss}x\right)$, where α_{loss} is the absorption coefficient and x is the optical path length.

Figure 2(b) shows the experimental results. The heights H of the template boxes of the specimens A–C were 10 nm, 20 nm, and 50 nm, respectively. They are proportional to the number N_z of NP_Ss that were vertically piled up. This figure shows the relation between the direct distance L and the light power emitted from NP_L. Broken lines represent the exponential functions fitted to the measured values. Since the output light power, normalized to the input power, is the transmittance T, this function is expressed as $T=\exp\left(-L/L_0\right)$, where L_0 is named the attainable distance.

Figure 2(c) shows the relations between H and L_0 for the specimens A–C. They indicate a monotonic increase in L_0 with an increase in H. Since the NP_Ss in the template box enable the formation of a longer path for the DP transfer by increasing H, decreases in the emitted light power are expected by this increase due to the increase in the amount of internal dissipation over the full

length of the path. However, the monotonic increase in Fig. 2(c) is contrary to this expectation. These unexpected results imply the intrinsic off-shell scientific features. They are: The DP selects a path that minimizes the decreases in the emitted light power. In other words, the DP autonomously finds the path so that it delivers the highest energy to the macroscopic system. This path is not necessarily the shortest of all the geometrically feasible paths in the box. That is, the principle for the path selection is different from the that of the on-shell scientific principle of least action.

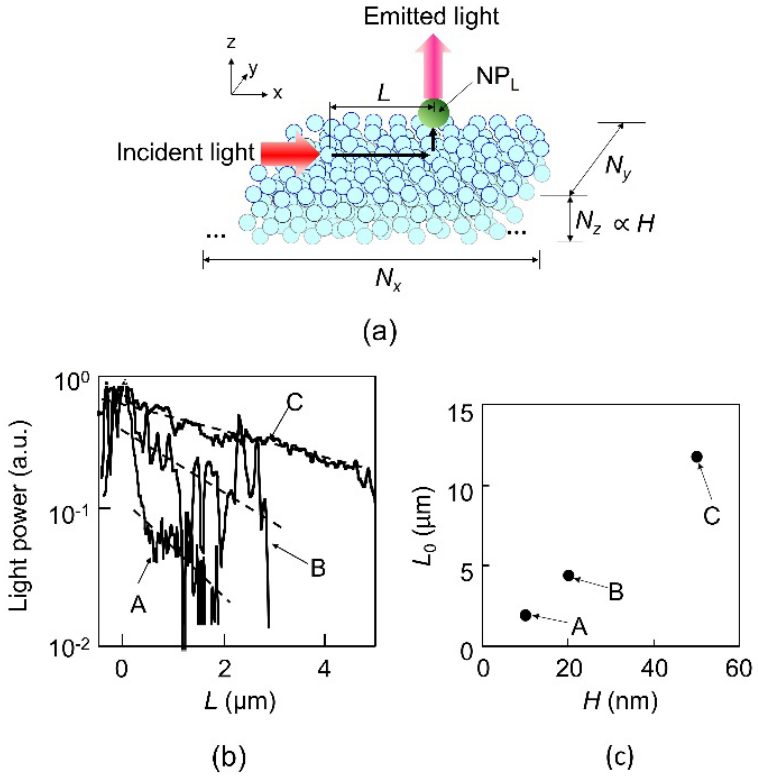

Fig. 2 Bi-directional DP transfer in a large number of small NPs (NP_Ss) and propagating light emitted from the large NP (NP_L).

(a) Schematic explanation of box-shaped arrangement. A semiconductor CuCl was used as the NP material.

(b) Measured relation between the direct distance L and the output light power emitted from NP_L. The heights H of the three-dimensional arrangements of NP_Ss of the specimens A–C were 10 nm, 20 nm, and 50 nm, respectively. Broken lines represent the exponential functions $\exp(-L/L_0)$ fitted to the measured values, where L_0 is the attainable distance.

(c) Relation between H and L_0 for the specimens A–C.

4. Theoretical model

Noting that interaction and dissipation are indispensable for describing the unique features of the DP [14], the QW has been used as a promising theoretical model for analyzing the DP transfer (**[2]** in Section 2) [6-10]. The contribution of dissipation was added to this model for deriving the probability

of the dressed-photon–phonon (DPP) created at the B atom-pair in a silicon (Si) crystal [11]. This section reviews the formulation of this model by starting from the case without energy dissipation.

By using of the light incident to the lower side of a two-dimensional lattice assumed for this model, a DP is created at each site in this lattice and travels in the upper or lower directions. During these travels, the DP repeats hopping from a site in the lattice to its nearest-neighbor site. The phonon does not hop due to its nonlocalized nature. Since the DPP is created as a result of coupling between two counter-travelling DPs and a phonon, a three-dimensional vector

$$\vec{\psi}_{t,(x,y)} = \begin{bmatrix} y_{DP+} \\ y_{DP-} \\ y_{Phonon} \end{bmatrix}_{t,(x,y)} \tag{1}$$

is used to represent its creation probability amplitude, where [ ] is the vector at time t and at the position (x, y) of the lattice site, y_{DP+} and y_{DP-} are the creation probability amplitudes of the DPs that travel by repeating the hopping in the upper or lower directions, respectively, and y_{Phonon} is that of the phonon.

For representing spatial-temporal evolution equations for the DPP that hops out from the site, the vectors

$$\left[\vec{\psi}_{t,(x,y)\leftrightarrow}\right] \equiv \begin{bmatrix} y_{DP+\rightarrow} \\ y_{DP-\leftarrow} \\ y_{Phonon} \end{bmatrix}_{t,(x,y)} \tag{2a}$$

and

$$\left[\vec{\psi}_{t,(x,y)\updownarrow}\right] \equiv \begin{bmatrix} y_{DP+\uparrow} \\ y_{DP-\downarrow} \\ y_{Phonon} \end{bmatrix}_{t,(x,y)} \tag{2b}$$

are used. In eq. (2a), the vector $\vec{\psi}_{t,(x,y)\leftrightarrow}$ represents the DPP, hopping out from the site, which is composed of two DPs ($y_{DP+\rightarrow}$ and $y_{DP-\leftarrow}$ that hop along the $\pm x$ axes) and a phonon (y_{Phonon}) at time t. In eq. (2b), the vector $\vec{\psi}_{t,(x,y)\updownarrow}$ represents the DPP, which is composed of two DPs ($y_{DP+\uparrow}$ and $y_{DP-\downarrow}$ that hop along the $\pm y$ axes) and a phonon (y_{Phonon}).

By using eqs. (2a) and (2b), the spatial-temporal evolution equation for the DPP is represented by

$$\vec{\psi}_{t,(x,y)} = \begin{bmatrix} \left[\vec{\psi}_{t,(x,y)\leftrightarrow}\right] \\ \left[\vec{\psi}_{t,(x,y)\updownarrow}\right] \end{bmatrix} = \begin{bmatrix} [0] & U \\ U & [0] \end{bmatrix} \begin{bmatrix} \left[\vec{\psi}_{t-1,(x,y)\leftrightarrow}\right] \\ \left[\vec{\psi}_{t-1,(x,y)\updownarrow}\right] \end{bmatrix}, \tag{3}$$

where

$$U \equiv \begin{bmatrix} \varepsilon_+ & J & \chi \\ J & \varepsilon_- & \chi \\ \chi & \chi & \varepsilon_0 \end{bmatrix} \tag{4}$$

and

$$[0] \equiv \begin{bmatrix} 0 & 0 & 0 \\ 0 & 0 & 0 \\ 0 & 0 & 0 \end{bmatrix}. \tag{5}$$

In eq. (4), U is a unitary matrix whose diagonal elements ε_+ and ε_- are the eigen-energies of the DPs (y_{DP+} and y_{DP-}), respectively, and ε_0 is that of the phonon. Off-diagonal elements J and χ represent the DP hopping energy and the DP-phonon coupling energy, respectively.

Next, the energy dissipation is introduced into this model [11]: The vector of eq. (1) is replaced by a four-dimensional vector

$$\vec{\psi}'_{t,(x,y)} = \begin{bmatrix} y_{DP+} \\ y_{DP-} \\ y_{Phonon} \\ y_{dis} \end{bmatrix}_{t,(x,y)} . \tag{6}$$

The fourth line y_{dis} represents the creation probability amplitude of the DPP dissipated from the lattice. The spatial-temporal evolution equation is represented by

$$\vec{\psi}'_{t,(x,y)} = \begin{bmatrix} \left[\vec{\psi}'_{t,(x,y)\leftrightarrow}\right] \\ \left[\vec{\psi}'_{t,(x,y)\updownarrow}\right] \\ \left[\vec{\psi}''_{t,(x,y),dis}\right] \end{bmatrix} = \begin{bmatrix} [0] & \sqrt{1-\kappa^2}U & [0] \\ \sqrt{1-\kappa^2}U & [0] & [\kappa] \\ [0] & [\kappa] & [0] \end{bmatrix} \begin{bmatrix} \left[\vec{\psi}'_{t-1,(x,y)\leftrightarrow}\right] \\ \left[\vec{\psi}'_{t-1,(x,y)\updownarrow}\right] \\ \left[\vec{\psi}''_{t-1,(x,y),dis}\right] \end{bmatrix}. \qquad (7)$$

The third line of the left-hand side vector corresponds to the dissipated DPP

$$\left[\vec{\psi}''_{t,(x,y),dis}\right] \equiv \begin{bmatrix} y_{DP+,dis} \\ y_{DP-,dis} \\ y_{Phonon} \end{bmatrix}_{t,(x,y)} . \qquad (8)$$

The first and second lines ($y_{DP+,dis}$ and $y_{DP-,dis}$) in eq. (8) represent the dissipated DPs that travel along the upper or lower directions in the lattice, respectively. Their sources are y_{DP+} and y_{DP-} in eq. (6), respectively.

The quantity κ in the matrix

$$[\kappa] \equiv \begin{bmatrix} \kappa & 0 & 0 \\ 0 & \kappa & 0 \\ 0 & 0 & 0 \end{bmatrix} \qquad (9)$$

on the right-hand side of eq. (7) is a phenomenologically introduced dissipation constant $(0 \le \kappa \le 1)$. As a result of introducing the matrix of eq. (9) into eq. (7), the coefficient matrix on the right-hand side of eq. (7) is transformed from unitary to non-unitary. The DPP energy stored in the lattice decreases as a result of the dissipation. The quantity $\sqrt{1-\kappa^2}$ represents the magnitude of the energy left in the lattice after dissipation.

Numerical calculations derived the values of the creation probabilities of DPP at the B atom-pairs in Si-light emitting devices and the light power emitted from the Si crystal to the external macroscopic space [11]. The calculated results agreed well with the experimental results. The remarkable finding revealed by these calculations is that there exists an optimum value κ_{opt} (=0.2) of the dissipation constant κ that maximizes the emitted light power, as is shown in Fig. 3.

The results shown in Fig. 3 give a clue for analyzing the intrinsic features of the experimental results of Fig. 2(d) when the B atom-pair in a Si crystal is replaced by NPs: After this replacement, the dissipation constant κ is given by the sum $(\kappa = \kappa_{in} + \kappa_{out})$ of the internal dissipation constant $\kappa_{in} (= N\alpha_{loss})$ at all the NPS (N: number of NPs in the box) and the dissipation constant κ_{out} at the output port NP_L. Since N is the product of the numbers N_x, N_y, N_z of the NPS along the x-, y-, and z-axes in the box and the height H is proportional to N_z, it is easily found that κ is proportional to H. This proportional relation implies that there exists an optimum value H_{opt} of H that maximizes the value of L_0 in Fig. 2(c).

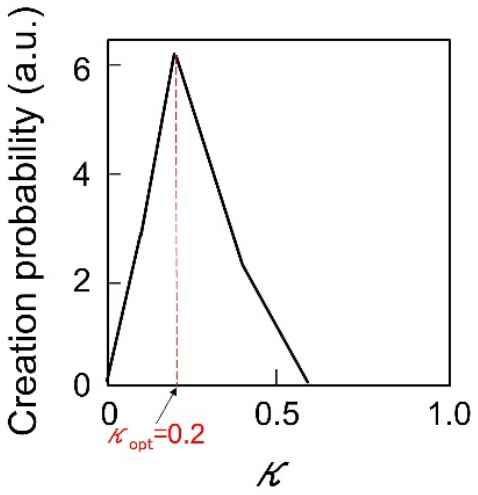

Fig. 3 Relation between the dissipation constant κ and the DPP creation probability at the B atom-pair.

5. Comparison with experimental results

Figures 4(a) and (b) are copies of Figs. 2(c) and 3, respectively. A comparison between them indicates that the monotonically increasing experimental values in Fig. 4(a) correspond to the calculated values in the area A ($H < H_{opt}$) in Fig. 4(b). This correspondence also indicates that the value of L_0 takes the maximum at $H = H_{opt}$ (the optimum path) and subsequently decreases with increasing H (the area B). This means that the optimum transfer path above is autonomously determined, resulting in minimizing the decreases in the emitted light power. For this path, the internal dissipation constant

$\kappa_{in}(=N\alpha_{loss})$ plays a leading role (**[3]** in Section 2) because the optimum path is realized by optimizing the constant κ to κ_{opt}. Furthermore, since the value of H_{opt} is finite, the optimum path is composed of a finite number of NPs. Finally, it is claimed that the features of the optimum path are intrinsic to off-shell science. In other words, this path is governed not by the on-shell scientific principle of least action but by the off-shell scientific principle of so-called largest output signal.

Future problems include how to describe H_{opt} in the formula and to identify the origin of the phenomenological dissipation constant κ.

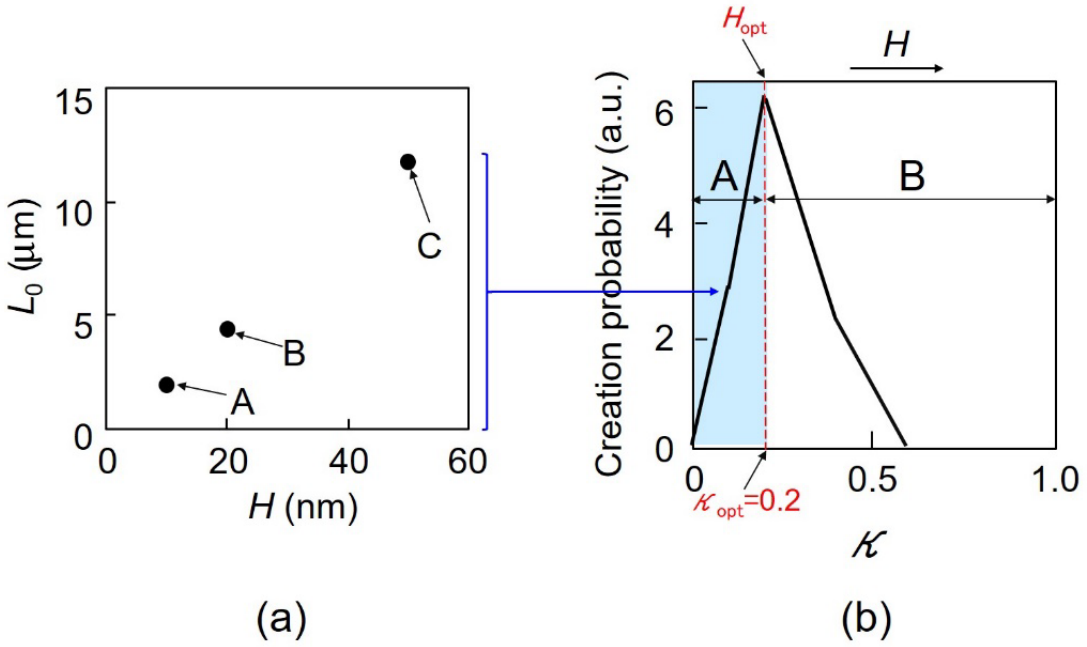

Fig. 4 Copies of Figs. 2(c) and 3 for comparing experimental and calculated results.
(a) Copy of Fig. 2(c). (b) Copy of Fig. 3.

6. Summary

This paper claimed that an optimum dissipation constant of DPP energy exists and that the transfer path with such optimum dissipation is autonomously determined to minimize the decreases in the emitted light power. In other words, this determination is governed not by the on-shell scientific principle of least action but by the off-shell scientific principle of largest output signal. These claims imply that there exists an optimum size of the three-dimensional arrangement of the NPs when it is applied to fabricate a novel nanometer-sized optical device. Future problems include how to describe H_{opt} in formula and to identify the origin of the dissipation constant κ.

Acknowledgements

The authors thank Prof. I. Ojima (RODreP), Dr. H. Sakuma (RODreP) and Prof. E. Segawa (Yokohama National Univ.) for their valuable suggestions on the DP creation theory and QW theory, respectively.

References

[1] M. Ohtsu, *Dressed Photons*, Springer, Heidelberg (2014) pp.89-214.

[2] M. Ohtsu, "Off-shell scientific nature of dressed photon energy transfer and dissipation," *Off-shell Archive* (April, 2024) Offshell: 2404R.001.v1, **DOI** 10.14939/2404R.001.v1, https://rodrep.or.jp/en/offshell/review_2404R.001.v1.html

[3] T. Kawazoe, K. Kobayashi, S. Sangu, and M. Ohtsu, "Demonstration of a nanophotonic switching operation by optical near-field energy transfer", Appl. Phys. Lett., Vol.82, No.18, May 2003, pp.2957-2959

[4] H. Sakuma, I. Ojima, M. Ohtsu, and T. Kawazoe, Drastic advancement in nanophotonics achieved by a new dressed photon study, "JEOS-RP (2021) **17**: 28.

[5] H. Sakuma, I. Ojima, and M. Ohtsu, "Perspective on an Emerging Frontier of Nanoscience Opened up by Dressed Photon Studies," *Nanoarchitectonics*, Vol. 5, Issue 1 (2024) pp.1-23.

[6] M. Ohtsu, "A Quantum Walk Model for Describing the Energy Transfer of a Dressed Photon," *Off-shell Archive* (September, 2021) OffShell: 2109R.001.v1. **DOI** 10.14939/2109R.001.v1, http://offshell.rodrep.org/?p=345

[7] M. Ohtsu, E. Segawa, and K. Yuki, "Numerical calculation of a dressed photon energy transfer based on a quantum walk model," *Off-shell Archive* (June, 2022) OffShell: 2206O.001.v1.**DOI** 10.14939/2206O.001.v1, https://rodrep.or.jp/en/off-shell/original_2206O.001.v1.html

[8] M. Ohtsu, E. Segawa, K. Yuki, and S. Saito, "Dressed-photon—phonon creation probability on the tip of a fiber probe calculated by a quantum walk model," *Off-shell Archive* (December, 2022) OffShell: 2212O.001.v1.
DOI 10.14939/2212O.001.v1, https://rodrep.or.jp/en/off-shell/original_2212O.001.v1.html

[9] M. Ohtsu, E. Segawa, K. Yuki, and S. Saito, "Spatial distribution of dressed-photon–phonon confined by an impurity atom-pair in a crystal," *Off-shell Archive* (January, 2023) Offshell: 2301O.001.v1.
DOI 10.14939/2301O.001.v1, https://rodrep.or.jp/en/off-shell/original_2301O.001.v1.html

[10] M. Ohtsu, E. Segawa, K. Yuki, and S. Saito, "Analyses of photon breeding with respect to photon spin by using a three-dimensional quantum walk model," *Off-shell Archive* (November, 2023) Offshell: 2311O.001.v110.
DOI 10.14939/2311O.001.v1, https://rodrep.or.jp/en/off-shell/original_2311O.001.v1.html

[11] M. Ohtsu, E. Segawa, K. Yuki, and S. Saito, "A quantum walk model with energy dissipation for a dressed-photon–phonon confined by an impurity atom-pair in a crystal," *Off-shell Archive* (April, 2023) Offshell: 2304O.001.v1.
DOI 10.14939/2304O.001.v1, https://rodrep.or.jp/en/off-shell/original_2304O.001.v1.html

[12] A.S. Wightman. "On the localizability of quantum mechanical systems," *Rev. Mod. Physics* **34**, 845 (1962).

[13] W. Nomura, T. Yatsui, T. Kawazoe, M. Naruse, and M. Ohtsu, "Structural dependency of optical excitation transfer via optical near-field interactions between semiconductor quantum dots, " Appl. Phys. B- Lasers and Optics, Vol. 100, No. 1, July 2010, pp. 181-187.

[14] I. Ojima, "Control over Off-Shell QFT via Induction and Imprimitivity," *Prog. in Nanophotonics.*, **5** (ed. T. Yatsui, Springer, 2018) pp. 108-135.

Off-shell scientific nature of dressed photon energy transfer and dissipation

M. Ohtsu

Research Origin for Dressed Photon,
3-13-19 Moriya-cho, Kanagawa-ku, Yokohama, Kanagawa 221-0022, Japan

Abstract

First, the principles of size-dependent resonance, bi-directional energy transfer, and subsequent energy dissipation are reviewed. Second, experimental results on energy transfer, dissipation, and light emission from multiple three-dimensionally arranged nanometer-sized particles are presented. These results imply that the dressed-photon (DP) energy transfers through a unique path via which the emitted light power takes the maximum value. Third, the results of preliminary numerical calculations carried out by using a random walk model are presented. These results show that there are serious problems originating from the principle of on-shell science assumed in the calculations. In order to solve these problems, a quantum walk is presented as a promising off-shell scientific model. Finally, it is suggested that the unique path above can be found by improving this quantum walk model.

1. Introduction

Extensive experimental studies on dressed photons (DPs) have found a large number of novel phenomena that originate from the unique nature of DP energy transfer and dissipation. They have been applied to realize innovative technologies [1]. These phenomena are totally different from those that have been popularly known in the field of conventional on-shell science. This paper reviews these phenomena and evaluates them from the viewpoint of novel off-shell science that is complimentary to the on-shell science [2]. After a review of experimental results in Sections 2 and 3, Section 4 introduces the result of preliminary numerical calculations for analyzing the experimental results. The results indicate that these calculations have serious problems, and numerical calculations based on an off-shell scientific quantum walk (QW) model are promising to solve these problems. Based on this unique off-shell scientific model, Section 5 presents a DP energy transfer path that can be possibly used to solve them. Section 6 presents a summary.

2. Energy transfer and dissipation of the dressed photon

This section reviews the mechanisms of DP creation, its energy transfer, and subsequent dissipation for measurements.

2.1 Creation and transfer

A DP is created on a microscopic material surface by the interaction between a light field and a microscopic material field. The DP creation process is described by the following three steps [3,4]:
(1) A microscopic material field (a timelike momentum field) interacts with a vector boson field[1)].
(2) In addition to a stable pair of the Majorana fermions (a spacelike momentum field)[1)], an unstable pair consisting of a Majorana particle and anti-particle (timelike momentum fields) is created (pair creation).
(3) Although this unstable pair annihilates within a short time duration (pair annihilation), a novel light field (a timelike momentum field) remains at the microscopic material. This is the DP.

In the case where the spins of the particle and anti-particle in (2) are anti-parallel, an electric DP (with spin 0) is created. When they are parallel, on the other hand, a magnetic DP (with spin 1) is created. The creation of these DPs has been experimentally confirmed [3-5].

A simple example of the microscopic material above is a nanometer-sized particle (NP) (Fig. 1(a)). That is, a DP is created on this NP by light irradiation. More realistic examples are the tip of a fiber probe, a bump on a rough material surface, and an impurity atom in a material.

If the second NP (NP_2) is placed in close proximity to the first NP (NP_1) (Fig. 1(b)), the energy of the DP on NP_1 transfers to NP_2 when the separation between the two NPs is shorter than the size of the NPs (a tunneling effect) because the spatial extent of the DP is equivalent to the size of the NP, as has been formulated by a Yukawa function [3, 4]. This transfer most probably occurs when the sizes of the two NPs are equal, which has been called size-dependent resonance [6]. This resonance can be interpreted as the resonance between the quantized energy levels of excitons in the NPs because the value of the quantized energy of the exciton is inversely proportional to the size of the NP[2)]. Here, it should be noted that this transfer is bi-directional between these NPs, which represents the interaction between the two NPs by exchanging a DP.

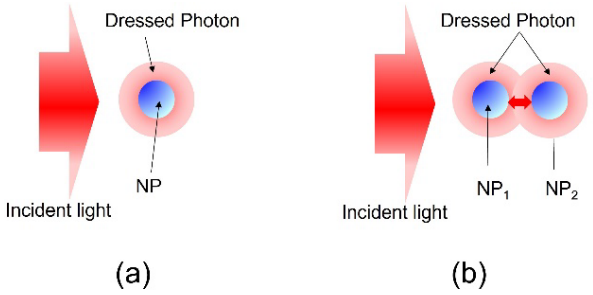

Fig. 1 Creation of DP on a nanometer-sized particle (NP) and its energy transfer.
(a) Creation. (b) Energy transfer.

1) This vector boson field is a spacelike momentum field that is indispensable for representing light–matter interaction. Theoretical studies have proved the existence of this field based on the concept of Clebsch dual representation. These studies have also successfully described that the spacelike momentum field for a classical electromagnetic field is created from condensed boson fields in a microscopic space that is composed of a pair of quantum mechanical Majorana fields (two Majorana fermions). The components of this pair are four-dimensionally orthogonal with each other. For reference, the Clebsch dual representation above uses a pair of scalar parameters (λ, ϕ), that has been introduced to represent the Hamiltonian structure with respect to the isentropic motion of an ideal fluid.

2) Since the DP is a photon–exciton coupled field, this phenomenon should be evaluated by the resonance between the DP on NP_1 and that on NP_2 instead of the resonance between the exciton energies. However, since the quantized energy of the DP is inversely proportional to the size of the NP [3, 4], the present interpretation is valid also for the quantized energy of the DP.

2.2 Dissipation for measurement

The DP energy transfer in Subsection 2.1 cannot be measured in macroscopic space because it occurs only in the microscopic space composed of the two NPs. For measurement, the DP energy must be dissipated from the microscopic to the macroscopic space. Figure 2 shows a method for inducing such dissipation, in which NP_2 in Fig. 1(b) is replaced by a larger NP (NP_L) [7]. In order to utilize the size-dependent resonance, the sizes of the two NPs are adjusted so that the lowest quantized energy E_{S1} of the smaller NP (NP_S) is tuned to the second-lowest quantized energy E_{L2} of NP_L. By this adjustment, annihilation of the exciton with energy E_{S1} in the smaller NP_S creates the DP that efficiently transfers to NP_L, resulting in the efficient creation of an exciton with energy E_{L2} in NP_L. This exciton rapidly relaxes from the second quantized energy level (E_{L2}) to the lowest level (E_{L1}) of NP_L. By this relaxation, a small amount of excess energy $E_{L2} - E_{L1}$ dissipates to the macroscopic heat bath in which these NPs are buried. After this relaxation, the exciton in NP_L rapidly annihilates and emits a photon. That is, the energy E_{L1} dissipates to the macroscopic space in the form of propagating light that can be measured.

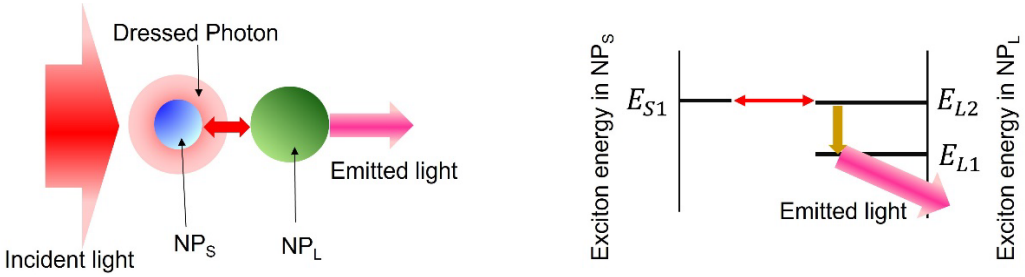

Fig. 2 DP energy dissipation.
NP_S and NP_L are smaller and larger NPs, respectively.

Black squares in Fig. 3 represent the measured values of the temporal variation of the optical power that was emitted from NP_L by pulsed light irradiation. A semiconductor (CuCl) was used as the

NP material. Curve A represents the exponential function $\exp\left(-t/\tau_{f1}\right)$ (τ_{f1}: decay time constant) fitted to the measured values of the short-time range ($0 \le t \le 2$ ns) immediately after pulsed light irradiation [8]. This short-time variation represents an off-shell scientific fast DP energy transfer that should be described by a quantum walk (QW) model. Curve B represents a slow exponential function $\exp\left(-\sqrt{t/\tau_{f2}}\right)$ (τ_{f2}: decay time constant) fitted to the measured values of the longer-time range. The quantity in this function $\sqrt{t}$ represents an on-shell scientific thermal relaxation phenomenon that can be described by a random walk (RW) model. For reference, similar temporal variation behaviors of CdSe NPs have been also measured [9].

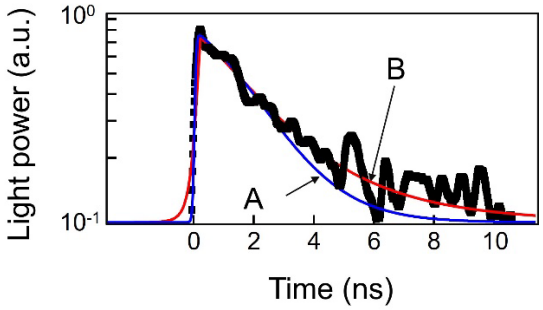

Fig. 3 Temporal variation of the optical power emitted from NP_L by pulsed right irradiation.
A semiconductor (CuCl) was used as the NP material. Curves A and B are the exponential functions $\exp\left(-t/\tau_{f1}\right)$ and $\exp\left(-\sqrt{t/\tau_{f2}}\right)$, respectively.

Even when increasing the number of NPs in Fig.1(b) from two to N (Fig. 4), bi-directional transfer of the DP energy in these NPs is also possible. Size-dependent resonance is also used here to maximize the efficiency of the DP energy transfer by using NPs of the same size. Figure 5 shows that a larger NP (NP_L) is placed at the end of the array of NP_Ss, as is the case of Fig. 2. After the DP energy reaches NP_L by repetitive bi-directional energy transfers between the adjacent NP_Ss, the DP energy is dissipated from NP_L to the macroscopic space in the form of propagating light which can be measured.

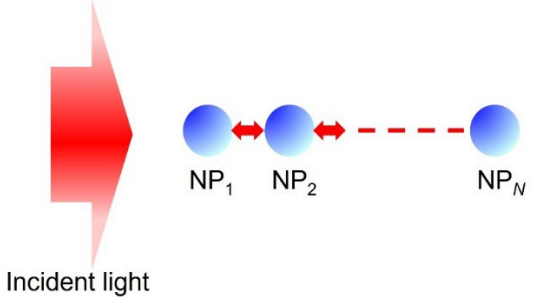

Fig. 4 Bi-directional transfer of the DP energy through linear array of NP_Ss (NP_1–NP_N).

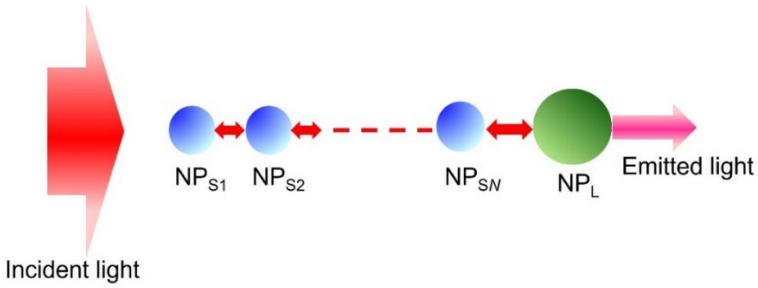

Fig. 5 DP energy dissipation.

NP_{S1}–NP_{SN} correspond to NP_1–NP_N in Fig. 4. NP_L is a larger NP.

By changing the number of NPs and by modifying their spatial layout as in Fig. 5, novel devices such as an optical switch [7], an optical nano-fountain (a super-resolution convex lens) [10], and an amoeba-inspired computing device [11] have been fabricated and their operations have been demonstrated. In the optical nano-fountain, a single NP_L is surrounded by multiple NP_Ss. Experiments on this device have confirmed that the efficiency of the DP energy dissipation from NP_L to the macroscopic space took a maximum when N=3. Preliminary numerical calculations have shown that it took a maximum when N=4, which nearly agreed with the experimental results above [12, 13]. Furthermore, these preliminary calculations have shown that the efficiency of this energy dissipation was higher when several paths of the energy transfer from the multiple NP_Ss to NP_L were cut off [13].

However, it should be pointed out that these preliminary numerical calculations have serious problems: They have dealt only with the uni-directional DP energy transfer by using a random walk (RW) model. That is, they are based on the principles of on-shell science. Furthermore, they required complicated fine adjustments of the values of relevant physical quantities in order to make the calculated results agree with the experimental values.

These problems originated from the nature of on-shell science, which did not deal with the interactions between the NPs mediated by DPs, and thus, neglected the bi-directional DP energy transfer.

3. Experimental results for three-dimensionally arranged nanometer-sized particles

This section discusses the DP energy transfer and dissipation when a large number of small NPs (NP_Ss) are arranged in box-shaped and channel-shaped templates.

3-1 Box-shaped template

Figure 6(a) schematically explains a large number of small NPs (NP_Ss) that were arranged in a box-shaped template. A large NP (NP_L) is arranged on the top of this box [14]. The size-dependent

resonance is also used here, as is the case in Fig. 5. Since the CdSe NPs used for the experiments absorb some amount of the light power, the DP energy may decrease by repeating the DP energy transfer between adjacent NPs. Thus, the propagating light power emitted from NP_L may decrease by increasing the number of NP_Ss arranged between the input and output ports (by increasing the direct distance L between these ports). For reference, in on-shell science, the rate of the decrease is formulated as $\exp(-\alpha_{abs}x)$, where α_{abs} is the absorption coefficient and x is the optical path length.

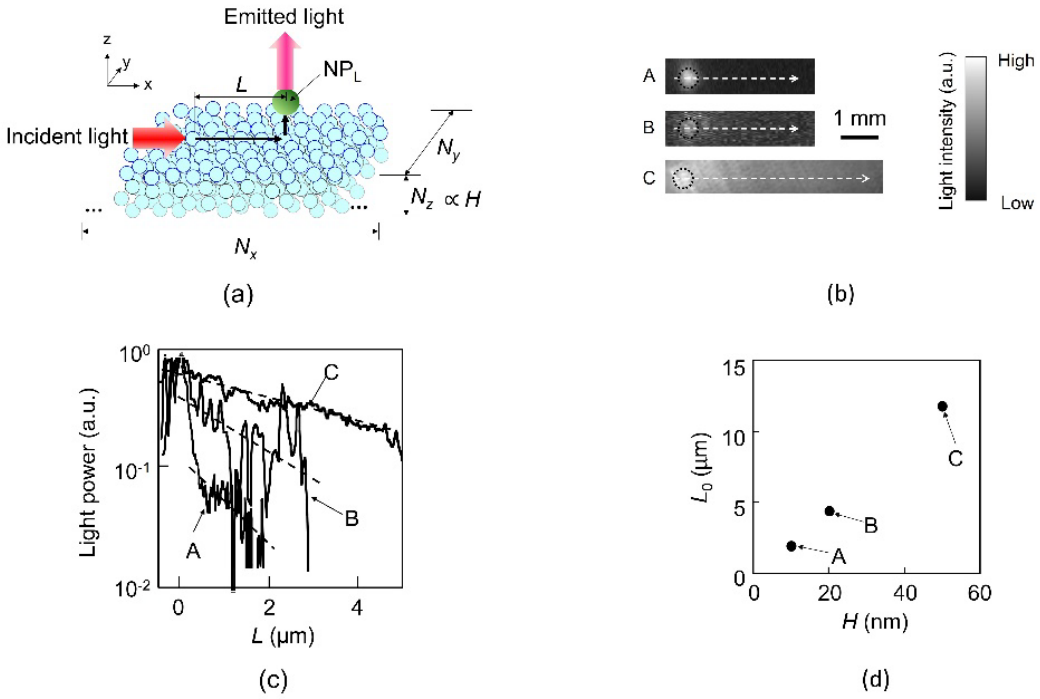

Fig. 6 Bi-directional DP energy transfer and dissipation in a large number of smaller-sized NPs (NP_Ss).

(a) Schematic explanation of the box-shaped arrangement. A semiconductor CuCl was used as the NP material.

(b) Near-field optical microscopic images of the DP energy transfer from NP_Ss to NP_L. The heights H of the three-dimensional arrangements of NP_Ss of the specimens A–C were 10 nm, 20 nm, and 50 nm, respectively.

(c) Measured relation between the direct distance L and the output light power emitted from NP_L for the specimens A–C. Broken lines represent the exponential functions $\exp(-L/L_0)$ fitted to the measured values, where L_0 is the attainable distance.

(d) Relation between H and L_0 for the specimens A–C.

However, the acquired experimental results, shown by Fig. 6(b), show the opposite features, as demonstrated by Fig. 6(c). Figure 6(c) shows the relation between the direct distance L and the output light power emitted from NP_L, where the heights H of the boxes of the specimens A–C were 10 nm, 20 nm, and 50 nm, respectively. They were proportional to the number N_z of NP_Ss that were vertically piled up. Broken lines in this figure represent the exponential functions fitted to the measured values. Since the output light power, normalized to the input power, corresponds to the transmittance

T, this function is expressed as $T = \exp(-L/L_0)$, where L_0 is named the attainable distance. Figure 6(d) shows the relations between H and L_0 for the specimens A–C. They clearly indicate an increase in L_0 with an increase of H, which is opposite to the decreasing feature in the on-shell scientific model described above.

Since the box-shaped arrangements of NPSs enables the formation of a longer path for the DP energy transfer by increasing H, monotonic decreases in the light power are expected by this increase, due to the increase in the amount of optical absorption over the full length of the path. However, the experimental results in Fig. 6(d) are contrary to this expectation. These unexpected results imply the following feature of the off-shell science:

[Feature 1] The DP selects a bi-directional path for maximizing the output light power. In other words, the DP chooses the path to contribute it energy most efficiently to the macroscopic system.

This path is not necessarily the shortest, as is schematically explained by Fig. 7(a). That is, the criterion for the path selection is different from that of the on-shell science in Fig. 7(b).

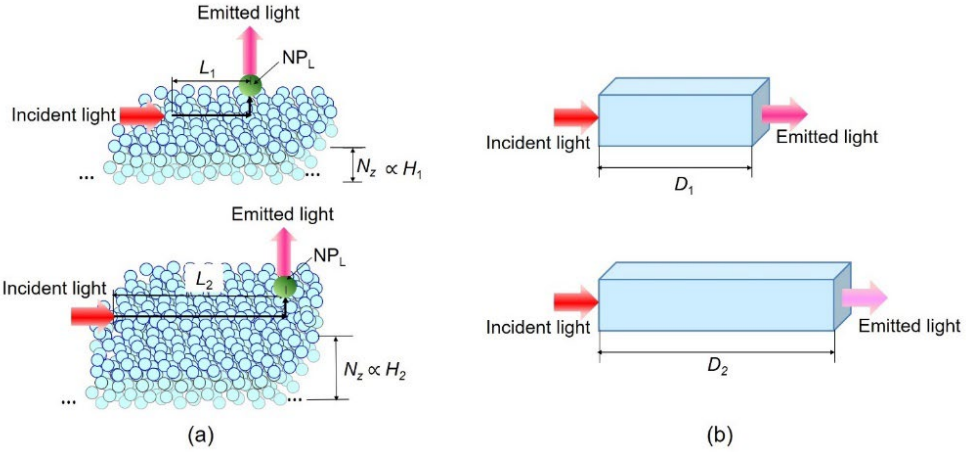

Fig. 7 Comparison between energy transfers of DP and conventional propagating light.

(a) DP energy transfer in a microscopic system (Fig. 6: off-shell science). NPs are smaller than 50 nm (smaller than the optical wavelength of about 1 μm). The size of the volume of the three-dimensionally arranged NPs is smaller than several μm, that is about 1/1,000th the material in (b).

(b) Energy transfer of the propagating light through a macroscopic system (optical wavelength of about 1μm: on-shell science). The optical path lengths D_1 and D_2 through the macroscopic materials are larger than several μm to several mm. In the case where $D_1 > D_2$, the transmittances of these materials satisfy the relation $T_1 > T_2$.

For reference, it should be pointed out that experiments have confirmed that the attainable distance L_0 was insensitive to the fluctuations of the separation between the adjacent NPSs [14]. This implies that accurate separation control is not required, which is advantageous when experimentally arranging a large number of NPs. Such a technical tolerance is also a unique feature of the off-shell science.

3.2 Channel-shaped template

Two pairs of CdSe NPs, consisting of NP_S and NP_L, were used [15]. Figure 8(a) illustrates these pairs, indicated as NP_{S1} and NP_{L1}, and NP_{S2} and NP_{L2}, respectively, for which the size-dependent resonance holds. On the other hand, the size-dependent resonance does not hold between NP_{S1} and NP_{L2}, and also between NP_{S2} and NP_{L1}.

These multiple NPs were arranged in channel-shaped templates, named as C_{S1}, C_{L1}, C_{S2}, and C_{L2} in Fig. 8(a). Figure 8(b) shows an atomic force microscope image of the area surrounded by the red square in Fig. 8(a). By irradiating light to the end of the channel C_{S1}, the DP energy created on NP_{S1}s at this end transfers bi-directionally through this channel and arrives at NP_{L1} in the intersection with the channel C_{L1}. Subsequently, the DP energy transfers through the channel C_{L1} due to the size-dependent resonance. If the DP in channel C_{S1} does not meet NP_{L1} in this intersection, it continues passing through the channel C_{S1}. Figure 8(c) shows a fluorescence microscope image of this transfer. The DP energy transfer from channel C_{S1} to C_{L1} shows two unique features:

[Feature 2]

(2-1) DP energy can transfer even though the channels C_{S1} and C_{L1} cross at right angles.

(2-2) The channels C_{S1} and C_{L2} do not show any crosstalk of DP energy transfer.

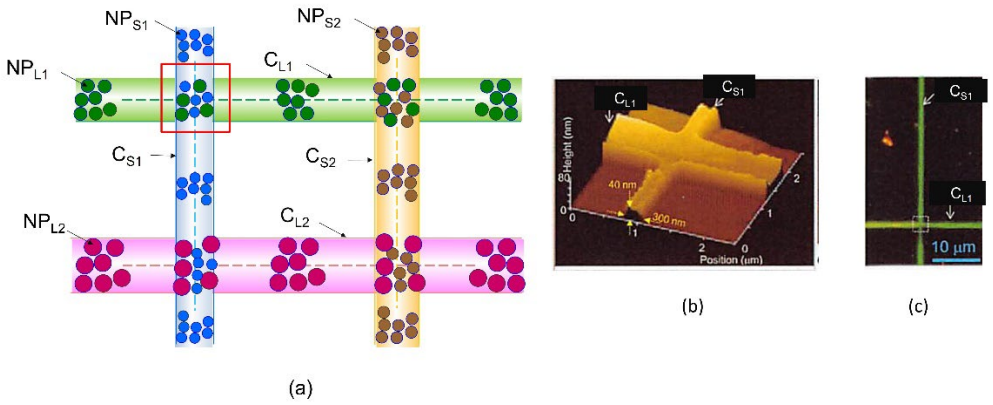

Fig. 8 Two pairs of NPs and their channel-shaped arrangements.

(a) Two pairs [NP_{S1} and NP_{L1}] and [NP_{S2} and NP_{L2}] and their channels C_{S1}, C_{L1}, C_{S2}, and C_{L2}.

(b) and (c) are atomic force microscope and fluorescence microscope images in the red square in (a), respectively.

Feature **(2-2)** indicates that the DP energy in channel C_{S1} does not transfer to NP_{L2} at the intersection with C_{L2}. This is because of the absence of size-dependent resonance between NP_{S1} and NP_{L2}. Channels C_{S2} and C_{L1} do not show any crosstalk either. The two features **(2-1)** and **(2-2)** above are schematically explained by Fig. 9(a), which imply the unique nature of the off-shell science. The DP energy transfer from C_{S2} to C_{L2} also has **[Feature 2]**. For comparison, in the case of the on-shell science in Fig. 9(b), the propagating light is scattered at the bends of a macroscopic optical waveguide or an optical fiber. No more stable propagation is expected downstream in the channel. Furthermore, light leaks from one waveguide to the adjacent one when the separation between their linearly aligned

sections is short, which results in large crosstalk.

Based on the off-shell scientific features above, an optical switch has been proposed which has a slightly different structure from the one presented at the end of Section 2 [16]. This device has been used to assemble a system for solving a multi-armed bandit problem [17].

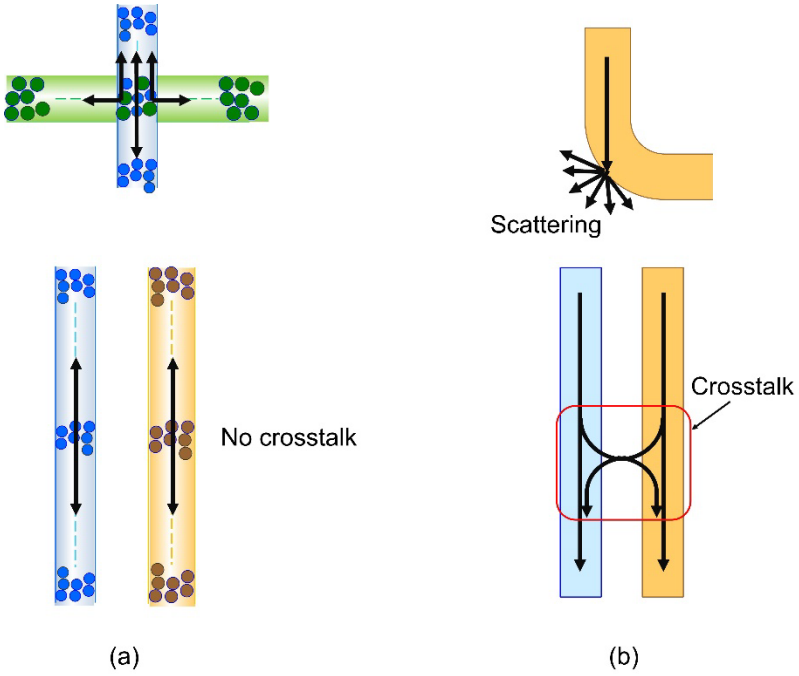

Fig. 9 Comparison between energy transfers of DP and conventional propagating light.

(a) DP energy transfer (double-pointed arrows) in a microscopic system (Fig. 8: off-shell science). NPs are smaller than 50 nm (smaller than the optical wavelength of about 1μm). The size of the volume of the channels for NPs is smaller than several μm, that is about 1/1,000th the devices in (b).

(b) Energy transfer of the propagating light (single-pointed arrows) through a macroscopic optical waveguide or an optical fiber (larger than the optical wavelength of about 1 μm: on-shell science).

4. Present status of numerical calculations and their problems

Preliminary numerical calculations have been carried out for the DP energy transfer among multiple NPs, as described in Subsection 3.1. The dependence of the attainable distance L_0 on the number N of NPs (Fig. 6(d)) has been analyzed by using the on-shell scientific method [18]. A random walk (RW) model was used by assuming that the DP energy transfer time was inversely proportional to the Yukawa function.

Although these calculations have derived the shortest percolation path [18], they had at least the two serious problems:

(1) The calculated quantity was not the creation probability of the DP but that of the exciton only.
(2) The calculation assumed a uni-directional exciton transfer ("excitation transfer" in ref. [18]), not bi-directional.

These problems originated from the principle of the on-shell science. That is, the on-shell science cannot derive the DP creation probability because it does not deal with the interaction. In order to solve these problems, the off-shell science is indispensable because it deals with the interaction, the creation probability of the DP, and its bi-directional transfer. Furthermore, it is expected that the off-shell science properly describes **[Feature 1]** and **[Feature 2]** in Subsections 3.1 and 3.2.

Furthermore, it is expected that the off-shell science can find a variety of natural phenomena that are similar to those in Section 3. It has preliminarily described these phenomena by using the terms such as autonomy and hierarchy [19]. With further progress, it is expected that a universal off-shell science will be established to analyze a variety of natural phenomena, including biological ones.

The interactions above have been dealt with by using an off-shell scientific quantum walk (QW) model that followed the suggestion given by the curve A in Fig. 3. It should be pointed out that the principles of the QW model and the nature of the DP have at least two common features:
(A) Nonreciprocity: Mathematical formulation of the QW uses nonreciprocal algebra composed of vectors and matrices. On the other hand, the DP is a field that mediates the interaction between NPs. Since the interaction is a typical nonreciprocal physical process, the QW and DP have a common feature, represented by nonreciprocity. This allows the QW model to describe the interaction and the bi-directional transfer of the DP energy.
(B) Site: The QW deals with the phenomenon of the energy transfer from one site to its neighbor. On the other hand, since the DP is spatially localized[3)], its quantum mechanical position operator can be defined. Thus, in the case where the site of the QW is the NP on which the DP is created, the position of the DP is equivalent to that of the site of the QW.

Based on these common features, the QW model has been used for numerical calculations of the following two subjects **(a)** and **(b)**:
(a) Energy transfer of DPP[4)] through a fiber probe [21]: Multiple atoms in the fiber probe and the atom at its apex corresponded to NP_Ss and NP_L in Fig. 5, respectively. Numerical calculations have successfully analyzed the dependence of the DPP creation probability at the apex on the profile of the fiber profile and on the magnitude of the DPP reflection at the slanted face of the fiber probe.
(b) DPP creation probability at a boron (B) atom-pair in a silicon (Si) crystal [22-24]: Multiple Si atoms and a few B atom-pairs corresponded to NP_Ss and NP_L, respectively. The DPP energy dissipates from the B atom-pair to emit photons to the outer macroscopic space. Numerical calculations have successfully analyzed the dependences of the DPP creation probability on the length and orientation of the B atom-pair. Furthermore, the photon breeding nature has also been successfully analyzed.

It has been confirmed that the results of the numerical calculations in **(a)** and **(b)** agreed with experimental results, which implies that the QW model can be used as a powerful tool for analyzing the nature of off-shell science[5)].

3) The theory of DP creation teaches that the spin of the electric DP is zero [3,4], which has also been experimentally confirmed. Such a zero-spin field is spatially localized, as indicated by Wightman's theorem [20].

4) DPP is a dressed-photon--phonon that is created by the coupling between a DP and a phonon.

5) It should be pointed out that such agreement has never been obtained by the on-shell scientific RW model or a wave-optical model.

5. Off-shell scientific path of DP energy transfer

A two-dimensional QW model for the DPP energy transfer has been built by referring to the two-dimensional lattice in Fig. 10 [25].

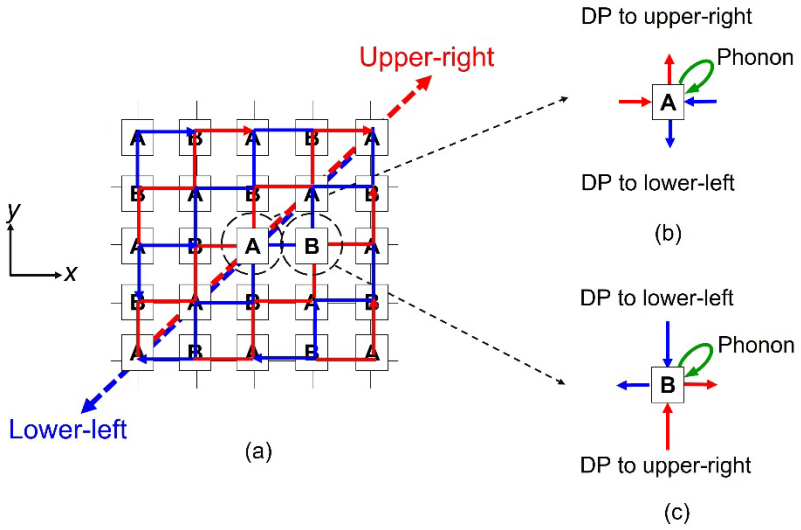

Fig. 10 Two-dimensional lattice.

(a) DPs travel to the upper-right and lower-left (red and blue broken arrows, respectively). The bent red and blue arrows represent the DP hopping from one lattice site to its neighbor, which repeats for these travels. The areas around the lattice sites A and B in (a) are magnified and shown in (b) and (c), respectively. The green loop represents a phonon.

For the following discussions, the magnitude and the direction of the input signal to the lattice are represented by a two-dimensional vector $\vec{K}_{\text{in}}$. Those of the output signal are represented by a vector $\vec{K}_{\text{out}}$, which is emitted from the site (sink) as the result of energy dissipation. Furthermore, those of the DPP energy transfer from site i to its neighbor site in the lattice are represented by a vector $\vec{k}_i$.

The energy conservation law requires the relation

$$\vec{K}_{\text{in}} + \sum_i \vec{k}_i = \vec{K}_{\text{out}}, \tag{1}$$

to hold, where $\sum_i \vec{k}_i$ represents the sum of the transferred DPP energy at all the sites in the lattice and is composed of the energies transferred toward the upper-right and lower-left directions in Fig. 10. These two directions correspond to the bi-directional energy transfer of the DPP that originates from the interaction, described in **(A)** in Section 4.

As a representative off-shell scientific experimental phenomenon, photon breeding generates the output signal $\vec{K}_{\text{out}}$ that is equal to the input signal $\vec{K}_{\text{in}}$ [22-24]. This means that photon breeding realizes a transmittance T as high as 100 %, which indicates **[Feature 1]** in Subsection 3.1. This can be realized if $\sum_i \vec{k}_i = 0$ in eq. (1) holds, which is possible by optimally adding the paths of bi-directional transfer towards the upper-right and lower-left directions above. That is, the optimal vectorial sum of the red and blue arrows in Fig. 10 can form a closed loop to realize $\sum_i \vec{k}_i = 0$. It should be pointed out that such perfect transmission corresponds to the QW nature of comfortability [26].

Since the number of paths is finite in an actual two-dimensional lattice due to its finite number of sites, a path with $\sum_i \vec{k}_i = 0$ may not exist. However, by increasing the number of sites, it is expected that the value of $\sum_i \vec{k}_i$ can gradually decrease and, finally, converge to zero. The possibility of this convergence has been indicated by the experimental results of Fig. 6(d), which demonstrated the increase in the attainable distance L_0 with the increase in the height H. In short, the DPP may transfer through the path with $\sum_i \vec{k}_i = 0$, as is schematically explained by Fig. 11(a), not through the shortest path given by the on-shell scientific model of Fig. 11(b).

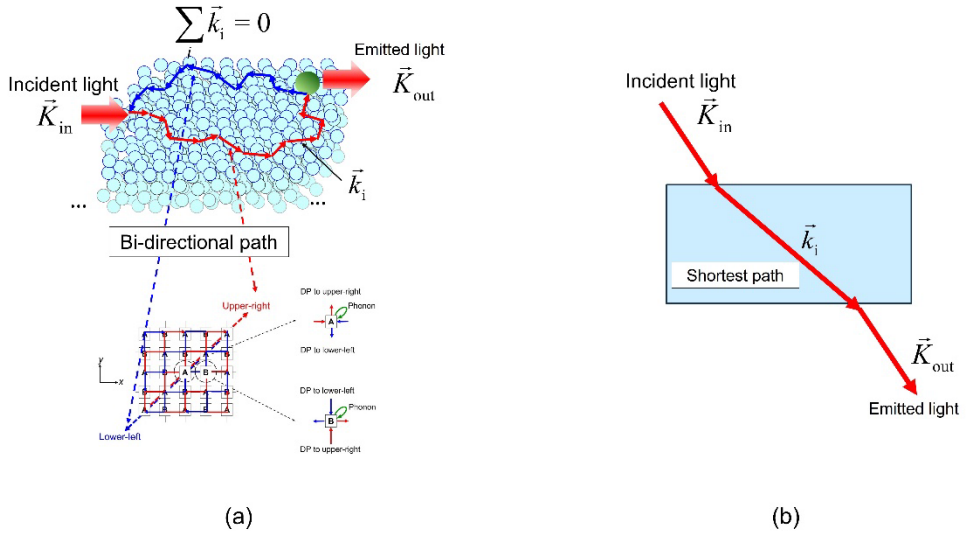

Fig. 11 Comparison between the paths of energy transfers of a DP and conventional propagating light. (a) Energy transfers of the DP in the systems in Fig. 7(a). (b) Energy transfer of the propagating light through the macroscopic systems in Figs. 7(b).

6. Summary

The first part of this paper reviewed the principles of size-dependent resonance, bi-directional energy transfer, and subsequent energy dissipation. The second part presented experimental results on energy transfer, dissipation, and light emission from multiple three-dimensionally arranged NPs. These results implied that the DP energy transferred not through the shortest path but through a unique path via which the emitted light power took the maximum value. The third part reviewed the results of preliminary numerical calculations by using a random walk model. The calculations had serious problems that originated from the principle of the on-shell science used in the model. In order to solve these problems, it was pointed out that numerical calculations using a quantum walk model based on the principle of off-shell science was promising. Finally, it was suggested that the unique path above can be found by further improvements of this quantum walk model.

Acknowledgements

The authors thank Dr. H. Sakuma (RODreP) and Prof. E. Segawa (Yokohama National Univ.) for their valuable suggestions on the DP creation theory and QW theory, respectively.

References

[1] M. Ohtsu, *Dressed Photons*, Springer, Heidelberg (2014) pp.89-214.

[2] M. Ohtsu, Off-shell Applications in Nanophotonics, Elsevier, Oxford (2021) pp.1-40.

[3] H. Sakuma, I. Ojima, M. Ohtsu, and T. Kawazoe, Drastic advancement in nanophotonics achieved by a new dressed photon study, "JEOS-RP (2021) **17**: 28.

[4] H. Sakuma, I. Ojima, and M. Ohtsu, “Perspective on an Emerging Frontier of Nanoscience Opened up by Dressed Photon Studies,” *Nanoarchitectonics*, Vol. 5, Issue 1 (2024) pp.1-23.

[5] T. Kadowaki, T. Kawazoe, and M. Ohtsu, “SiC transmission-type polarization rotator using a large magneto-optical effect boosted and stabilized by dressed photons,” *Sci. Reports*, (2020) 10: 12967.
https://doi.org/10.1038/s41598-020-69971-3

[6] M. Ohtsu, Dressed Photon, Springer, pp.33-36.

[7] T. Kawazoe, K. Kobayashi, S. Sangu, and M. Ohtsu, “Demonstration of a nanophotonic switching operation by optical near-field energy transfer”, Appl. Phys. Lett., Vol.82, No.18, May 2003, pp.2957-2959

[8] M. Ohtsu , T. Kawazoe, & H. Saigo, (2017). Spatial and Temporal Evolutions of Dressed Photon Energy Transfer. *Off-shell Archive,* Offshell:1710R.001.v1. doi 10.14939/1710R.001.v1. http://offshell.rodrep.org/?p=79

[9] W. Nomura, T. Yatsui, T. Kawazoe, and M. Ohtsu, “The observation of dissipated optical energy transfer between CdSe quantum dots,” J. Nanophoto., Vol. 1, November 2007, pp. 011591 1-7

[10] T. Kawazoe, K. Kobayashi, and M. Ohtsu, “Optical nanofountain: A biomimetic device that concentrates optical energy in a nanometric region”, Appl. Phys. Lett., Vol.86, No.10, March 2005, pp.103102-1 –3

[11] M. Aono, M. Naruse, S-J. Kim, M. Wakabayashi, H. Hori, M. Ohtsu, and M. Hara, “Amoeba-Inspired Nanoarchitectonic Computing: Solving Intractable Computational Problems Using Nanoscale Photoexcitation Transfer Dynamics,” Langmuir, Vol. 29, April 2013, pp. 7557-7564.

[12] M. Naruse, T. Kawazoe, R. Ohta, W. Nomura, and M. Ohtsu, “Optimal mixture of randomly dispersed quantum dots for optical excitation transfer via optical near-field interactions,” Physical Review B, Vol. 80, No. 12, September 2009, (pp. 125325 1-7).
(selected for Virtual Journal of Nanoscale Science & Technology-- September 5, 2009, Vol. 20, Issue 14).

[13] M. Naruse, K. Leibnitz, F. Peper, N. Tate, W. Nomura, T. Kawazoe, M. Murata, and M. Ohtsu, “Autonomy in excitation transfer via optical near-field interactions and its implications for information networking,” Nano Communication Networks, Vol. 2, No. 4, December 2011, pp. 189-195.

[14] W. Nomura, T. Yatsui, T. Kawazoe, M. Naruse, and M. Ohtsu, “Structural dependency of optical excitation transfer via optical near-field interactions between semiconductor quantum dots, ” Appl. Phys. B- Lasers and Optics, Vol. 100, No. 1, July 2010, pp. 181-187.

[15] W. Nomura, T. Yatsui, T. Kawazoe, E. Runge, and C. Lienau, and M. Ohtsu, “Direct observation of optical excitation transfer based on resonant optical near-field interaction,” Appl. Phys. B Lasers and Optics, Vol. 107, Number 2, May 2012, pp. 257-262.

[16] W. Nomura, M. Naruse, M. Aono, S.-J. Kim, T. Kawazoe, T. Yatsui, and M. Ohtsu, “Demonstration of Controlling the Spatiotemporal Dynamics of Optical Near-field Excitatoin Transfer in Y-Junction Structure Consisting of Randomly Distributed Quantum Dots,” Advances in Optical Technologies, Vol.2014, April 2014, Article ID 569684 (8 pages).

[17] M. Naruse, W. Nomura, M. Aono, M. Ohtsu, Y. Sonnefraud, A. Drezet, S. Huant, and S.-J Kim, “Decision making based on optical excitation transfer via near-field interactions between quantum dots,” Journal of Applied Physics, Vol. 116, No. 15, October 2014, pp.154303-1～8.

[18] M. Naruse, S.J. Kim, T. Takahashi, M. Aono, K. Akahane, M. D’Acunto, H. Hori, L. Thylen, and M. Ohtsu, “Percolation of optical excitation mediated by near-field interactions,” Physica A (2017) pp.162-168.

[19] M. Ohtsu, “Indications from dressed photons to macroscopic systems based on hierarchy and autonomy,” *Off-shell Archive* (June, 2019) Offshell: 1906R.001.v1. **DOI** 10.14939/1906R.001.v1, http://offshell.rodrep.org/?p=201

[20] A.S. Wightman. “On the localizability of quantum mechanical systems,” *Rev. Mod. Physics* **34**, 845 (1962).

[21] M. Ohtsu, E. Segawa, K. Yuki, and S. Saito, “Dressed-photon—phonon creation probability on the tip of a fiber probe calculated by a quantum walk model,” *Off-shell Archive* (December, 2022) OffShell: 2212O.001.v1.
DOI 10.14939/2212O.001.v1 https://rodrep.or.jp/en/off-shell/original_2212O.001.v1.html

[22] M. Ohtsu, E. Segawa, K. Yuki, and S. Saito, “Spatial distribution of dressed-photon–phonon confined by an impurity atom-pair in a crystal,” *Off-shell Archive* (January, 2023) Offshell: 2301O.001.v1.
DOI 10.14939/2301O.001.v1 https://rodrep.or.jp/en/off-shell/original_2301O.001.v1.html

[23] M. Ohtsu, E. Segawa, K. Yuki, and S. Saito, “A quantum walk model with energy dissipation for a dressed-photon–phonon confined by an impurity atom-pair in a crystal,” *Off-shell Archive* (April, 2023) Offshell: 2304O.001.v1.
DOI 10.14939/2304O.001.v1 https://rodrep.or.jp/en/off-shell/original_2304O.001.v1.html

[24] M. Ohtsu, E. Segawa, K. Yuki, and S. Saito, “Analyses of photon breeding with respect to photon spin by using a three-dimensional quantum walk model,” *Off-shell Archive* (November, 2023) Offshell: 2311O.001.v110.
DOI 10.14939/2311O.001.v1 https://rodrep.or.jp/en/off-shell/original_2311O.001.v1.html

[25] M. Ohtsu, “A Quantum Walk Model for Describing the Energy Transfer of a Dressed Photon,” *Off-shell Archive* (September, 2021) OffShell: 2109R.001.v1. **DOI** 10.14939/2109R.001.v1, http://offshell.rodrep.org/?p=345

[26] K. Higuchi, T. Komatsu, N. Konno, H. Morioka, and H. Segawa, “A Discontinuity of the Energy of Quantum Walk in Impurities,” *Symmetry* **2021**,13, 1134.

[IV] PREPRINT DEPOSITORIES

[IV-2] arXiv

International Journal of Geometric Methods in Modern Physics

REEXAMINATION OF THE HIERARCHY PROBLEM FROM A NOVEL GEOMETRIC PERSPECTIVE

HIROFUMI SAKUMA†, IZUMI OJIMA§

Research Origin for Dressed Photon,
Yokohama City, Kanagawa 221-0022, Japan *
†*sakuma@rodrep.or.jp,* §*ojima@gaia.eonet.ne.jp*

KAZUYA OKAMURA

College of Engineering
Chubu University Center for Mathematical Science and Artificial Intelligence
1200 Matsumoto-cho, Kasugai-shi, Aichi 487-8501, Japan
k.okamura.renormalizable@gmail.com

Received (Day Month Year)
Revised (Day Month Year)

A lucid interpretation of the longstanding hierarchy problem is proposed based on the unconventional model of the universe recently proposed by the authors. Our heuristic cosmological model is developed by considering Penrose and Petit's original ideas as the Weyl curvature hypothesis, conformal cyclic cosmology, and the twin universe model. The uniqueness of our model lies in its incorporation of *dark energy and matter*, and its single key parameter, adjusted by observational data, is the radius (R_{dS}) of a four-dimensional ($4D$) hypersphere called de Sitter space. We presuppose that our $4D$ universe originated from the spontaneous conformal symmetry (SCS) breaking of a light field with a null distance. We show that in this SCS breaking state, the energy–momentum tensor of the space-like electromagnetic field, whose existence is inevitable for quantum electromagnetic field interactions (Greenberg–Robinson theorem), becomes isomorphic to the divergence-free Einstein tensor in the general theory of relativity. Furthermore, we reveal the R_{dS} dependency of the $4D$ gravitational field. Based on these findings, we show an intriguing relation between the magnitude of the gravitational coupling constant and R_{dS}. A solution to the hierarchy problem is derived by assuming that R_{dS} depends on the "newly defined cosmological time".

Keywords: hierarchy problem; coupling constant; dark energy; dark matter; conformal symmetry breaking, algebraic QFT, micro–macro duality, extra dimension.

1. Introduction

This study aims to shed new light on the unresolved hierarchy problem in particle physics. The problem stems from the incredible difference existing between, for instance, the magnitudes of electromagnetic and gravitational cou-

*Bldg.1-1F, 3-13-19 Moriya-cho, Kanagawa-ku, Yokohama, Kanagawa, 221-0022 Japan

pling constants. This inspired the investigations of Dirac[1,2], Milne[3], and other researchers' [4,5,6,7], wherein they refute the hypothesis on the invariance property of physical constants, particularly of gravitational constant G. To understand the problem, the possibility of simultaneous temporal change of all physical constants was examined first by Troitskii[8] and explored further by Petit[9,10]. At the end of the 20th century, an entirely different approach to explaining the hierarchy problem was presented by Randoll and Sundrum[11], who introduced a notion of warped extra dimensions based on the brane dynamics in superstring theory. Notably, our model is distinct from the abovementioned two in the sense that it incorporates dark energy and matter as crucial components. However, our model inherits important characteristics from those preceding researches. For instance, it addresses the "temporal"evolution of the magnitude of the cosmological constant associated with the extra expansion of the universe in the fifth dimension (D) perpendicular to our $4D$ universe.

The elucidation of new ideas is frequently accompanied by the dissemination of important knowledge. Although such knowledge might be new or old, it is often not widespread in the relevant community. In our case, we have three pieces of such important knowledge: two of which, the Greenberg–Robinson (GR) theorem[12,13] and the micro–macro duality (MMD) theory of Ojima[14,15], are considered old information, whereas the Clebsch dual space-like electromagnetic (CDSE) theory[16,17,18] built on the two preceding pieces of knowledge is considered new knowledge. As demonstrated by the Schrödinger's cat, the prevailing understanding of the invisible microscopic quantum world and its connection to the visible macroscopic world is unsatisfactory. The MMD theory, built on the basic philosophy of the Araki–Haag–Kastler formulation of the algebraic quantum field theory (QFT), is an ambitious scheme aiming to provide a solution to the Schrödinger's cat problem in quantum physics. Notably, herein, the term "quantum physics" denotes relativistic quantum physics unless otherwise stated.

In the field of quantum physics, the prevailing knowledge is quantum mechanics (QM) with finite degrees of freedom. The knowledge required for this study is not that on QM but on QFT with *infinite degrees of freedom*, whose dynamical behaviors are considerably more complex than those of QM. Moreover, the crucial difference between QM and QFT lies in the number of sectors, where a sector is defined as the dynamical domain in which the principle of superposition on the quantum states holds good. For a QM system, only one sector exists (Stone–von Neumann theorem[19]), whereas for a system described by QFT, multiple unitarily inequivalent sectors exist (initially highlighted by van Hove in 1952). Initially, the abovementioned van Hove phenomena were considered as the pathological characteristics of a QFT-based system with infinite degrees of freedom. However, later, the existence of such multiple sectors was determined to be the source of dynamical richness with which the visible macroscopic world can emerge from the invisible quantum microscopic world.

Ojima's MMD theory was developed from the Doplicher–Haag–Roberts (DHR)'s original sector theory[20,21], which attempted to formulate the QFT based solely on the maximal set of observables. In addition, Ojima developed the theory further by generalizing it in such a way that it could cope with the important physical mechanism of (spontaneous) symmetry breaking of given quantum fields. Notably, in the MMD theory, the original sector notion based on irreducible representations is revised into a generalized one with factor representation. In the revised variant, the factor representation centers feature attributes of either trivial or nontrivial, corresponding to microquantum or macroclassical factor representations, respectively. In addition, these generalized sectors are mutually disjoint (separated by the absence of intertwiners), which is a stronger notion than unitary inequivalence. Thus, the MMD theory became a comprehensive QFT, which can consistently connect the quantum world, where the algebra of physical quantities obeys the noncommutative law, to the classical world, where the corresponding algebra is replaced by the one with commutative law. Thus, the *MMD theory embodies the mathematically rigorous quantum–classical correspondence*. A plain explanation of the essence of the MMD theory without resorting to sophisticated mathematical representations has been provided by Sakuma et al.[22].

Clarifying the mechanism of nonlinear field interactions would pose the biggest dynamical challenge in QFT studies. As is well known, the essential features of Fock spaces, such as the positive energy spectra in the state vector space generated by repeated applications of the creation operators on the Fock vacuum $|0\rangle$ (under the cyclicity assumption), are derived from the following Eq. (1):

$$\phi^{(f)}(x^0,\tilde{x}) = \int \frac{d^3\tilde{k}}{\sqrt{(2\pi)^3 2E_k}}[a(\tilde{k})\exp(-ik_\nu x^\nu) + a^\dagger(\tilde{k})\exp(ik_\nu x^\nu)], \qquad (1)$$

where $(a^\dagger(\tilde{k}),\ a(\tilde{l}))$ and $(\tilde{x}$ and $\tilde{k})$, respectively, denote a pair of creation–annihilation operators and of three vectors comprising spatial components of x^μ and k_ν, with E_k defined by $E_k := \sqrt{(\tilde{k})^2 + (m_0)^2}$. Although the ϕ^f field thus constructed embodies the wave–particle duality of a quantum system, the ϕ^f field and the associated 4-momentum p^μ are, respectively, restricted by the following linear Klein–Gordon (KG) equation and the on-shell condition of the form

$$[\hbar^2\partial^\nu\partial_\nu + (m_0c)^2]\phi^{(f)} = 0, \quad p_\nu p^\nu = (m_0c)^2 \geq 0, \qquad (2)$$

where the sign convention of $(+,-,-,-)$ is used for the Lorentzian metric tensor. Regarding these expressions, however, with the linearity of Eq. (2) overlooked, the abovementioned characteristic features of Fock spaces are frequently misinterpreted as the universal structure to be found in interacting multiparticle systems. Accordingly, $|0\rangle$ becomes as mysterious as the creation of everything from emptiness.

In the quest to clarify quantum field interactions, the GR theorem stands as a noteworthy forerunner. In fact, it provides a clear-cut mathematical criterion for distinguishing nonlinear quantum field interactions from the time evolution

of the free modes ($\phi^{(f)}$) with the second quantization described in Eq. (1). The GR theorem states that *if the Fourier transform ($\varphi(p)$) of a given quantum field ($\varphi(x)$) does not contain an off-shell space-like momentum (p_μ) satisfying $p_\nu p^\nu < 0$, then $\varphi(x)$ is a generalized free field.* We believe that this theorem highlights the missing factor in the presently incomplete QFT. In the appendix, we provide a sketchy overview of the theorem derived based on Wightman axioms. In the field of elementary particle physics, such off-shell quantities are conventionally dismissed as nonphysical ghosts or extremely short-lived transitory entities. Consequently, the wide physical science communities have not come to an important research conclusion on off-shell quantities in general, despite their importance.

In conventional quantum electrodynamics (QED), the longitudinal mode of a field is eliminated as a nonphysical mode, although, classically, the Coulomb mode plays an important role in electromagnetic field interactions. This well-known fact highlights the limitation of the prevailing QED theory in affording a satisfactory explanation of the consistent connection between the quantum world and classical one. As the first step to a solution, based on the GR theorem and MMD theory, the first author successfully extended a free electromagnetic field into a space-like momentum domain [23]. As this extension was achieved by introducing Clebsch variables [24] used in the study of the Hamiltonian structure of barotropic fluid, we call the extended electromagnetic field the Clebsch dual (CD) field. Notably, energy–momentum tensor of the field assumes the same form as Einstein's tensor in the theory of general relativity. Namely, the CD field bears the characteristics of spacetime itself in the sense of general relativity and can be shown to be a promising candidate for understanding the enigmatic dark energy field [17]. As the CD field plays an important role in our discussion of the hierarchy problem, we will recapitulate its necessary points in Section 2.

As stated at the beginning of this section, we aim to present a novel view of the hierarchy problem in Section 3. To do that, we think it is inevitable to explore the different ideas published recently in our series of papers[17,25,26]. Accordingly, considering that majority of readers would be unfamiliar with those ideas, in Section 2, we provide a bird's eye view of the grand design of our research. The overview encompasses all individual aspects necessary in the pursuit of what we call "off-shell science", originating from dressed photon (DP) studies in the field of nanophotonics. Thereafter, in Section 4, we highlight an intriguing finding on the meaning of Maldacena duality[27] in superstring theory, which applies to the early stages of our new model of the universe. Finally, the summary and conclusions are presented in Section 5.

2. Overview of our ongoing research on reformulating the quantum field theory

As stated in the preceding section, one of the focal points of our research on the *extended light field* is off-shell quantum fields involving quantum field interactions.

The existence of off-shell (superluminal wave-) momenta implies, as in the case of quantum spin entanglement, an instantaneous connectedness of the entire universe. This naturally leads us to some cosmological problems that are not necessarily within the scope of this study. As cosmology remains a vast, unknown frontier in the physical sciences, in dealing with mysterious cosmological problems, we adopt a simple and effective approach, the Occam's razor principle.

In line with studying the *extended light field*, we use a unique hypothesis. The hypothesis is similar to the conformal cyclic cosmology (CCC) concept proposed by Penrose[28], whose characteristics were explained in Sakuma and Ojima[25], and hereinafter, it will be referred to as CCC of the second kind (CCC-2nd). According to it, as in the case of the creation and annihilation of the matter and antimatter pair, the twin universes as metric spacetimes are birthed by a certain kind of spontaneous conformal symmetry breaking of a light field with null distance ($ds^2 = 0$). The twin universes thus created are divided by an event horizon intrinsically embedded in the de Sitter space structure, caused by the most dominant component of dark energy. Eons later, the twins meet at the event horizon to return to the original light field, and this cycle repeats forever. In our cosmological hypothesis, the flatness, isotropy, and horizon problems are resolved, respectively, by the observed existence ratio of dark energy to matter, the Weyl curvature hypothesis proposed by Penrose[29], and the existence of a superluminous off-shell electromagnetic field.

In this section, we first explain the emergence of a space-like domain known as de Sitter space mentioned above, which is necessary for quantum field interactions. The emergence mechanism of the familiar time-like domain to which not only the classical but also partial quantum fields belong must be quite different from that of the space-like domain. Second, we provide a clear explanation of the mechanism based on our new interpretation of conformal gravity.

2.1. *Conformal symmetry breaking and emergence of spacetime*

Concerning the symmetry breaking of quantum fields, the MMD theory states that the symmetric space (G/H) studied by Cartan[30], which has various desirable properties, emerges in the generalized sector classifying space if the symmetry of a given system, described by a Lie group (G), is broken up into its subgroup, H, remaining unbroken. A concrete example of this case will be explained in this subsection concerning the emergence of spacetime, *not as a purely mathematical concept having nothing to do with physics, but as a physical entity.* Recall that $4D$ spacetime occupies a special position in differential topology. A most notable example would be the one highlighted by Donaldson [31]. In the context of our present research on QFT, the following properties of $4D$ spacetime are deemed important: (i) the free Maxwell equation on electromagnetism is scale free only in $4D$ spacetime and (ii) the Weyl (conformal) curvature can be defined in spacetimes with dimensions larger than or equal to 4.

If we combine the statement of the MMD theory on an emerging symmetric

space (G/H) with property (i), i.e., the free Maxwell field that can play the role of H, then one of the assertions of our cosmological theory (CCC-2nd) proposing a $4D$ spacetime theory is restated as follows: *the universe as a symmetric space (G/H) emerges as the conformal symmetry breaking of the H field with H being an important remaining unbroken subgroup.* In our series of papers cited in Section 1, we show how space- and time-like domains of G/H emerge from H. Next, we briefly recapitulate the main points of those emergence processes, starting from the simple space-like case.

2.1.1. *Emergence of the space-like domain*

The energy–momentum tensor ($T_\mu{}^\nu$) of the free Maxwell field assumes the form of $T_\mu{}^\nu = F_{\mu\sigma}F^{\nu\sigma}$ with $F_{\mu\sigma} = \nabla_\mu A_\sigma - \nabla_\sigma A_\mu$, where ∇_μ denotes the covariant derivative and other notations are conventional. As is well known, this free field is characterized by a couple of conditions:

$$F_{\nu\sigma}F^{\nu\sigma} = 0 \quad \text{and} \quad F_{01}F_{23} + F_{02}F_{31} + F_{03}F_{12} = 0. \tag{3}$$

In extending this null field to the space-like momentum domain, focusing on the properties of the Riemann curvature tensor ($R_{\alpha\beta\gamma\delta}$) and the mixed form of the Ricci tensor ($R_\mu{}^\nu$), as shown below, is quite helpful:

$$R_{\beta\alpha\gamma\delta} = -R_{\alpha\beta\gamma\delta}, \;\; R_{\alpha\beta\delta\gamma} = -R_{\alpha\beta\gamma\delta}, \;\; R_{\gamma\delta\alpha\beta} = R_{\alpha\beta\gamma\delta}, \tag{4}$$

$$R_{\alpha\beta\gamma\delta} + R_{\alpha\gamma\delta\beta} + R_{\alpha\delta\beta\gamma} = 0, \;\; R_\mu{}^\nu := R_{\mu\sigma}{}^{\nu\sigma}. \tag{5}$$

Here, the first equation in Eq. (5) is called the first Bianchi identity, which is closely related to the second equation in Eq. (3), namely, the orthogonality of electric and magnetic fields.

In relativistic fluid dynamics, if the vorticity tensor field ($\omega_{\mu\nu}$) satisfies the second equation in Eq. (3), then the fluid is classified as a barotropic (isentropic) fluid (cf. [26]). This observation motivates us to use Clebsch parameterization (CP) to represent the electromagnetic vector potential (U_μ) in space-like momentum domains. We can achieve this because the rotational part of the barotropic fluid velocity (u_μ) can be represented by two Clebsch parameters, λ and ϕ, to give $u_\mu = \lambda\nabla_\mu\phi$ [24]. Notably, λ and ϕ serve as the canonically conjugate variables for the Hamiltonian structure of the barotropic fluid motions. In our case, the two gradient vectors, $C_\mu := \nabla_\mu\phi$ and $L_\mu := \nabla_\mu\lambda$, with the orthogonality condition, $C^\nu L_\nu = 0$, provide a dynamical basis on which electric and magnetic fields can be successfully introduced into the space-like momentum domain.

To understand the meaning of CP, we first explain the light-like case to compare it with the conventional quantization of the light field. In the second part on the pure space-like case, we will show that the energy–momentum tensor ($\hat{T}_\mu{}^\nu$) in the extended space-like domain becomes isomorphic to the Einstein tensor in the theory of general relativity. This will reveal that the extended electromagnetic field

automatically possesses the property of spacetime through which quantum electromagnetic field interactions occur (GR theorem). Namely, this spacetime, including the light-like case, plays the role of "virtual photons" in the conventional QED.

Light-like case: $U^\nu(U_\nu)^* = 0$, where $(\cdot)^*$ denotes the complex conjugate of $(\cdot)$. For Clebsch variables λ and ϕ satisfying

$$\nabla^\nu\nabla_\nu\lambda - (\kappa_0)^2\lambda = 0, \;\; L_\mu = \nabla_\mu\lambda, \quad \nabla^\nu\nabla_\nu\phi = 0, \;\; C_\mu = \nabla_\mu\phi, \tag{6}$$

$$C^\nu(L_\nu)^* = 0, \;\; U_\mu := \lambda C_\mu, \tag{7}$$

where $(\kappa_0)^{-1}$ is DP constant $l_{dp} \approx 50$ nm, determined by Ohtsu[17], we have

$$U^\nu\nabla_\nu U_\mu = 0, \;\; S_{\mu\nu} := \nabla_\mu U_\nu - \nabla_\nu U_\mu = L_\mu C_\nu - L_\nu C_\mu, \tag{8}$$

$$\hat{T}_\mu{}^\nu = S_{\mu\sigma}S^{\nu\sigma} = \rho C_\mu C^\nu, \;\; \rho := L^\nu(L_\nu)^* < 0, \;\; \nabla_\nu\hat{T}_\mu{}^\nu = 0. \tag{9}$$

Notice that $\hat{T}_\mu{}^\nu$ has a dual wave $(S_{\mu\sigma}S^{\nu\sigma})$ and particle $(\rho C_\mu C^\nu)$ representation. The latter is consistent with the conventional quantization of QED where this mode is eliminated from the physically meaningful domain as the particle density (ρ) in Eq. (9) becomes negative. As referenced in the introduction, in re-examining the Nakanishi–Lautrup formalism of the abelian gauge theory, Ojima[32] highlighted that the nonparticle form corresponding to $(S_{\mu\sigma}S^{\nu\sigma})$ in our model plays substantial physical roles, which is consistent with the GR theorem.

Space-like case: $U^\nu(U_\nu)^* < 0$.
In this case, we modify Eq. (6) as follows:

$$\nabla^\nu\nabla_\nu\lambda - (\kappa_0)^2\lambda = 0, \;\; \nabla^\nu\nabla_\nu\phi - (\kappa_0)^2\phi = 0, \;\; C^\nu(L_\nu)^* = 0, \tag{10}$$

$$U_\mu : = (\lambda C_\mu - \phi L_\mu)/2. \tag{11}$$

By doing so, the associated energy–momentum tensor $(\hat{T}_\mu{}^\nu)$ now becomes

$$\hat{T}_\mu{}^\nu = S_{\mu\sigma}S^{\nu\sigma} - \frac{1}{2}g_\mu{}^\nu S_{\sigma\tau}S^{\sigma\tau}. \tag{12}$$

Considering the definition of the Ricci tensor $(R_\mu{}^\nu)$ in Eq. (5), we see that Eq. (12) is isomorphic to the Einstein tensor $(G_\mu{}^\nu = R_\mu{}^\nu - g_\mu{}^\nu R/2)$.

As Dirac's equation $((i\gamma^\nu\partial_\nu + m)\Psi = 0)$ is the square root of the time-like KG equation $((\partial^\nu\partial_\nu + m^2)\Psi = 0)$, the quantum field $(\Psi_{(M)})$ that satisfies the square root of the space-like KG equation $((\partial^\nu\partial_\nu - (\kappa_0)^2)\Psi = 0)$ is shown to be the electrically neutral Majorana fermionic field $(\{(\gamma^\nu_{(M)}\partial_\nu - \kappa_0)\Psi_{(M)} = 0\})$. As the space-like $\Psi_{(M)}$ represents a nonparticle mode, we denote it as the *Majorana fermionic field* instead of the Majorana fermion. Owing to Pauli's exclusion principle, $\Psi_{(M)}$ with a half-integer spin of 1/2 cannot occupy the same state. A possible configuration where a couple of $\Psi_{(M)}$s form a bosonic $S_{\mu\nu}$ field can be identified using the Pauli–Lubanski 4-vector (W_μ), which describes the spin states of moving particles.

$$W_\mu = \frac{1}{2}\epsilon_{\mu\nu\lambda\sigma}M^{\nu\lambda}p^\sigma, \tag{13}$$

where $\epsilon_{\mu\nu\lambda\sigma}$ denotes the $4D$ totally antisymmetric Levi–Civita tensor, $M^{\nu\lambda}$ and p^{σ} are angular and linear momenta, respectively. As Eq. (13) is rewritten as

$$\begin{pmatrix} W_0 \\ W_1 \\ W_2 \\ W_3 \end{pmatrix} = \begin{pmatrix} 0 & M^{23} & M^{31} & M^{12} \\ -M^{23} & 0 & M^{03} & -M^{02} \\ -M^{31} & -M^{03} & 0 & M^{01} \\ -M^{12} & M^{02} & -M^{01} & 0 \end{pmatrix} \begin{pmatrix} p^0 \\ p^1 \\ p^2 \\ p^3 \end{pmatrix}, \tag{14}$$

we can see that two different fields, $(M^{\mu\nu}, p^{\mu})$ and $(N^{\mu\nu}, q^{\mu})$, which satisfy the orthogonality condition ($p^{\nu}q_{\nu} = 0$, corresponding to $C^{\nu}(L_{\nu})^{*} = 0$ in Eq. (10)), can share the same W_{μ} and hence combine to form a spin 1 bosonic field, $S_{\mu\nu}$.

The CDSE field ($S_{\mu\nu}$) has another noteworthy geometric feature, which is particularly important for its application in cosmology. A plane wave of the form, $\psi = \hat{\psi}_c \exp[i(k_{\nu}x^{\nu})]$, satisfies the equation of a couple of λ and ϕ fields in Eq. (10) with $\partial^{\nu}\psi(\partial_{\nu}\psi)^{*} = -(\kappa_0)^2[\hat{\psi}_c(\hat{\psi}_c)^{*}]$. Therefore, for vector L_{μ}, we have

$$L^{\nu}(L_{\nu})^{*} = -(\kappa_0)^2[\hat{\lambda}_c(\hat{\lambda}_c)^{*}] = const. < 0, \tag{15}$$

whose structure resembles that of the tangent vector on de Sitter space. Notably, the importance of this space in the context of spacetime quantization was first noted by Snyder[33]. A pseudo-hypersphere with radius R_{dS} embedded in R^5 is called de Sitter space, which is represented as

$$(\eta_0)^2 - (\eta_1)^2 - (\eta_2)^2 - (\eta_3)^2 - (\eta_4)^2 = -(R_{dS})^2 = -3(\Lambda_{dS})^{-1}. \tag{16}$$

Here, $3(\Lambda_{dS})^{-1} := (R_{dS})^2$ is a frequently employed alternative expression of R_{dS}. Snyder showed that the spacetime (x^{μ}) together with the 4-momentum (p_{μ}), defined as

$$p_{\mu} = \frac{\hbar}{l_p}\frac{\eta_{\mu}}{\eta_4}, \ \ (0 \le \mu \le 3), \ \ p^{\nu}p_{\nu} = \left(\frac{\hbar}{l_p}\right)^2\left[1 - \left(\frac{R_{dS}}{\eta_4}\right)^2\right] < 0, \tag{17}$$

can be quantized without breaking Lorentz's invariance, where l_p denotes Planck's length. We have already seen that an isomorphism exists between the Einstein tensor ($G_{\mu}{}^{\nu}$) and ($\hat{T}_{\mu}{}^{\nu}$) in Eq. (12) whose r.h.s. can be quantized with the Majorana field. Thus, we conjecture that the spacetime quantization scheme of Snyder is consistent with the quantization of $\hat{T}_{\mu}{}^{\nu}$. Eq. (15 and 17) show that L_{μ} and p_{μ} are on the submanifold of de Sitter space, parameterized by $\eta_4 = const.$

As nonlinear electromagnetic field interactions are ubiquitous, the incessant occurrence of instantaneous excitation–deexcitation processes in the $S_{\mu\nu}$ field must be prevalent in the universe. In such processes, we can show that a unique state exists, $|M3\rangle_g$, of $S_{\mu\nu}$, which behaves as if it is "the ground state"of $S_{\mu\nu}$ in the sense that $|M3\rangle_g$ is occupied by $S_{\mu\nu}$ at every moment. To observe this phenomenon, we consider Eq. (13) again. As the spatial dimension of our spacetime is three, the maximum number of space-like momentum vectors satisfying the orthogonality condition (10): ($p^{\nu}q_{\nu} = 0$), is also three. That is, for three different sets of ($M^{\mu\nu}$, p^{μ}),

$(N^{\mu\nu},\ q^{\mu})$, and $(L^{\mu\nu},\ r^{\mu})$ with $p^{\nu}q_{\nu}=0;\ p^{\nu}r_{\nu}=0;\ q^{\nu}r_{\nu}=0$, the following unique spin vector configuration exists:

$$2W_{\mu}=\epsilon_{\mu\nu\lambda\sigma}M^{\nu\lambda}p^{\sigma}=\epsilon_{\mu\nu\lambda\sigma}N^{\nu\lambda}q^{\sigma}=\epsilon_{\mu\nu\lambda\sigma}L^{\nu\lambda}r^{\sigma}. \tag{18}$$

This indicates the existence of a compound state of the Majorana fermionic field with spin 3/2, called the Rarita–Schwinger state ($|M3\rangle_g$). Notice that a bosonic field, $S_{\mu\nu}$, can be constructed by any pair in the set of $\{(M^{\mu\nu},\ p^{\mu}),\ (N^{\mu\nu},\ q^{\mu})$, and $(L^{\mu\nu},\ r^{\mu})\}$ mentioned above. In our scenario of the electromagnetic field interactions in which the ubiquitous field interactions induce the incessant occurrence of excitation–deexcitation processes, the $|M3\rangle_g$ state behaves like "the ground state" of $S_{\mu\nu}$ in the sense that any vacant configuration of $S_{\mu\nu}$, if it exists, must be reoccupied in a moment. This makes $|M3\rangle_g$ a constantly occupied state from a macroscopic timescale.

The key question regarding $|M3\rangle_g$ is whether it is an observable quantity in either a direct or an indirect fashion as $S_{\mu\nu}$, as a space-like quantity, is not observable in general. First, we can say that, within the framework of relativistic QFT, any observable, without exception, associated with the given internal symmetry is the invariant under the action of the transformation group materializing the symmetry under consideration. The second helpful observation is that, as was highlighted after Eq. (17), Lorentz's invariance still holds for Snyder's quantum version of the isomorphism between Einstein tensor $G_{\mu}{}^{\nu}$ and the Majorana version of $\hat{T}_{\mu}{}^{\nu}$ given in Eq. (12). This is in addition to the fact that Lorentz's invariance, indicating an external symmetry, is related to the internal ones through supersymmetry. Based on these observations, we assume that $\{|M3\rangle_g := \Sigma_{(i=1)}^{(3)}\hat{T}_{\nu}{}^{\nu}(x^i)\rightarrow R\}$, *as the invariant of the general coordinate transformations, is an observable as it is indirectly related to the actual observable quantity, i.e., the expansion rate of the universe.*

The simplest model of dark energy is expressed as a cosmological term, $\Lambda_{(de)}g_{\mu\nu}$, with $\Lambda_{(de)}<0$ in the following Einstein field equation, with the sign convention $R>0$ for a matter-dominated closed universe:

$$R_{\mu}{}^{\nu}-\frac{R}{2}g_{\mu}{}^{\nu}+\Lambda_{(de)}g_{\mu}{}^{\nu}=-\frac{8\pi G}{c^4}T_{\mu}{}^{\nu}. \tag{19}$$

From the discussions developed thus far, we can identify observable $\Lambda_{(de)}$ as

$$\Lambda_{(de)}=|M3\rangle_g=\Sigma_{(i=1)}^{(3)}\hat{T}_{\nu}{}^{\nu}(x^i)<0. \tag{20}$$

Recall that the key parameter (κ_0) in Eq. (6) for determining Clebsch variables λ and ϕ is the DP constant, which has been experimentally determined. Using the experimental value of $(\kappa_0^{-1})\approx 50$ nm, we obtain $\Lambda_{(de)}=-2.47\times 10^{-53}m^{-2}$. Conversely, the value of Λ_{obs} derived by Planck satellite observations [34] is estimated as $\Lambda_{(obs)}\approx -3.7\times 10^{-53}m^{-2}$.

2.1.2. *Emergence of the time-like domain*

As shown above, the CP used to develop our dark energy model as a space-like electromagnetic field is an analytic approach that sheds light on the characteristics

of *barotropic (isentropic) fluid motions*. Next, we show that the knowledge on fluid dynamics is again quite helpful in identifying a promising dark matter model, which can be derived by considering *baroclinic (nonisentropic) fluid motions*. For clarity, we begin with the definitions of barotropic and baroclinic fluids. For simplicity, let us consider the nonrelativistic equation of motion of ideal gas flows:

$$\partial_t v_\mu + v^\nu \partial_\nu v_\mu = -\partial_\mu p/\rho = -C_p \partial_\mu T + T\partial_\mu s, \tag{21}$$

where v_μ denotes the $3D$ velocity field; p, ρ, T, and s denote pressure, density, absolute temperature, and specific entropy, respectively; and C_p denotes specific heat at constant pressure. A given fluid motion is barotropic if $\partial_\mu s = 0$ (namely isentropic); otherwise, it is baroclinic. A particularly important conserved quantity for the general baroclinic case is Ertel's potential vorticity (Q[35]), which has the following form:

$$Q := \frac{1}{\rho}(\vec{\nabla} \times \vec{v}) \cdot \vec{\nabla} s, \implies \partial_t Q + v^\nu \partial_\nu Q = 0. \tag{22}$$

Notice that Q can be adopted to label the fluid particles defined in the Lagrangian specification of the flow field. Alternatively, Q may play the role of the "physical coordinates"of the space in which a given baroclinic fluid system undergoes time evolution.

To clarify the underlying mechanism of the interpretation of dark matter in terms of Q, Sakuma et al.[26] examined the novel relativistic representation (Ω_T) of Q. They found that *under the assumption of a low energy limit within which the conservation of the fluid particle number (n) having the form of* $\nabla_\nu(nu^\nu) = 0$ *holds,*

$$\Omega_T := \Omega/T, \;\; \Omega := \omega_{01}\omega_{23} + \omega_{02}\omega_{31} + \omega_{03}\omega_{12}, \tag{23}$$

$$\Omega_T u^\mu = \nabla_\nu[^*(\omega^{\mu\nu})(\sigma/n)], \implies \nabla_\nu(\Omega_T u^\nu) = 0. \tag{24}$$

Here, u^μ, $\omega_{\mu\nu}$, $^*\omega^{\mu\nu}$, T, σ, and n are the nondimensional 4-velocity vector, relativistic vorticity tensor, Hodge's dual of $\omega^{\mu\nu}$, absolute temperature, specific entropy, and particle number per unit volume, respectively. Furthermore, the current ($\Omega_T u^\mu$) is identified as gravitational entropy current. In additional, the conservation law given in the second equation in Eq. (24) shows that the first equation may be considered as "Maxwell's equation" in which $\Omega_T u^\mu$ plays the role of the "electric current". They further derived the following important relations valid among metric tensor $g^{\mu\nu}$, Weyl curvature tensor $W^{\alpha\beta\gamma\delta}$, and relativistic vorticity tensor $\omega^{\mu\nu}$ under the assumption of $W^2\Omega^2 \neq 0$

$$g^{\mu\nu} = \frac{W^{\mu\alpha\beta\gamma}W^{\nu}{}_{\alpha\beta\gamma}}{W^2/4} = \frac{^*\omega^{\mu\sigma}(^*\omega^{\kappa\lambda})\omega^\nu{}_\sigma\omega_{\kappa\lambda}}{(^*\omega^{\kappa\lambda}\omega_{\lambda\kappa})^2/4} = \frac{^*\omega^{\mu\sigma}(^*\omega^{\kappa\lambda})\omega^\nu{}_\sigma\omega_{\kappa\lambda}}{(4\Omega)^2/4}, \tag{25}$$
$$W^2 := W^{\alpha\beta\gamma\delta}W_{\alpha\beta\gamma\delta}, \;\; \Omega := {}^*\omega^{\kappa\lambda}\omega_{\lambda\kappa}.$$

These suggest the existence of the minimum values of $(W_0)^2$ and $(\Omega_0)^2$. In general, $g^{\mu\nu}$ is a purely mathematical concept as it is dependent on the choice of the coordinates. *However, Eq. (25) assigns a unique physical characteristic to* $g^{\mu\nu}$ *such that*

the emergent symmetric space (G/H) in our cosmological theory, as a metric space, assumes the form of a certain kind of spin-network to which the skew-symmetric properties of Eq. (4) are reflected. In relativistic dynamics, mass distribution is directly related to the distribution of scalar curvature $R_\nu{}^\nu$. By contrast, from Eq. (25), we observe that W^2 is directly correlated with $(4\Omega)^2$ and that $\Omega_T u^\mu = (\Omega/T)u^\mu$ behaves like a conserved density current. As the pure Weyl curvature represents the vacuum of relativistic dynamics, a relatively strong current $(\Omega_T u^\mu)$ in a cosmological environment with a negligible value of $R_\nu{}^\nu$ compared with Ω_T would behave like the invisible density current, which is the model of dark matter in our theory. Using Aoki et al.'s[36] recent research outcomes on relativistic conserved charges and entropy current, Sakuma et al.[26] also showed that *the entropy current $\Omega_T u^\mu$ is dynamically associated with an energy–momentum tensor of the form, $\lambda g_{\mu\nu}$, with λ being a positive constant, where $g_{\mu\nu}$ is to be interpreted by Eq. (25).*

Thus, a series of the above analyses on $\Omega_T u^\mu$ suggests that the energy–momentum tensor of dark matter assumes the form of $\Lambda_{(dm)} g_{\mu\nu}$, where constant $\Lambda_{(dm)}$ is to be determined by observations. The consensus ranges of the estimated percentage of dark energy and dark matter are (68%–76%; mean = 72%) and (20%–28%; mean = 24%), respectively. Thus, the following equation:

$$\Lambda_{(dm)} \approx \hat{\Lambda}_{(de)} := -\Lambda_{(de)}/3 = \Lambda_{dS}/3 = 1/(R_{dS})^2, \tag{26}$$

is an estimate consistent with the observation, where R_{dS} and $\Lambda_{dS}/3$ denote the radius of de Sitter space and its alternative expression defined in Eq. (16).

Notably, in our cosmological scenario of CCC-2nd, $\hat{T}_\mu{}^\nu$ in Eq. (12), shown to be isomorphic to the space-like Einstein tensor $(G_\mu{}^\nu)$ and $\Lambda_{(dm)} g^{\mu\nu}$ with $g^{\mu\nu}$ given by Eq. (25), provide *the physical* space- and time-like spacetimes, respectively. These spacetimes emerged from the spontaneous symmetry breaking of the *primordial* light field with null distance $(ds^2 = 0)$. To consolidate our CCC-2nd scenario here, we show that a unique vector boson exists in our model, which plays the role of the Nambu–Goldstone boson (NGB) associated with the spontaneous symmetry-breaking process.

To start, we consider again the space-like CP of U^μ explained in Eq. (10, 11). The field strength $(S_{\mu\nu})$ defined by the curl of U_μ assumes the same form as the one in the light-like case given in the second equation in Eq. (8). Contrarily, the null geodesic equation $(U^\nu \nabla_\nu U_\mu = 0)$ in Eq. (8) is replaced by

$$U^\nu \nabla_\nu U_\mu = -S_{\mu\nu} U^\nu + \nabla_\nu (U^\nu U_\nu/2) = 0; \;\; U^\nu U_\nu < 0. \tag{27}$$

In relativistic fluid dynamics, the magnitude of U^μ, defined by $V := U^\nu U_\nu/2$, can be normalized as $V = 1$[37]. As the equations on λ and ϕ in Eq. (10) are linear, we can introduce a similar normalization for $L_\mu = \nabla_\mu \lambda$ and $C_\mu = \nabla_\mu \phi$. The natural normalization would be

$$L^\nu L_\nu = -(m_\lambda)^2 \lambda^2, \;\; C^\nu C_\nu = -(m_\phi)^2 \phi^2, \tag{28}$$

where the wavenumber vector, k^μ, of the respective plane-wave solutions satisfies $k^\nu k_\nu = -(m_\lambda)^2$ and $k^\nu k_\nu = -(m_\phi)^2$. For the space-like CP of U^μ discussed thus

far, we have

$$(m_\lambda)^2 = (m_\phi)^2 = (\kappa_0)^2. \tag{29}$$

Using the orthogonality condition, $C^\nu (L_\nu)^* = 0$, in Eq. (10) and Eq. (28), a couple of important characteristics of space-like U^μ fields can readily be expressed as

$$\nabla_\nu U^\nu = 0, \quad V = -\frac{1}{8}\lambda^2\phi^2[(m_\lambda)^2 + (m_\phi)^2]. \tag{30}$$

Now, revisiting Eq. (10), we consider a different case in which we only replace the second equation, $\nabla^\nu\nabla_\nu\phi - (\kappa_0)^2\phi = 0$, with $\nabla^\nu\nabla_\nu\phi + (\kappa_0)^2\phi = 0$. With this change, Eq. (29) changes into $(m_\lambda)^2 = (\kappa_0)^2 = -(m_\phi)^2$. Consequently, V in Eq. (30) vanishes, and U^μ becomes a null vector. Notably, the form of $S_{\mu\nu}U^\nu$ in Eq. (27) is similar to that of Lorentz force, $F_{\mu\nu}(ev^\nu)$, where $F_{\mu\nu}$ and ev^ν denote the background electromagnetic field and an electric current with charge e, respectively. A direct expression of $-S_{\mu\nu}U^\nu$ is

$$\begin{aligned} -S_{\mu\nu}U^\nu &= -(L_\mu C_\nu - L_\nu C_\mu)(\lambda C^\nu - \phi L^\nu)/2 \\ &= -\lambda\phi(\kappa_0)^2(\phi L_\mu - \lambda C_\mu)/2 = \lambda\phi(\kappa_0)^2 U_\mu. \end{aligned} \tag{31}$$

Conversely, as we have $\nabla_\nu U^\nu = -\lambda\phi(\kappa_0)^2$, in this case, Eq. (31) becomes

$$S_{\mu\nu}U^\nu = -\lambda\phi(\kappa_0)^2 U_\mu = (\nabla_\nu U^\nu)U_\mu \neq 0. \tag{32}$$

Eq. (32) expresses that *the null vector U^μ with a nonvanishing irrotational part* is a vector field for which κ_0 and $i\kappa_0$ play the role of the field source as in the case of $\pm e$ in electromagnetism. Furthermore, the field source behaves as if it is an "electrically charged virtual photon" responsible for nonlinear electromagnetic field interactions. In our CCC-2nd scenario, the emergence of a couple of these sources (κ_0 and $i\kappa_0$) is interpreted as the consequence of the spontaneous symmetry breaking of the light vector field whose temporal and spatial components exist in a balanced manner. Thus, we believe that the vector field, U^μ, with the abovementioned characteristics plays the role of NGB in our cosmological scenario. Moreover, it plays substantial roles in the nonlinear field interactions between the quantum generalized sectors defined by Ojima[14], existing on not only time-like but also space-like domains, and the classical generalized sectors on time-like domains. In the subsequent section, we show that the DP constant ($l_{dp} \approx 50$ nm), defined as the inverse of κ_0, gives the scale of the Heisenberg cut dividing the whole universe into micro-quantum and macro-classical worlds (cf. Eq. (42)).

Interestingly, we can unravel many conceptual aspects of QFT from such a specific theory as the description of the behaviors of DPs. Here, the concentration of the momentum support of the dressed photon field in the space-like domain ($p^2 = p_\mu p^\mu < 0$) plays the most important role, which is in sharp contrast to the time-like momenta owing to the particle-like excitations. This contrast between the space- and time-like momenta should not be superficially considered. However, the important factor is the medium or environment constructed by the space-like

momenta, in contrast to the particle-like motions associated with the time-like momenta. From this viewpoint, the distribution of different sizes of space-like momenta ($p^2 < 0$) describes the difference among different media, which constitutes the categorical background of algebraic QFT constructed by arrows of space-like momenta. Therefore, this kind of interpretation of space-like momenta associated with dressed photons exhibits the categorical essence of QFT.

Along this line, we promote new research on the relevance of Kan extentions in the QFT of dressed photons. This is applicable if the four terms constituting MMD are recombined into the three terms of micro-dynamical systems (comprising micro-dynamics acting on the micro-algebra) and macro-states, together with a macro-classifying space constructed by the classifying parameters of macro-states.

3. Approach to the hierarchy problem

The Einstein field equation incorporating our dark energy and matter model is expressed as follows:

$$R_\mu{}^\nu - \frac{R}{2} g_\mu{}^\nu + \Lambda_{(dm)} g_\mu{}^\nu = -\frac{8\pi G}{c^4}[T_\mu{}^\nu + \{\Lambda_{(de)} g_\mu{}^\nu\}], \tag{33}$$
$$\Lambda_{(dm)} = -\Lambda_{(de)}/3 + \epsilon > 0.$$

Here, our present concern is the dark matter field, $\Lambda_{(dm)} g_\mu{}^\nu$, as the main source of the gravitational field. As the first step, by comparing Coulomb's law with the universal law of gravitation, we obtain

$$F_e = \frac{1}{4\pi\epsilon_0}\frac{q_1 q_2}{r^2}, \quad F_g = G\frac{m_1 m_2}{r^2}. \tag{34}$$

Let us examine the F_e/F_g ratio, where the notations used in Eq. (34) are conventional. By doing so, it would be natural to choose the fundamental electric charge (e) for $q_1 = q_2$. However, for $m_1 = m_2$, we encounter a serious challenge as we cannot single out "the fundamental mass charge" like e in the case of F_e. To overcome this problem, recall first that, for our dark energy model, a unique state, $|M3\rangle_g$, exists, which behaves like "the ground state" of $S_{\mu\nu}$. Through Eq. (20) and Eq. (26), this "ground state" is directly related to $\Lambda_{(dm)}$. By contrast, in Eq. (25), we highlight the existence of the minimum value of W^2, i.e., $(W_0)^2 \neq 0$, associated with the conformal symmetry breaking of the light field (H). Thus, we naturally assume that $\Lambda_{(dm)} = |W_0|$. Notably, in our previous studies where we did not consider the possibility of the "temporal change" of $\Lambda_{(dm)}$ in the dark matter field ($\Lambda_{(dm)} g_{\mu\nu}$), we simply asserted $\Lambda_{(dm)} = W_0 = const.$ However, in the present discussion where we consider the "temporal change" of $\Lambda_{(dm)}$, we assume that W_0 is a certain positive constant that satisfies

$$W_0 := Min\{\Lambda_{(dm)}\}. \tag{35}$$

Under this new hypothesis, we can regard $\Lambda_{(dm)}$ as the fundamental mass of the gravitational field; the justification will be provided shortly.

As the dimension of $\Lambda_{(dm)}$ is (length)$^{-2}$, we introduce m_λ having the dimension of mass, corresponding to $\Lambda_{(dm)}$. Substituting e and m_λ into F_e and F_g in Eq. (34), respectively, we obtain

$$\frac{F_e}{F_g} = \frac{e^2}{4\pi\epsilon_0}\frac{1}{G(m_\lambda)^2} = \frac{e^2}{4\pi\epsilon_0 c\hbar}\frac{c\hbar}{G(m_\lambda)^2} = \alpha\left(\frac{m_p}{m_\lambda}\right)^2, \tag{36}$$

$$\alpha := \frac{e^2}{4\pi\epsilon_0 c\hbar}, \quad m_p := \sqrt{\frac{c\hbar}{G}}, \tag{37}$$

where α and m_p are the coupling constant of the electromagnetic field and Planck's mass. For $\Lambda_{(dm)}$, using Eq. (26), namely, $\Lambda_{(dm)} \approx -\Lambda_{(de)/3}$, and using the concrete expression of Eq. (20) obtained in reference [17], we have

$$\Lambda_{(dm)} \approx \frac{4\pi G h}{c^3}\frac{(\kappa_0)^2}{\epsilon} = \frac{8\pi^2 G\hbar}{c^3}\frac{(\kappa_0)^2}{\epsilon} = 8\pi^2(l_p)^2\frac{1}{\epsilon(l_{dp})^2};\ \ l_{dp} := (\kappa_0)^{-1}. \tag{38}$$

Here, l_p and l_{dp} are the Planck length and DP length defined as the inverse of the *DP constant* in Eq. (6); ϵ denotes a dimension adjusting coefficient of *unit length squared*. Two reasons exist for the appearance of ϵ in the expression of $\Lambda_{(dm)}$. First, the quantity, $\Lambda_{(de)} = \Sigma_{(i=1)}^{(3)}\hat{T}_\nu{}^\nu(x^i)$, in Eq. (20) is related to the "radiation pressure" of the $S_{\mu\nu}$ field. Second, the calculation of such a quantity is required to make the energy quantization of the light-like $S_{\mu\nu}$ field consistent with $E = h\nu$ for the usual radiation field. As we have introduced m_λ as the elemental mass corresponding to $\Lambda_{(dm)}$, we can determine it by the following formal identification using Einstein's field equation:

$$\Lambda_{(dm)}g_\mu{}^\nu = \frac{8\pi G}{c^4}[(\rho_\lambda c^2)u_\mu u^\nu],\ \ \Rightarrow\ \ \Lambda_{(dm)}(l_\epsilon)^3 = \frac{8\pi G}{c^2}m_\lambda,\ \ m_\lambda = \rho_\lambda(l_\epsilon)^3, \tag{39}$$

where l_ϵ denotes unit length. Therefore, using Eq. (36), Eq. (37), Eq. (38), and Eq. (39), we finally obtain

$$\frac{F_e}{F_g} = \frac{\alpha}{\pi^2}\frac{(l_{dp})^4}{(l_p)^2}\frac{1}{\epsilon}. \tag{40}$$

Substituting $\alpha = 7.3\times10^{-3}$, $\pi^2 = 9.9$, $l_p = 1.6\times10^{-35}$m, $l_{dp} \approx 5.0\times10^{-8}$m, and $\epsilon = 1\text{m}^2$ into Eq. (40), we obtain

$$\frac{F_e}{F_g} = 1.7\times10^{37}, \tag{41}$$

which appears to be consistent with the conventional rough estimates obtained without using $\Lambda_{(dm)}$.

Having derived Eq. (40), now we examine the consequence of the "temporal change" of $R_{dS}(=1/\sqrt{\Lambda_{(dm)}})$ applicable to F_e/F_g in Eq. (40). In the introduction, we cited previous studies on (cosmological) time-dependent physical constants. Suppose that $\Lambda_{(dm)}$ is such a time-dependent quantity, then $\Lambda_{(dm)}g_\mu{}^\nu$ in Eq. (33) ceases to be a divergence-free term. Notice, however, that as $\Lambda_{(dm)}$ is directly related to the radius (R_{dS}, in Eq. (26)) of de Sitter space (Eq. (16)), the partial derivative of

$\Lambda_{(dm)}$ with respect to the cosmological coordinate (x^μ) vanishes. This is because the shape of the isotropic universe is given by a de Sitter space and $\nabla_\mu R_{dS}$ $(0 \leq \mu \leq 3)$ is on the tangent hyperplane of $R_{dS} = const.$, on which the gradient of the local $4D$ spacetime coordinate (x^μ) exists. Thus, in this sense, $\Lambda_{(dm)} g_\mu{}^\nu$ remains a divergence-free term, although the radius can either expand or shrink in the fifth dimension perpendicular to the gradient of the $4D$ coordinates (x^μ). The "temporal change" of $\Lambda_{(dm)}$ that we consider is the change in the magnitudes of the dark energy and matter fields.

For simplicity, in our discussion, except for $\Lambda_{(de)}$ and the related $\Lambda_{(dm)}$, we assume that all physical constants are fixed quantities. From Eq. (26, 38), we readily obtain

$$l_{dp} \approx \frac{2\sqrt{2}\pi}{\sqrt{\epsilon}} \frac{l_p}{\sqrt{\Lambda_{(dm)}}} = \frac{2\sqrt{2}\pi}{\sqrt{\epsilon}} l_p R_{dS}, \tag{42}$$

which implies that the DP length (l_{dp}) affords the geometric mean of the smallest Planck length (l_p) and the largest scale of our universe (R_{dS}). Furthermore, under the assumption that $l_p = const.$, l_{dp} becomes proportional to R_{dS}. Thus, we can choose l_{dp} as the unique geometrical parameter of our cosmological model. From the viewpoint of the unification of four forces, examining the case where we have $F_e/F_g = 1$ is interesting. A simple calculation shows that

$$\text{the present value}: \quad \frac{F_e}{F_g} = 1.7 \times 10^{37}; \quad l_{dp} \approx 5.0 \times 10^{-8}\text{m} \tag{43}$$

$$\text{the unification value}: \quad \frac{F_e}{F_g} = 1; \qquad\qquad l_{dp} \approx 2.4 \times 10^{-17}\text{m}. \tag{44}$$

Thus, using Eq. (38), we observe that the unification value of $\Lambda_{(dm)}(u)$ is $(4.4{\times}10^{18})$ times larger than the present value of $\Lambda_{(dm)}(p)$.

We focus on dark energy and matter mainly because of their extreme predominance over material substances. This implies that, in thermodynamic terminology, the dark matter field $(\Lambda_{(dm)} g_{\mu\nu})$ with positive $\Lambda_{(dm)}$ resulting from *Weyl curvature* and dark energy field $(\Lambda_{(de)} g_{\mu\nu})$ with negative $\Lambda_{(de)} g_{\mu\nu}$ resulting from *Ricci curvature* would work as high- and low-temperature reservoirs, respectively, for the gravity-driven temporal evolution of such material systems as stars, galaxies, clusters of galaxies, and the large-scale structure of the cosmos. Moreover, in this cosmic thermodynamical system, $\Omega_T u^\mu$, defined in Eq. (24), gives the gravitational entropy flow. As the energy density of the two thermal reservoirs are finite, the initial "temperature difference" between them, measured by $\Lambda_{(dm)}(u) - \Lambda_{(de)}(u) \approx 4\Lambda_{(dm)}(u)/3 = 4[R_{dS}(u)]^{-2}/3$, would decrease with the temporal evolution of material systems. This result can be observed as the extra expansion (increase of R_{dS}) of our universe in the fifth dimension, directly related to the temporal increase in the ratio of the previously discussed coupling constants, $F_e/F_g \propto (R_{dS})^2$. Although the dynamics we have discussed are unrelated to superstring theories, it is interesting to bring our attention to Witten's noteworthy

remark[38] made at *Strings '95*: "eleven-dimensional supergravity arises as a low energy limit of the ten-dimensional Type IIA superstring." This appears to be qualitatively similar to our present situation, in which our $4D$ universe undergoes an extra expansion into the surrounding fifth-dimensional space. The expansion starts from the initial high-energy state of $F_e/F_g \approx 1$ with a negligible magnitude of W^2 in Eq. (25) to low energy states having large values of W^2 as the measure of conformal gravity.

4. Implication of Maldacena (AdS/CFT) duality

In subsection 2.1.1, we saw that the CDSE field ($S_{\mu\nu}$) is closely related to de Sitter space having the well-known scale-free property. Recall first that spinor is an irreducible representation of the universal covering group, $SU(2)$ of $SO(3)$. For the $4D$ spacetime case, in which we have the Lorentz transformation group ($SO(1,3)$), the Lorentzian spinor ($SL(2,C)$) corresponds to $SU(2)$ in the case of $SO(3)$. When we further extend $SO(1,3)$ into the $4D$ conformal transformation group ($SO(2,4)$), $SL(2,C)$ is extended into $SU(2,2)$, which operates on Penrose's twistor in the $4D$ complex spacetime. As in the case of the above extension of spinor, we can also consider a similar extension of the electromagnetic field ($F_{\mu\nu}$) as the $U(1)$ gauge field. We believe that the CP (explained in subsection 2.1.1) applied to extend $F_{\mu\nu}$ into a space-like momentum domain is what is required for such an extension of conformal transformation, which is closely related to the important notion of modular form.

The fact that the emergence of de Sitter space through CP is an inevitable consequence of the extension of $SL(2,C)$ can be readily verified from the following properties of the Lorentzian spinor, $\Psi(V^\mu)$:

$$\Psi(V^\mu) = V^{\mu(\mu)'} = \begin{bmatrix} V^{00'} & V^{01'} \\ V^{10'} & V^{11'} \end{bmatrix} = \frac{1}{\sqrt{2}} \begin{bmatrix} V^0 + V^3 & V^1 + iV^2 \\ V^1 - iV^2 & V^0 - V^3 \end{bmatrix}, \tag{45}$$

$$det\Psi(V^\mu) = \frac{1}{2}[(V^0)^2 - (V^1)^2 - (V^2)^2 - (V^3)^2]. \tag{46}$$

For the space-like vector, V^μ, $det\Psi(V^\mu)$ becomes negative so that Eq. (46) becomes isomorphic to the second equation in Eq. (17). As Eq. (16) and Eq. (17) are connected by a one-to-one correspondence through parameter η_4 and the latter is isomorphic to Eq. (46), we thus see that de Sitter space and $\Psi(V^\mu)$ share the same symmetry.

Now, we compare the following forms of $g^{\mu\nu}$:

$$g^{\mu\nu}_{(I)} = \frac{-1}{\Lambda_{(I)}} \left(R^{\mu\nu}_{(I)} - \frac{R_{(I)}}{2} g^{\mu\nu}_{(I)} \right), \ (W^{\alpha\beta\gamma\delta} = 0), \ (I = 1 \text{ or } 2), \tag{47}$$

$$g^{\mu\nu} = \frac{W^{\mu\alpha\beta\gamma} W^{\nu}{}_{\alpha\beta\gamma}}{W^2/4} \ (W^2 \neq 0), \tag{48}$$

where Eq. (47) represents either de Sitter space with $\Lambda_{(1)} = \Lambda_{(de)} < 0$ or anti de Sitter space (AdS) with $\Lambda_{(2)} = \Lambda_{(dm)} > 0$, depending on the index (I).

In our CCC-2nd hypothesis, the isotropy of an early universe is explained by the small amplitude of W^2 (the Weyl curvature hypothesis proposed by Penrose[29]), which motivates us to examine the possibility that the following limit exists:

$$g^{\mu\nu} = \frac{W^{\mu\alpha\beta\gamma}W^{\nu}{}_{\alpha\beta\gamma}}{W^2/4} \longrightarrow g^{\mu\nu}_{(2)} = \frac{-1}{\Lambda_{(2)}}\left(R^{\mu\nu}_{(2)} - \frac{R_{(2)}}{2}g^{\mu\nu}_{(2)}\right), \text{ as } W^2 \to 0. \quad (49)$$

Within the framework of our CCC-2nd hypothesis, this gives a diffeomorphism defined as the time reversal of a given cosmological time development. As $g^{\mu\nu}$ on the l.h.s. gives the gravitational field, whereas the r.h.s. represents AdS, Eq. (49) can be regarded as the "Maldacena (AdS/CFT) duality"[27] in CCC-2nd.

5. Summary and conclusion

Using our recently developed unconventional model incorporating dark energy and matter, we re-examined the hierarchy problem. As the model itself is not well known, we began our discussion by recapitulating the key concepts used in our new theory to elucidate an elusive phenomenon called *DP* in the field of nanophotonics. This phenomenon unexpectedly inspired the novel perspective on cosmological problems addressed in this study. The concepts include the GR theorem for nonlinear quantum field interactions, Ojima's MMD theory developed from DHR's original sector theory in QFT, and CDSE field developed by the first author, together with the unconventional introduction of conformal gravity explained in subsection 2.1.

In addition, as an outstanding feature of our cosmological theory, we use the basic view that our universe is undergoing an infinite cycle of birth and death as in the case of CCC. However, a crucial difference exists between CCC and our theory (CCC-2nd), namely, the twin structure of a universe arising from the intrinsic property of de Sitter space. Our reason for supporting such a view is twofold. First, we believe that the basic principle of the universe is not complicated but simple. The creation and annihilation mechanisms of the matter and antimatter pair through the intervention of a light field observed in laboratories can also be applied naturally to the case of a twin universe configuration. Once we accept this conceptually simple view on the creation of the universe, we need not worry about complicated parameter tuning processes used in the widely prevailing theory of cosmic inflation, which favors the creation of everything from emptiness.

Second, as mentioned in the introductory section, the idea of the creation of everything from emptiness appears to be conceived from either the misinterpretation or the extended interpretation of Fock vacuum $|0\rangle$, which is, as far as QFT is concerned, introduced within the framework of linear dynamics on free modes. In our cosmological theory, as Eq. (26) shows, the universe expands, keeping a quasi-equilibrium between $\Lambda_{(dm)}$ and $\hat{\Lambda}_{(de)}$, which behave as "high and low temperature reservoirs", respectively, for the temporal evolutions of systems in the universe. Thus, the essential global aspect of the expanding universe in a quasi-equilibrium state should be described by the Tomita–Takesaki theory[39] as a thermodynamic

Kubo–Martin–Schwinger (KMS) state with infinite degrees of freedom. As the KMS state is a mixed one, its corresponding Gel'fand–Naimark–Segal representation is reducible. Therefore, for $\mathcal{M}$, defined as a von Neumann algebra on Hilbert space $\mathfrak{H}$, there exists its commutant, $\mathcal{M}'$, which satisfies the following inversion relation:

$$J\mathcal{M}J = \mathcal{M}', \quad e^{itH}\mathcal{M}e^{-itH} = \mathcal{M}, \quad J^2 = 1, \tag{50}$$

$$JHJ = -H, \tag{51}$$

where H and J denote the Hamiltonian and antiunitary operators called modular conjugation, respectively. Notice that the spectrum of the Hamiltonian is symmetric with respect to its sign, which indicates the existence of states with negative energy. We believe that the result of the Tomita–Takesaki theory applies to the case of a twin universe configuration and to the thermodynamics of the observed cosmic background radiation whose energy-spectrum distribution is given by the black body radiation.

Eq. (40) stands as the central result in our study, showing the clear causal relation between the existence of noncompactified extra dimension and F_e/F_g, in which the DP length (l_{dp}) plays the key role in determining the value of F_e/F_g. Through Eq. (42), we see that l_{dp} divides the universe into two domains. Furthermore, its present value, given in Eq. (43), suggests that l_{dp} affords the scale of the Heisenberg cut dividing the micro-quantum and the macro-classical worlds.

As the final remark on our study, we wish to make a few brief comments on the innovative observational outcomes of the James Webb Space Telescope (JWST). One of the quite unexpected findings of the *JWST Advanced Deep Extragalactic Survey* is that the events considered to have occurred in the very early stages of the universe actually occurred much earlier than expected. We have shown that the magnitudes of $\Lambda_{(dm)}$ and $\Lambda_{(de)}$ given in Eq. (26) in the early stage of the universe were considerably greater than those in the present one. Thus, we conjecture that the standard ΛCDM model used in cosmological simulations is not suitable for simulating the temporal development of the early universe. Eq. (33) shows that the isotropic expansion owing to $\Lambda_{(de)}g_{\mu\nu}$ on the r.h.s. manifests itself through a conformally flat Ricci curvature. Conversely, the local gravitational attraction owing to $\Lambda_{(dm)}g_{\mu\nu}$ on the l.h.s. is highly nonisotropic because of the intrinsic property of the Weyl curvature. Data from CEERS survey by JWST show that most of the very early galaxies assumed elongated shapes similar to noodles or surfboards, which appears to be consistent with our conjecture on the gravitational effect arising from the nonisotropic Weyl curvature. Presumably, the observed large-scale structure of the present universe comprising galaxy filaments and voids is also the manifestation of this nonisotropic Weyl curvature effect.

Regarding the cosmic age problem relating to the very early formation of primordial galaxies, in his 2023 paper, Gupta[40] proposed an intriguing resolution derived from the outcome of a hybrid cosmological model called CCC(*covarying coupling constants*) + TL(*tired light*). The idea of CCC is similar to that of Dirac's hypothesis on varying physical constants, such as gravitational constant (G) and

speed of light (c). Gupta introduced the CCC model as an extended version of the ΛCDM model with *a variant cosmological constant*. In that sense, our model with a varying $\Lambda_{(dm)}(\approx -\Lambda_{(de)}/3)$ is similar to the CCC model. However, a crucial difference exists between these two models. In Gupta's model, parameter α, called *the strength of the coupling constant's variation*, plays a substantial role, whereas in our model, all usual physical constants, except for Λ, are assumed to be non-variant. We adopt this assumption because it is the simplest one. Therefore, the question of whether physical constants are unchanging or not remains unanswered. Qualitatively, much larger value of $\Lambda_{(dm)}$ in our model of the very early universe and much larger value of gravitational constant G in Gupta's model would have a similar impact on the formation of early galaxies. The most important characteristics of our model is the possibility of the universe expansion in fifth dimensional direction, which reveals that our universe as a $4D$ Riemannian manifold is not a closed entity but is open to a higher dimensional realm.

Acknowledgments

All of the authors express their sincere appreciation for the distinguished leadership of M. Ohtsu, Prof. Emer. of the University of Tokyo, who has been and is still driving unique "off-shell science project" originated from his lifelong dressed photon research in the field of nanophotonics.

Appendix A. Greenberg-Robinson theorem

The essence of the theorem is that off-shell fields is never compatible with the on-shell condition characterizing (generalized) free fields in the special relativistic situation. To precisely state the theorem, we briefly present the Wightman system of axioms. In this appendix, we use the natural system of units, the unit system such that $c = 1$ and $\hbar = 1$.

The following family of four axioms is referred to as the Wightman system of axioms:

[1. Field operator] For a neutral field, a field operator $\phi(x)$, $x \in \mathbb{R}^4$, is defined by an operator on a Hilbert space $\mathcal{H}$.

[2. The covariance condition] A (projective) unitary representation (U) of the Poincaré group exists, $\mathcal{P}_+^\uparrow = \mathbb{R}^4 \rtimes \mathcal{L}_+^\uparrow$ on $\mathcal{H}$ such that

$$U(a, L)\phi(x)U(a, L)^* = \phi(Lx + a) \tag{A.1}$$

for all $(a, L) \in \mathcal{P}_+^\uparrow = \mathbb{R}^4 \rtimes \mathcal{L}_+^\uparrow$.

[3. The causality condition] $\phi(x)$, $x \in \mathbb{R}^4$, satisfy the local commutativity, that is,

$$[\phi(x), \phi(y)] = \phi(x)\phi(y) - \phi(y)\phi(x) = 0 \tag{A.2}$$

for all pairs (x, y) of mutually space-like points.

[4. Vacuum state and the spectrum condition] A unit vector, Ω of $\mathcal{H}$, called the vacuum vector and a spectral measure (E) of $\mathbb{R}^4$ on $\mathcal{H}$ exist, satisfying the following two conditions:

4.1 Ω satisfies $U(a,L)\Omega = \Omega$ for all $(a,L) \in \mathcal{P}_+^\uparrow$. E satisfies

$$U(a,I) = \int_{\overline{V_+}} e^{ia\cdot p}\, dE(p) \tag{A.3}$$

for all $a \in \mathbb{R}^4$, where $\overline{V_+} = \{x = (x^\mu) \in \mathbb{R}^4 \,|\, x^2 = x_\mu x^\mu \geq 0 \text{ and } x^0 \geq 0\}$ and $a \cdot p = a^\mu p_\mu$ (Ω then satisfies $E(\{0\})\Omega = \Omega$).

4.2 Ω is cyclic for $\mathcal{P}(\mathbb{R}^4)$, the polynomial algebra over $\mathbb{C}$ generated by $\{\phi(x) \,|\, x \in \mathbb{R}^4\}$, i.e., $\mathcal{H} = \overline{\mathcal{P}(\mathbb{R}^4)\Omega} = \overline{\{X\Omega \,|\, X \in \mathcal{P}(\mathbb{R}^4)\}}$.

Strictly, every field operator is defined as an operator-valued distribution. However, we omit the detail (see [41] for example). Moreover, no field operator is defined at each point x of the Minkowski space, so that $\phi(x)$ is simply a symbolic notation.

A neutral field $\phi(x)$ is *irreducible* if it satisfies the following condition: If B is a bounded linear operator on $\mathcal{H}$ such that

$$\langle\Omega|B\phi(x_1)\phi(x_2)\cdots\phi(x_m)\Omega\rangle = \langle\phi(x_m)^*\phi(x_{m-1})^*\cdots\phi(x_1)^*\Omega|B\Omega\rangle \tag{A.4}$$

for every natural number m and points $x_1, \cdots, x_m$ of the Minkowski space, then it is of the form $B = kI$, where $k \in \mathbb{C}$ and I is the identity operator on $\mathcal{H}$.

The Fourier transform $\hat{\phi}(p)$ of a field operator $\phi(x)$ is defined by

$$\hat{\phi}(p) = \frac{1}{(2\pi)^2}\int_{\mathbb{R}^4} e^{-ip\cdot x}\phi(x)\, d^4x. \tag{A.5}$$

A field $\phi(x)$ is called a *generalized free field* if it satisfies the commutation relation

$$[\phi(x), \phi(y)] = iP(x-y)I \tag{A.6}$$

for all $x, y \in \mathbb{R}^4$. The function $P(x)$ is called the function defined by

$$P(x) = \int_0^\infty D_{\sqrt{\xi}}(x)\, d\sigma(\xi), \tag{A.7}$$

where σ is a measure on $\mathbb{R}_{\geq 0} = \{x \in \mathbb{R} \,|\, x \geq 0\}$,

$$D_m(x) = \frac{1}{(2\pi)^3}\int_{\mathbb{R}^3} \sin(p^0x^0)e^{-i\boldsymbol{p}\cdot\boldsymbol{x}}\frac{d\boldsymbol{p}}{p^0} \tag{A.8}$$

and $p^0 = \sqrt{\boldsymbol{p}^2 + m^2}$. The free Klein-Gordon field $\varphi(x)$ with square mass $m^2(>0)$, a typical example, satisfies the commutation relation $[\varphi(x), \varphi(y)] = iD_m(x-y)I$ for all $x, y \in \mathbb{R}^4$.

Theorem 1 (Greenberg-Robinson [42,43]). *Let $\phi(x)$ be an irreducible neutral field. If an open subset exists, O, of $\mathbb{R}^4\backslash\overline{V_\pm}$ such that $\hat{\phi}(p) = 0$ for all $p \in O$, where $\overline{V_\pm} = \{x \in \mathbb{R}^4 \,|\, x^2 = x_\mu x^\mu \geq 0\}$, then $\phi(x)$ is a generalized free field.*

The contraposition of this theorem implies that

If an irreducible neutral field $\phi(x)$ is not a generalized free field, it holds that $\hat{\phi}(x) \neq 0$ for all $p \in \mathbb{R}^4$.

This fact indicates that the involvement of off-shell momenta is specific to interacting quantum fields and is never observed in (generalized) free fields at the four-dimensional Minkowski space.

References

[1] P. A. M. Dirac, Letters to the Editor, *NATURE* **139** (1937), 323.
[2] P. A. M. Dirac, Long Range Forces and Broken Symmetries, *Proceedings of the Royal Society, London A* **333** (1973), 403–418.
[3] E. A. Milne, *Kinematic Relativity* (Oxford, 1948).
[4] V. Canuto and J. Lodenquai, Dirac cosmology, *Astrophys. J.* **211** (1977), 342–356.
[5] T. C. Van Flandern, Is the gravitational constant changing? *International Astronomical Union Colloquium* **63** (1981), 207–208.
[6] H. Reeves, On the origin of the light elements ($Z < 6$), *Rev. Mod. Phys.* **66** (1994), 193.
[7] P. J. E. Peebles and B. Ratra, Cosmology with a Time-Variable Cosmological "Constant", *Astrophysical J. Lett.* **325** (1988), L17.
[8] V. S. Troitskii, Physical Constants and Evolution of the Universe, *Astrophysics and Space Science* **139** Issue 2, (1987), 389–411.
[9] J. P. Petit, AN INTERPRETATION OF COSMOLOGICAL MODEL WITH VARIABLE LIGHT VELOCITY, *Mod. Phys. Lett. A* **3**, No.16, (1988), 1527-1532.
[10] J. P. Petit and M. Viton, GAUGE COSMOLOGICAL MODEL WITH VARIABLE LIGHT VELOCITY: III. COMPARISON WITH QSO OBSERVATIONAL DATA, *Mod. Phys. Lett. A* **4**, No. 23, (1989), 2201–2210.
[11] Lisa Randall and Raman Sundrum, Large Mass Hierarchy from a Small Extra Dimension, *Phys. Rev. Lett.* **83** (1999), 3370.
[12] R. Jost, *The General Theory of Quantized Fields*; (American Mathematical Society: Providence, RI, USA, 1963.)
[13] G. F. Dell'Antonio, Support of a field in p space. *J. Math. Phys.* **2** (1961), 759–766.
[14] I. Ojima, A unified scheme for generalized sectors based on selection criteria-order parameters of symmetries and of thermal situations and physical meanings of classifying categorical adjunctions. *Open Syst. Inf. Dyn.* **10** (2003), 235–279.
[15] I. Ojima, Micro-Macro duality and emergence of macroscopic levels. *Quantum Probab. White Noise Anal.* **21** (2008), 217–228.
[16] H. Sakuma, I. Ojima, M. Ohtsu, Gauge symmetry breaking and emergence of Clebsch-dual electromagnetic field as a model of dressed photons. *Appl. Phys. A* **123** (2017), 750.
[17] H. Sakuma, I. Ojima, M. Ohtsu, and H. Ochiai, Off-Shell Quantum Fields to Connect Dressed Photons with Cosmology, *Symmetry* **12(8)** (2020), 1244; doi:10.3390/sym12081244.
[18] H. Sakuma, Virtual Photon Model by Spatio-Temporal Vortex Dynamics. In *Progress in Nanophotonics* **Vol. 5**, pp. 53–77, T. Yatsui, Ed., (Springer Nature, Switzerland, 2018).
[19] G. W. Mackey, A theorem of Stone and von Neumann. *Duke Math. J.* **16** (1949), 313–326.
[20] S. Doplicher, R. Haag and J. E. Roberts, *Comm. Math. Phys.* **13** (1969), 1–23; **15** (1969), 173–200; **23** (1971), 199–230 & **35** (1974), 49–85.

[21] S. Doplicher and J. E. Roberts, *Comm. Math. Phys.* **131** (1990), 51–107; *Ann. Math.* **130** (1989), 75–199 (1989); *Inventiones Math* **98** (1989), 157–218.
[22] Sakuma, H., Ojima, I. and Ohtsu, M., Perspective on an Emerging Frontier of Nanoscience Opened up by Dressed Photon Studies, Nanoarchitectonics **Vol. 5** Issue 1, (2024), 1 – 23.
[23] H. Sakuma, I. Ojima, and M. Ohtsu, Dressed photon in a new paradigm of off-shell quantum fields, Progress in Quantum Electronics **Vol. 55**, (2017), 74 – 87.
[24] Lamb, S. H. *Hydrodynamics*, 6th ed. Cambridge University Press: Cambridge, UK, (1930), 248–249.
[25] H. Sakuma and I. Ojima, On the Dressed Photon Constant and Its Implication for a Novel Perspective on Cosmology, *Symmetry* **13**, issue 4, (2021), p. 593; https://doi.org/10.3390/sym13040593.
[26] H. Sakuma, I. Ojima, H. Saigo and K. Okamura, Conserved relativistic Ertel's current generating the vortical and thermodynamic aspects of space-time, *Int. J. Mod. Phys. A* **37** No. 22, 2250155 (2022), https://doi.org/10.1142/S0217751X2250155X.
[27] Maldacena, J. The large N limit of superconformal field theories and supergravity. *Adv. Theor. Math. Phys.* (1998), 2, 231-252.
[28] R. Penrose, Before the Big Bang: an outrageous new perspective and its implications for particle physics, *Proceedings of EPAC* (2006), https://accelconf.web.cern.ch/e06/PAPERS/THESPA01.PDF
[29] R. Penrose, Singularities and Time-Asymmetry, *General Relativity: An Einstein Centenary Survey* (Cambridge Univ. Press,) (1979), pp. 581-638.
[30] S. Helgason, Differential Geometry, Lie Groups, and Symmetric Spaces (Academic press, New York) (1978).
[31] S. K. Donaldson, An application of gauge theory to four-dimensional topology, *Journal of Differential Geometry*, **18** (2), (1983), 279-315.
[32] I. Ojima, Nakanishi-Lautrup B-Field, Crossed Product & Duality, *RIMS Kokyuroku* **1524** (2006), 29–37.
[33] H. S. Snyder, Quantized space-time, *Phys. Rev.* **71**, (1947), 38.
[34] Liu, H. {Available online:} What-is-the-best-estimate-of-the-cosmological-constant. {https://www.quora.com} (accessed on 1 January, 2021).
[35] H. Ertel, *Meteorol. Z.* **59** (9), (1942), 277-281.
[36] S. Aoki, T. Onogi and S. Yokoyama, Charge conservation, entropy current and gravitation, *Int. J. Mod. Phys. A* 36, No. 29 2150201 (2021).
[37] Landau, L.D.; Lifshitz, E.M. *Course of Theoretical Physics*, 2nd ed.; Volume 6 Fluid Mechanics; Elsevier: Oxford, UK, (1987).
[38] E. Witten, STRING THEORY DYNAMICS IN VARIOUS DIMENSIONS, arXiv:hep-th/9503124v2 (1995).
[39] M. Takesaki, *Lecture Notes Math.* **128** (Springer 1970). doi:10.1007/BFb0065832, ISBN 978-3-540-04917-3
[40] R. P. Gupta, *JWST* early Universe observations and ΛCDM cosmology, *Monthly Notices of the Royal Astronomical Society*, Vol. 524, Issue 3, (2023), 3385-3395. https://doi.org/10.1093/mnras/stad2023
[41] R.F. Streater and A.S. Wightman, *PCT, Spin and Statistics, and All That*, (Princeton Univ. Press, 2000).
[42] O.W. Greenberg, Heisenberg fields which vanish on domains of momentum space, J. Math. Phys. **3** (1962), 859–866.
[43] D.W. Robinson, Support of a field in momentum space, Helv. Phys. Acta **35** (1962), 403–413.

[V] PUBLISHED BOOKS

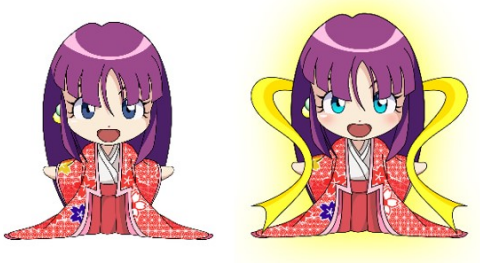

[VI] PRESENTATIONS

IN DOMESTIC CONFERENCES

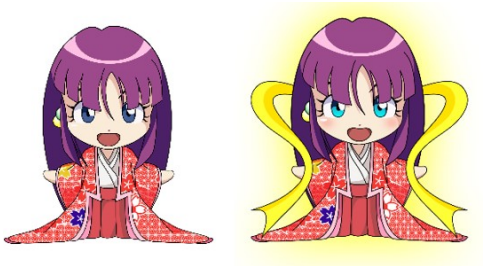

流れが誘導する平衡から遠い量子構造 IV

Current-induced Non-equlibrium Structure IV

○ 坂野　斎　(山梨大院)

○Itsuki Banno　(Univ. of Yamanashi)

E-mail: banno@yamanashi.ac.jp

川添，大津らの開発したフォトンブリーディング（PB）[1] は間接遷移型半導体から高効率発光デバイス作成を可能にし，その発光波長を決めるのは物質のバンドギャップではなくプロセス中の照射光波長である．同時に巨大磁気光学効果 [2] や強磁性 [3] を発現する特徴をもつ．

本理論 [4] の目的は内在電磁場を原因として発光や磁気光学効果が増強される仕組みの解明である．前回は間接遷移型半導体の発光増強のトイモデルを提案した．モデルの特徴は，内在ベクトルポテンシャルが存在し，(a) 波数過剰というオフシェル性を持つこと，(b) 非相対論性を起源とした非線形性を有し，非摂動論的に考慮すると強調因子となること (c) 光学フォノンなどの外電流密度（流れ）と結合する 1 次摂動の存在であり，「基底状態から遠い定常状態」の出現が示唆された．そのシナリオは，非線形性と流れのインタープレイという意味で，非平衡熱力学の散逸構造 [5] と類似のものである．

本発表の内容は：(1) 磁気光学効果にも上記 (b) と同様の強調因子が現れること，(2) 上記モデルの尤もらしさ；(a) オフシェル性,(b) 非線形性,(c) 1 次摂動の強度の検証，(3) モデルが依拠しているオンシェル，オフシェル電磁場の従う Mawell 方程式を導く変分原理．

特に，(3) の変分原理は強い非線形性がある系を非摂動論的に／変分法で扱う際に有効である．

$$\mathcal{I}_{\mathrm{EM+}} = \frac{1}{2}\int \mathrm{d}^4x \int \mathrm{d}^4x_1\, \Delta A_\mu(x)\frac{-1}{c^2}\kappa^\mu_{\mu_1}(x,x_1)\Delta A^{\mu_1}(x_1) + \frac{-1}{c^2}\int \mathrm{d}^4x\, \Delta A_\mu(x)\left\{\hat{j}^{(ext)\mu}(x) + \int_0^1 \mathrm{d}\zeta\, \hat{j}^{(ind)\mu}(x;[\zeta\Delta A^\nu])\right\}$$

$$\frac{-1}{c^2}\kappa^\mu_{\mu_1}(x,x_1) \equiv \frac{\epsilon_0}{c}(\partial_\sigma\partial^\sigma\delta^\mu_{\mu_1} - \partial^\mu\partial_{\mu_1})\delta^4(x-x_1)$$

誘導電流密度の部分が電磁ポテンシャルの振幅のパラメータ積分で書かれ，構成方程式（$\hat{j}^{(ind)}$ の ΔA 依存性）は自由に設定できる；第 1 原理で導いてもよいし，現象論として導入してもよい．この作用積分の電磁ポテンシャルによる最適化により，次の通常のマクスウェル方程式が導かれるので，光学全般に使えるものである．

$$(\partial_\sigma\partial^\sigma\delta^\mu_{\mu_1} - \partial^\mu\partial_{\mu_1})\Delta A^{\mu_1}(x) = \frac{1}{\epsilon_0\, c}\left(j^{(ext)\mu}(x) + j^{(ind)\mu}(x;[\Delta A])\right).$$

謝辞

大津元一博士が主宰されるドレスト光子研究起点 (RODreP) での研究会のメンバーの方々に感謝いたします. この研究の一部はドレスト光子研究起点からの援助を受けています.

参考文献

[1] T. Kawazoe and M. A. Mueed and M. Ohtsu, Appl. Phys. B, **104** p.747–754(2011); M. A. Tran, T. Kawazoe, and M . Ohtsu. Appl. Phys. A, **115** p.105-111(2014); M. Ohtsu, "Silicon Light-Emitting Diodes and Lasers" (Springer International Publishing, Swit- sland, 2016).

[2] N. Tate, T. Kawazoe, W. Nomura, and M. Ohtsu, Scientific Reports **5** p.12762-1-7 (2015); M. Ohtsu, in Off-shell archive (http://offshell.rodrep.org), DOI: 10.14939/1809R.001.v1.

[3] 門脇 拓也, 川添 忠, 大津 元一, 佐野 雅彦, 向井 孝志.「ドレスト光子による誘導放出を利用した波長 1.3~1.9 μ m 帯の非冷却型 Si 受光素子], 応用物理学会 2021 年春期学術講演会, 17p-Z14-8.

[4] 坂野　斎,「流れが誘導する平衡から遠い量子構造」2023 年春季学術講演会，16a-A201-1；坂野　斎,「流れが誘導する平衡から遠い量子構造 II」2023 年秋季学術講演会，22p-A310-1；坂野　斎,「流れが誘導する平衡から遠い量子構造 III」2024 年春季学術講演会，24a-11F-1.

[5] G. ニコリス，I. プリゴジーヌ,「散逸構造 – 自己秩序形成の物理学的基礎」(岩波書店，1980).

オフシェル科学と因果性

Off-shell Sciences and Causality

○ 西郷 甲矢人 (長浜バイオ大学)

○Hayato Saigo (Nagahama Institute of Bio-Science and Technology)

E-mail: h_saigoh@nagahama-i-bio.ac.jp

ドレスト光子研究をその嚆矢とするオフシェル科学は、相対論的な意味で「空間的」な領域の間の「つながり」を正面から受け止める科学であるともいえる。この種の「つながり」は、直接的に因果的な関係ではない一方で、因果性と矛盾するどころか、間接的な形では因果性と深く関連しあっている。したがって、オフシェル科学を推進するうえで、「因果性」とは何かを深く掘り下げることは不可避的に重要である。これは、「時空」概念を問い直すことと表裏一体である。

これまでの本学会における講演では、[2, 3] に基づき、量子場とその状態を「(部分的な) 対合構造をもつ圏上の圏代数とその上の状態」として定義することにより、圏構造としての相対論的構造と非可換確率構造としての量子論的構造を直接に統合できることを示し、代数的量子場理論や位相的量子場理論などの先行するアプローチとの概念的関係についても論じた。またこれらを踏まえてオンシェル・オフシェルの概念を見直し、時空を「(構造づけられた) 点集合」としてではなく「圏」—より詳細にいえば「(部分的な) 対合構造を持つ因果的圏」[3]—として見直すことが、ドレスト光子研究 [1] に端を発するオフシェル科学にとって核心的であるという見方を提示した。ここでいう「因果的圏」は、きわめて抽象的な概念であって、因果性とは何かについては一旦横に置く形で定式化されているが、これを現実的な因果性概念と関連付けることは、現象とそのモデルの関係性を明らかにするうえで根本的である。

本講演では、そもそも因果性とは何であるかを反省し、「時空：圏」「量子場：圏代数」「量子場の状態：圏上の状態」という対応の枠組みにおいて「量子場の (局所) 状態の遷移に関する (非決定論的な) 法則性」(それは「(局所) 状態の類」「(局所) 圏代数の間の完全正値写像の類」の概念を用いて書ける) として定式化する。また、こうした法則性が因果的圏としての時空の構造から誘導できることを示し、量子場の動力学を、この意味での因果性の様相として捉え直すことを提案する。

Acknowledgments

本研究は (社) ドレスト光子研究起点の助成を得た。

参考文献

[1] M. Ohtsu: *Dressed Photons* (Springer, Berlin Heidelberg 2014)

[2] Saigo, H. Category Algebras and States on Categories. *Symmetry* **2021**, *13* 7, 1172. https://doi.org/10.3390/sym13071172

[3] Saigo, H. Quantum Fields as Category Algebras. *Symmetry* **2021**, *13* 9, 1727. https://doi.org/10.3390/sym13091727

ネットワーク量子場からのドレスト光子

Dressed photons from network quantum fields

中部大工[1]，　○岡村 和弥[1]

Chubu Univ.[1], ○Kauzya Okamura[1]

E-mail: k.okamura.renormalizable@gmail.com

ネットワーク量子場の観点からドレスト光子のモデリングについての講演を行う。ネットワーク量子場とは，ネットワークおよび離散的な構造上に定義される量子場のことであり，量子場として有限自由度系から無限自由度系まで扱う対象である。本講演で重視する観点および研究目標は以下の 3 点である：

(1) 近年では量子ウォークによるモデリングが盛んになっている。それ以前のドレスト光子のモデリング [1, 2] の意義をネットワーク量子場として見直したい。

(2) そして，連続時間量子ウォークによるモデリングの可能性を議論できる体系（枠組み）を構築したい。ここにおいては三宮氏のアプローチ [3] との比較も重要になる。

(3) ドレスト光子が関わる系に対する量子測定理論の開拓をしたい。

(1) と (2) は，ドレスト光子をオフシェル量子場として記述する試みにおいて，先行研究の意義を明確にする目的がある。第一に，量子ウォーク以前のモデルをネットワーク量子場の特殊な場合として位置づけられることを説明する。量子ウォーク以前のモデルは量子場として記述できているが，関わる物質の非一様性や欠陥などドレスト光子のモデリングにおいて特徴的な系の構造，そしてダイナミクスを記述する目的には徹底されていなかった。非一様性や欠陥などについては，量子ウォークモデルにおいて克服されており，ネットワーク量子場によるモデリングにおいても当然組み込まれるべき観点である。量子ウォークモデルは離散時間でのダイナミクスの記述である一方，今回提案するモデルは 1 粒子状態においては連続時間量子ウォークモデルに対応するモデルである。そのため，離散時間と連続時間でのモデリングの差については今後の検討課題である。

ネットワーク量子場における量子測定理論，そしてドレスト光子のモデリングと量子測定理論の関係の追究が (3) である。講演者が研究してきた（相対論的状況をふくめた）量子場の測定理論 [4, 5] の知見を活かし，ネットワーク量子場およびドレスト光子のモデリングに対する測定理論を継続的に研究している。今回は，上で行ったネットワーク量子場によるモデルが測定状況で被る変化について行った解析の紹介を行う。ドレスト光子が関わる系においては，合成系の構築が物理量代数のテンソル積に基づく有限自由度系とは異なるため，量子場の測定理論の知見が不可欠である。この事実について実験と数理が対応することを説明する。

参考文献

[1] 大津 元一，小嶋 泉 編著,『ここからはじまる量子場 ―ドレスト光子が開くオフシェル科学―』, (朝倉書店, 2020).

[2] 大津 元一,『ドレスト光子』, (朝倉書店, 2013）.

[3] S. Sangu, H. Saigo, Symmetry **13** (2021), 1768.

[4] K. Okamura and M. Ozawa, J. Math. Phys. **57** (2016), 015209.

[5] K. Okamura, Symmetry **13** (2021), 1183.

正則グラフ上の量子ウォークの波動関数について

The wave functions of quantum walks on regular graphs

工学院大学
○ 齋藤正顕
Kogakuin University
○Seiken Saito

ドレスト光子（DP）を説明するモデルとして, 大津–瀬川 [3] によって 3 状態の量子ウォーク (QW) モデル（ドレスト光子の量子ウォークモデル）が提案され, 次元が 2 以上の場合に, その数値的な挙動が調べられている [4]. 本研究では, より基礎的なグラフ上の量子ウォークを扱う. 具体的には, グラフ $G = (V, E)$ の隣接行列を A とするとき, 時間発展行列を $U(t) = e^{itA/2}$ とし, 初期状態を $\Psi(0) \in \mathbf{C}(V)$ とするとき, 時刻 $t \geq 0$ における状態が

$$\Psi(t) = U(t)\Psi(0)$$

によって定められる連続時間量子ウォークについて考察する. このような量子ウォークモデルは, グラフ上のシュレディンガー方程式として, 昔から研究されてきた. グラフ G が 1 次元格子 $\mathbf{Z}$, サイクルグラフ C_N, 正則木 T_{q+1} の場合については, [2] などがある. 詳しくは,[1], [2], [5], [6] 等を参照のこと. しかしながら, 特定の種類のグラフの族だけを扱った研究が多く, 正則グラフを統一的な視点で扱う研究は少ないようである. 本研究では, 跡公式の観点から正則グラフの時間発展行列の統一的な表示を与える. これは, [2] で扱っているいくつかの例が示唆するように J-ベッセル関数を含む式で表され, またグラフのパスの個数に関する幾何的な情報を持った数列を含む. 併せて頂点推移的で, girth が発散するような正則グラフの増大列 (G_n) の場合についても考察した.

謝辞 この研究の一部はドレスト光子研究起点の支援を受けています.

参考文献

[1] C. Godsil and H. Zhan, Hanmeng Discrete quantum walks on graphs and digraphs, London Math. Soc. Lecture Note Ser., 484 Cambridge University Press, Cambridge, 2023, xii+138 pp.

[2] 今野紀雄, 量子ウォークの数理, 産業図書, 2008.

[3] M. Ohtsu, A Quantum Walk Model for Describing the Energy Transfer of a Dressed Photon, Preprint, 2021, Offshell: 10.14939/2109R.001.v1.

[4] 大津元一, 瀬川悦生, 結城謙太, 量子ウォークモデルによるドレスト光子エネルギー移動のシミュレーション, 2022 年第 83 回応用物理学会秋季学術講演会 (講演番号 22a-A101-6).

[5] R. Portugal, Quantum walks and search algorithms, Quantum Sci. Technol., Springer, New York, 2013, xii+222 pp.

[6] S. E. Venegas-Andraca, Quantum walks: a comprehensive review, Quantum Inf. Process.11(2012), no.5, 1015–1106.

ドレスト光子の自律的移動経路を決める最適散逸

Optimum dissipation for governing the autonomous transfer of dressed photons

ドレスト光子[1]，横浜国大[2]，Middenii[3]，工学院大[4]

○大津元一[1]，瀬川悦生[2]，結城謙太[3,4]，齋藤正顕[4]

Res. Origin Dressed Photon[1], Yokohama Ntnl. Univ[2], Middenii[3], Kogakuin Univ.[4]

○Motoichi Ohtsu[1], Etsuo Segawa[2], Kenta Yuki[3,4], Seiken Saito[4]

E-mail: ohtsu@rodrep.or.jp

【まえがき】多数のナノ寸法粒子（NP:NP_S）の三次元配列の光照射位置に発生したドレスト光子（DP）はフォノンと結合してドレスト光子フォノン（DPP）を生成し、NP_S間を自律的に移動し出口のNP(NP_L)に達して外部に光放射する。この現象は従来のOn-shell科学を支配する最小作用の原理には従わない。本講演ではこの現象への散逸過程の関わりを示す。

【方法】実験によれば出口までのDPPの到達可能距離L_0は三次元配列の厚さHの増加とともに増加する（図1(a)）[1]。理論面に目を向けるとDPの特性解析には相互作用、さらには散逸が本質であることがわかっている[2]。相互作用は非可換な物理過程なので、非可換代数の量子ウォーク（QW）モデルが有効である。このモデルに散逸の効果を取り入れたこれ迄の計算結果は実験結果と整合している[3]。さらにSi結晶中のB原子対に局在するDPPの生成確率は散逸係数κが0.2（$=\kappa_{opt}$）のときに最大となる（図1(b)）。B原子対をNPに置き換えれば図1(a)が解析可能である。

【結果】散逸係数κは内部散逸係数$\kappa_{internal}$(=$N\cdot\alpha_{loss}$)（N: NPの数、α_{loss}:各NPでの損失係数)と出口（NP_L）での放射緩和に起因する散逸係数κ_{out}の和である。ここでNは三次元配列の三軸方向のNPの数N_x, の積に比例し、また、配列の厚みHはN_zに比例するから$\kappa\propto H$である。これは上記の最適値κ_{opt}はHにも最適値H_{opt}があることを意味するので、図1(a)の実験結果は図1(b)中の領域A（$H<H_{opt}$）に対応する。するとL_0は$H\fallingdotseq H_{opt}$において最大となり（最適経路)、その後はHの増加とともに減少することがわかる（領域B：$H>H_{opt}$)。この最適経路は有限数のNPにより構成されるのであり、以上の特性は最小作用の原理とは異質であり、オフシェル科学固有である。

【まとめ】QWモデルによりDPエネルギー移動後の放射光パワーを最大とする最適散逸量、最適経路があることを示した。これは新しいナノ寸法光デバイスを作るには三次元配列には有限値の最適寸法があることを示唆する。

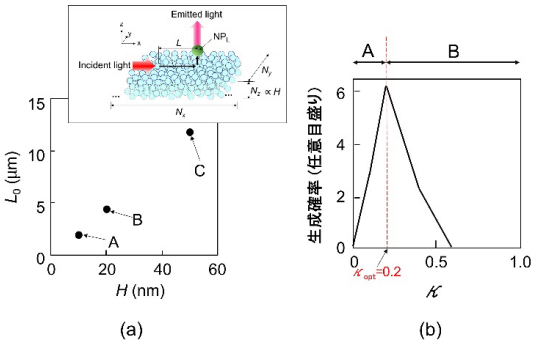

図1　最適経路の条件

【文献】

[1] W. Nomura, et al, *Appl. Phys.* B. **100**, (2010), pp. 181-187. [2] I. Ojima, in *Progress in Nanophotonics* 5, (ed. T. Yatsui, Springer, 2018) pp. 107-135. [3]大津他、第84回応物秋講演会(2023/9)22p-A310-7.

量子ウォークモデルから見たドレスト光子が自律的に選択するグラフ上のパス

Paths on the graph chosen autonomously by dressed photons from the quantum walk model

○ 瀬川悦生 (横浜国大)[1]，斎藤正顕 (工学院大)[2]，　結城謙太 (Middenii)[3], 大津元一 (ドレスト光子)[4],
○ Etsuo Segawa(Yokohama Nat. Univ.)[1], Seiken Saito(Kogakuin Univ.)[2], Kenta Yuki(Middenii)[3], Motoichi Ohtsu(Dressed photon)[4].
E-mail: segawa-etsuo-tb@ynu.ac.jp

任意のグラフ上のドレスト光子のエネルギー移送問題 [1] の量子ウォークによる素子化モデル [2], を提案する. グラフ上の各頂点にその隣接頂点に関する巡回置換 (ローテーション) を与える。そして、元のグラフの隣接構造を保ちつつ、各頂点をこの巡回置換にしたがった有向サイクルに置き換えたグラフを拡張グラフと呼ぶ。したがって、この拡張グラフの各頂点において、元のグラフの隣接構造から由来するするものと、各頂点のローテーションから由来する 2 種類の有向辺が存在する。これをドレスト光子の各頂点における局所的な 2 種類の跳躍経路とみなす。さらにフォノンによる跳躍の抑止性を与えるため、その各頂点にセルフループを設ける。この各頂点上に適切な 3 次元のユニタリ行列 $H = (h_{i,j})_{i,j=1,p,2}$ を与えることで、量子ウォークによる素子化モデルの時間発展を定義することができる。このときの定常状態において、ドレスト光子がどのような振る舞いをするのかについて考察する。まず、定常性とフォノンのこのモデルにおける役割により、ドレスト光子の 2 種類の跳躍の中に、フォノンの役割を反映させた次のような 2 次元のユニタリ行列 $\tilde{H}$ による時間発展として書き直すことができる。

Lemma 1. 既約化された量子コイン $\tilde{H} = (\tilde{h}_{ij})_{i,j=1,2}$ は次のように書き表される。

$$\begin{aligned}\tilde{h}_{ij} &= h_{ij} + \frac{h_{ip}h_{pj}}{1-h_{pp}} \\ &= \frac{1}{1-h_{pp}}\left(h_{ij} - (-1)^{i+j}\mathrm{Det}(H)\bar{h}_{\neg i,\neg j}\right)\end{aligned}$$

この Lemma と $\tilde{H}$ のユニタリ性から次の事が導出される.

Theorem 1. 定常状態において, $h_{11} = \mathrm{Det}(H)\bar{h}_{22}$ を満たすとき, ドレスト光子はローテーションによって誘導されるグラフの閉曲面埋め込みにおける各面の境界に沿って動く.

この定理の条件を満たすものは, [2] によって提案されている典型的な量子ウォークのドレスト光子シミュレーションモデルの中で現れている. しかしながら, [1] の結果との整合性の観点から, この条件を緩和させ $h_{11} - \mathrm{Det}(H)\bar{h}_{22} \in \mathbb{R}$ となるものが良いことが [3] から示唆できる.

参考文献

[1] M. Naruse et al., Nano Communication Networks **2** (2011) 189–195.

[2] M. Ohtsu et al., Off -shell archive: 2304O.001.v1 (2013).

[3] Yu. Higuchi and E. Segawa, arXiv:2402.00360.

物質構造を介したドレスト光子高励起状態の生成

Generation of Highly Excited States of Dressed Photon via Matter Structure

(株) リコー ○三宮 俊

Ricoh Co., Ltd.

○Suguru Sangu

E-mail: suguru.sangu@jp.ricoh.com

1. はじめに

ドレスト光子は原子や量子ドットなどの質点を表わすノードに束縛された準粒子としてモデル化することができる。このモデルを用い、ドレスト光子を介在した物理現象(不純物位置の固定化や発光現象など)の解明を試みている[1]。これらの現象はナノ物質系から外界へのエネルギー散逸が重要な役割を担っており、その制御方法の確立や高効率化は将来的な技術課題である。著者らは近年、散逸現象とドレスト光子の高励起状態(複数個のドレスト光子を内在する状態)との関係に注目し、理論検討を進めている。高励起状態は Dicke の超放射と類似の基底状態[2]で記述することができ、空間対称性に起因した高速な緩和現象の発現が示唆される。また、ドレスト光子が主役となるナノ物質系は人工的に製造可能であり、多様な光学機能実現への展開が期待される。

本発表では、上述内容の予備的検討として数値シミュレーションを基に、ドレスト光子の高励起状態を効率的に生成する物質構造について検討した結果を報告する。

2. 数値シミュレーション

数値シミュレーションでは、散逸を加味した量子密度行列の運動方程式(Lindblad 方程式)の定常解を数値的に算出し、各基底状態の占有確率を評価する。ここで、基底状態とはドレスト光子が物質を表わすノードに束縛された状態を示し、これは物質励起、光子、フォノンの混合状態を準粒子と見なした描像である。物質構造とドレスト光子の励起状態との関係を調べるため、本講演では最近接距離に配置したノード対を中央に固定し、その周囲にランダムにノードを配置した物質モデルを解析対象としている。

3. 数値解析例と考察

Fig. 1 は、6 ノードの物質モデル多数生成し、ドレスト光子基底状態の占有確率を算出した結果の一例を示す。ノード間の配置に規則性がない場合、占有確率は平坦な分布となるが、幾つかの物質モデルでは Fig. 1(b)に示すように、3 個のドレスト光子を内在する状態(3DP 状態)において基底状態の選択的な励起が観測できる。3DP 状態は基底の数が多く、ノードの空間配置に依存して励起および緩和のレートが異なるために、占有確率に偏りが現れるものと推察される。構造の特徴として、対配置または鎖状配置を有する物質モデルにおいて占有確率の分散性が高くなる傾向を確認しているが、より詳細な物理的解釈さらにはノード数影響等について現在検討を進めており、講演ではその内容も含めて報告する。

参考文献

[1] 三宮・他, 2024 年第 71 回応用物理学会春季学術講演会 講演予稿集(2024) 24a-11F-7.

[2] M. Gross and S. Haroche, Phys. Rep. 93 (1982) 301.

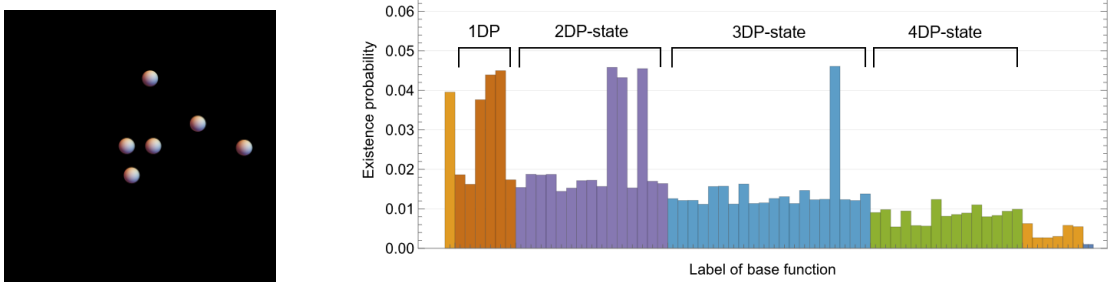

(a) 物質モデル(6 ノード)　(b) 基底状態の占有確率

Fig. 1: 非平衡定常状態におけるドレスト光子状態の数値解析例

レーザー学会　レーザー普及セミナー（2024 年 8 月 12 日）福井大学遠赤外領域開発研究センター

〔招待講演〕

ドレスト光子の自律的移動とその原理

○大津元一[1]、瀬川悦生[2]、結城謙太[3]、齋藤正顕[4]

[1]（一社）ドレスト光子研究起点、[2]横浜国大、[3]Middenii、[4]工学院大

講演概要: 微視系内部でのドレスト光子(DP)の移動は従来の最小作用の原理には従わない。本講演ではその実験結果を紹介し、次にそれを説明するための量子ウォーク理論を提示する。両者を比較し、この移動は DP から巨視系に放射され る光パワーを最大にするように自律的に調整されることを示す。いわば DP の 移動は出力最大化の原理に従う。その際、微視系内部でのエネルギー散逸が重要な役割を果たすことを指摘する。以上の議論はドレスト光子に限らず、 生物系など、複雑系の振る舞いなどにも適用可能である。

流れが誘導する平衡から遠い量子構造 III

Current-induced Non-equlibrium Structure III

○ 坂野　斎　(山梨大院)

○Itsuki Banno　(Univ. of Yamanashi)

E-mail: banno@yamanashi.ac.jp

川添，大津らの開発したフォトンブリーディング（PB）[1] は間接遷移型半導体から高効率発光デバイス作成を可能にし，その発光波長を決めるのは物質のバンドギャップではなくプロセス中の照射光波長である．また，高効率の発光と同時に巨大磁気光学効果 [2] や強磁性 [3] を発現する特徴をもつ．この理論 [4] の目的は内在電磁場を原因として発光や磁気光学効果が増強される仕組みの解明であり，概要は以下のとおり．今回の発表の新規の部分は (5) 以下である．

(1) PB プロセスで製作されたデバイス（PB デバイス）の磁気的効果の発現から内在ベクトルポテンシャル (VP) の関与を，現象の強さからコヒーレント長が大きな電子系の存在を想定する．

(2) 電子の場と電磁場ポテンシャルを変数する通常の量子電磁力学の半古典的作用を出発点とする．開放系熱力学の散逸構造の類似として，(a)「流れ（1 次摂動）」と (b)「非線形性」の存在によって，基底状態から遠いところに最小作用の原理に適う動的状態が現れることを期待し，作用積分中に (a) として内在 VP を伴う光学フォノンを，(b) として内在 VP への非線形応答を考慮する．

(3) ４元誘導電流密度を線形・非線形感受率のハイゼンベルグ演算子により表し，その式中の電磁ポテンシャルのスケール積分によって物質場のラグランジアンを構成する．この処方は作用積分中の電子の場の最適化に相当する．

(4) 非相対論系特有の非線形効果として内在 VP の自己相関と電荷密度の結合がある．電磁ポテンシャルと感受率の変換で誘導電流密度を不変に保つものを利用して，この効果をスカラーポテンシャルの一部として無限次数まで取り込む．このように用意した作用積分の演算子を非線形感受率演算子に対して再帰的な電子状態で期待値を取る．４元電流密度演算子の非可換性により，内在 VP の非線形効果が発光や磁気光学効果を担う誘導電流密度の変調因子をもたらす．

(5) 作用積分における電磁ポテンシャルの最適化は外電流密度と内在 VP で変調された誘導電流密度の下でマクスウェル方程式を解くことである．大振幅の VP の解があれば，最小作用の原理に適う基底状態から遠い動的状態である．その実現には，作用積分における (4) の非線形効果の非摂動論的扱いと電磁ポテンシャルがマクスウェル方程式の解であることの相乗効果が必要である．

(6) 以上より，トイモデルの提案を目指す．また，内在電磁場を量子場とする必要性を検討する．

謝辞

大津元一博士が主宰されるドレスト光子研究起点 (RODreP) での研究会のメンバーの方々に感謝いたします. この研究の一部はドレスト光子研究起点からの援助を受けています.

参考文献

[1] T. Kawazoe and M. A. Mueed and M. Ohtsu, Appl. Phys. B, **104** p.747–754(2011); M. A. Tran, T. Kawazoe, and M . Ohtsu. Appl. Phys. A, **115** p.105-111(2014); M. Ohtsu, "Silicon Light-Emitting Diodes and Lasers" (Springer International Publishing, Swit- sland, 2016).

[2] N. Tate, T. Kawazoe, W. Nomura, and M. Ohtsu, Scientific Reports **5** p.12762-1-7 (2015); M. Ohtsu, in Off-shell archive (http://offshell.rodrep.org), DOI: 10.14939/1809R.001.v1.

[3] 門脇 拓也, 川添 忠, 大津 元一, 佐野 雅彦, 向井 孝志.「ドレスト光子による誘導放出を利用した波長 1.3~1.9 μ m 帯の非冷却型 Si 受光素子], 応用物理学会 2021 年春期学術講演会, 17p-Z14-8.

[4] 坂野　斎,「ドレスト光子 / 内在電磁場と最小作用の原理」2022 年春季学術講演会，22a-E103-1; 坂野　斎,「最小作用の原理で達成される内在電磁場を伴う散逸構造の理論」2022 年秋季学術講演会，22a-A101-1. 坂野　斎,「流れが誘導する平衡から遠い量子構造」2023 年春季学術講演会，16a-A201-1；坂野　斎,「流れが誘導する平衡から遠い量子構造 II」2023 年秋季学術講演会，22p-A310-1.

時空領域の創発とドレスト光子の存在について

On the emergence of spacetime and existence of dressed photon

ドレスト光子研究起点、佐久間弘文

RODreP, Hirofumi Sakuma

E-mail: sakuma@rodrep.or.jp

ドレスト光子（DP）研究起点の設立と共に、開始された DP の新理論研究は、未解明の量子場の深い意味を、DP 現象を切り口として、改めて考えて見るという挑戦である。素粒子物理においては、長らく、（１）粒子状の物質と（２）物質の相互作用を担う力の場が主要テーマとなっていたが、最近では、これに加え、entanglement による量子相関が時空を創発するのではという事も言われている。時空という概念は、物理系を記述する上で必須な概念であり、この事は、宇宙論における未解明なダークマター (DM) およびダークエネルギー (DE) の記述に対しても同様である。通常物質が宇宙全体で占める割合は数パーセントとで、残りは DM と DE であるという事実は、時空は 通常物質以上に、DM と DE の存在と密接に関係しているのではという推論を有力視する根拠を与えている。

量子場の相互作用には spacelike momentum 場が必須であるという事を示した Greenberg-Robinson (GR) 定理から出発し、ここ２，３年間に達成した DP の理論研究の成果 [1] は、まさにその事ー時空と DE 及び DM との密接な関係ーを示すものであった。具体的に言えば、spacelike な電磁場が spacelike な時空である DE を形成すると同時に、DE と連動する形で、「光」の場の “共形不変性” の破れに対応する形で創発される timelike な “Weyl conformal gravity” 場が DM の場として理解され、この場が timelike な時空を構成すると言う事である。

小嶋の代数的量子場理論に基づく「量子・古典対応」 (MMD) [2] においては、DHR のセクター理論を発展させた generalized sector (GS) が導入されて、GS は factor 表現により明確に、非可換な表現を持つ量子的 GS と可換な表現を持つ古典的 GS に分類され、ミクロの量子場の無数の集積により古典場が生じているという自然な形で量子場と古典場が結び付く事が示される。GR 定理から量子場には timelike および spacelike な時空が随伴している一方、古典場には timelike な時空のみが随伴していると仮定する事は自然な仮定であると思われる。その様な仮定の下では、量子的 GS と古典的 GS との相互作用は、必然的に timelike な時空と spacelike な時空との相互作用を伴うという事が導かれる。

今回の発表においては、「光」の場の “共形不変性” の自発的破れに伴う仮想粒子としての南部・Goldstone (NG) boson とは DP 理論においていかなる表現をとるのかを考察し、更には、この観測にはかからない仮想粒子が、量子的 GS と古典的 GS との相互作用を担う質量ゼロの “gauge boson” 的役割を果たしているのではという可能性を考察する。発表者のこれまでの研究 [3] により、長さの次元を持つ DP 定数 (≈ 40 nanometer) は、量子的領域と古典的領域の境界を示す Heisenberg cut に対応している事が示されているが、その事も、今回の考察と整合的であると思われる。DP の生成、移動、消滅というナノ光学にとって重要な一連の現象は、物理学的にはナノ光学という一分野を越えて、量子および古典的領域の相互作用にとって中核的なものである可能性を考察する。

参考文献

[1] Sakuma, H. et al. *Int. J. Mod. Phys. A* (2022) 2250155. (https://doi.org/10.1142/S0217751X2250155X).

[2] 小嶋泉、量子場とミクロ・マクロ双対性、2013、丸善出版。

[3] Sakuma, H. and Ojima, I. *Symmetry* 2021, 13, 593, doi:10.3390/sym13040593.

ドレスト光子の物理量代数について

Off-shell Science and the Concept of Spacetime

○ 西郷 甲矢人 (長浜バイオ大学)

○Hayato Saigo (Nagahama Institute of Bio-Science and Technology)

E-mail: h_saigoh@nagahama-i-bio.ac.jp

ドレスト光子の振る舞いを量子場として理解する上で欠かせないのがその「物理量代数」の構造である。そもそも量子場は、代数的量子場理論の観点よりすれば、時空領域に対しそこで意味を持つ物理量代数を対応させる対応付けであってしかるべき公理を満たすものと考えられるが、本講演においては、このような意味での時空/物理量代数の構造が、いかにしてドレスト光子に対して与えられるかを「圏代数」の概念を用いて明らかにする。

2022 年春・2022 年秋の本学会における講演では、[2, 3] に基づき、量子場とその状態を「(部分的な) 対合構造をもつ圏上の圏代数とその上の状態」として定義することにより、圏構造としての相対論的構造と非可換確率構造としての量子論的構造を直接に統合できることを示し、代数的量子場理論や位相的量子場理論などの先行するアプローチとの概念的関係についても論じた。また、内部自由度を持つ状態空間の取り扱いを通じて、このアプローチがオフシェル科学への量子ウォークからのアプローチやネットワーク上の「(一般化された) 生成消滅演算子」を活用するアプローチとも深く関連していることを明らかにしてきた。また、2023 年春にはこれらを踏まえてオンシェル・オフシェルの概念を見直し、2023 年秋には時空を「(構造づけられた) 点集合」としてではなく「圏」—より詳細にいえば「(部分的な) 対合構造を持つ因果的圏」[3]—として見直すことが、ドレスト光子研究 [1] に端を発するオフシェル科学にとって核心的であるという見方を提示した。

本講演では、ナノ粒子の相互関係から上記の意味での一般化された時空構造が生じ、そこから自然に定まる圏代数がドレスト光子の物理量代数に他ならない、とする理論的提案を行う。さらに、この提案の物理的妥当性を検討するとともに、それが通常の有限自由度量子力学の枠組み (特にそこで用いられる通常の行列代数) からいかに異なっているかを論じる。以上を通じて、圏論・作用素環論・非可換確率論及び量子ウォークの数学的理論とドレスト光子の研究がいかに関連するか (すべきか) を明らかにしたい。

Acknowledgments

本研究は (社) ドレスト光子研究起点の助成を得た。

参考文献

[1] M. Ohtsu: *Dressed Photons* (Springer, Berlin Heidelberg 2014)

[2] Saigo, H. Category Algebras and States on Categories. *Symmetry* **2021**, *13* 7, 1172. https://doi.org/10.3390/sym13071172

[3] Saigo, H. Quantum Fields as Category Algebras. *Symmetry* **2021**, *13* 9, 1727. https://doi.org/10.3390/sym13091727

代数的量子場の測定理論

Measurement theory for algebraic quantum fields

中部大工[1]，　○岡村和弥[1]

Chubu Univ.[1]，　○Kauzya Okamura[1]

E-mail: k.okamura.renormalizable@gmail.com

本講演では，量子場の測定理論について発表する。代数的量子場理論（AQFT）による量子場の定式化 [1] に基づき，量子場の自由度および状態空間の構造と関連させて測定の中心概念である**量子インストルメント**（quantum instrument）を量子場において定義する。

以下のトピックについて，講演者は近年注力している：

(1)　量子場の概念と数理の深化

(2)　量子場における量子測定理論とその数理

(1) に関しては，現行様々に提案している定式化のどれも，相対論的状況下では具体例は自由場を除いて（存在証明や構成において）多くの数学的困難と直面することが動機となっている。それ故，新しい手法が必要であるが，より根本的に量子場の概念や定式化そのものを吟味するアプローチを採用し研究を行っている。一方で，(2) の量子場の測定理論ついては，単に量子力学系での量子測定理論を踏襲するだけでは不足で，量子場特有の「事情」を考慮して概念を組み立てていかなければならず，概念から吟味しなおす研究が不可欠である。本講演はその一環である。これはドレスト光子 [1, 2] のモデリングとも無関係でないばかりか，ドレスト光子が関わる現象に対する測定の定式化とも直結する。

上の量子場特有の「事情」とは，量子場のもつ局所性（より正確には因果構造）やダイナミクスのことである。物理量代数のレベルにおいて，局所性とは，互いに空間的な領域にあるそれぞれの領域の物理量は互いに可換となることである。そして，有界な時空領域で行う測定は空間的な領域に影響しないという条件を課すことが，局所性の測定における扱いである。ダイナミクスに関しては，相対論的量子場は非相対論的な状況とは大きく異なり，自由場と相互作用場のギャップが Greenberg-Robinson の定理などとして示されている。

Haag-Kastler [3] で導入された AQFT の概念を参照しつつ，本講演では量子場の測定理論を展開する。量子場の時空局所的に測定可能な物理量のなす代数の集まりである**局所ネット**（local net）と，既存の量子インストルメントの数理 [4, 5, 6] を統合させた理論について講演では紹介をする。

参考文献

[1] 大津 元一，小嶋 泉 編著，『ここからはじまる量子場 ―ドレスト光子が開くオフシェル科学―』，(朝倉書店, 2020).

[2] 大津 元一,『ドレスト光子』,（朝倉書店, 2013）.

[3] R. Haag and D. Kastler, J. Math. Phys. **5** (1964), 848–861.

[4] M. Ozawa, J. Math. Phys. **25** (1984), 79–87.

[5] K. Okamura and M. Ozawa, J. Math. Phys. **57** (2016), 015209.

[6] K. Okamura, Symmetry **13** (2021), 1183.

量子ウォークは近道を探せるか？

Can quantm walk find the shortest path ?

○ 瀬川悦生 (横浜国大)[1]，大野博道 (信州大)[2]，　松岡雷士 (広工大)[3]

○ **Etsuo Segawa(Yokohama Nat. Univ.)[1], Hiromichu Ohno(Shishu Univ.)[2], Leo Matsuoka(Hiroshima Inst, Tech.)[3].**

E-mail: segawa-etsuo-tb@ynu.ac.jp

本研究では, ドレスト光子のエネルギー移送問題の素子化モデル [1] として考えられている量子ウォーク [2] が, 最短経路を探し出せるかどうかについて考察する. 今回は簡単のため, Grover walk で考察する. そのために, 連結単純グラフの 2 点を選び, 入口, 出口とし, 迷路とみなす. この 2 つにセルフループを加え, さらに入口にシンクである葉も加える. 初期状態として, 入口頂点のセルフループからスタートさせ, 時間発展は Grover walk による時間発展とする. すると, まず次の事が示せる.

Proposition 1. $\mu_t \in [0,1]^V$ を時刻 t での各頂点における生存確率とする. すると

$$\exists \lim_{t\to\infty} \mu_t =: \mu_\infty.$$

さらに, 初期状態を ψ_0 とおくと,

$$\mu_\infty(u) = \sum_{t(a)=u} |(\Pi_C \psi_0)(a)|^2$$

ここで, Π_C は *[4]* の *Case C* もしくは *D* に相当する固有空間への射影作用素である.

この事実を用いると次のようなことが導かれる.

Theorem 1. オリジナルのグラフがツリーのとき, スタートとゴールを結ぶ最短経路 $\xi = (a_1, \dots, a_r)$ とおくと,

$$\mathrm{supp}(\mu_\infty) = \{a_1, \dots, a_r\} \cup \{ \text{セルフループ} \}$$

ツリーにはサイクルがないので, まわり道が存在しない. そこで, 次のように沢山周りに道を用意したイジワルな迷路はどうなるかを考える. 縦 m, 横 ℓ の長方形が横方向に r 個連なった階段を考える. さらにこの左上端と右上端にそれぞれ長さ ℓ のパスをつけ, その端点をそれぞれ入口と出口とする. このグラフを Γ_r とする. すると

Theorem 2. グラフ Γ_r の各長方形を左から順に $C_1, \dots, C_r$ とする. 各 C_j の横の辺が観測される確率を p_j とする. すると $p_j > p_{j+1}$ となる.

参考文献

[1] M. Naruse et al., Nano Communication Networks **2** (2011) 189–195.

[2] M. Ohtsu et al., Off -shell archive: 2304O.001.v1 (2013).

[3] Yu. Higuchi and E. Segawa, J. Phys. A Math. Theor. **52** (2009) 395202.

[4] N. Konno, E. Segawa, and M. Stefanak. Relation between quantum walks with tails and quantum walks with sinks on finite graphs, Symmetry, 3, pp. 1169–2021.

偏光に関する光子ブリーディングの 3 次元量子ウォーク解析

Three-dimensional quantum walk analyses of photon breeding with respect to photon spin

ドレスト光子 [1]，横浜国大 [2]，Middenii[3]，工学院大 [4]

○大津元一 [1]，瀬川悦生 [2]，結城謙太 [3,4]，齋藤正顕 [4]

Res. Origin Dressed Photon[1], Yokohama Ntnl. Univ[2], Middenii[3], Kogakuin Univ.[4]

○Motoichi Ohtsu[1], Etsuo Segawa[2], Kenta Yuki[3,4], Seiken Saito[4]

E-mail: ohtsu@rodrep.or.jp

【まえがき】間接遷移型半導体である Si 結晶にドレスト光子（DP）とフォノンの結合場（DPP）を用いたアニールを施して製作した発光素子（LED、レーザーなど）は光子ブリーディング（PB）という際立った性質を有する。これ迄に発光の光子エネルギー、スピンに関する PB が観測されている [1]。運動量に関しては量子ウォーク（QW）モデルにより再現されている [2]。即ちこれらは DPP 援用アニール時に照射する光のそれらの複製になっている。本講演では光子のスピン（偏光）に関する PB を QW モデルにより解析した結果を報告する [3]。

【方法】ここでは Si 結晶中の B 原子対の方向が x 軸方向のとき、y 軸方向の直線偏光の入射光により生成する DPP がこの対に閉じ込められる確率が大きいことを示す。偏光を取り扱うために 3 次元 QW モデルを用いる [4]。Si 結晶を表す 3 次元立方体状格子への入射光（直線偏光は y 軸方向）により各サイトに生成した DP は x 軸方向に跳躍し、またフォノンと結合して DPP を形成する。次に y 軸、z 軸方向に順次跳躍する。これを繰り返し格子中心に配置された B 原子対に到達し閉じこめられる。格子のサイト数は 21x21x21。DP の跳躍エネルギーJ、フォノンとの結合エネルギーχの比は B 原子の位置ではχ/J=20、その他では 1 とした。

【結果と考察】B 原子対の位置での DPP の閉じ込めの確率の計算結果を図 1 に示す。

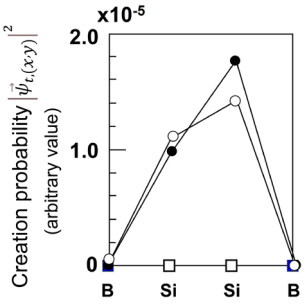

図 2 DPP の閉じ込めの確率

図中●、○は B 原子対が各々x 軸、y 軸方向を向いている場合の結果であり、前者の値が大きいことがわかる。これをもとに PB の度合いを表す尺度 *DoPB* を求めると 2%であった。これは発光の偏光度の測定値と整合し [1]、偏光に関する PB を再現することができた。

【まとめ】3 次元 QW モデルを用い偏光に関する PB を解析した。その結果は実験結果と整合した。

【文献】 1) M. Ohtsu, *Silicon Light-Emitting Diodes and Lasers*, Springer, Heidelberg (2016) Chapter 3.

2) 大津、瀬川、結城、齋藤、第 84 回応用物理学会秋季学術講演会（2023 年 9 月）講演番号 22p-310-7.

3) M. Ohtsu et al., *Off-shell Archive* (November, 2023) 2311O.001.v1. **doi** 10.14939/2311O.001.v1.

4) M. Ohtsu, *Off-shell Archive* (September, 2021) 2109R.001.v1. **doi** 10.14939/2109R.001.v1.

ドレスト光子の局在および散逸における物質系の幾何学的構造の影響

Influence of Matter-System Geometry on Dressed-Photon Localization and Dissipation

(株) リコー[1]，長浜バイオ大[2]，ドレスト光子研究起点[3] ○三宮 俊[1]，西郷 甲矢人[2]，大津 元一[3]

Ricoh Co., Ltd[1], Nagahama Inst. Bio-Sci. Tech.[2], Res. Origin Dressed Photon[3]

○Suguru Sangu[1], Hayato Saigo[2], Motoichi Ohtsu[3]

E-mail: suguru.sangu@jp.ricoh.com

1. はじめに

ドレスト光子を起源とする特異な物理現象の機能光学デバイスへの応用が期待されている。例えば、従来、光学禁制とされていた間接遷移型半導体による発光素子や、非磁性材料を用いた巨大磁気光学効果デバイスなどが報告されている[1, 2]。このような光機能は遠方場において観測されるため、ドレスト光子の特性を自由光子に転写し、効率よく物質系外へ取り出すことが必要である。本発表では、数値シミュレーションを足掛かりに、ドレスト光子から自由光子への変換に際して物質系の非対称性の果たす役割について考察するとともに、自由光子の取出しに求められる構造の要件について議論を行う。

2. 数値シミュレーションによる知見

これまでの研究[3]を踏襲し、ドレスト光子を複数のノードに束縛された調和振動子としてモデル化し、それぞれのノードを占有し得る全てのドレスト光子の組み合わせを基底状態とした量子密度行列の運動方程式（Lindblad 方程式）を数値的に解き、各基底状態の占有確率または基底状態間の遷移確率を算出する数値シミュレーションを行った。ここで、ドレスト光子が全てのノードを占有する高励起状態まで基底状態として考慮している点を強調しておきたい。本数値シミュレーションを用い物質系の対称性の影響を調べるため、Fig. 1 に示す計算例では 6 個のノードを円中央と円周部に配置したモデルを考え、非平衡定常状態におけるドレスト光子の占有確率を算出した。グラフの横軸は取り得る基底準位のラベルであり、ドレスト光子の個数に応じて色分けしている。各ノードを等間隔に配置した系(Fig. 1(a))と乱数によりクラスタ構造を生成した系(Fig. 1(b))において明らかな差異が確認でき、非対称な構造が特定の（高励起）基底状態の占有確率を選択的に高めることが明らかとなった。

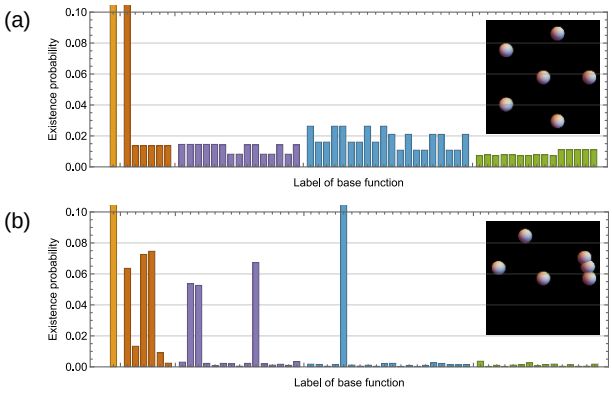

Fig. 1: 基底状態の占有確率の数値シミュレーション結果。(a)等方配置、(b)クラスタ構造あり

3. 考察

上述のように、特定の基底状態が選択励起され、この状態が双極子遷移許容な状態である（ドレスト光子の個数を変える遷移が確認できる）ことから、非対称性を有する系では効率的な自由光子の放出が示唆される。また、占有確率の低い基底状態はダーク状態に相当し、ダーク状態の存在がエネルギー移動を阻害することで散逸経路を限定し、特定の基底状態の占有を促している。講演では、自由光子放出の効率を評価指標とした最適構造の探索についても議論したい。これはドレスト光子を介した自律的な構造形成とも密接な関係があるものと推察する。

参考文献

[1] M. Ohtsu, *Silicon Light-Emitting Diodes and Lasers: Photon Breeding Devices Using Dressed Photons (Nano-Optics and Nanophotonics)* (Springer, 2016).
[2] N. Tate, et al., Sci. Rep. 5 (2015) 12762.
[3] 三宮・他，第 84 回応用物理学会秋季学術講演会 講演予稿集(2023) 22p-A310-8.

招待講演

レーザ光制御マイクロ液滴ロボット

Laser light controlled microdroplet robot

○納谷 昌之[1,2]，佐藤 守[1]、白田 真也[1]、三友 秀之[3]、居城 邦治[3]、斎木 敏治[1]
(慶應義塾大学理工学部[1]、納谷ラボ[2]、北海道大学電子科学研究所[3])
○Masayuki Naya, Mamoru Sato[1], Shinya Hakuta[1], Hideyuki Mitomo[1], Kuniharu Ijiro[1], Toshiharu Saiki[1]
([1]Keio Univ. ,[2]Naya-lab., [3]Hokkaido Univ.)

1.

1. はじめに

自らが推進力を持って自己駆動する物質をアクティブマターと呼ぶ[1)]。アクティブマターは、非平衡状態における物理現象、生命活動の起源、環境を利用した自然知能などにつながる重要な基礎科学であると同時に、新たな微小駆動源、微小流体による精密な物質輸送などへの応用などが期待され、近年、物理、化学、生物、情報、機械など、さまざまな分野からの注目が高くなっている。多くの研究は、あらかじめ存在する個体微粒子や液滴などの、個々あるいは集団的な運動を取り扱っている。これに対し、我々は、光を用いることで、発生から消滅、輸送、運動など、そのすべてのプロセスを人為的に自由にコントロールできるアクティブマターの実現を目指している。本講演では、レーザ光の ON/OFF によって発生・消滅し、さらにレーザ光のパワーなどに依存して自発的運動や変形をするマイクロ液滴ロボットについて報告する。

2. 実験系

高揮発性かつ低表面張力の液体と低揮発性かつ高表面張力の液体の混合液の薄膜の一部に光を照射し、光熱効果で局所的な高温領域を形成することで、光を照射した領域に液滴が発生する。これは、光熱効果による局所的発熱による液体の蒸発、熱マランゴニ対流、濃度マランゴニ対流の相乗作用によってレーザ光照射領域に局所的高表面張力領域が生じて液が集合することで生じる現象である[2)]。

我々は、レーザ光照射によって蒸発する気体が閉じ込められるサンドイッチ構造によって、開放系と比べて、より微小な液滴や、サンドイッチ構造内でのメニスカス架橋液滴が発生し、さらにはレーザ光の操作で液滴の移動が可能であることを示した[3)]。さらに、照射するレーザ光の強さやビーム形状に依存して、発生した液滴が自己駆動運動することを見出した[4)]。図１にサンドイッチ構造の実験系を示す。用いた液体は、エタノール（高揮発性かつ低表面張力）とポリエチレングリコール(PEG200:不揮発性かつ高表面張力）の混合液である。この液を、金の薄膜を形成したガラス基板ともう一枚のガラス基板に挟み込むことで、液が上下の基板間で

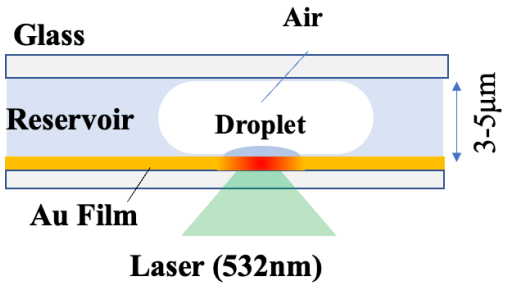

図 1. サンドイッチ構造中での液滴発生

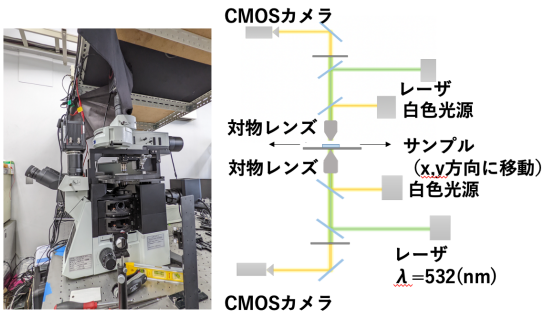

図 2. 実験光学系

メニスカス架橋したリザバー部と、架橋していない空気層が形成される。図２に示す実験系により、空気層の金膜にレーザ光（波長 532nm）を照射すると、金の光熱効果によって局所的加熱が生じ、それによってレーザ光の照射位置に液滴が発生する。液体が架橋していない空気層で液滴が発生する理由は、一見、液体が無いと見える場所にも、表面張力によって数十 nm 程度の薄い液体の前駆膜（プリカーサ膜）が形成されているためである[5)]。

3. 実験結果

(a) 金薄膜基板での実験

図３は、厚さ 25nm の金膜を形成した光熱変換基板を用いた実験の結果である。この系では、空気層の右下側は基板エッジ部で大気に解放されている。図に示す通り、レーザ光を ON することで何もなかった領域に微小な液滴が発生し、レーザ光を OFF することで液滴が開放側に向かって飛び去っていくことが観測された。直進運動の原因としては、エタノールの選択蒸発によ

招待講演

り、プリカーサ膜の PEG 濃度が開放側に向かって高くなっており、そのような濃度勾配の中で、濃度マランゴニ対流、及びに Fick 則による液滴からの PEG の拡散による駆動力が生じているためと考えられる。

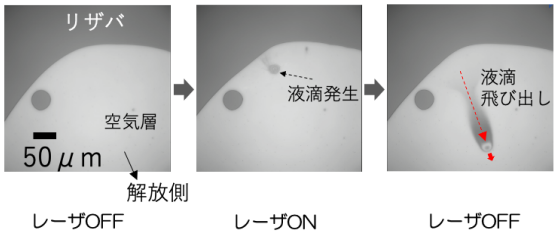

図 3.　液滴の発生と飛び出し

空気層が気泡となって密閉されている場合には、レーザ光照射位置を中心とした液滴の自励的な回転運動が生じる。この原因としては、液滴の中に非線形流れが生じること、液滴中に PEG 濃度の不均一性、表面張力不均一分布が発生し、拡散やマランゴニ対流の非対称性によって駆動力が生じていることなどが考えられる。

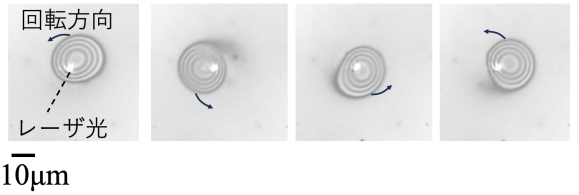

図 4.　液滴の自励回転

(b)　金ナノ粒子分散基板での実験 [6]

複数の微小な光熱変換点の間の複雑な流体ネットワークが生じるときの液滴の挙動を探索するため、我々は直径 40nm の金ナノ微粒子を表面にランダムに分散した基板を用いた実験を行った。基板上に波長 532nm のレーザ光をデフォーカスして広い範囲に照射すると、光スポット領域に存在する複数の微粒子を包含する単一の液滴が形成される。フォーカスビームの時に生じる液滴の形状は真円なのに対し、デフォーカスビームでは微粒子の分散状況に依存したアメーバ状の形状となる。さらに、液滴は、レーザスポットの位置の移動に応じて複雑に変形しながらレーザ光に追従する。それは、あたかも液滴が自分の生存のために最適な光熱スポットを狙って動いているように見える(Fig. 2)。この現象は、金ナノ粒子のプラズモン共鳴の発熱によるエタノールの蒸発による散逸を補う対流、およびに局所的な PEG 濃縮で生じる濃度マランゴニ対流に加え、一体化した液滴が複数の微粒子を跨いで自分の表面積を最小に保とうとする表面張力の統合的な作用によるものと考えられる。

図 5.　金ナノ粒子分散基板実験系

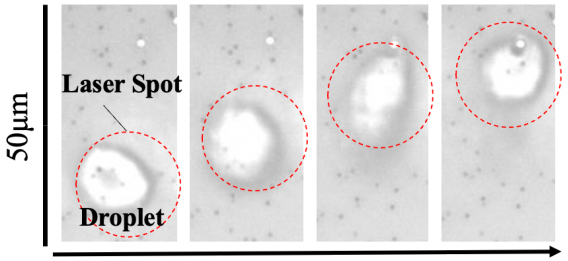

図 6.　デフォーカス光の移動により変形する液滴の変形

4.　まとめ

液体の架橋・非架橋部を含むサンドイッチ密閉構造を用いることで、レーザ光の照射によって、微小液滴の発生・移動・消滅を制御することが可能であることを示した。生じる液滴は自励的な運動や変形をすることから、この液滴はアクティブソフトマターと考えて良い。人為的に操作しているのはレーザスポットの照射・移動のみであるにもかかわらず、液滴が自ら複雑に形を変えるのは、制御対象（液滴）と環境（金微粒子分布など）との物理相互作用によるものである。我々は、このような動作を利用して、未知の環境に適応して駆動する身体性を有するロボットや、脳に依存しない自然知能への応用を考えている。

本研究は、文部科学省「光・量子飛躍フラッグシッププログラム」、「科研費学術変革研究(A)」、及びに「物質・デバイス領域共同研究拠点」の助成を受けている。

参考文献

1) S. Ramaswamy, Annual Review of Condensed Matter Physics. **1** (1): 323–345.
2) A. Ksenia, et al., Colloids and Surfaces A: Physicochem. Eng. Aspects 521(2017) 22-29.
3) Y. Takamatsu, et al., Micromachines, 14(7), (2023),1460
4) 納谷昌之他，第 69 回応用物理学会春季学術講演会(2022)　講演予稿集 23a-D315-6.
5) Yonatan Dukler, et.al., Phys. Rev. Fluids 5(2020) 034002
6) 納谷昌之他，第 70 回応用物理学会春季学術講演会(2023)　講演予稿集 18p-A201-5.

シンポジウム

エネルギー散逸のあるドレスト光子の量子ウォークモデル

A quantum walk model for dressed photons with energy dissipation

大津　元一 ((一社)ドレスト光子研究起点)

Motoichi Ohtsu (Research Origin for Dressed Photon)

1. はじめに

ドレスト光子（DP）は光が照射されたナノ寸法粒子（NP）や原子に光子、電子（励起子）との相互作用にて生成される量子場であり、それはさらにフォノンとも結合してドレスト光子フォノン（DPP）を生成する。DP の実験研究は大きな進歩を遂げた [1]。理論研究も次のように最近著しく発展している。

[1] DP の生成の理論：光・物質相互作用を記述するオフシェル科学が展開された。そして NP における局所的な光・物質相互作用の結果、spacelike マヨラナ場からの転移により timelike マヨラナ粒子と反粒子の対が生成し、その対消滅により生成するボゾン場が DP であることが示された。さらに DP の最大寸法が導出され、この理論と宇宙論との繋がりが見出された [2,3]

[2] DP のエネルギー移動：移動に際し、ランダムウォーク（RW）モデルで記述される時間的変化よりもずっと高速に変化すること、NP の間を自律的に移動することなどが実験により確認されている [1]。これらは量子ウォーク（QW）モデルが必要であることを示唆している。なぜなら QW モデルは高速現象の記述が可能 [4]であるのみでなく、空間的局在性を有する量子場の記述に適合し [5]、これまでの QW 理論研究の複数の帰結が DP エネルギー移動の自律性などとの類似性を示唆しているからである。さらにその時空発展方程式は行列を使った非可換代数の形式をとり、それは上記の相互作用の非可換性と整合するからである。本講演では QW モデルを使った数値計算を展開し、実験と比較しつつ DP エネルギー移動を記述する手法の試みを報告する。

2. エネルギー散逸の導入

ここではシリコン（Si）結晶を用いた発光素子の例を取り上げる。すなわちその製作のために施す DPP 援用アニールによって自律的に生成された B 原子対による DPP の生成/閉じ込めの現象を解析する。これまでの QW モデルによる数値計算により B 原子対が DPP 援用アニール用の照射光の伝搬方向と垂直面内にあ場合、さらに B 原子対の長さが Si 格子定数の 2-3 倍の場合、B 原子対に生成し閉じこめられる DPP の確率が最大になることが導出され、実験結果とよく合致した [6]。

これらの数値計算では Si 結晶の内部での事象を扱っている。しかし可観測(observable)物理量は製作された S 発光素子から出射する伝搬光のエネルギー、偏光、伝搬方向などであることに注意されたい。それらの評価を可能にするため、Si 結晶内部で生成された DPP のエネルギー散逸が解析できる QW モデルを構築する必要がある。

以下ではこの構築の事例として光子の運動量に関する光子ブリーディング(PB)の現象を取り上げる。なお、光子のエネルギーに関する PB はすでに実験により確認されているが [7]、運動量に関しては未だ確認されていない。そこで実験に先立って QW モデルによる解析で確認する。

ここで光子の運動量に関する PB とは、Si 結晶中の原子に生成した DP が最近接の原子に跳躍する際、照射光の運動量と同方向に跳躍する確率が高いことを意味する。しかしこれらの現象を評価できるのは Si 結晶中の DPP のエネルギーが散逸して Si 結晶外部に放射される伝搬光の特性を通じてのみである。すなわち可観測物理量としてのエネルギー散逸量を記述できる QW モデルが必要とされる。そのために 2 次元格子モデルを仮定すると、DPP の状態ベクトルは次のように表される [8]。

$$\vec{\psi}_{t,(x,y)} = {}^{T}\left[y_{DP+} \quad y_{DP-} \quad y_{Phonon} \quad y_{dis} \right]_{t,(x,y)} \tag{1}$$

ここで第 1-3 成分は Si 結晶中の DPP を表し y_{DP+}、y_{DP-} は互いに反対方向に跳躍する DP の存在確率振幅、y_{Phonon} はフォノンのそれを表す。第 4 成分はエネルギー散逸の結果 Si 結晶外部に放射する成分を表し、それは

$$\left[y_{dis,t,(x,y),} \right] \equiv {}^{T}\left[y_{DP+,dis} \quad y_{DP-,dis} \quad y_{Phonon\bigcirc} \right]_{t,(x,y)} \tag{2}$$

である。その第 1、第 2 成分 $y_{DP+,dis}$、$y_{DP-,dis}$ の発生源は各々式(1)の第 1 目、第 2 成分の y_{DP+}、y_{DP-} であり、各々入射光の進む方向と同じ方向、逆方向に進む。また、フォノンは $y_{Phonon\bigcirc}$ によって表されているが、これはサイト間を跳躍しないのでエネルギーの散逸は関与しない。

また式(1)が従う時空発展方程式の係数行列の和はもはやユニタリ行列ではなく、その中に現

象論的な散逸定数 κ を含む。なお $0 \le \kappa \le 1$ である。

3. 結果と考察

図 1 は $|y_{DP+,dis}|^2$、$|y_{DP-,dis}|^2$ の値を計算した結果である。これは B 原子対に発生した y_{DP+}、y_{DP-} に起因する散逸エネルギーを B 原子対中の各サイトの関数として記したものである。すべてのサイトにおいて $|y_{DP+,dis}|^2 > |y_{DP-,dis}|^2$ であることから、入射光の運動量と同じ方向に散逸して Si 結晶外部に放射された光量が多いこと、すなわち運動量に関する光子ブリーディングを示している。

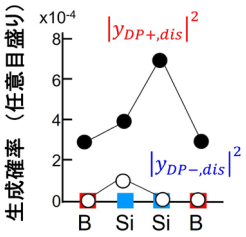

図 1 エネルギー散逸量の B 原子対サイト依存性

図 2 は散逸エネルギーの B 原子対内の全サイトの総和を散逸係数 κ の関数として示している。この図でも $|y_{DP+,dis}|^2 > |y_{DP-,dis}|^2$ であることから、運動量に関する光子ブリーディングが再確認される。この図ではさらに κ=0.2 において散逸エネルギーが最大となっている。これは Si 結晶外部に取り出すエネルギーを最大にするための最適な散逸係数があることを示している。

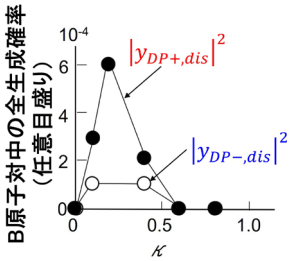

図 2 散逸係数 κ とエネルギー散逸量との関数

最後に図 3(a)、(b)は散逸係数 κ と Si 結晶内部の DPP の全エネルギー、外部に散逸した全エネルギーとの関係を示す。両図中の値は各々散逸係数 κ の増加とともに単調減少、単調増加しており、その和は係数 κ に依存せず一定である。すなわち Si 結晶内部と外部とを合わせた全空間ではエネルギーが保存していることを示している。

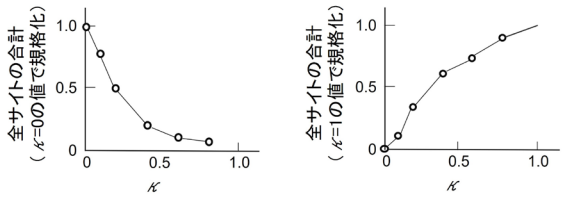

図 3 散逸係数 κ と Si 結晶内外（(a)、(b)）のエネルギー量との関係

4. まとめと展望

本研究では可観測物理量を扱うため QW モデルにエネルギー散逸の概念を導入した。その結果、光子の運動量に関する光子ブリーディングを確認することができた。さらに

(1) 散逸定数 κ=0.2 の時に外部へのエネルギー量放出量は最大となった。
(2) Si 結晶中外の全空間でのエネルギー保存則は保証された。

(1)、(2)により微視系、巨視系（各々Si 結晶内部、外部）の特性を相互矛盾なく説明された。

今後は可観測(observable)物理量、エネルギー散逸とオフシェル科学のける量子測定論 [9]との連携を探ることが重要となる。

謝辞

QW モデルの概念に関しご教示頂いた瀬川悦生氏（横浜国大）、齋藤正顕氏（工学院大学）、三宮俊氏（リコー）に、多くの数値計算を実施された結城謙太氏（Middenii）に感謝致します。

参考文献

1) M. Ohtsu: Dressed Photon (Springer, Heidelberg, 2014) pp.1-246.
2) H. Sakuma and I. Ojima: Symmetry. **13** (2021) 593.
3) H. Sakuma, et al.: J. Euro. Opt. Soc. **17** (221) 28.
4) N. Konno: Quantum Walk, Chapter 8, Quantum Potential Theory, ed. by U. Franz and M. Schumann (Springer, Heidelberg, 2008). p.309.
5) H. Saigo: Quantum Probability for Dressed Photons, Chapter 3, Progress in Nanophotonics 5, ed. by T. Yatsui (Springer, Heidelberg, 2018) p.79.
6) 大津元一 他、第 70 回応用物理学会春季講演会（2023 年 3 月）、16a-A201-4.
7) M. Ohtsu: Silicon Light-Emitting Diodes and Lasers (Springer, Heidelberg, 2016) pp.8-11.
8) 大津元一 他、第 84 回応用物理学会秋季講演会（2023 年 9 月）、162p-A310-7.
9) K. Okamura, “Towards a Measurement Theory for Off-Shell Quantum Fields,” Symmetry **13** (2021) 1183.

シンポジウム

量子ウォークのエネルギー遷移問題の数理

Mathematics of energy transfer problem of quantum walks

瀬川 悦生 [1] (横浜国立大学)

Etsuo Segawa [1] (Yokohama National Univ.)

1. はじめに

栓が抜けた水槽に蛇口から水を入れ続け, 水面が一定になっていることを想像してみる. 水槽内の水量は一定なので, 定常的な状態になっている. これは, 蛇口から入ってきた水(流入)と, 栓から出ていく(流出)が釣り合うことによって起こる. これと似たようなことが量子コンピュータの中で, 量子探索アルゴリズム [1]やハミルトニアンの高速シミュレータ [2]として駆動することが期待されている量子ウォークでも起こせる.

量子ウォークの時間発展作用素は系全体ではユニタリ作用素で与えられるため, 固有値が複素平面内の単位円周上に分布している. そのため, 時間発展を行うと, 固有値はその単位円周上を周ることになり, 力学系としての固定点への収束は期待できない. 一方で, その対応モデルであるエルゴードで非周期的なランダムウォークにおいては, 固有値が(-1,1]に分布し, 時刻無限大で 1 以外の固有値が 0 に指数関数的に縮退するため, 固有値 1 の固有ベクトルへ定常状態として収束する. このような性質があるため, 電気回路との繋がりやカットオフ現象など, 豊かな性質について論じることができる.

そこで, 冒頭で述べた例の類推で, 有限で連結なグラフを水槽に見立て, 頂点から境界にあたるもの任意に選び, それを蛇口と栓に見立てて, 量子ウォークの流出入が行われるように設定する. すると, この量子ウォークモデルは定常状態に収束することが証明された [1]. 実は, この量子ウォークモデルの定常状態の中に, ドレスト光子のエネルギー遷移の挙動と幾つかの類似性を見出すことができる. 特に, 最大出力を得るために必要な空間構造を導出するような計算量を要する問題には, ドレスト光子ダイナミクスの素子化モデルとして, 量子ウォークが着目されつつある [3].

本研究では, この量子ウォークモデルの中で最も基本的な Grover walk と呼ばれるもので考察し, その不思議な定常状態の性質について議論する.

2. 拡張型ラプラシアン

有限で連結なグラフを $G = (V, E)$ とし, その隣接行列を M, 次数行列を D とすると, L=M-D はラプラシアン, Q=M+D は符号付ラプラシアンと呼ばれており, 多くの研究が行われている. 量子ウォークの流出入が行われる頂点の集合を δV とし, そこから振幅 α, 振動数 θ で毎時刻流入が行われているとする. このときの量子ウォークの定常状態を記述する上で重要な作用素が次に定義する拡張型ラプラシアンである.

定義 (拡張型ラプラシアン)

$$L(\theta) = M - \cos\theta D + i \sin\theta \Pi.$$

ここで, Π は境界 δV に対応するところは 1 それ以外が 0 の対角行列である.

特に, $\theta=0$ のときはラプラシアン, $\theta=\pi$ のときは, 符号付ラプラシアンになっており, 両者がパラメータ(振動数) θ によって連続的に接続されている.

3. 主結果

定常状態を ϕ_∞ とすると, 次のような量子ウォーク版の回路方程式が得られる.

定理 1（量子ウォークの回路方程式）

$$i \sin\theta \, \phi_\infty = \partial_\theta \nu;$$
$$L(\theta)\nu = i \sin\theta \, \alpha'.$$

ここで, 任意の頂点 V 上の関数 f に対して,
$(\partial_\theta f)(a) = f(t(a)) - \exp(i\theta) f(o(a))$.

最初の式は, キルヒホッフの電圧則, 最後の式は, キルヒホッフの電流測に対応している.

定常状態における流出量を $|\delta V|$ 次元のベクトル値 β で表すと, 流入値 α との間に関係性がある. この関係性は定常性と時間発展のユニタリ性から, 流入量に依存しない, ある $|\delta V|$ 次元のユニタリ行列で記述できる. これを S とおくと $\beta = S\alpha$ となり, S は次のように表される.

定理 2 (散乱行列)

$$S = \chi_\delta (2i\sin\theta \, L^{-1}(\theta) - I) \chi_\delta^*.$$

ここで χ_δ は V から境界 δV への制限を表現する $|\delta V| \times |V|$ の長方行列.

内部では定常状態でどのくらい量子ウォークが存在するかを測る指標として,

$$E = 1/2 \, \| \phi_\infty \|^2_G$$

で定義する快適度を考える [4]. これは冒頭の例でいうところの水槽にたまっている水量に相当する. すると次のように拡張型ラプラシアンによるシンプルな表示が与えられる.

定理 3 (快適度)

$$E= < L^{-1}(\theta)\boldsymbol{\alpha}, (D-\cos\theta M) L^{-1}(\theta)\boldsymbol{\alpha} >.$$

4. 除去可能特異点

定理 2，3 の左辺の表現に拡張型ラプラシアンの逆行列が表れている．θ の値によっては，特異点になるように見える．例えば，$\theta=0$ のときは，ラプラシアンそのものになり，ラプラシアンは all 1 ベクトルは固有値 0 の固有ベクトルになるから，逆行列を持たない．しかしながら，実はそれらが除去可能特異点となっていることが加藤の摂動論を用いて示せる． 例えば，$\theta=0$ のときはまさに電気回路の方程式が現れる．

しかしながら，この特殊な振動数は除去可能とはいえ，量子ウォークとしては特別な挙動を見せることを，グラフとして完全グラフにおける快適度を例にして，紹介する．冒頭にあげた，水槽の例で，たくさんの栓がついているほど，それだけ出口が多いのだから，水は溜まりにくい．この直感は入力振動数 θ が 0 のときにはマッチする．つまり，$E(\theta, \ell)$ を頂点数 N の完全グラフにおいて，入力振動数 θ，出口の個数 ℓ における快適度とすると，

$$E(0, N)> E(0, N-1)>\ldots>E(0,1)$$

である．ところがある特殊な振動数で入力をすると非直感的な現象が次のように起こる． $\theta=\theta_*$ のとき（但し $\cos\theta_*=-1/(N-1)$ ）

$$E(\theta_*, N-1)> E(\theta_*, \ell-2)>\ldots> E(\theta_*, 1)> E(\theta_*, N)$$

となる．つまり，沢山の出口があるにもかかわらず，中に量子ウォークが溜まりやすくなっていくだけでなく，さらに(調子に乗って)全ての頂点を出口にすると，快適度は最下位に陥落するという，追い打ちをかける非直感的現象が起こっている．

この振動数 θ_* は完全反射を起こし，特殊な挙動を示す．実は $\cos\theta_*$ は完全グラフ上のランダムウォークの固有値に一致している．しかも実は，この θ は $L(\theta)$ を不可逆にするので，まさに除去可能特異点になっている．そして，ほとんどの境界の個数において， 頂点が十分に大きいと，振動数 θ を動かして，快適度を計算すると，$\theta=\theta_*$ で快適度が最大になる．

このような振動数は，より一般のグラフにおいて， θ が 0 と π 以外のとき，ランダムウォークの確率遷移行列の，境界 δV にオーバーラップがない左固有ベクトルが起因している．実際，完全グラフの場合は，そのような固有ベクトルが境界の個数 ℓ に依存して複数とることができることが容易にわかる．

5 今後の展望

Grover walk においては，拡張型ラプラシアン行列を導入することによって， 問題を簡略化することができた． 特に逆行列による表現が出てくるので，ランダムウォークの hitting time や訪問回数に類似した表現方法に焼き直すことにより， 一見すると不思議に思えるこの現象の説明をより身近に感じられる解釈によって説明がなされることが期待される．また Grover walk はグラフの隣接関係のみに依存するもっともシンプルな量子ウォークモデルの 1 つであるがゆえに，ドレスト光子を記述するには挙動の類似性があるとはいえ，物足りない．現在その最有力候補として参考文献 3)で提案されているモデルが挙げられ，数値計算と並行して，その解析的な考察が進められている．

参考文献

1) R. Portugal, Quantum Walks and Search Algorithms, 2nd Ed., Springer, Switzerland (2018).
2) S. Apers, A. Sarlette, Quantum fast-forwarding: Marcov chains and graph property testing, Quantum Information and Computation, 19 (2019) pp.181-213.
3) Yu. Higuchi and E. Segawa, Dynamical system induced by quantum walks, J. Phys. A: Math. Theor. 52 (2019), 395202.
4) M. Ohtsu, A quantum walk model for describing the energy transfer of a dressed photon, DOI : 2109R.001.v1.
5) Yu. Higuchi, M. Sabri and E. Segawa, A comfortable graph structure for Grover walk, J. Phys. A: Math. Theor. 56 (2023) 275203.

シンポジウム

欠陥構造が引き起こすドレスト光子の超放射過程

Superradiance process of dressed photons induced by spatial defect structures

○三宮　俊 (株式会社リコー)

Suguru Sangu (Ricoh Company, Ltd.)

1.

1.　はじめに

ドレスト光子の局在・散逸と物質系に含まれる欠陥の空間配置には密接な関係がある．その一例として，間接遷移型半導体であるシリコンの発光デバイスが知られている [1]．本デバイスの作製過程では光を照射しながらドーパント(ボロン)をアニールすることで，ドーパントの対構造が自律的に形成され，本デバイスの発光過程ではこのドーパント対を介することで禁止されている状態間の発光が得られる。ここで欠陥位置におけるドレスト光子の局在とフォノン場を巻き込んだ相互作用がドーパント対形成や発光を引き起こすものと解釈されている．

我々は上述のようなドレスト光子介在の物理現象を数値シミュレーションにより紐解き，説明することを目指している．構築中のシミュレーションでは，ドレスト光子を自由光子，物質励起，フォノンの全ての寄与を含んだ準粒子二準位系)と見なし，その静的および動的振る舞いを解析する。つまり，上述のフォノンの効果を切り分けて議論することはせずに，強い局在性を有する基底状態や空間的に広がった分布を有する基底状態といった，基底状態の保有する性質にその機能を負わせている．

最近では，物質系内にドレスト光子が複数個含まれる状態に注目し，上述の欠陥構造の自律形成および発光現象を説明できる予備的知見を得ている [2]．数値シミュレーションにより，複数欠陥の配置に依存して，輻射遷移に関わる主要な基底状態が変化し，緩和寿命が変化することで，ドレスト光子エネルギーを物質系外に効率的に放出したり，内部に留めたりする機能が制御される可能性を確認している．なお，二準位系の集団内の励起個数に分類し，線形和として基底状態を表現した状態はディッケ状態と呼ばれ，高速な発光である超放射現象を引き起こすことが知られている [3]．

本論文では，上述したドレスト光子を複数含む基底状態およびドレスト光子の個数に変化をもたらす遷移に改めて着目し、欠陥構造の自律形成や発光現象への関与する様子を数値シミュレーヨンにより浮き彫りにするとともに，ディッケの超放射現象との類似性に着目してその物理的解釈を与えることを検討する。

2.　ドレスト光子シミュレーションの概略

本数値シミュレーションは，物質系のサイトに束縛されたドレスト光子(調和振動子)を基本要素とし，このサイトを空間的に自由に配置した系を，量子密度行列を用いて記述する．量子

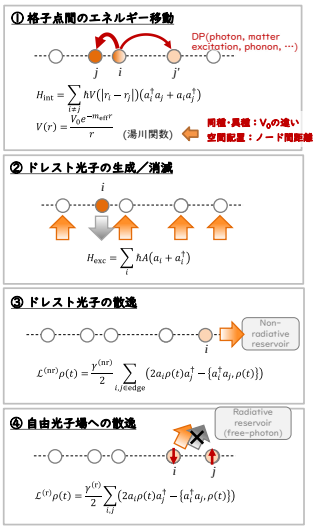

図 1　運動方程式の構成要素

密度行列のダイナミクスは Lindblad 方程式と呼ばれる散逸を近似的に導入した時間発展方程式で記述する [4]．数式の詳細な記述は省略し，量子密度行列の運動方程式の構成要素について図 1 に説明する．系内のドレスト光子の移動は，①に示すように，任意のサイト間の相互作用強さにより与える．相互作用強さはドレスト光子が質量をもつ準粒子と見なせることから相互作用距離が有限となる湯川関数で与える．ドレスト光子の入力は，②に示すように，生成、消滅演算子の和，すなわち電気双極子励起を模倣した形で与え、系内の全サイトをコヒーレントに励起する．エネルギー散逸はサイト端部からの非輻射緩和(③)と自由光子としての輻射緩和(④)を考慮する．ここで，輻射緩和は全サイトの和の形で与えており、これは反対称な空間分布をもつ励起状態からの輻射が禁制される状況を含んでいる．数値シミュレーションは系内にドレスト光子を含まない状態から開始し，連続的に入力を与えた状態で非平衡定常状態に達するまで計算を継続する．

3.　欠陥の空間配置による影響の考察

本節では代表的な計算結果について説明する。図 2 は不純物サイトを含む 1 次元物質系(6 サイト)に対し本数値シミュレーションを実施した結果であり，量子密度行列の対角成分，すなわちドレスト光子基底状態の占有確率をグラフ化している．ここでいうドレスト光子基底状態とは，6 サイトに対してドレスト光子が 0 個から 6 個配置できるすべての組み合わせの要素を意味

している．左から茶色，紫色，青色，緑色の表示はドレスト光子 1 個から 4 個を含む基底状態をグルーピングしたものである．図 2(a)は 1 個の不純物サイトを含む場合であり、図 2(b)は 2 個の不純物サイトが 1 サイト間隔を空けて配置された場合の結果である。不純物サイトが所定位置に配された場合に，ドレスト光子 1, 2 個の基底状態の占有確率が低下し，ドレスト光子 3 個の基底状態の占有確率が増加する様子が確認できる．この結果は，6 サイトにドレスト光子を配置できる組み合わせの数がドレスト光子 3 個の場合が最も多くなり、基底状態の数が最大となるためと考えられる．また，本結果では顕わに表現できていないが，ドレスト光子の占有確率が高くなると，光子密度が上がるために誘導放出が促され，自由光子の放出が活性化し，発光を促すとともに，系を冷却し，不純物の自律的な位置決めにつながると推察している．誘導放出に関しては，対象となる基底状態の寿命がその効率を決めるパラメータとなることから，外部へ光子を放出しやすいモードの抽出(基底状態の変換)が必要であり，その方法については現在検討中である．その要点についてのみ，次節に取り上げる．

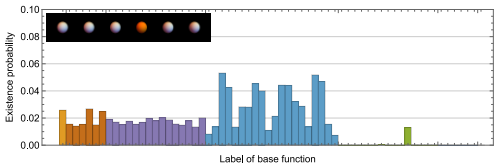

(a) 不純物を 1 個含む系

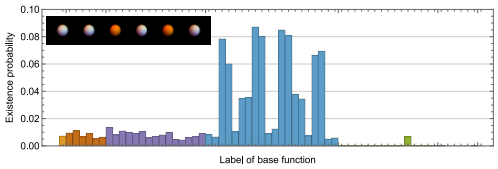

(b) 不純物を 2 個含む系

図 2　一次元系モデルにおけるドレスト光子占有確率の計算結果

4.　基底変換方法の提案

ドレスト光子の個数ごとに主要な基底状態を抽出する方法について検討している．一つの方法として、非平衡定常状態に達した密度行列のドレスト光子の個数に依存した部分行列を対角化する方法を提案する．図 3 はその概略を説明する図である。図 3 の上図はサイトで分解した基底状態による量子密度行列である．この量子密度行列を図中の枠線で表わすドレスト光子の個数ごとに分けた部分行列を対角化するように全体の変換行列を定義する．図 3 下図は変換後の量子密度行列の算出結果の一例である．変換後に得られた基底状態について緩和時間や主要

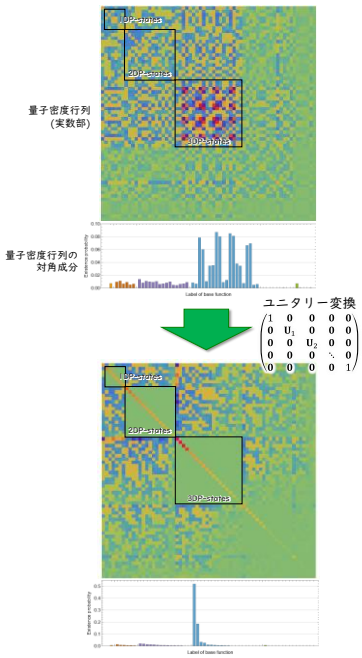

図 3 ドレスト光子の個数に依存した基底変換の方法

な遷移先基底状態を調べることで，本稿冒頭で述べた自律的構造形成や発光現象の許容化に関わる物理的解釈が進むものと考えており、現在可視化等の手段を模索中である．この基底変換はサイトの励起状態の集合からなる基底状態の線形和により異なる基底状態を定義するプロセスであり，冒頭で述べた超放射現象を説明するディッケ状態に類推する基底状態を抽出している．したがって，一部の基底状態においてディッケ状態と同様の散逸の加速が生じることが期待される．

5.　まとめ

光子，物質励起，フォノンを個々に識別することなく「ドレスト光子」と見なし、そのダイナミクスを，量子密度行列を用いて数値シミュレーションする方法を構築中である。系内のドレスト光子の個数に依存した特徴的な振る舞いが現れることを見出し，その状況が超放射現象に類推するものであることを指摘した．その解読方法については現在模索中であり，講演時にその進捗状況についても紹介したい．

参考文献

1) M. Ohtsu and T. Kawazoe, Adv. Mat. Lett. **10** (2019) 860.
2) 三宮・他，第 84 回応用物理学会秋季学術講演会（2023 年 9 月），22p-A310-8.
3) R. H. Dicke, Phys. Rev. **93** (1954) 99.
4) S. Sangu, et al., Symmetry 13 (2021) 1768.

[VII] AWARDS AND CONFERMENTS

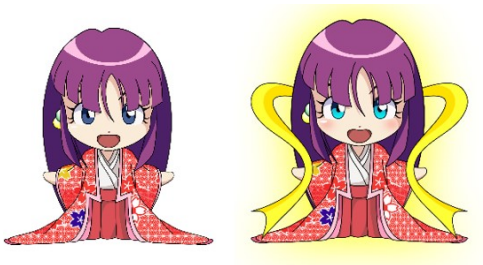

（左）賞状（盾）、（右）副賞（トロフィ）